Bressay Bridge
Lerwick, Shetland

Ground investigation

April 2003

REPORT ON PRESSUREMETER TESTS

Reference: CIR 1099/03

CAMBRIDGE INSITU
Little Eversden
Cambridge
ENGLAND
CB3 7HE

Tel:- (01223) 262361 Fax:- (01223) 263947 Email:- caminsitu@aol.com
Web site:- Cambridge-Insitu.com

CONTENTS

1 INTRODUCTION
- 1.1 Instrument
- 1.2 Analysis
- 1.3 Report
- 1.4 Notation
- 1.5 Units
- 1.6 Personnel
- 1.7 Headers and Footers

2 A LIST OF TESTS CARRIED OUT

3 COMMENTS ON THE TESTS AND THE ANALYSIS
- 3.1 Comments on tests
- 3.2 Shear modulus
- 3.3 Shear strength
- 3.4 Insitu stress
- 3.5 Friction angle

4 SUMMARY OF RESULTS

Table 1	General results
Table 2	Frictional results
Table 3	Shear modulus parameters

5 FULL RESULTS AND PLOTS

APPENDICES:

A. DESCRIPTION OF THE EQUIPMENT
1. Outline
2. The Membrane
3. The Pressurising System
4. Electronics Interface Unit
5. Data Logging/Analysis Software

B. THE CALIBRATION PROCEDURE
1. Scale Factors
2. The displacement measuring system
3. Pressure measuring transducers
4. Reference ('zero') outputs
5. Membrane stiffness
6. Instrument compliance
7. Membrane thinning
8. Repeatability
9. Orientation
10. Table of measured scalar values
11. Table of membrane correction for HPD tests

C. THE TEST PROCEDURE
1. Coring the pocket
2. Description of the Test
3. Tests in material that can be failed –Type A
4. Tests in material where all deformation is elastic – Type B
5. Concluding remarks

D. INTERPRETATION OF PRESSUREMETER TESTS
1. Introduction
2. Analyses for expansion
3. Shear Modulus
4. Interpretation of Pressuremeter tests in rock

E. CONVERTING RAW DATA TO ENGINEERING UNITS

F. REFERENCES

1. INTRODUCTION

Ten High Pressure Dilatometer (HPD) tests were carried out for Seacore at Lerwick as part of the site investigation for the proposed Bressay Bridge.

The HPD testing was carried out in a series of boreholes, following the line of the proposed bridge from Lerwick to Bressay Island. There was one test in each borehole, nominally 2 metres into competent rock. All except one gave good tests. The rock was mainly sandstone, fractured in places, with bands of conglomerate.

Work continued on a 24hour basis, except when delayed by wind. Two operators were available and the testing was shared between them.

The probe used for the first two tests (Scotty) developed a fault on one arm – probably connected with the sudden loss of pressure when the membrane punctured. The spare probe (Tilly) was used for all subsequent tests.

The instrument expands in an approximately circular manner, even if the resultant circle is offset to one side. The results have been analysed using the average expansion, as this gives the best overall picture of the soil properties. The exception to this is the test in Borehole 8, where one arm reached maximum expansion at very low pressure. Only one pair of arms gives realistic results. Some of the tests had the lowering recorded separately, but these have now been incorporated into the test itself as this makes it easier to determine the zeros for the sensors.

For the analysis, therefore, all tests are known as B*T1.

1.1 Instrument

The pressuremeter used was a 95mm diameter Cambridge High Pressure Dilatometer. This instrument, based on an earlier design by Dr J.M.O Hughes, was developed to carry out a pressuremeter test in soft to weak rock. In use the instrument is lowered into a 100mm pocket made by a rotary coring rig as a consequence of obtaining an H sized core. Once in position, oil or gas pressure is applied down an umbilical cord and a membrane covered the central third of the probe inflates and thus loads the borehole wall. The expansion of the membrane is monitored by sensitive feelers and the pressure applied is measured by a transducer in the probe. The output of the probe is a stream of digital data, which when converted to engineering units gives a pressure/displacement curve of the horizontally orientated loading test. It is a complex instrument by normal site standards, uses strain gauged transducers throughout and includes a microprocessor controlled data acquisition system.

Although developed to test ground of the strength of weak rock, the pressure and displacement resolution of the instrument is such that it can operate at two extremes of ground conditions. The first is weak rock, where it is likely the ground will only deform elastically and the 20MPa pressure capability of the instrument will determine the end of the test. The second condition is typically firm to very stiff clay, when the soil will experience substantial plastic deformation at modest pressures, and the strain range of the probe will determine the limit of the test. All tests on this contract showed some plastic deformation.

1.2 Analysis

The pressuremeter loading curve can be solved directly using mathematical expressions for the expansion of a cylindrical cavity. The solution is conventionally quoted in terms of strength parameters for the material, specifically shear modulus, shear strength or friction angle as appropriate, and the insitu lateral stress. This fundamental approach is not the only way to interpret pressuremeter data, but is common practice in the UK.

The success of this method is dependent on the validity of the assumptions that have to be made:

- Assumptions about the soil response include the following: that the material is fully saturated, homogeneous, isotropic, behaving as a continuum that fails in shear only.
- An important assumption about the instrument is that the length to diameter ratio of the expanding section is large enough for end effects to be negligible allowing the test to be modelled as a plane strain expansion.
- A major assumption concerning the test procedure is that the loading path be either undrained or fully drained. If undrained the loading takes place at constant volume and only shear strains need be considered. This loading path would be appropriate for a test in clay. If the expansion is drained, then the material is treated as behaving with the characteristics of sand and shear and volumetric strains must be accounted for.

Conventionally, it is the pressuremeter loading curve that is analysed. Strength parameters have been obtained using the method first proposed by Gibson & Anderson (1961) for an undrained expansion. This is probably not strictly applicable to this material, as the data does generally show a constantly increasing shear stress. The Hughes et al (1977) analysis for sands has also been applied, with some success. The method requires the user to input a value for ϕ_{cv} – 'typical' values have been used, in the absence of any further information.

Plausible and consistent data for shear modulus have been obtained from the pressuremeter tests, derived from the slope of the chord that bisects small cycles of elastic unloading and reloading. At least two such cycles were incorporated into each HPD test. This procedure implies the material response is linear elastic. A non-linear elastic evaluation of the unload/reload data has also been carried out using the procedure proposed by Bolton & Whittle (1999). Loops begun after the onset of failure show some non-linearity.

Note that all modulus parameters quoted are shear modulus G and have not been converted to Young's modulus E. If the material is isotropic then the relationship $E = 2G(1+\mu)$ can be used where μ is Poisson's ratio. Where drained Young's modulus E′ is required μ is often taken to be 0.25 or 0.3.

Values are given for the cavity reference pressure P_o using the construction proposed by Marsland & Randolph (1977). P_o is often taken to be the insitu lateral stress, but for an HPD test this assumption is unwise. The cavity reference pressure may mask a contribution due to tensile failure, and this is not taken account of in the methods of analysis used here.

Details of the analysis methods used are given in Appendix D.

1.3 Report

Although it is necessary to make judgements when analysing the data, this remains a factual report. The parameters derived represent what seems a reasonable choice having applied a particular analysis. However other choices are certainly possible, and the intention is that this report provides a full description of the tests and analytical methods employed so that the choices made here can be checked or modified.

Where necessary, significant details of individual tests have been mentioned, and this includes any problems with the equipment or procedure that may have influenced the results.

Note that the test data is available on disk as files of readings in engineering units in a format easily accessed by several common spreadsheet programs.

1.4 Notation

The data collection system employed on site utilises a limited keyboard that restricts the options for describing a test. In particular it stores tests in the form B** T** where ** must be a number. The 'B' is intended to refer to the borehole and the 'T' refers to the individual test, so a typical test reference is B1T1 - the test in borehole 1. Note that some tests were initially called B*T11 (B6T11 for example). This was because B6T1 had been used to monitor the lowering.

Calibration tests to evaluate membrane stiffness and compression are reported in a similar manner, but using a test number that cannot be confused with an actual test. Only one calibration test was required for each probe used on this contract, C999T99 for Tilly and C499T99 for Scotty.

1.5 Units

Pressure is quoted throughout in Pascal's. The smallest unit of pressure quoted is 1 kPa. Displacements are quoted in millimetres; once an estimate of the insitu lateral stress has been made, hence allowing the original cavity diameter to be inferred, then these are converted to percent cavity strain. Lengths are quoted in metres.

1.6 Personnel

The field work for these tests was carried out by Pat Finlay and Philip Hawkins of Cambridge Insitu, with coring of the test pockets the responsibility of Seacore personnel. The analysis and reporting has been done by Philip Hawkins, also of Cambridge Insitu.

1.7 Headers and Footers

The header used on every page of this text report refers to the contract and the approximate date of the field work. The footer is for CI internal use only and refers to the document name and the date of printing.

2. A LIST OF TESTS CARRIED OUT

Test	Date	Depth (m) below sea bed	Probe	Maximum pressure (MPa)	Notes
B6 T11	10/04/03	3.5	Scotty	21	Very stiff. Very little movement.
B5 T1	11/04/03	3.3	"	11	Much weaker after initial failure. Membrane burst just above arms.
B8 T1	12/04/03	7.5	Tilly	0.8	Large pocket. One arm out to maximum expansion.
B9 T11	"	3.1	"	5.0	Conglomerate. Nice test.
B7 T11	13/04/03	4.6	"	15	Failing nicely.
B10T11	"	5.1	"	10	Weakens at ~3.5MPa?
B13T11	14/04/03	3.3	"	2.2	Pebbly. Arms very different. Expanding at end of membrane?
B14T1	16/04/03	5.4	"	7.5	Failing nicely.
B12T11	"	3.0	"	8.8	Conglomerate. Clayey?
B11T1	17/04/03	3.1	"	10	Failing nicely. Kink at ~7MPa.

Notes:

- Depth is given in metres below sea bed level to the centre of the membrane of the probe, where displacements are measured.
- Where the test is called B*T11, the designation B*T1 was used to record the lowering of the probe to test depth.

3. Site Specific Commentary

3.1 Test comments

The first test (B6T11) turned out to be in the stiffest material encountered. There was very little movement, even at maximum pressure. A closer look, however, revealed a sudden jump just after the second reload loop (at about 8MPa), with a definite softening of the material. This behaviour was to be repeated in some of the subsequent tests.

The second test (B5T1) was one such, with the change in properties very marked. Unfortunately a small puncture in the membrane stopped this test slightly prematurely, and prompted a change to the spare probe.

The third test (B8T1) was marred by a different phenomenon. One arm expanded rapidly into a cavity. The maximum pressure reached was only 750kPa, by which time this arm was at more than 23mm expansion.

Subsequent testing proved uneventful, with the material failing nicely at modest pressure. The only test to show any worrying behaviour was B13T11, in pebbly material. The borehole wall was obviously very uneven and the arms were behaving differently, so the test was stopped as soon as possible.

Most tests had four reload loops, with just two having three.

3.2 Shear Modulus

It most tests it would appear that the higher the stress, the higher the modulus – this implies that the mean effective stress is increasing throughout the expansion, which is what would be expected from a frictional material. In those tests that show a sudden expansion, the modulus afterwards is reduced – at least initially.

Ignoring those loops which are obviously below the Insitu Stress, most show slight non-linearity. This tends to become more noticeable after failure.

The initial modulus is generally less than that from the reload loops, typical for a soil where the material fails on removal of the core barrel. Some tests, however, show an initial modulus of similar magnitude to that from the loops, giving the possibility of using this to estimate the Insitu Stress.

3.3 Shear Strength

The tests have been analysed as undrained expansions, probably an unrealistic assumption. The material is certainly frictional in behaviour, so the figure quoted is merely the maximum shear stress reached, but some tests do seem to have reached a constant value.

It is customary to assume that the undrained shear strength is half the unconfined compressive strength.

3.4 Insitu Stress

The Marsland and Randolph method for estimating the Insitu stress becomes somewhat subjective when using 'End of Creep' points, as there tend to be rather few of them and they are often rather scattered. These tests are better than most, and one of the reasons

that the results given here differ from the preliminary results is that the creep points have been carefully re-inspected.

In those tests which show a sudden jump, it is the part prior to the jump that is used for the Marsland and Randolph procedure. In test B6T1 this means that there are not enough points, so a value has been estimated.

The Insitu stress is used to define the strain origin. Where the second part of the test is completely separate, a new strain origin has been used to determine the shear strength.

For those tests that have not suffered from the loss of stress on removal of the core barrel, the Initial modulus has been used to give an estimate of the Insitu stress.

3.5 Friction angle

Most tests can be analysed as a drained expansion, and give sensible results. One even appears to reach constant volume expansion. The results are reasonably consistent.

The Hughes, Wroth & Windle analysis for peak friction angle requires a value for the friction angle at constant volume. A value of 33° has been assumed for the sandstone, and the slightly higher value of 35° for the conglomerate. This latter is on the basis of test B9T1 which appears to reach constant volume expansion.

4. Summary of Results

Table 1 General results

Test	Depth (mtr)	P_{max}	Pocket dia.	P_o (M&R)	P_o (G_i)	P_f	C_u	P_L	G_i	G_{ur1}	G_{ur2}	G_{ur3}	G_{ur4}
	(bsb)	(MPa)	(mm)	(MPa)	(MPa)	(MPa)	(MPa)	(MPa)	(GPa)	(GPa)	(GPa)	(GPa)	(Gpa)
B5T1	3.3	10.8	99.5	5.0	-	5.5	4.9	24	0.69	1.15	1.35	0.75	0.83
B6T1	3.5	20.6	100.1	-	4.7	~8	12	73	2.05	1.30	2.79	2.28	2.85
B7T1	4.6	14.8	99.2	2.6	(0.3)	6.1	7.5	38	0.37	0.19	0.71	0.96	1.34
B8T1	7.5	0.8	*100.9*	-	-	-	-	-	0.02	0.02	0.04	0.05	0.08
B9T1	3.1	4.9	99.1	1.2	-	2.2	1.7	11	0.24	0.31	0.61	0.57	-
B10T1	5.1	10.3	99.8	2.0	-	3.2	4.4	23	0.29	0.60	0.80	0.70	-
B11T1	3.1	10.2	99.1	2.0	-	6.7	6.1	26	0.11	0.58	0.57	0.49	0.59
B12T1	3.0	8.7	98.6	2.0	1.3	3.9	3.8	23	0.41	0.22	0.56	0.77	0.85
B13T1	3.3	2.2	99.9	1.1	0.6	1.9	0.9	6.5	0.14	0.02	0.04	0.27	0.37
B14T1	5.4	7.4	102.7	1.5	-	2.9	4.2	17	0.08	0.10	0.19	0.25	0.31

Notes on Table 1:

1. **P_{max}** This is the maximum pressure reached during the test.

2. **P_o (M & R)** These results for cavity reference pressure are derived from the Marsland & Randolph (1977) method.

3. **P_o (G_i)** An interpolation from the Initial Modulus, where it falls within the range of Reload Moduli.

4. **Pocket dia.** Given a value for P_o (an estimate is used if no reliable value is available) a corresponding displacement is derived. This when added to the probe diameter gives the diameter of the cavity in its *insitu* condition. For B8T1 this is the smallest of the arm pairs, from which the results given are obtained.

5. **P_f** This is the observed yield stress of the material, being the total stress where the loading curve departs from the initial straight line. In a linear elastic/perfectly plastic material this will be p_o+c_u.

6. **C_u** This is the undrained shear strength, derived from the slope of a semi-log plot of total pressure versus current shear strain.

7. **P_L** This is the limit pressure of the material, from the intercept of a semi-log plot of total pressure versus current shear strain.

8. **G_i** The shear modulus derived from the slope of the initial linear part of the expansion. In a pre-bored pressuremeter test they are unlikely to be representative of the true elastic properties of the material.

9. **G_{urn}** The shear modulus derived from the slope of the chord bisecting cycles of unloading and reloading. This procedure is valid provided the material response is linear elastic. If not, then a slightly more complex procedure is required and these results are given in Table 2.

Table 2 Frictional results

Test	Depth (mtr) (bsb)	Friction angle (const vol) --Assumed --	(Peak) friction angle	Angle of dilation	Remarks
B5T1	3.3	33°	42°	12°	After initial failure.
B6T1	3.5	"	44°	15°	"
		"	(56°)	(31°)	Apparently stiffer at large strain?
B7T1	4.6	"	47°	18°	Good straight line plot.
B8T1	7.5	-	-	-	Not enough to analyse.
B9T1	3.1	35°	47°	16°	Conglomerate. Peak values.
		"	35°	0°	At large strain – constant volume?
B10T1	5.1	33°	47°	18°	Stiffer at large strain?
B11T1	3.1	"	54°	28°	Unambiguous high values?
B12T1	3.0	35°	49°	19°	Conglomerate. Good straight line.
B13T1	3.3	-	-	-	Not really enough to analyse.
B14T1	5.4	33°	51°	24°	Good straight line plot.

Notes on Table 2:

1. The angles of friction and dilation are found using the method of Hughes et al (1977).

2. The method requires a value for ϕ_{cv} - the angle of friction at constant volume. I have used 33° as a typical value for the sandstone and 35° for the conglomerate (this as a result of test B9T1). Results for other values may be found from the equations

$$\sin \phi' = S/[1 + (S - 1) \sin \phi_{cv}]$$
$$\sin \Psi = S + (S - 1) \sin \phi_{cv}$$

where ϕ' is the peak angle of friction
ϕ_{cv} is the constant volume angle of friction
Ψ is the angle of dilation.
S is the slope of the 'Hughes' plot.

3. Only tests B8T1 and B13T1 do not have enough expansion to analyse.

Table 3 Shear modulus parameters

		Linear elastic interpretation					Non-linear elastic interpretation				
Test	**Loop**	**Value**	ε_c	p_c	$\Delta\varepsilon_c$	Δp_c	β	α	$\gamma=10^{-4}$	$\gamma=10^{-3}$	$\gamma=10^{-2}$
		(MPa)	(%)	(MPa)	(%)	(MPa)		(MPa)	(MPa)	(MPa)	(MPa)
B5T1	1	1148	-0.12	2.5	0.09	1.9	1	-	-	-	-
	2	1350	-0.01	3.5	0.11	3.1	1	-	-	-	-
	3	750	0.94	3.6	0.08	1.1	0.845	233	971	680	476
	4	830	2.69	5.8	0.12	1.9	0.85	297	1182	837	593
B6T1	1	1303	-0.17	2.2	0.05	1.3	1	-	-	-	-
	2	2794	-0.06	5.2	0.07	3.9	1	-	-	-	-
	3	2277	0.10	5.8	0.09	3.9	0.915	1219	2667	2193	1803
	4	2847	0.33	10.0	0.10	5.6	1	-	-	-	-
B7T1	1	190	-0.39	0.6	0.10	0.4	1	-	-	-	-
	2	712	-0.14	1.6	0.05	0.7	0.835	190	868	594	406
	3	960	0.13	2.9	0.09	1.7	0.94	638	1109	966	841
	4	1335	0.78	6.6	0.11	2.9	0.94	890	1547	1347	1173
B8T1	1	20	-1.69	0.3	0.19	0.08	-	-	-	-	-
Arm	2	39	-1.05	0.3	0.15	0.12	-	-	-	-	-
Pair	3	54	-0.50	0.4	0.18	0.2	-	-	-	-	-
3 & 6	4	76	0.05	0.6	0.13	0.2	-	-	-	-	-
B9T1	1	314	-0.05	0.9	0.06	0.4	1	-	-	-	-
	2	606	0.31	2.0	0.10	1.2	0.94	394	685	596	519
	3	570	0.97	3.2	0.18	2.1	0.85	209	832	589	417
B10T1	1	599	-0.08	1.3	0.05	0.6	1	-	-	-	-
	2	800	0.13	2.3	0.07	1.1	0.95	530	840	749	667
	3	697	0.62	3.5	0.15	2.1	0.855	274	1042	746	534
B11T1	1	576	-0.16	1.3	0.04	0.5	1	-	-	-	-
	2	573	0.11	1.9	0.07	0.8	0.955	449	680	613	552
	3	489	0.49	2.4	0.18	1.7	0.855	195	741	531	380
	4	585	1.11	3.6	0.17	1.9	0.82	178	934	617	408
B12T1	1	220	-0.23	0.7	0.08	0.3	1	-	-	-	-
	2	561	-0.02	1.6	0.11	1.2	1	-	-	-	-
	3	771	0.20	3.0	0.14	2.1	0.985	761	874	844	815
	4	851	0.37	3.9	0.18	3.0	0.93	544	1037	882	751
B13T1	1	17	-1.08	0.1	0.10	0.03	1	-	-	-	-
	2	38	-0.71	0.2	0.15	0.12	1	-	-	-	-
	3	270	0	1.0	0.11	0.6	1	-	-	-	-
	4	369	0.25	1.5	0.13	0.9	0.88	164	495	376	285
B14T1	1	97	-0.58	0.6	0.17	0.3	1	-	-	-	-
	2	186	0.07	1.3	0.16	0.6	1	-	-	-	-
	3	254	0.88	2.4	0.21	1.0	0.875	121	383	287	215
	4	305	2.25	3.7	0.37	2.2	0.885	160	461	354	272

Notes on Table 3

1. The table gives a comprehensive breakdown of the shear modulus data for this contract. The linear elastic columns give the slope of the chord bisecting the cycle. Also quoted is the pressure and strain amplitude of the cycle, and the pressure and strain co-ordinate of the centre of the cycle. Strain here is cavity strain.

2. ε_c Cavity strain

3. p_c Total pressure at the cavity wall.

4. The non-linear elastic interpretation uses a power law to approximate the degradation of stiffness with strain. The multiplier and exponent of a power law are obtained from the intercept and slope of reloading data plotted in log-log space.

5. β The slope of a log-log plot of reloading data, where 1 is linear elasticity.

6. α The shear stress constant.

7. γ Plane shear strain, being approximated by $2\varepsilon_c$

8. $\gamma=10^{-4}$ This column and the next two quote shear modulus at three magnitudes of shear strain. The equation is $G_s = \alpha\gamma^{\beta-1}$, where G_s is secant shear modulus. Note for the sake of completeness that tangential shear modulus G_t is given by $\alpha\beta\gamma^{\beta-1}$

TEST RECORD SHEET - HIGH PRESSURE DILATOMETER

SITE	Date	Day	Borehole	Test No	Depth
LERWICK	11-4-03	FRI	5	1	3-3

Material SANDSTONE

Weather	Water Table	Time Now	Drilling End	Orientation	CHL
OK	SEA LEVEL			—	✓

Drilling	Pocket

Diameter	Distance	Rate	Core Description	Length

Wet/Dry	Rig	Driller	Core Quality	Size
WET	SKATE 2)			

Pres/Incrmnt	Wait Time	Creep Time	Cycle Time	Disc No.	Operator	Engineer
			10 sec	1		

ZERO READINGS: SCOTTY Machine Diameter 95 mm

Arm 1	Arm 2	Arm 3	Arm 4	Arm 5	Arm 6	T/Press.	Battery
A 5	B 6	T 1				A: B:	

Calibrations:

Strain Arm Calibration date:	20-03-03	Test No:
Total Pressure Cell Calibration date:	"	Test No:
Membrane Stiffness Calibration date:	24-03-03	Test No: C499T99
Membrane Compression Calibration date:	"	Test No: "
New Membrane fitted date:	20-03-03	

Test Comments:

Time	Line No.	Start Test at: 04:57
04:40	0	START LOWERING
04:57	100	START PUMPING
	148	LOOP (1)
	~180	PRESSURE LOSS ?
	192	LOOP (2)
	233	LOOP (3) EXPANDING CAVITY
	280	LOOP (4)
	332	BURST !

Test Ends at 05:37

Max. Pressure reached: 11 MPa

General Comments:

COMPLETELY DIFFERENT AFTER LOOP (2) - MUCH LESS STIFF.

CAMBRIDGE INSITU, Little Eversden, Cambridge, England CB3 7HE
Telephone: 01223 262 361 . Fax:- 01223 263 947

HIGH PRESSURE DILATOMETER RESULTS SUMMARY SHEET

Site:- Bressay Bridge Test :- B5T1 Test Date :- 11th April 2003
Material :- Sandstone Depth (m) :- 3.3 Water depth (m) :- -

Analysis of Insitu Lateral Stress (Po) :-

		Arm Av.
Marsland and Randolph (Iterative Analysis)	kPa	4994
Best Estimate of Po	kPa	5000
Assessed diameter of borehole	mm	99.5

Analysis of Undrained Shear Strength (Cu) :-

Gibson and Anderson	kPa	4858
Failure pressure (Pf)	kPa	5503
Limit Pressure (P_L)	MPa	24

Strength of Sands Analysis (Hughes, Wroth & Windle)

Friction angle at const. vol.	deg	33	(assumed)
Angle of Friction	deg	42	
Angle of Dilation	deg	12	

Analysis of Shear Modulus (G) :-

Initial Modulus (Gi)	MPa	685

Linear Analysis of Reload Loops (Gr) :-

Loop no.	Value (MPa)	Co-ordinate Strain %	Co-ordinate Pressure kPa	Amplitude Strain %	Amplitude Pressure kPa
1	1148	-0.12	2486	0.085	1944
2	1350	-0.01	3475	0.114	3091
3	750	0.94	3554	0.075	1121
4	830	2.69	5844	0.12	1940

Non-linear Analysis of Reloading data :-

Loop no.	Linearity exponent (β)	Radial Stress Coeff. (MPa)	Shear Stress Coeff. (MPa)
3	0.845	276	233
4	0.85	349	297

Test Analysed By :- PGH
Date :- 27th May 2003

SCREEN DUMP Test: B5T1 Date: 11/04/03 Depth: 3.30m
HPD95 Pressuremeter tests Bressay Bridge Site Investigation
Cambridge Insitu for Seacore April 2003

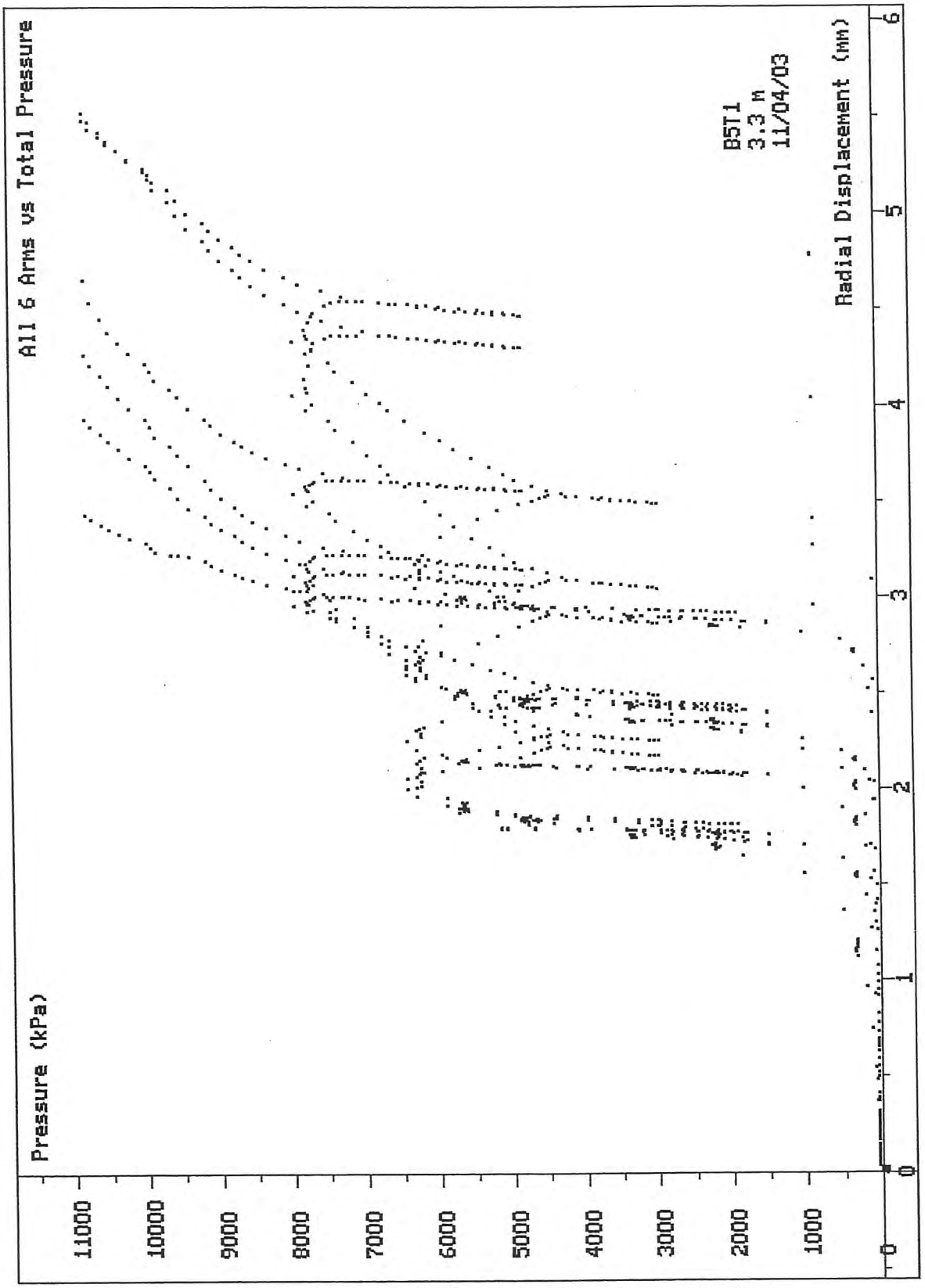

SCREEN DUMP Test: B5T1 Date: 11/04/03 Depth: 3.30m
HPD95 Pressuremeter tests Bressay Bridge Site Investigation
Cambridge Insitu for Seacore April 2003

HPD95 Pressuremeter tests
Cambridge Insitu for Seacore

Bressay Bridge Site Investigation
April 2003

Total Pressure/Log(a) (ΔV / V) Arm Ave
Test B5T1
Date 11 Apr 03
Depth 3.3 m
Cu 4858 kPa
Pl 24 MPa
Ir 27
G(min) 131 MPa
11
4
-8
-1
Total Pressure (MPa)
Ln 1-(1/(1+E)²)

Log(e) Effective Strass/Log(e) Strain Arm Ave
Gradient 0.48
Øcv 33 °
Ø' 42 °
Dilation 12 °
Test B5T1
Date 11 Apr 03
Depth 3.3 m
Log (e) Effective Radial Stress
Log (e) Cavity Strain
9.3
8.6
-5
-4

HPD95 Pressuremeter tests
Cambridge Insitu for Seacore

Bressay Bridge Site Investigation
April 2003

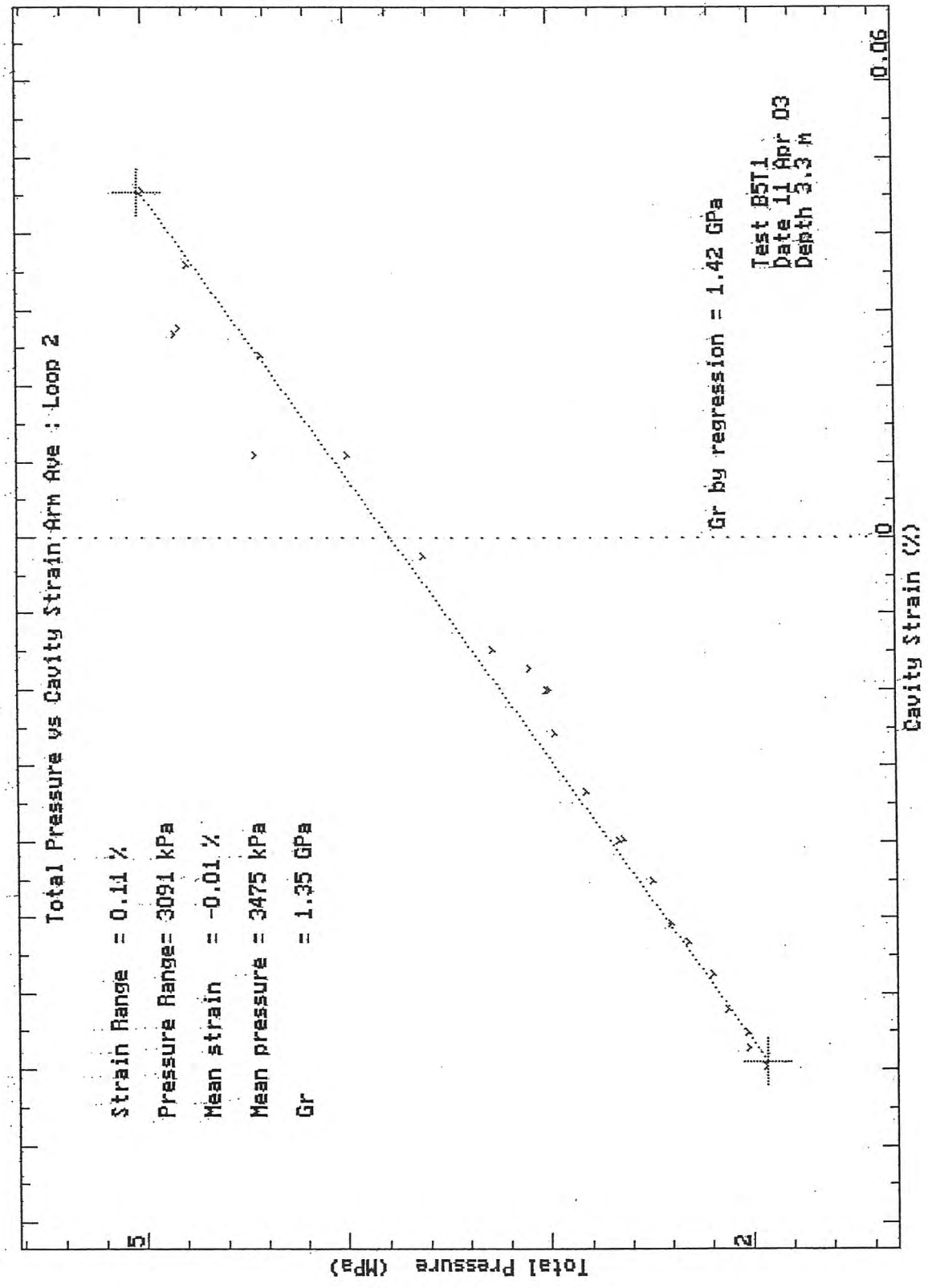
Total Pressure vs Cavity Strain Arm Ave : Loop 2
Strain Range = 0.11 %
Pressure Range= 3091 kPa
Mean strain = -0.01 %
Mean pressure = 3475 kPa
Gr = 1.35 GPa
Gr by regression = 1.42 GPa
Test BST1
Date 11 Apr 03
Depth 3.3 m
Total Pressure (MPa)
Cavity Strain (%)
5
2
0
0.06

Total Pressure vs Cavity Strain Arm Ave : Loop 3
Strain Range = 0.08 %
Pressure Range= 1121 kPa
Mean strain = 0.94 %
Mean pressure = 3554 kPa
Gr = 750 MPa
Gr by regression = 654 MPa
Test B5T1
Date 11 Apr 03
Depth 3.3 m
Total Pressure (MPa)
Cavity Strain (%)
4
3
0.9
1

Ln(Radial Stress) vs Ln(Shear Strain) Arm Ave : Loop 3
Elastic exponent = 0,844
Radial stress constant = 276,310 MPa
Shear stress constant = 233,206 MPa
Test BST1
Date 11 Apr 03
Depth 3.3 m
Ln Radial Stress
Ln Shear Strain
7
4
-10
-6

HPD95 Pressuremeter tests
Cambridge Insitu for Seacore

Bressay Bridge Site Investigation
April 2003

Ln(Radial Stress) vs Ln(Shear Strain) Arm Ave : Loop 4
Elastic exponent = 0.850
Radial stress constant = 349.343 MPa
Shear stress constant = 296.969 MPa
Test BST1
Date 11 Apr 03
Depth 3.3 m
Ln Radial Stress
Ln Shear Strain
8
5
-9
-6

TEST RECORD SHEET - HIGH PRESSURE DILATOMETER

Site	Date	Day	Borehole	Test No	Depth
LERWICK	10.4.03	THURS	6	11	3.5

Material: SANDSTONE

Weather	Water Table	Time Now	Drilling End	Orientation	CHL
FINE & DRY	SEA LEVEL	16.50	18.10	NK	✓

Drilling	Pocket

Diameter	Distance	Rate	Core Description	Length

Wet/Dry	Rig	Driller	Core Quality	Size
WET	STATE II D		GOOD	

Pres/Incrmnt	Wait Time	Creep Time	Cycle Time	Disc No.	Operator	Engineer
			10SEC	DAY-1		

ZERO READINGS: SCOTTY — Machine Diameter 95 mm

Arm 1	Arm 2	Arm 3	Arm 4	Arm 5	Arm 6	T/Press.	Battery
-21308	-1.9972	-18327	-1.8308	-19281	-1.9835	A: ~~-.0706~~ B: .1128	12.42

Calibrations:

Strain Arm Calibration date: 20-03-03 Test No:

Total Pressure Cell Calibration date: " Test No:

Membrane Stiffness Calibration date: 24-03-03 Test No: C499 T99

Membrane Compression Calibration date: " Test No: "

New Membrane fitted date: 20-03-03

Test Comments:

Time	Line No.	Start Test at: 18.13
		1ST LOOP @ L 70 — 2.9 mPa APP.
		LOOP 2 @ L 125 — 7.1 mPa
		LOOP 3 @ L 155
		LOOP 4 @ L 205 — 13 mPa
		TO UNLOAD L 270

Test Ends at:

Max. Pressure reached: 20.6 mPa

General Comments:

VERY STIFF

CAMBRIDGE INSITU, Little Eversden, Cambridge, England CB3 7HE
Telephone: 01223 262 361 Fax:- 01223 263 947

HIGH PRESSURE DILATOMETER RESULTS SUMMARY SHEET

Site:- Bressay Bridge Test :- B6T1 Test Date :- 10th April 2003
Material :- Sandstone Depth (m) :- 3.5 Water depth (m) :- -

Analysis of Insitu Lateral Stress (Po) :-

		Arm Av.
Interpolation from Initial Modulus	kPa	4712
Best Estimate of Po	kPa	8000

Assessed diameter of borehole mm 100.1

Analysis of Undrained Shear Strength (Cu) :-

Gibson and Anderson	MPa	12
Failure pressure (Pf)	MPa	~8
Limit Pressure (P_L)	MPa	73

Strength of Sands Analysis (Hughes, Wroth & Windle)

Friction angle at const. vol.	deg	33	(assumed)	At large strain
Angle of Friction	deg	44		56
Angle of Dilation	deg	15		31

Analysis of Shear Modulus (G) :-

Initial Modulus (Gi) MPa 2045

Linear Analysis of Reload Loops (Gr) :-

Loop	Value	Co-ordinate		Amplitude	
no.	(MPa)	Strain %	Pressure kPa	Strain %	Pressure kPa
1	1303	-0.17	2248	0.049	1266
2	2794	-0.06	5200	0.069	3875
3	2277	0.10	5751	0.087	3943
4	2847	0.33	10008	0.098	5586

Non-linear Analysis of Reloading data :-

Loop	Linearity exponent	Radial Stress Coeff.	Shear Stress Coeff.
no.	(β)	(MPa)	(MPa)
3	0.915	1331	1219

Test Analysed By :- PGH
Date :- 27th May 2003

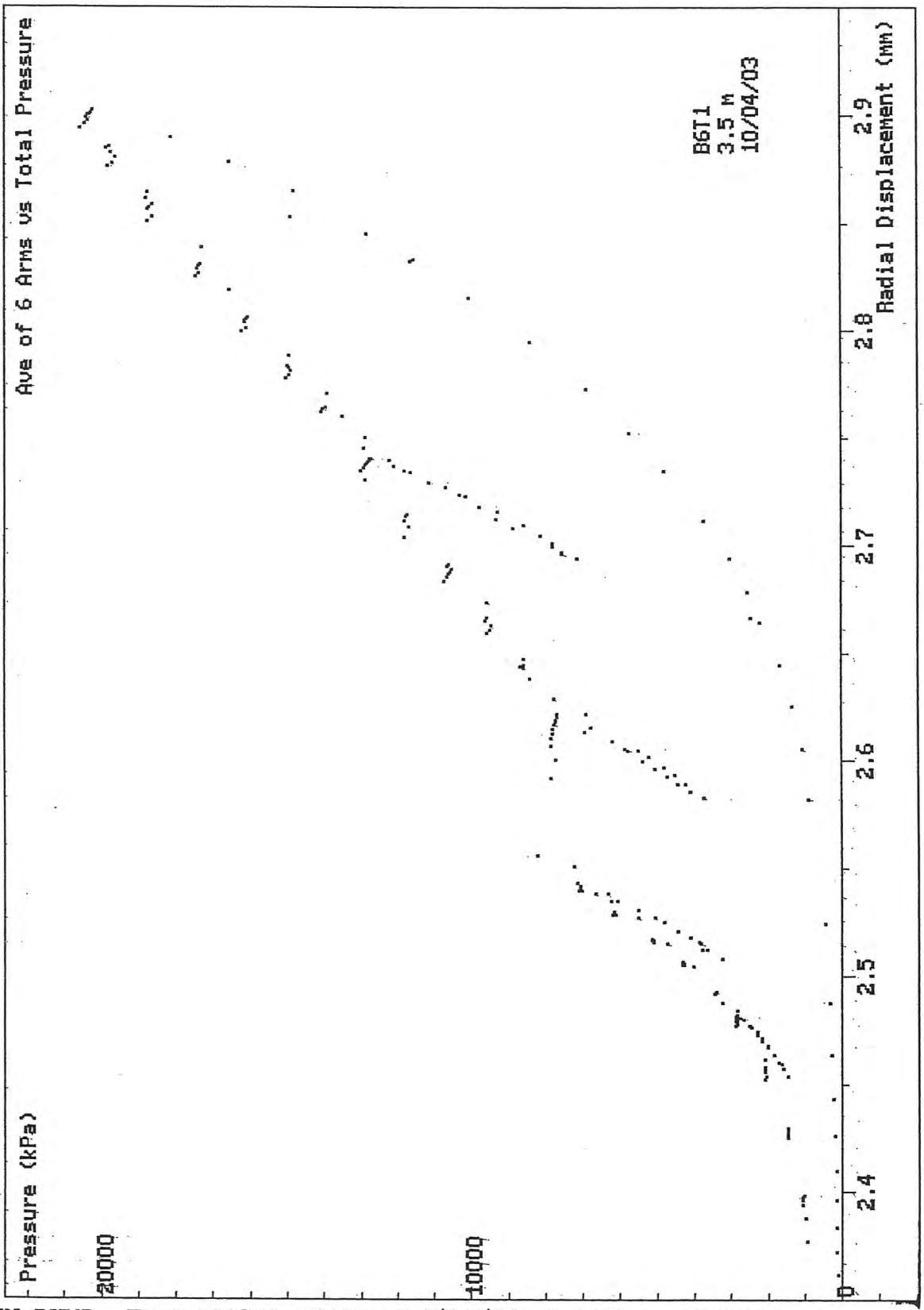

SCREEN DUMP Test: B6T1 Date: 10/04/03 Depth: 3.50m
HPD95 Pressuremeter tests Bressay Bridge Site Investigation
Cambridge Insitu for Seacore April 2003

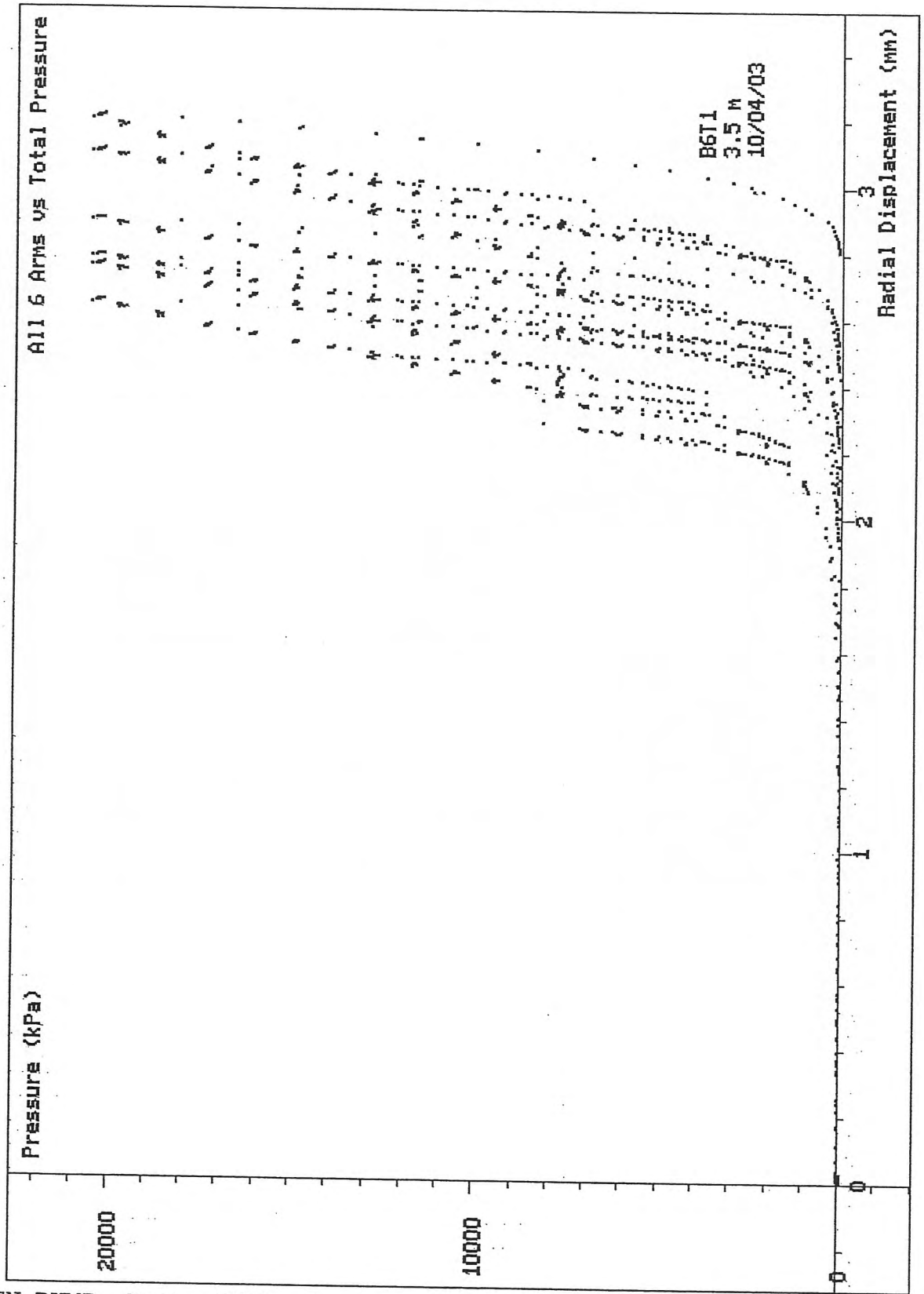

SCREEN DUMP Test: B6T1 Date: 10/04/03 Depth: 3.50m
HPD95 Pressuremeter tests Bressay Bridge Site Investigation
Cambridge Insitu for Seacore April 2003

Marsland and Randolph Pressure/Strain Arm Ave
Gi 2.04 GPa
Test B6T1
Date 10 Apr 03
Depth 3.5 m
P/Log(e) E
Pressure (MPa)
Radial displacement (mm)
0
2.4
2.49
9
Creep
0.01 mm

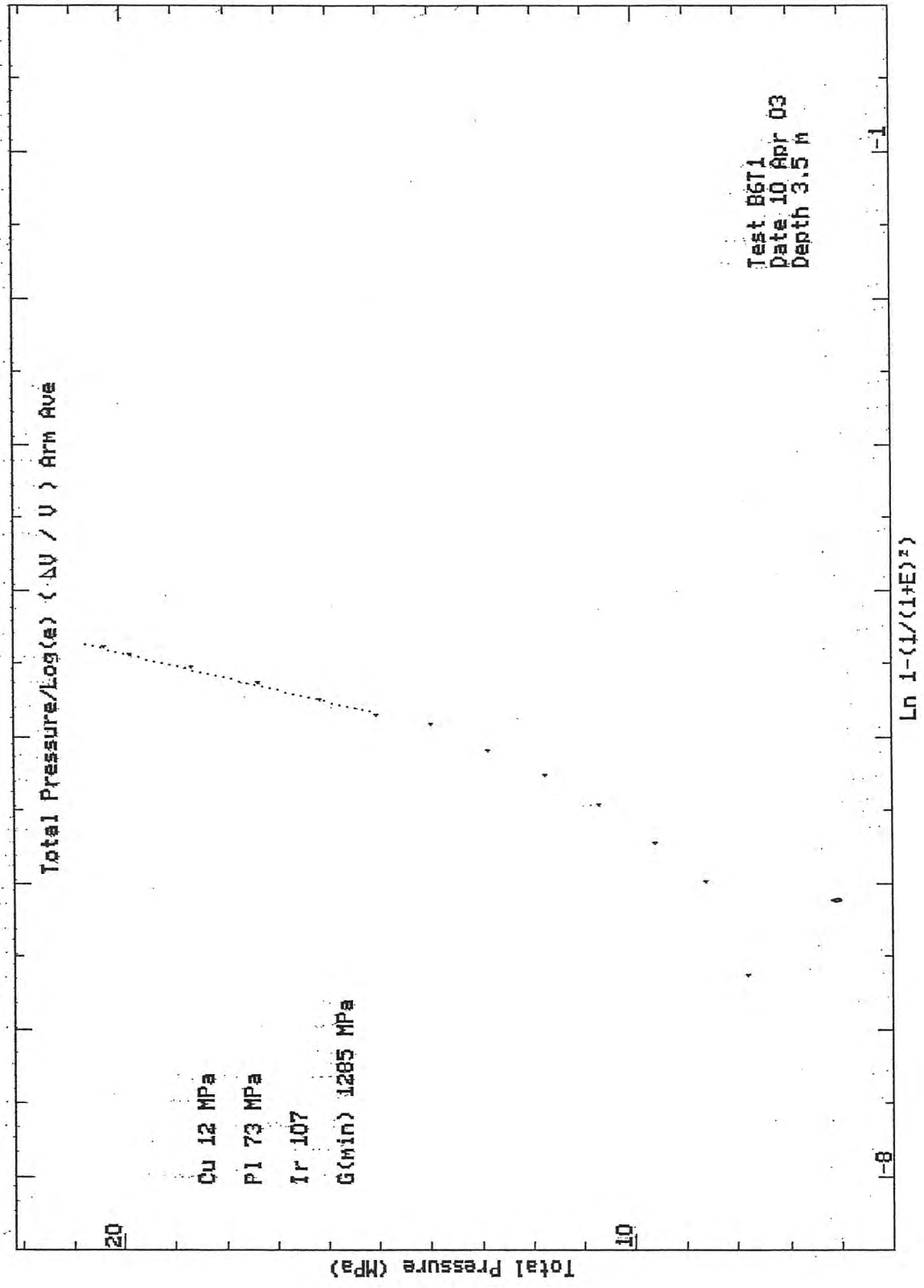
Total Pressure/Log(a) (ΔV / V) Arm Ave
Test B671
Date 10 Apr 03
Depth 3.5 m
Cu 12 MPa
Pl 73 MPa
Ir 107
G(min) 1285 MPa
20
10
Total Pressure (MPa)
-8
-1
Ln 1-(1/(1+E)²)

Log(e) Effective Stress/Log(e) Strain Arm Ave
Gradient 0.52
Øcv 33 °
ø' 44 °
Dilation 15 °
Test B6T1
Date 10 Apr 03
Depth 3.5 m
Log (e) Effective Radial Stress
Log (e) Cavity Strain
-10
-9
-7
-5

Log(e) Effective Stress/Log(e) Strain Arm Ave
Gradient 0.69
φcv 33 °
φ' 56 °
Dilation 31 °
Test B6T1
Date 10 Apr 03
Depth 3.5 m
Log (e) Effective Radial Stress
Log (e) Cavity Strain
10
9
-7
-5

Total Pressure vs Cavity Strain Arm Ave : Loop 1
Strain Range = 0.05 %
Pressure Range= 1266 kPa
Mean strain = -0.17 %
Mean pressure = 2248 kPa
Gr = 1.3 GPa
Gr by regression = 1.3 GPa
Test B6T1
Date 10 Apr 03
Depth 3.5 m
Total Pressure (MPa)
Cavity Strain (%)
3
2
-0.21
-0.14

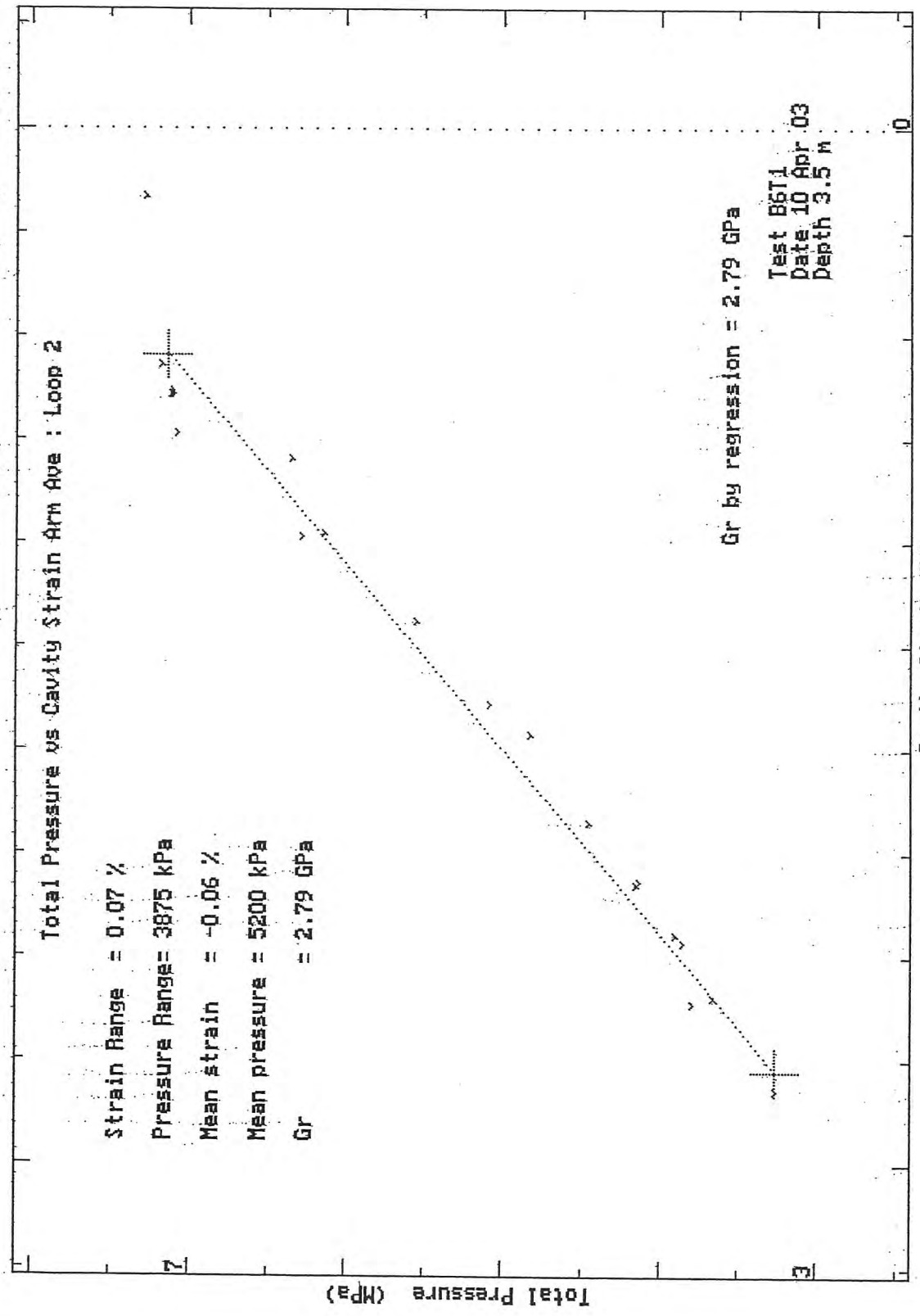

HPD95 Pressuremeter tests
Cambridge Insitu for Seacore

Bressay Bridge Site Investigation
April 2003

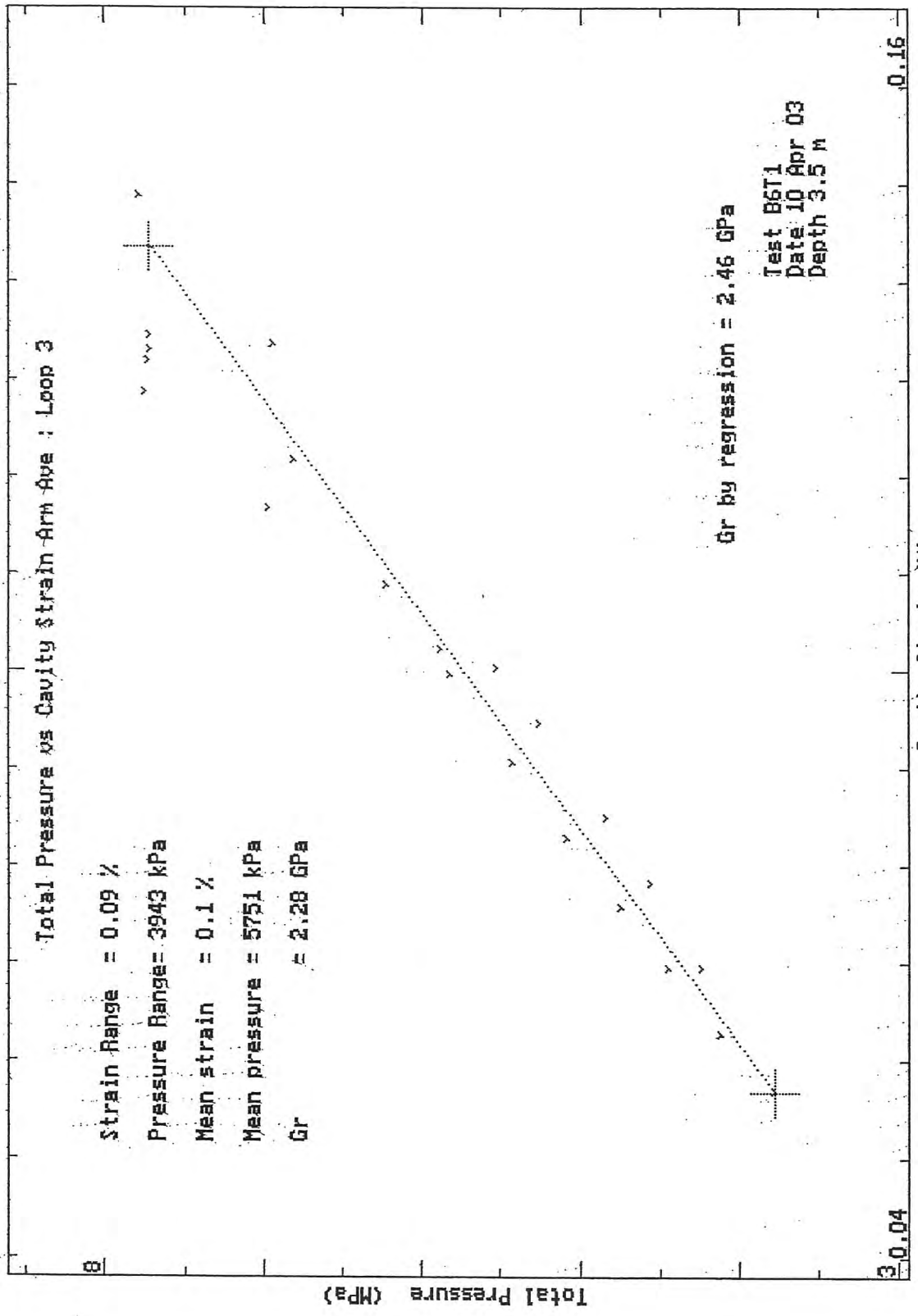
Total Pressure vs Cavity Strain Arm Ave : Loop 3
Strain Range = 0.09 %
Pressure Range= 3943 kPa
Mean strain = 0.1 %
Mean pressure = 5751 kPa
Gr = 2.28 GPa
Gr by regression = 2.46 GPa
Test B6T1
Date 10 Apr 03
Depth 3.5 m
Total Pressure (MPa)
Cavity Strain (%)
8
3
0.04
0.16

Ln(Radial Stress) vs Ln(Shear Strain) Arm Ave : Loop 3
Elastic exponent = 0.916
Radial stress constant = 1330.953 MPa
Shear stress constant = 1218.585 MPa
Test B6T1
Date 10 Apr 03
Depth 3.5 m
Ln Radial Stress
Ln Shear Strain
-8
-9
-6

Total Pressure vs Cavity Strain Arm Ave : Loop 4
Strain Range = 0.1 %
Pressure Range= 5586 kPa
Mean strain = 0.33 %
Mean pressure = 10 MPa
Gr = 2.85 GPa
Gr by regression = 2.92 GPa
Test B6T1
Date 10 Apr 03
Depth 3.5 m
Total Pressure (MPa)
Cavity Strain (%)
13
6
0.3
0.39

TEST RECORD SHEET - HIGH PRESSURE DILATOMETER

Site	Date	Day	Borehole	Test No	Depth
LERWICK	13-4-03	SUN	7	1	4·6

Material SANDSTONE

Weather	Water Table	Time Now	Drilling End	Orientation	CHL
	SEA LEVEL				✓

Drilling	Pocket

Diameter	Distance	Rate	Core Description	Length

Wet/Dry	Rig	Driller	Core Quality	Size
WET	SKATE 2			

Pres/Incrmnt	Wait Time	Creep Time	Cycle Time	Disc No.	Operator	Engineer
			10sec	2		

ZERO READINGS: TILLY Machine Diameter 95 mm

Arm 1	Arm 2	Arm 3	Arm 4	Arm 5	Arm 6	T/Press.	Battery
						A: B:	

Calibrations:

Strain Arm Calibration date:	2-10-02	Test No:
Total Pressure Cell Calibration date:	6-3-03	Test No: C999 T99
Membrane Stiffness Calibration date:	19-3-03	Test No: "
Membrane Compression Calibration date:	"	Test No: "
New Membrane fitted date:	"	

Test Comments:

Time	Line No.	Start Test at: 06:40
	24	HOLD ⇒ LOOP ① (~200kPa)
	~70	LOOP ②
	160	LOOP ③
	245	LOOP ④
	323	DOWN - OUT OF CREEP

Test Ends at 06:40

Max Pressure reached: 15 MPa

General Comments

CAMBRIDGE INSITU, Little Eversden, Cambridge, England CB3 7HE
Telephone: 01223 262 361 Fax:- 01223 263 947

HIGH PRESSURE DILATOMETER RESULTS SUMMARY SHEET

Site:- Bressay Bridge Test :- B7T1 Test Date :- 13th April 2003
Material :- Sandstone Depth (m) :- 4.6 Water depth (m) :- -

Analysis of Insitu Lateral Stress (Po) :-

		Arm Av.
Marsland and Randolph (Iterative Analysis)	kPa	2600
Interpolation from Initial Modulus	kPa	279
Best Estimate of Po	kPa	2600
Assessed diameter of borehole	mm	99.2

Analysis of Undrained Shear Strength (Cu) :-

Gibson and Anderson	kPa	7469
Failure pressure (Pf)	kPa	6106
Limit Pressure (P_L)	MPa	38

Strength of Sands Analysis (Hughes, Wroth & Windle)

Friction angle at const. vol.	deg	33	(assumed)
Angle of Friction	deg	47	
Angle of Dilation	deg	18	

Analysis of Shear Modulus (G) :-

Initial Modulus (Gi)	MPa	367

Linear Analysis of Reload Loops (Gr) :-

Loop	Value	Co-ordinate		Amplitude	
no.	(MPa)	Strain %	Pressure kPa	Strain %	Pressure kPa
1	190	-0.39	561	0.104	398
2	712	-0.14	1555	0.049	700
3	960	0.13	2932	0.087	1663
4	1335	0.78	6604	0.108	2863

Non-linear Analysis of Reloading data :-

Loop	Linearity exponent	Radial Stress Coeff.	Shear Stress Coeff.
no.	(β)	(MPa)	(MPa)
2	0.835	228	190
3	0.94	678	638
4	0.94	946	890

Test Analysed By :- PGH
Date :- 27th May 2003

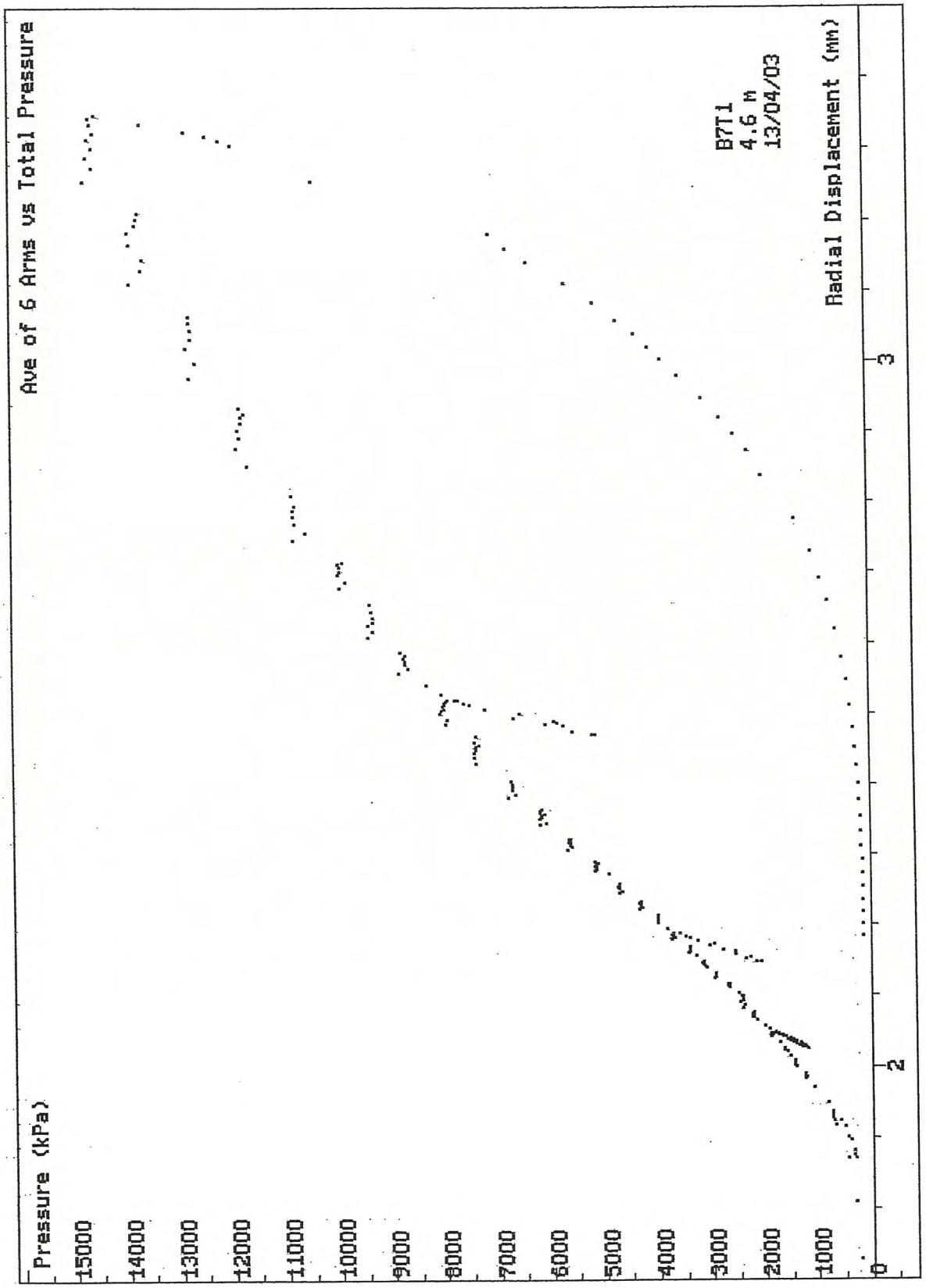

SCREEN DUMP Test: B7T1 Date: 13/04/03 Depth: 4.60m
HPD95 Pressuremeter tests Bressay Bridge Site Investigation
Cambridge Insitu for Seacore April 2003

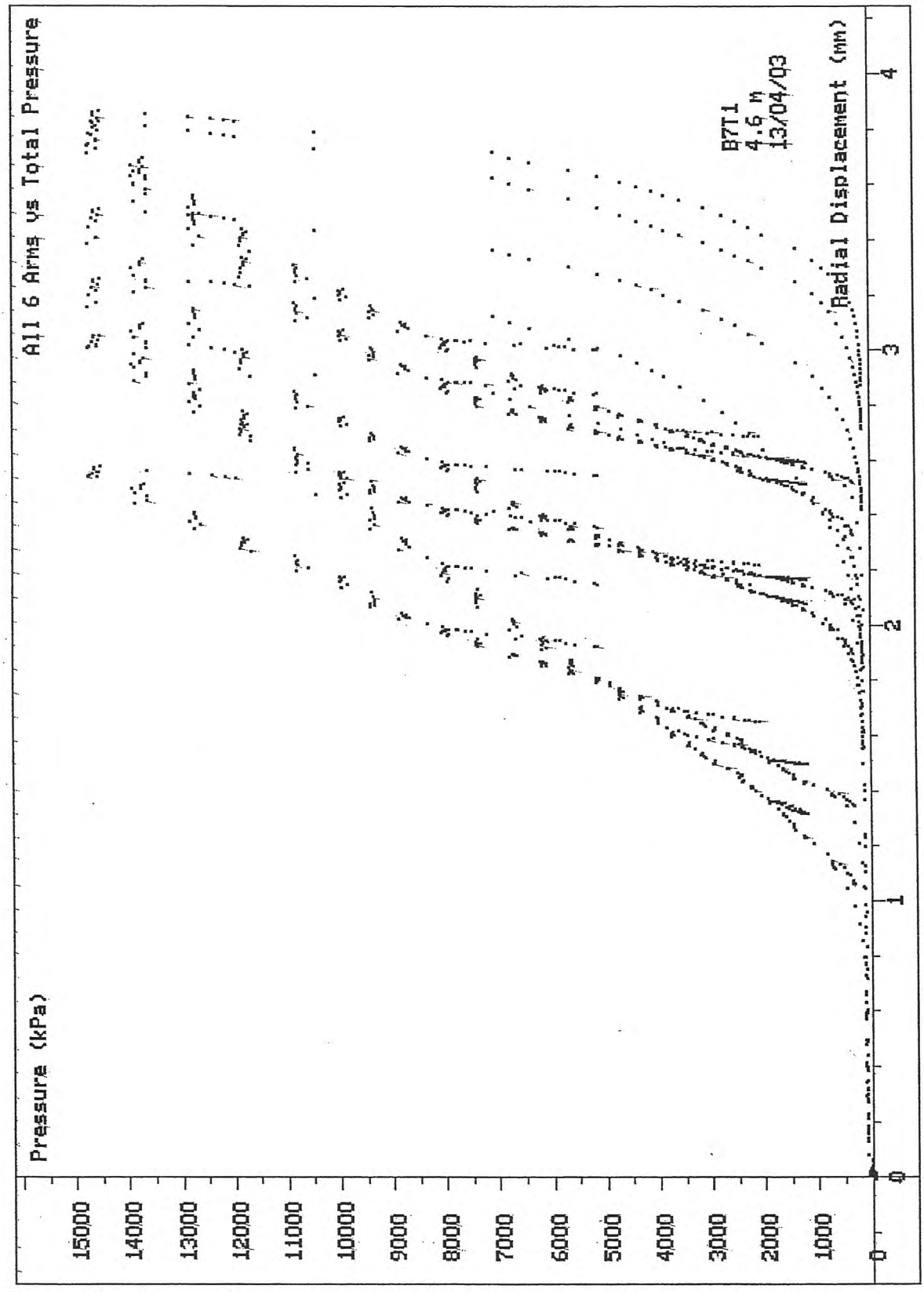

SCREEN DUMP Test: B7T1 Date: 13/04/03 Depth: 4.60m
HPD95 Pressuremeter tests Bressay Bridge Site Investigation
Cambridge Insitu for Seacore April 2003

Marsland and Randolph Pressure/Strain Arm Ave
Gi 367 MPa
Pf 6106 kPa
Po 2600 kPa
Tf 3503 kPa
Po+Tf
Pf
Po
P/Log(e) E
Test B7T1
Date 13 Apr 03
Depth 4.6 m
Pressure (MPa)
Radial displacement (mm)
0.7
2.3
6
Creep
0.04 mm

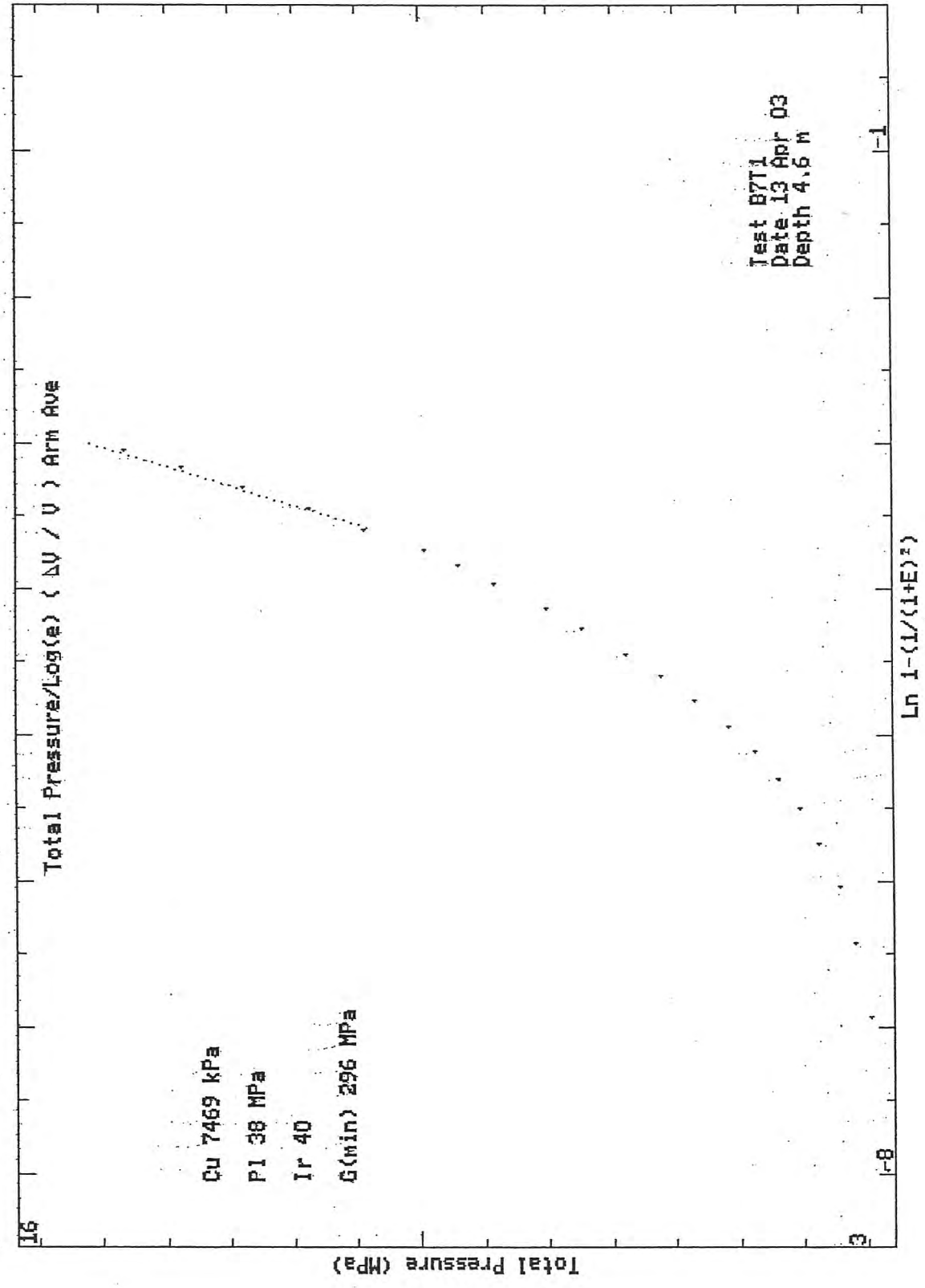
Total Pressure/Log(e) (ΔV / V) Arm Ave
Test B7T1
Date 13 Apr 03
Depth 4.6 m
Cu 7469 kPa
Pl 38 MPa
Ir 40
G(min) 296 MPa
16
3
-8
-1
Total Pressure (MPa)
Ln 1-(1/(1+E)²)

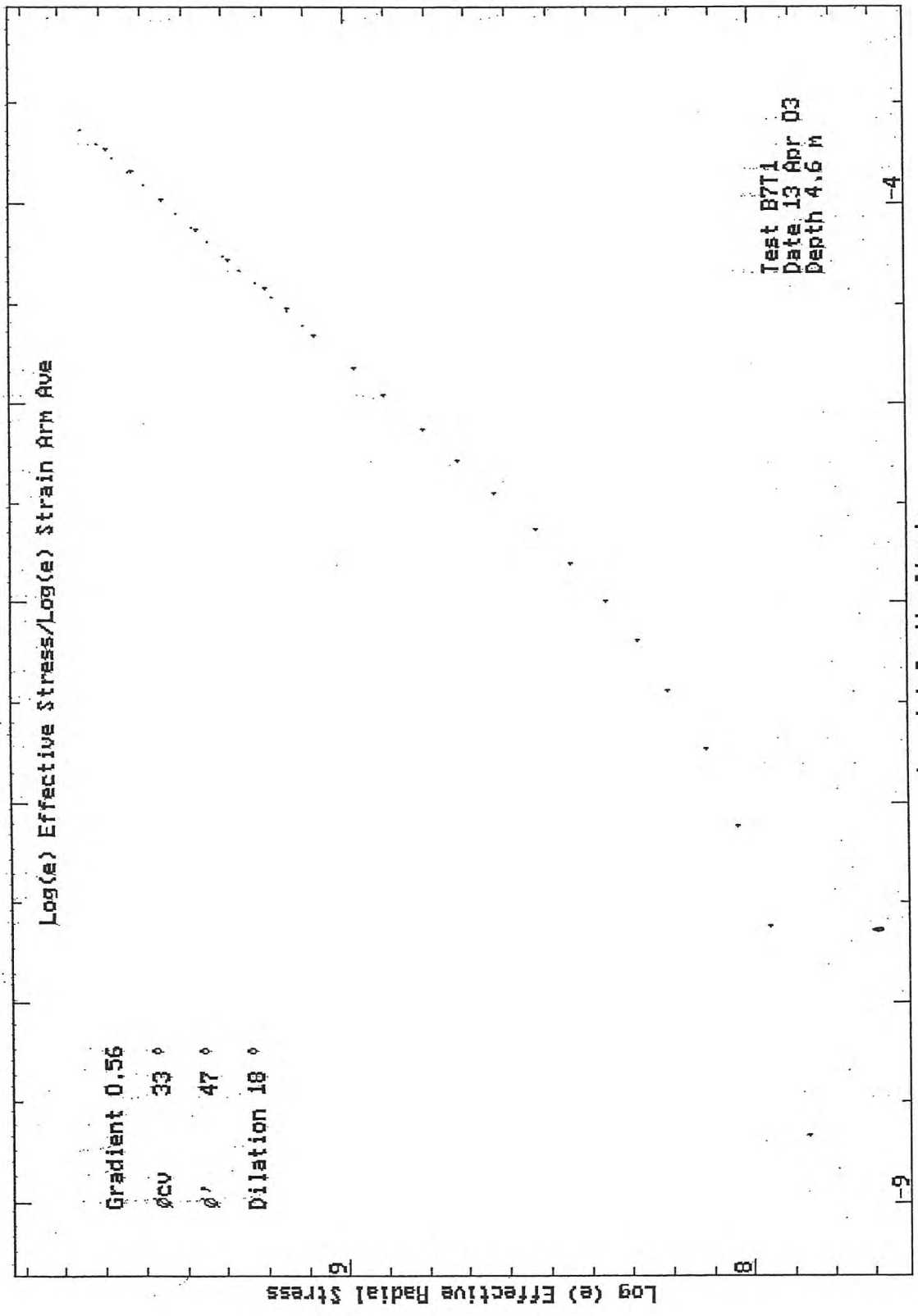
Log(e) Effective Stress/Log(e) Strain Arm Ave
Gradient 0.56
φcv 33 °
φ' 47 °
Dilation 18 °
Test B7T1
Date 13 Apr 03
Depth 4.6 m
Log (e) Effective Radial Stress
Log (e) Cavity Strain
-9
-8
-6
-4

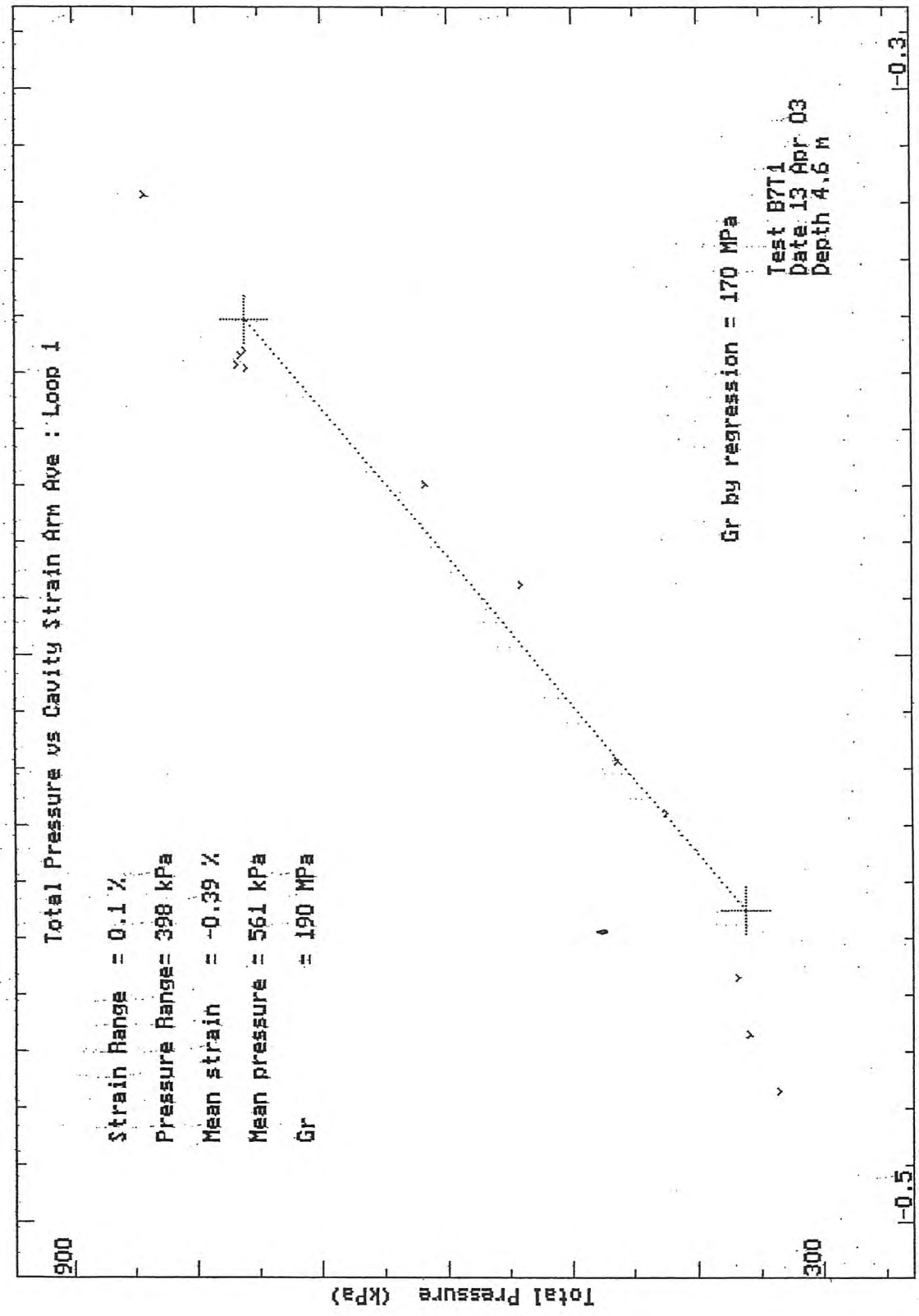
Total Pressure vs Cavity Strain Arm Ave : Loop 1
Strain Range = 0.1 %
Pressure Range= 398 kPa
Mean strain = -0.39 %
Mean pressure = 561 kPa
Gr = 190 MPa
Gr by regression = 170 MPa
Test B7T1
Date 13 Apr 03
Depth 4.6 m
900
300
-0.5
-0.3
Total Pressure (kPa)
Cavity Strain (%)

Total Pressure vs Cavity Strain Arm Ave : Loop 2
Strain Range = 0.05 %
Pressure Range= 700 kPa
Mean strain = -0.14 %
Mean pressure = 1555 kPa
Gr = 712 MPa
Gr by regression = 712 MPa
Test B7T1
Date 13 Apr 03
Depth 4.6 m
Total Pressure (MPa)
Cavity Strain (%)
1.1
-0.17
-0.11
2

Ln(Radial Stress) vs Ln(Shear Strain) Arm Ave : Loop 2
Elastic exponent = 0.835
Radial stress constant = 227.984 MPa
Shear stress constant = 190.459 MPa
Test B771
Date 13 Apr 03
Depth 4.6 m
Ln Radial Stress
Ln Shear Strain
-6
-4
-10
-7

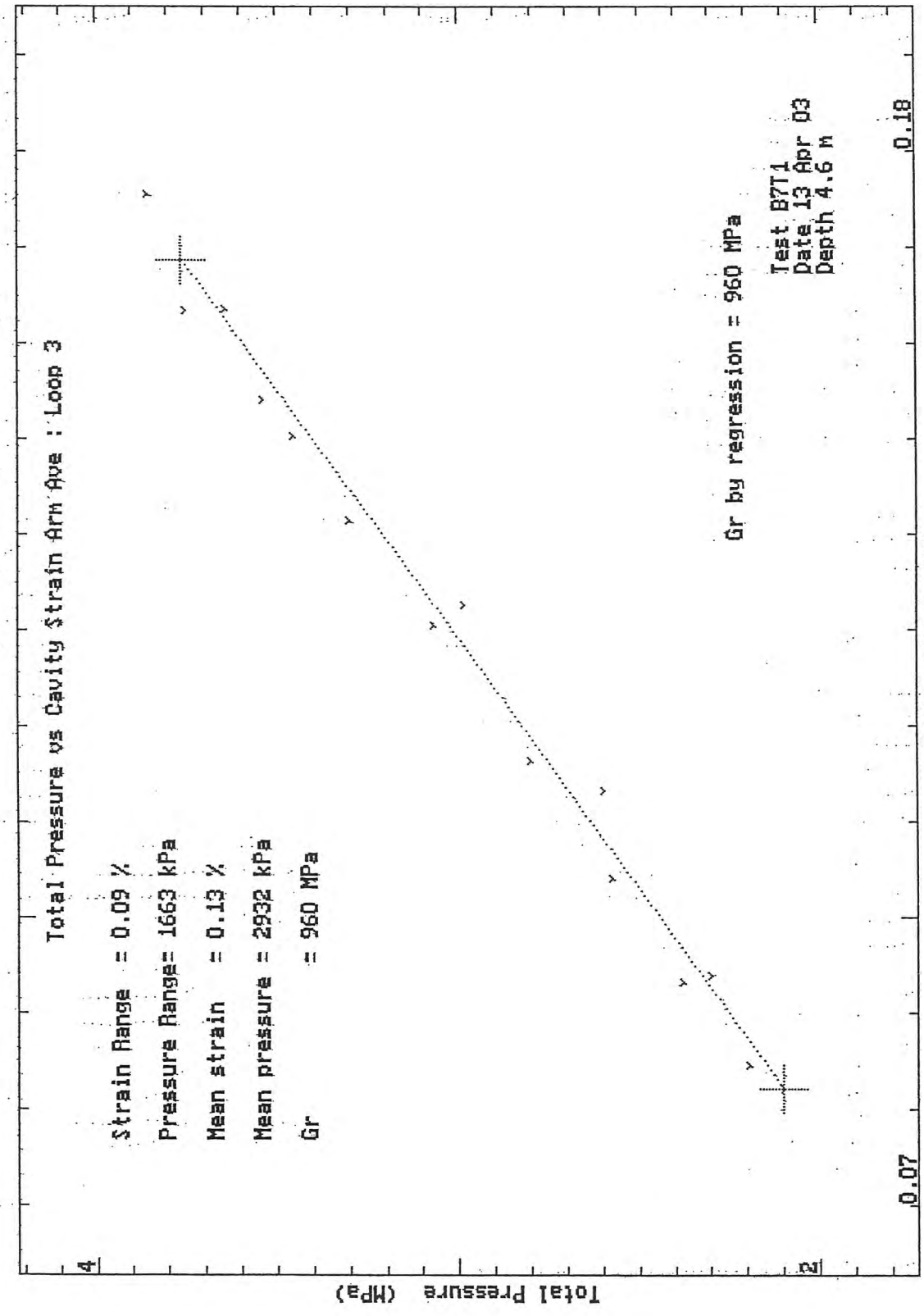
Total Pressure vs Cavity Strain Arm Ave : Loop 3
Strain Range = 0.09 %
Pressure Range= 1663 kPa
Mean strain = 0.13 %
Mean pressure = 2932 kPa
Gr = 960 MPa
Gr by regression = 960 MPa
Test B7T1
Date 13 Apr 03
Depth 4.6 m
Total Pressure (MPa)
Cavity Strain (%)
0.07
0.18
4
2

Ln(Radial Stress) vs Ln(Shear Strain) Arm Ave : Loop 3
Elastic exponent = 0,941
Radial stress constant = 678,228 MPa
Shear stress constant = 638,385 MPa
Test B7T1
Date 13 Apr 03
Depth 4,6 m
Ln Radial Stress
Ln Shear Strain
-5
-6
-7
-9

Total Pressure vs Cavity Strain Arm Ave : Loop 4
Strain Range = 0.11 %
Pressure Range= 2863 kPa
Mean strain = 0.78 %
Mean pressure = 6604 kPa
Gr = 1.33 GPa
Gr by regression = 1.38 GPa
Test B7T1
Date 13 Apr 03
Depth 4.6 m
Total Pressure (MPa)
Cavity Strain (%)
8
5
0.8

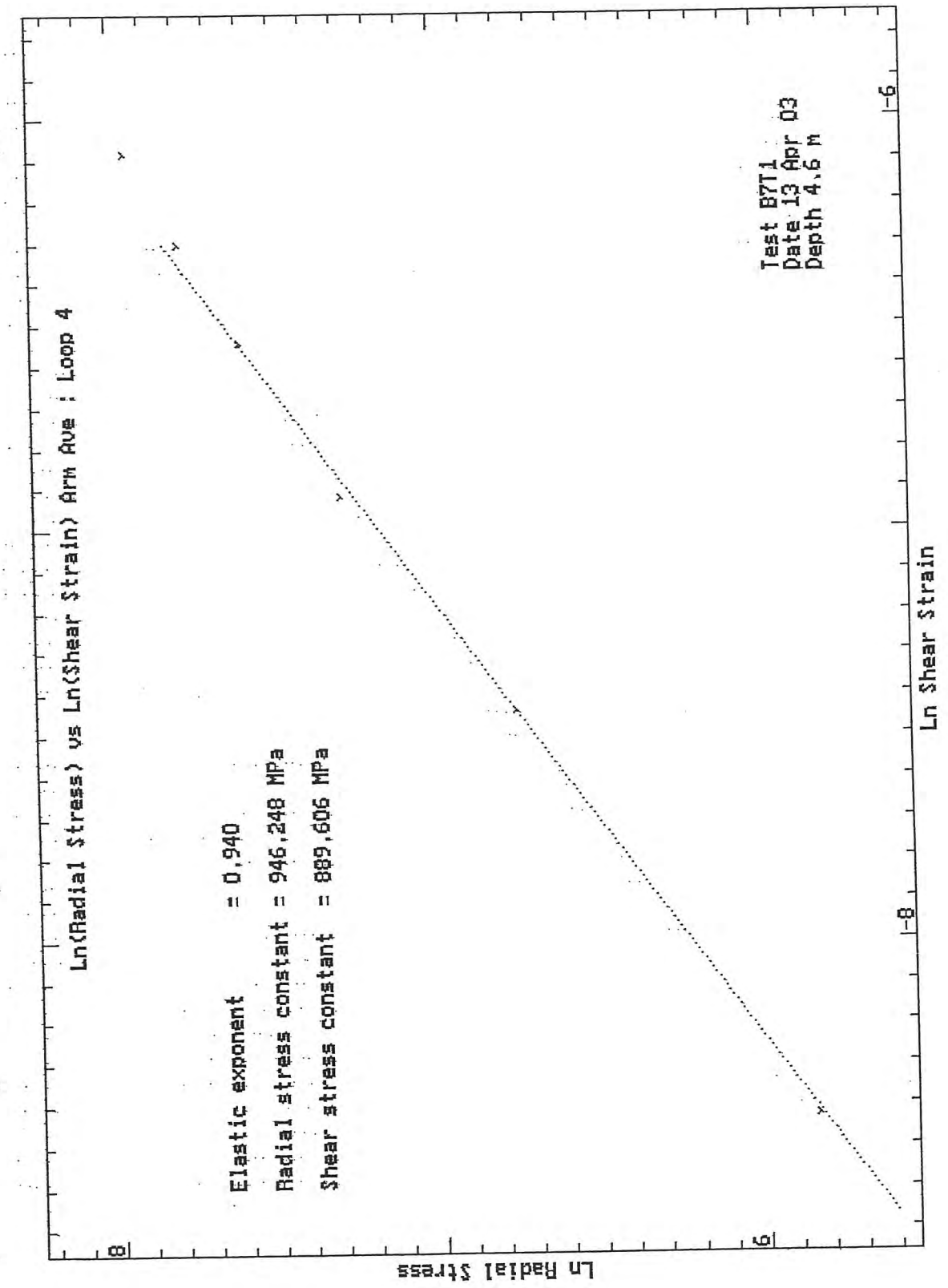
Ln(Radial Stress) vs Ln(Shear Strain) Arm Ave : Loop 4
Test B7T1
Date 13 Apr 03
Depth 4,6 m
Elastic exponent = 0,940
Radial stress constant = 946,248 MPa
Shear stress constant = 889,606 MPa
Ln Radial Stress
Ln Shear Strain
-8
-6
9
8

TEST RECORD SHEET - HIGH PRESSURE DILATOMETER

Site	Date	Day	Borehole	Test No	Depth
LOANWICK	12-4-03	SAT	B	BST 1	7.5m

Material: SANDSTONE

Weather	Water Table	Time Now	Drilling End	Orientation	CHL
OK	SEA LEVEL				✓

Drilling	Pocket

Diameter	Distance	Rate	Core Description	Length

Wet/Dry	Rig	Driller	Core Quality	Size
WET	SKATO 2)			

Pres/Incrmnt	Wait Time	Creep Time	Cycle Time	Disc No.	Operator	Engineer
			10sec	2		

ZERO READINGS: TICCY — Machine Diameter 95 mm

Arm 1	Arm 2	Arm 3	Arm 4	Arm 5	Arm 6	T/Press.	Battery
-1.4068	-1.6427	-1.5459	-1.3679	-1.4837	-1.5396	A: 0.0080 B: 0.0874	12.2

Calibrations:

Strain Arm Calibration date:	2-10-02	Test No:
Total Pressure Cell Calibration date:	6-3-03	Test No:
Membrane Stiffness Calibration date:	19-3-03	Test No: C999 T99
Membrane Compression Calibration date:	"	Test No: "
New Membrane fitted date:	—	

Test Comments:

Time	Line No.	Start Test at: 03:45
03:45	155	START — STUMBLED RECORDING !
03:58	18	RE-START
	46	HOLD ⇒ LOOP ① ~300 kPa
		ARM ① ~ 14 mm
	82	LOOP ②
	121	LOOP ③ ARM ① ⇒ 20 mm
	157	LOOP ④
	184	UNLOAD

Test Ends at: 04:40

Max Pressure reached: 0.8 MPa

General Comments

ARM ① INTO CAVITY - VERY LOW PRESSURE. ARM PAIR ③ & ⑥ GIVE STIFFEST RESPONSE.

CAMBRIDGE INSITU, Little Eversden, Cambridge, England CB3 7HE
Telephone: 01223 262 361 Fax:- 01223 263 947

HIGH PRESSURE DILATOMETER RESULTS SUMMARY SHEET

Site:- Bressay Bridge Test :- B8T1 Test Date :- 12th April 2003
Material :- Sandstone Depth (m) :- 7.5 Water depth (m) :- -

Analysis of Insitu Lateral Stress (Po) :-

		Arm Pair 3 & 6
Working value of Po	kPa	700
Assessed diameter of borehole	mm	100.9

Analysis of Shear Modulus (G) :-

Initial Modulus (Gi)	MPa	16

Linear Analysis of Reload Loops (Gr) :-

Loop	Value	Co-ordinate		Amplitude	
no.	(MPa)	Strain %	Pressure kPa	Strain %	Pressure kPa
1	19.6	-1.69	268	0.191	76
2	38.8	-1.05	344	0.151	118
3	54.0	-0.50	443	0.181	196
4	75.5	0.05	574	0.132	199

Arm 1 expanding into a cavity, with Arm 2 also affected.
Only Arm pair 3 & 6 is worth analysing, but it is still not very useful as the maximum pressure is so low. There is not enough to do any analysis of the expansion curve.

Test Analysed By :- PGH
Date :- 22nd April 2003

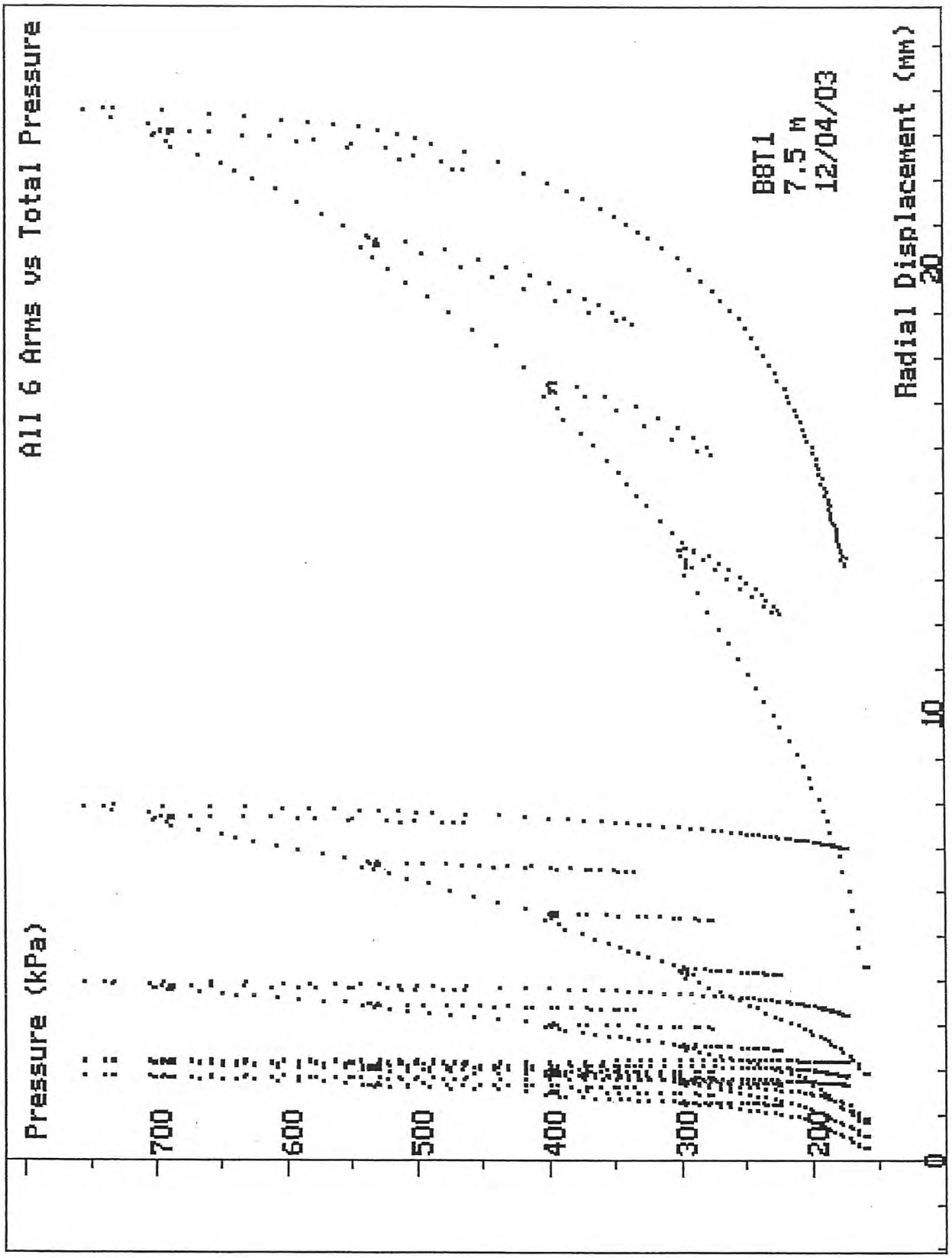

SCREEN DUMP Test: B8T1 Date: 12/04/03 Depth: 7.50m
HPD95 Pressuremeter tests Bressay Bridge Site Investigation
Cambridge Insitu for Seacore April 2003

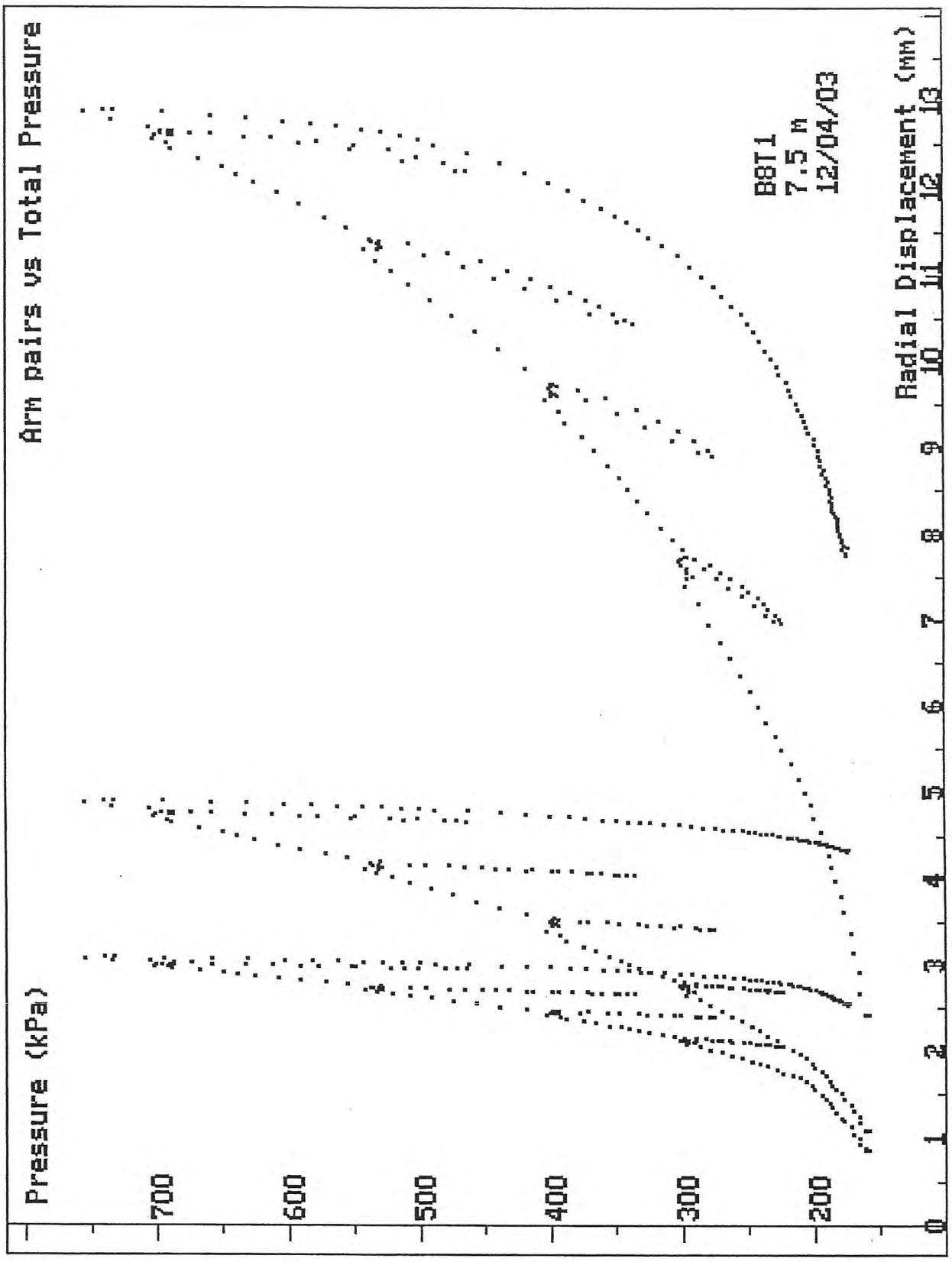

SCREEN DUMP Test: B8T1 Date: 12/04/03 Depth: 7.50m
HPD95 Pressuremeter tests Bressay Bridge Site Investigation
Cambridge Insitu for Seacore April 2003

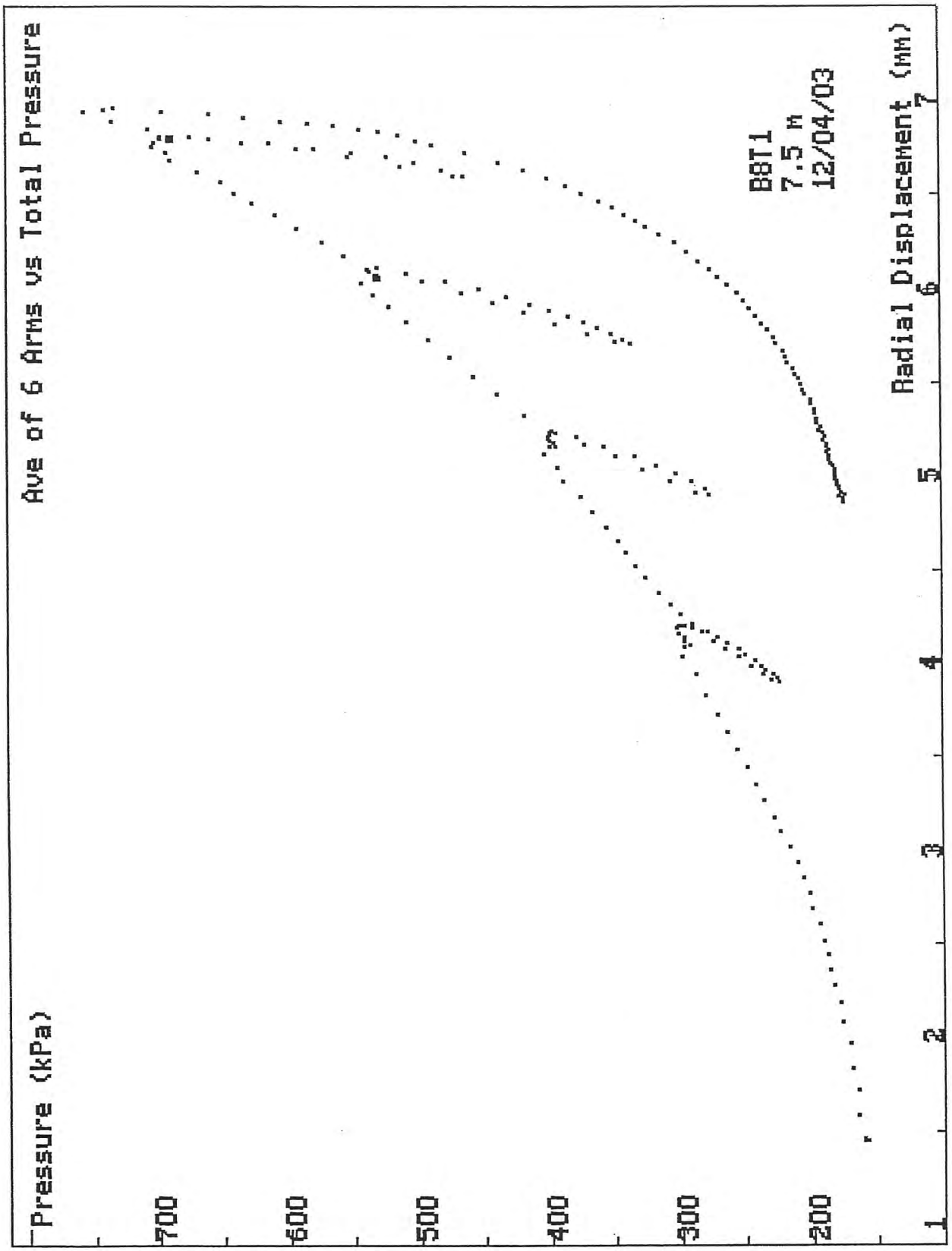

SCREEN DUMP Test: B8T1 Date: 12/04/03 Depth: 7.50m
HPD95 Pressuremeter tests Bressay Bridge Site Investigation
Cambridge Insitu for Seacore April 2003

HPD95 Pressuremeter tests
Cambridge Insitu for Seacore

Bressay Bridge Site Investigation
April 2003

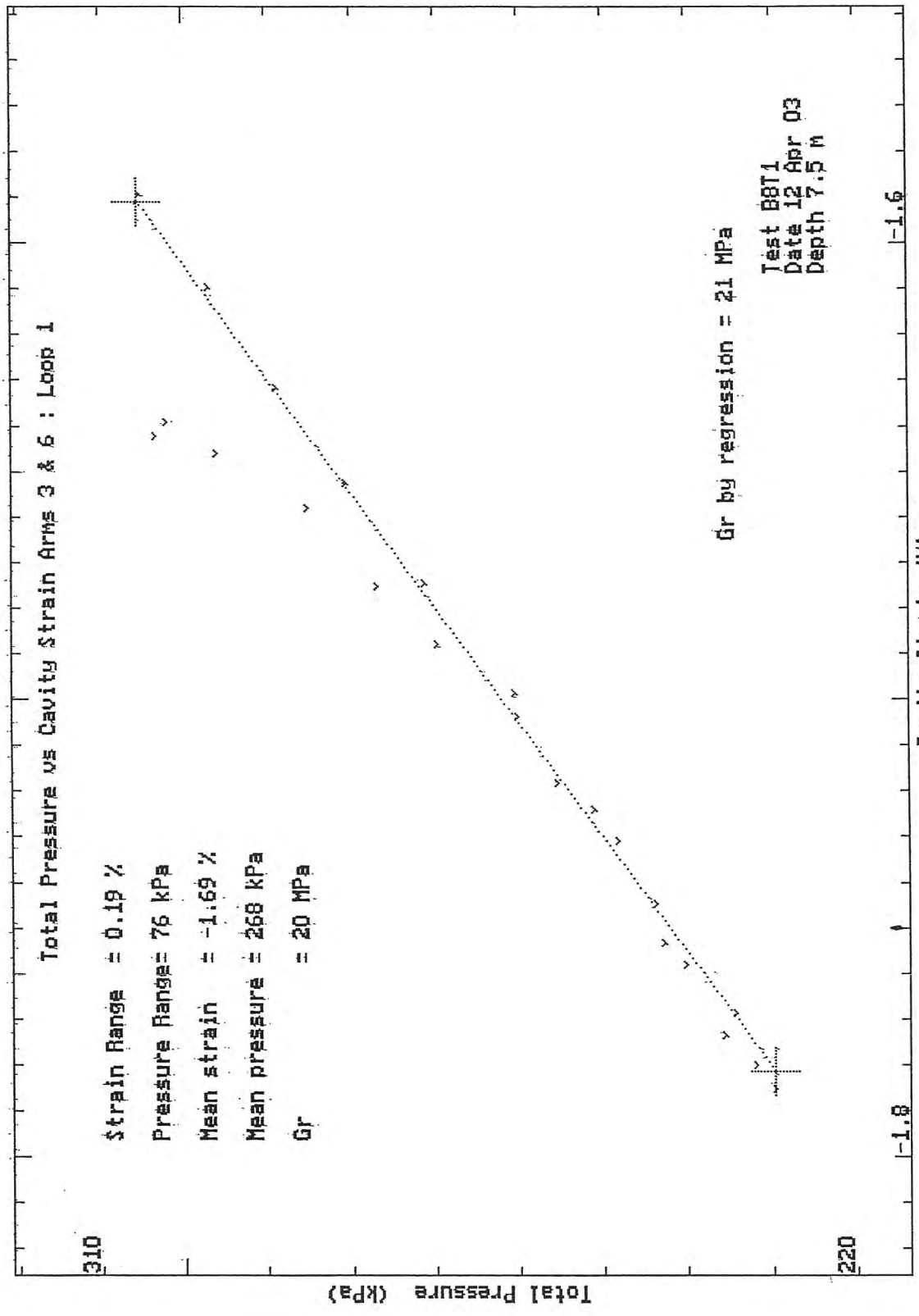
Total Pressure vs Cavity Strain Arms 3 & 6 : Loop 1
Strain Range = 0.19 %
Pressure Range= 76 kPa
Mean strain = -1.69 %
Mean pressure = 268 kPa
Gr = 20 MPa
Gr by regression = 21 MPa
Test B8T1
Date 12 Apr 03
Depth 7.5 m
310
220
-1.8
-1.6
Total Pressure (kPa)
Cavity Strain (%)

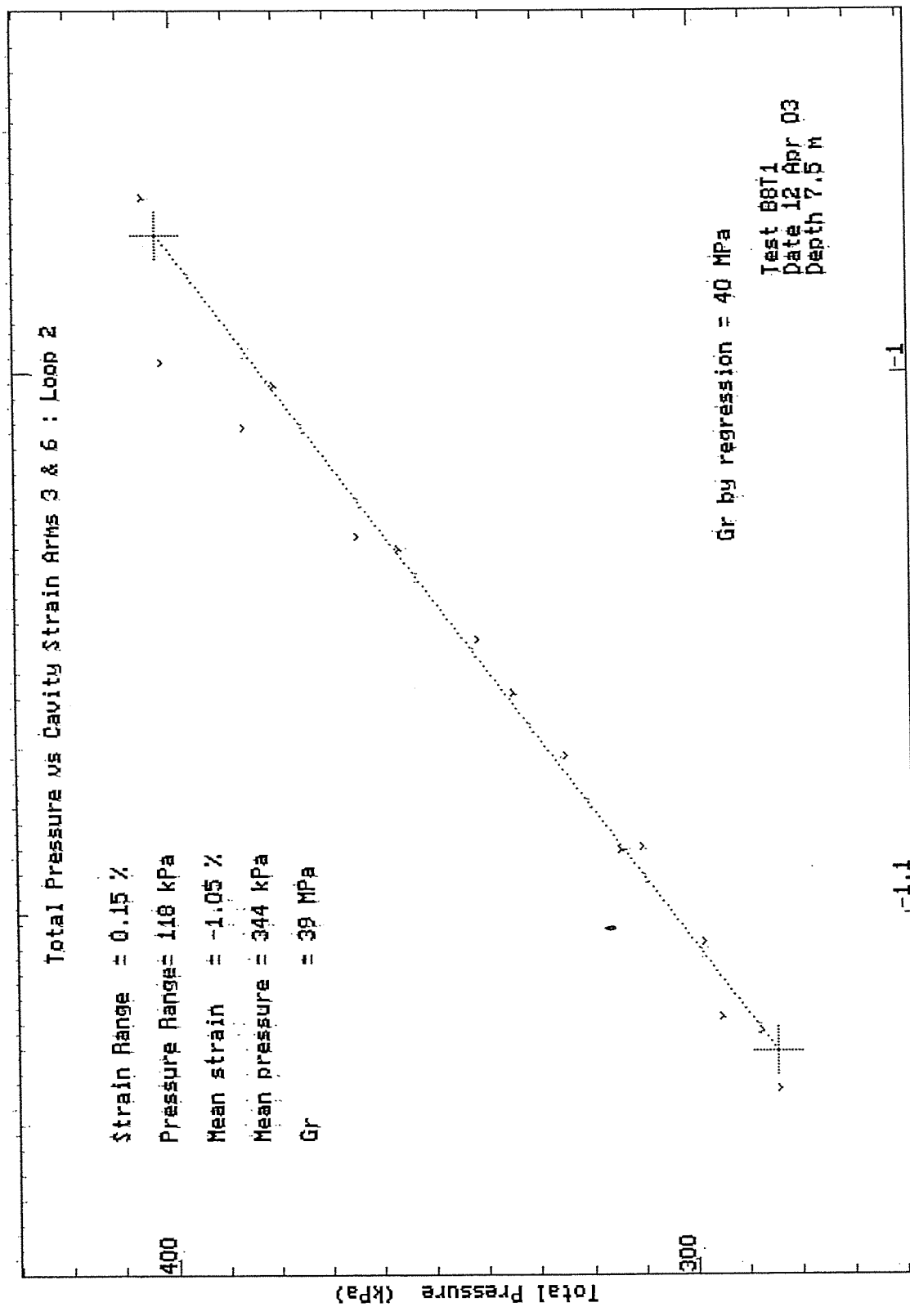
Total Pressure vs Cavity Strain Arms 3 & 6 : Loop 2
Strain Range = 0.15 %
Pressure Range= 118 kPa
Mean strain = -1.05 %
Mean pressure = 344 kPa
Gr = 39 MPa
Gr by regression = 40 MPa
Test BBT1
Date 12 Apr 03
Depth 7.5 m
400
300
-1.1
-1
Total Pressure (kPa)
Cavity Strain (%)

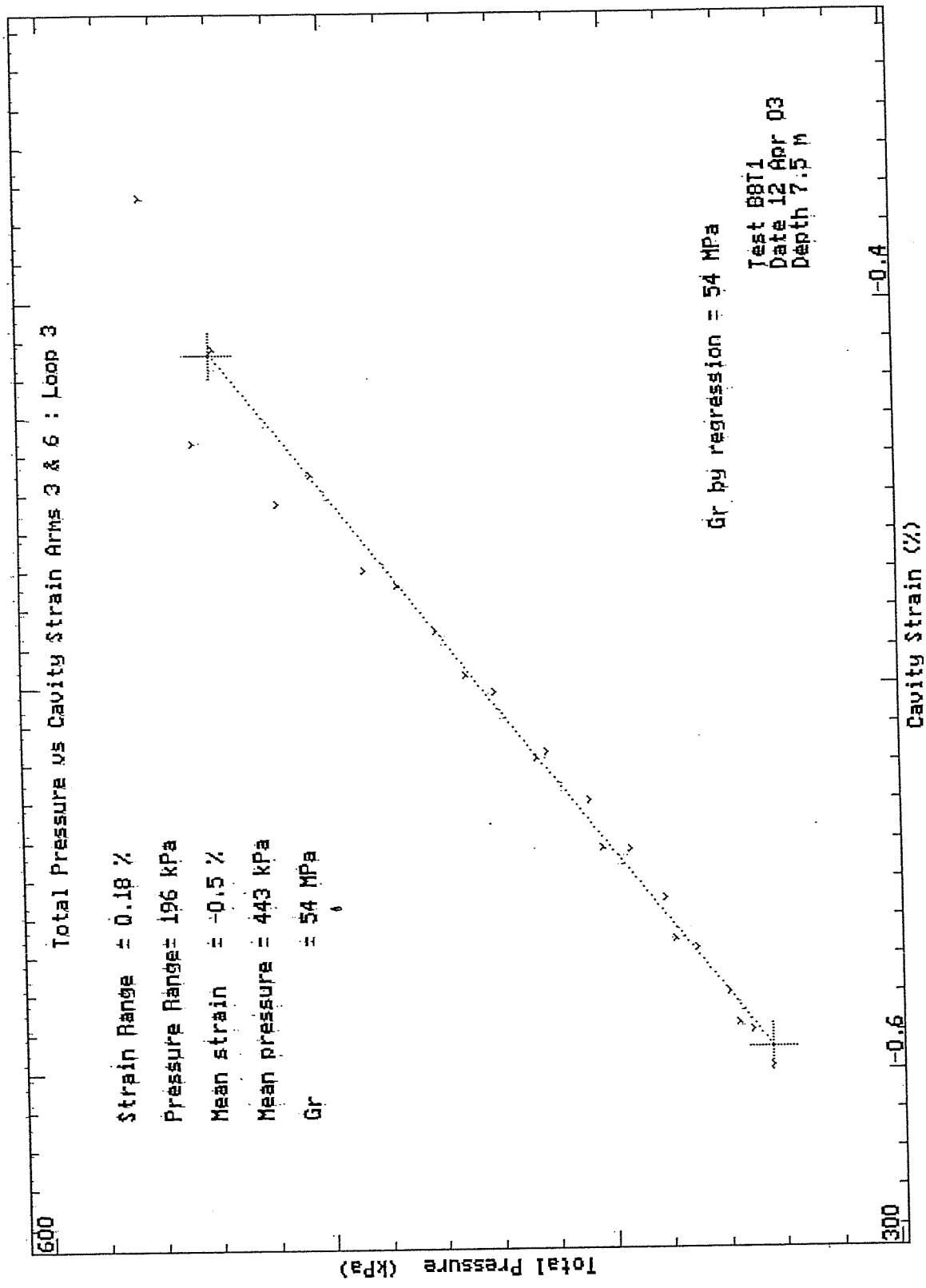
Total Pressure vs Cavity Strain Arms 3 & 6 : Loop 3
Strain Range = 0.18 %
Pressure Range= 196 kPa
Mean strain = -0.5 %
Mean pressure = 443 kPa
Gr = 54 MPa
Gr by regression = 54 MPa
Test BBT1
Date 12 Apr 03
Depth 7.5 m
600
300
-0.4
-0.6
Total Pressure (kPa)
Cavity Strain (%)

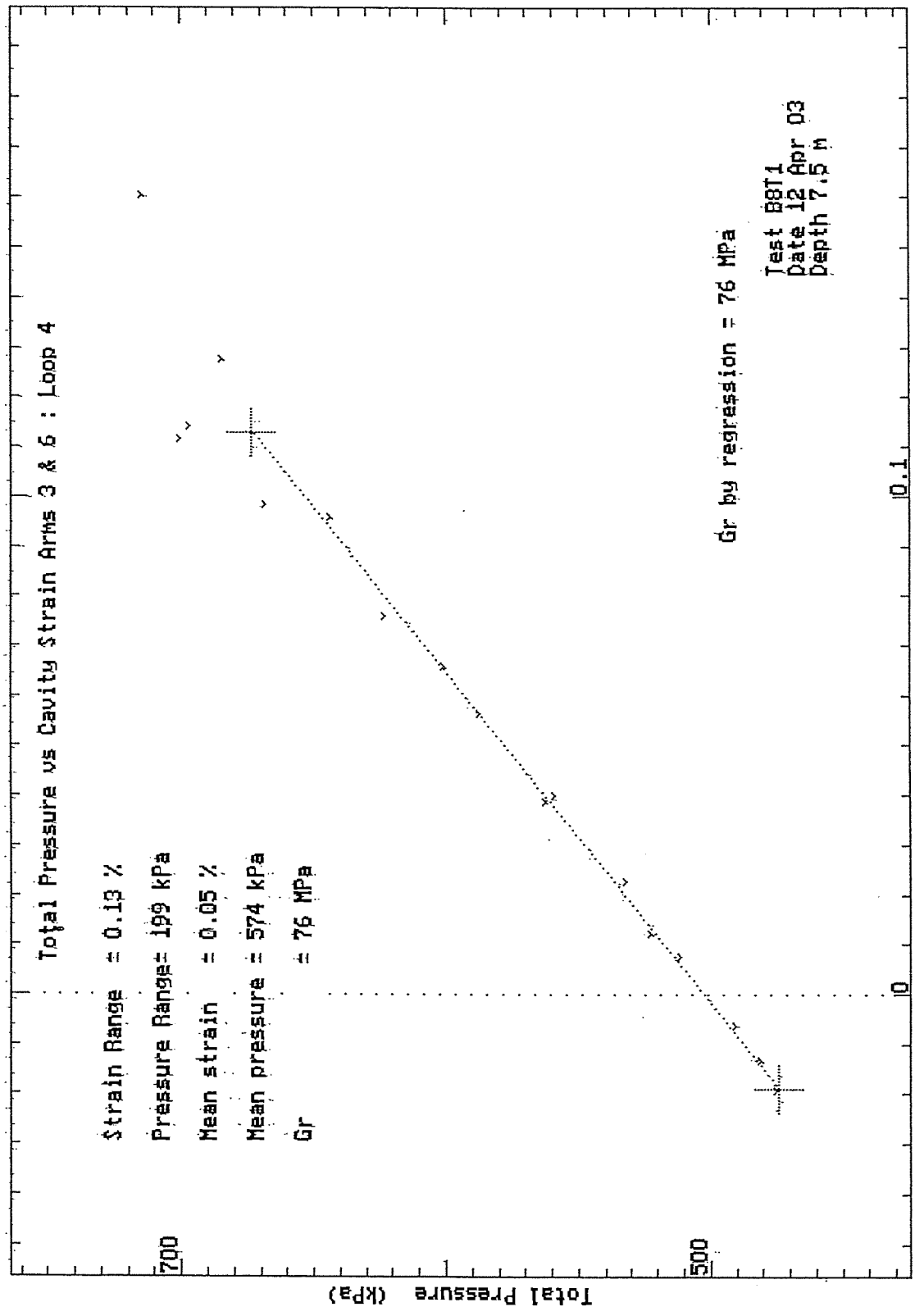
Total Pressure vs Cavity Strain Arms 3 & 6 : Loop 4
Strain Range ± 0.13 %
Pressure Range± 199 kPa
Mean strain ± 0.05 %
Mean pressure ± 574 kPa
Gr ± 76 MPa
Gr by regression = 76 MPa
Test BBT1
Date 12 Apr 03
Depth 7.5 m
Total Pressure (kPa)
Cavity Strain (%)
700
500
0
0.1

TEST RECORD SHEET - HIGH PRESSURE DILATOMETER

Site	Date	Day	Borehole	Test No	Depth
LERWICK FOR SHAFOCE	12.4.03	SAT	9	1	3.1

Material: CONGLOMERATE

Weather	Water Table	Time Now	Drilling End	Orientation	CHL
SUNNY & BREEZY	SEA LEVEL		15.30 APPROX	NE	V

Drilling	Pocket

Diameter	Distance	Rate	Core Description	Length

Wet/Dry	Rig	Driller	Core Quality	Size
WET	STARTER II D	MARTIN WILLY		

Pres/Incrmnt	Wait Time	Creep Time	Cycle Time	Disc No.	Operator	Engineer
			10 SEC	2		

ZERO READINGS: TILLY Machine Diameter 95 mm

Arm 1	Arm 2	Arm 3	Arm 4	Arm 5	Arm 6	T/Press.	Battery
-1.3835	-1.6569	-1.5607	-1.3726	-1.4775	-1.5400	A: .0102 B: .0888	12.30 DECK LEVEL

Calibrations:

Strain Arm Calibration date:	2-10-02	Test No:
Total Pressure Cell Calibration date:	6-3-03	Test No:
Membrane Stiffness Calibration date:	19-3-03	Test No: C999T99
Membrane Compression Calibration date:	"	Test No: "
New Membrane fitted date:	"	

Test Comments:

Time	Line No.	Start Test at: 17.20
		1ST LOOP @ L 65 1.1MPa
		LOOP 2 @ L 35 (RE STARTED TEST) 2.7MP
		LOOP 3 @ L 95
		TO UNLOAD L 130
		LOW OIL LEVEL
		MEM BALLOONING

Test Ends at: 18.10

Max. Pressure reached: 5MPa APROX

General Comments:

3 RELOADS - MATERIAL MOVEMENT

INST IS TILLY

CAMBRIDGE INSITU, Little Eversden, Cambridge, England CB3 7HE
Telephone: 01223 262 361 Fax:- 01223 263 947

HIGH PRESSURE DILATOMETER RESULTS SUMMARY SHEET

Site:- Bressay Bridge Test :- B9T1 Test Date :- 12th April 2003
Material :- Conglomerate Depth (m) :- 3.1 Water depth (m) :- -

---

Analysis of Insitu Lateral Stress (Po) :-

		Arm Av.
Marsland and Randolph (Iterative Analysis)	kPa	1203
Best Estimate of Po	kPa	1200
Assessed diameter of borehole	mm	99.1

Analysis of Undrained Shear Strength (Cu) :-

Gibson and Anderson	kPa	1672
Failure pressure (Pf)	kPa	2205
Limit Pressure (P_L)	MPa	11

Strength of Sands Analysis (Hughes, Wroth & Windle)

Friction angle at const. vol.	deg	35	(assumed)	At large strain
Angle of Friction	deg	47		35
Angle of Dilation	deg	16		0

Analysis of Shear Modulus (G) :-

Initial Modulus (Gi) MPa 243

Linear Analysis of Reload Loops (Gr) :-

Loop no.	Value (MPa)	Co-ordinate Strain %	Co-ordinate Pressure kPa	Amplitude Strain %	Amplitude Pressure kPa
1	314	-0.05	882	0.06	379
2	606	0.31	2022	0.103	1249
3	570	0.97	3152	0.184	2074

Non-linear Analysis of Reloading data :-

Loop no.	Linearity exponent (β)	Radial Stress Coeff. (MPa)	Shear Stress Coeff. (MPa)
2	0.94	419	394
3	0.85	247	209

Test Analysed By :- PGH
Date :- 27th May 2003

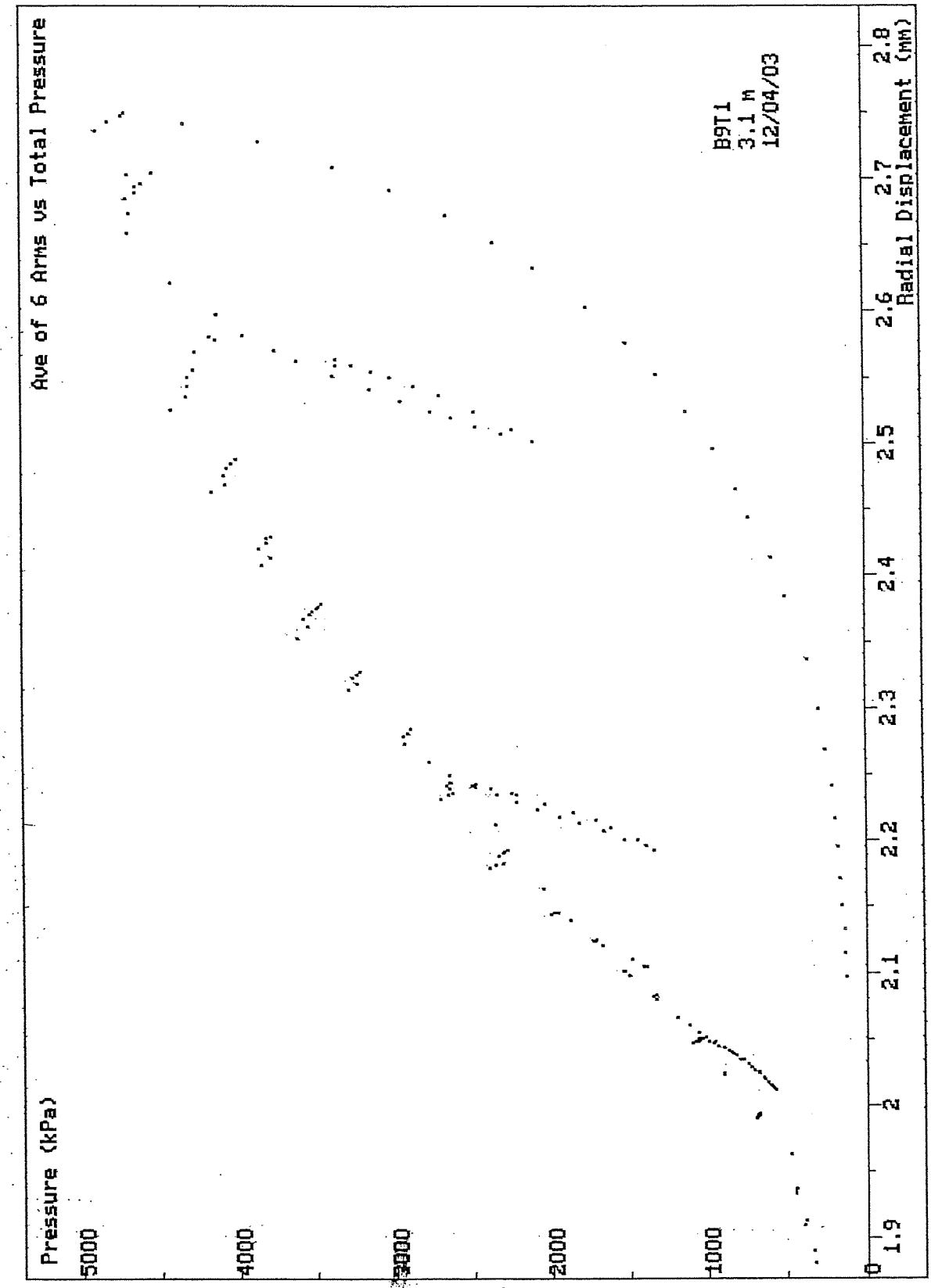

SCREEN DUMP Test: B9T1 Date: 12/04/03 Depth: 3.10m
HPD95 Pressuremeter tests Bressay Bridge Site Investigation
Cambridge Insitu for Seacore April 2003

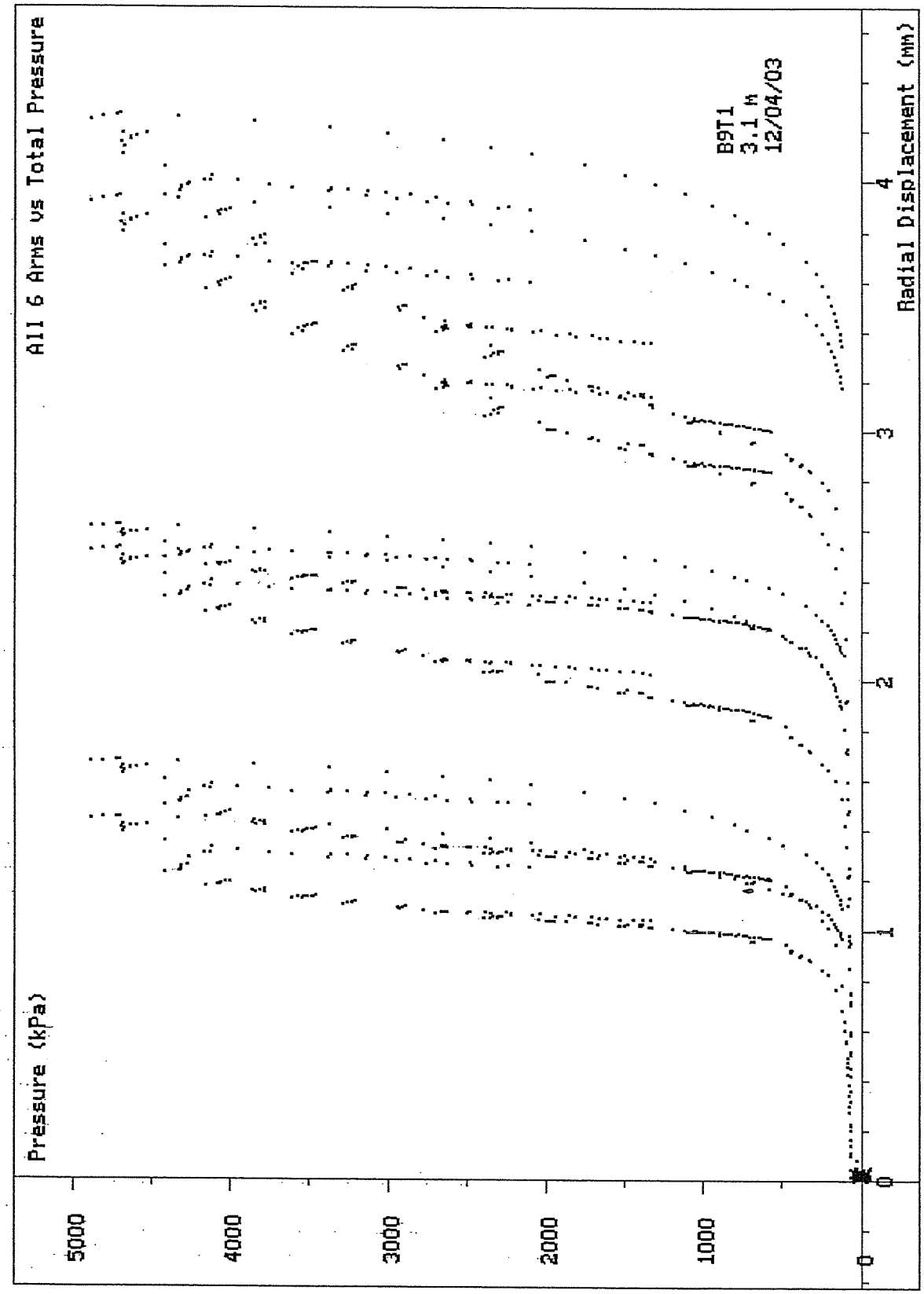

SCREEN DUMP Test: B9T1 Date: 12/04/03 Depth: 3.10m
HPD95 Pressuremeter tests Bressay Bridge Site Investigation
Cambridge Insitu for Seacore April 2003

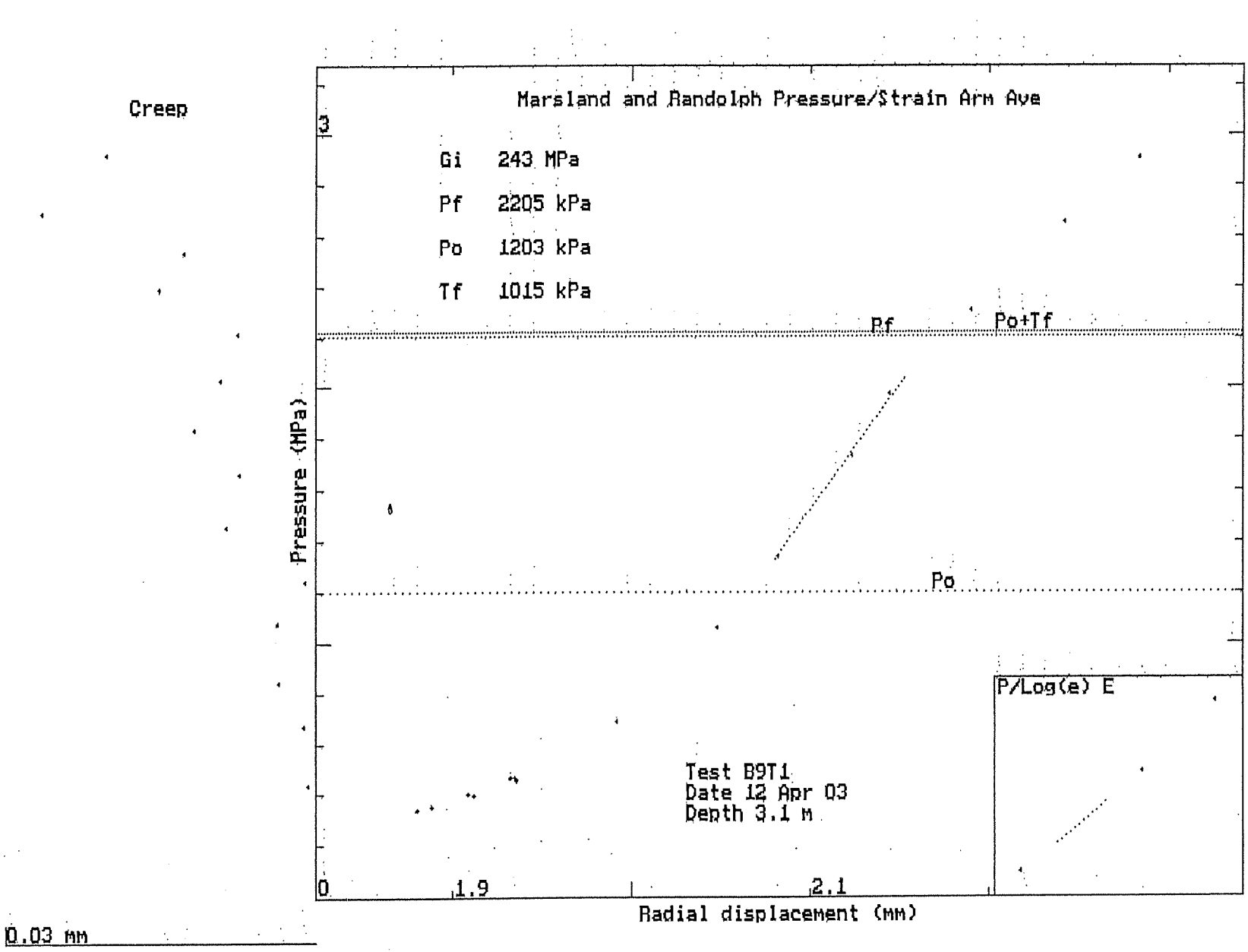
Creep
0.03 mm
Marsland and Randolph Pressure/Strain Arm Ave
Gi 243 MPa
Pf 2205 kPa
Po 1203 kPa
Tf 1015 kPa
Pf
Po+Tf
Po
Pressure (MPa)
3
P/Log(e) E
Test B9T1
Date 12 Apr 03
Depth 3.1 m
0
1.9
2.1
Radial displacement (mm)

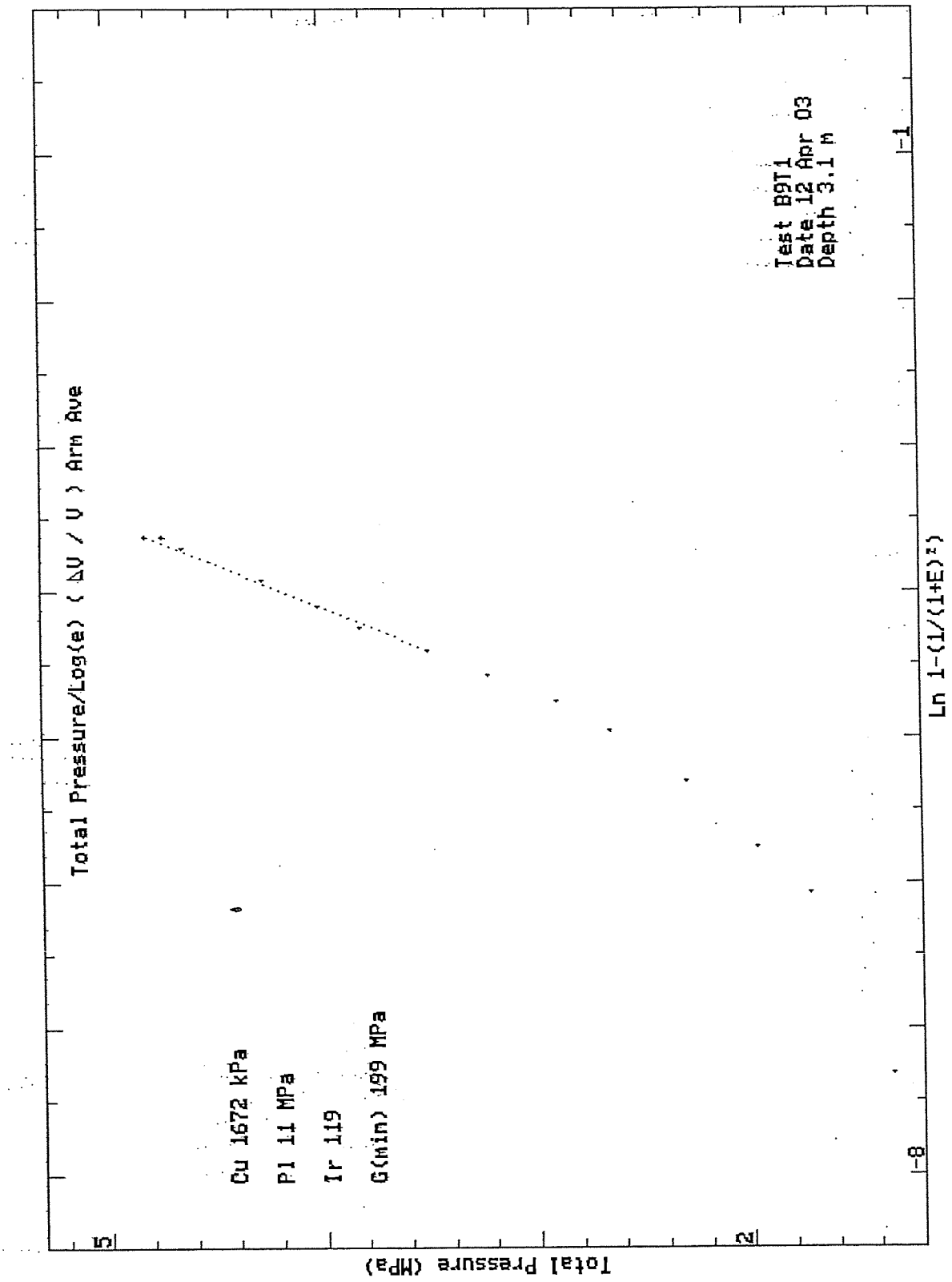

HPD95 Pressuremeter tests
Cambridge Insitu for Seacore

Bressay Bridge Site Investigation
April 2003

Log(e) Effective Stress/Log(e) Strain Arm Ave
Gradient 0.54
øcv 35 °
ø' 47 °
Dilation 16 °
Test BBT1
Date 12 Apr 03
Depth 3.1 m
Log (e) Effective Radial Stress
Log (e) Cavity Strain
-4
-8
7
8

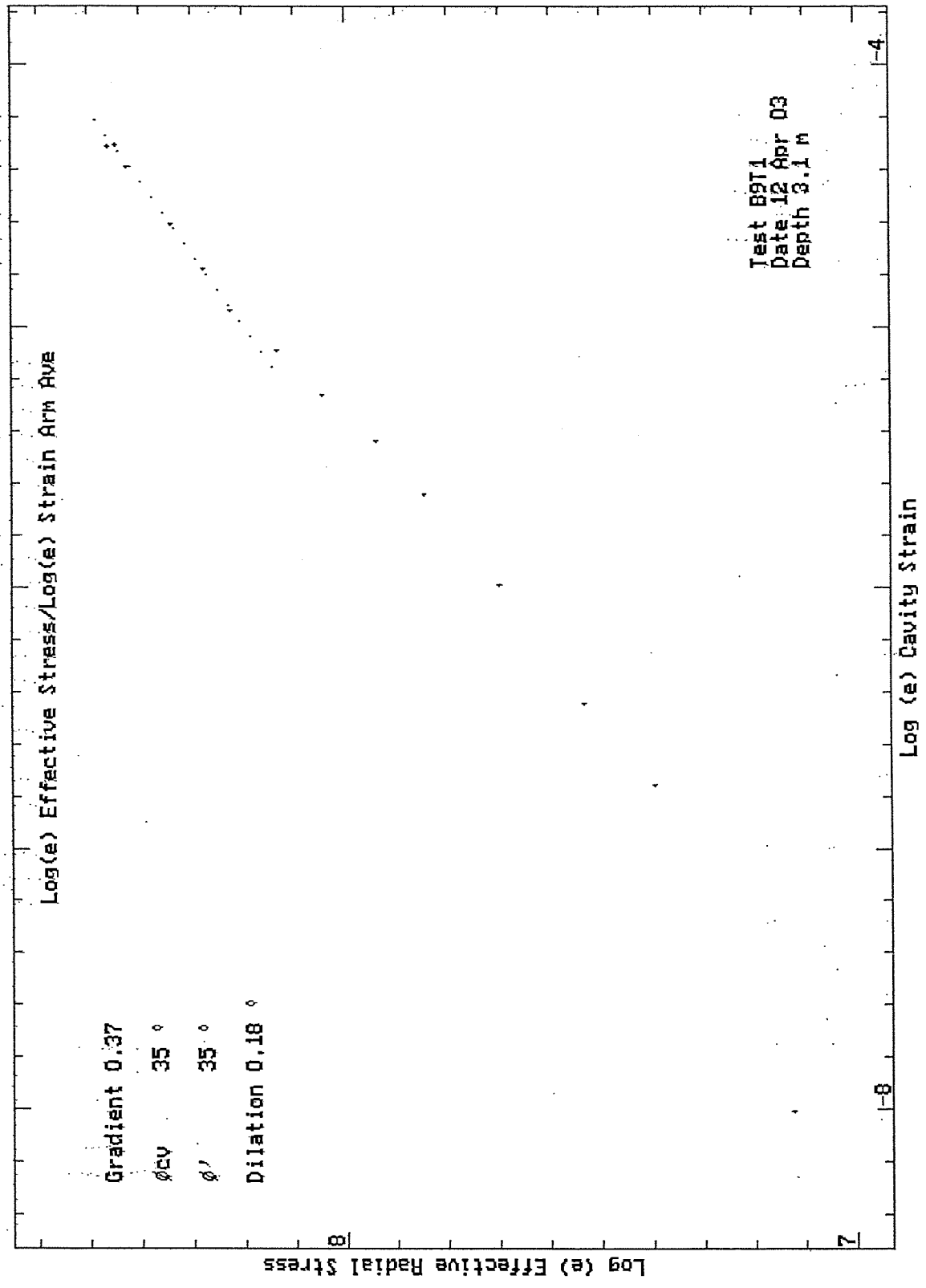
Log(e) Effective Stress/Log(e) Strain Arm Ave
Test B9T1
Date 12 Apr 03
Depth 3.1 m
Gradient 0.37
Øcv 35 °
Ø' 35 °
Dilation 0.18 °
Log (e) Effective Radial Stress
Log (e) Cavity Strain
-4
-8
7
8

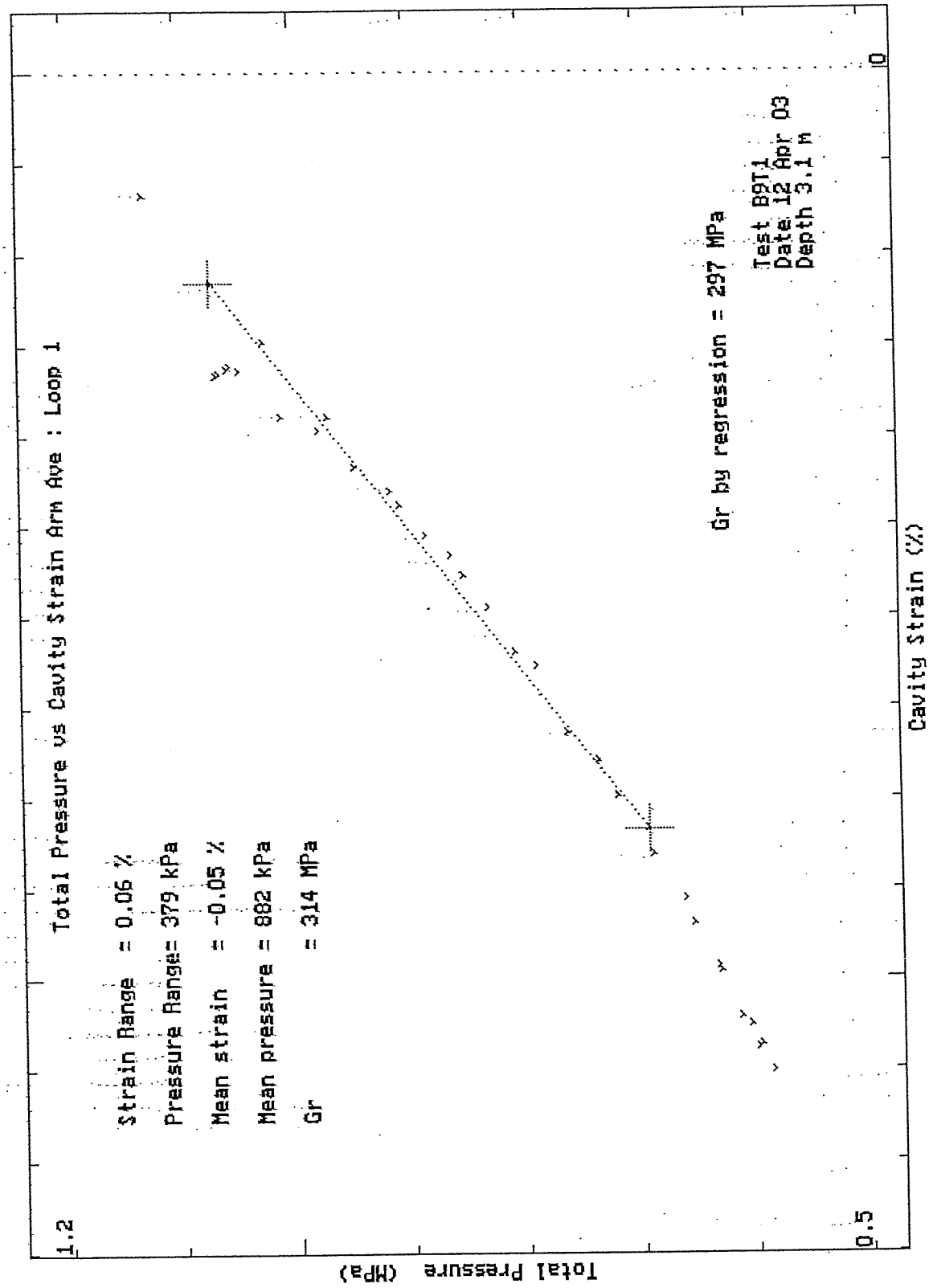

HPD95 Pressuremeter tests
Cambridge Insitu for Seacore

Bressay Bridge Site Investigation
April 2003

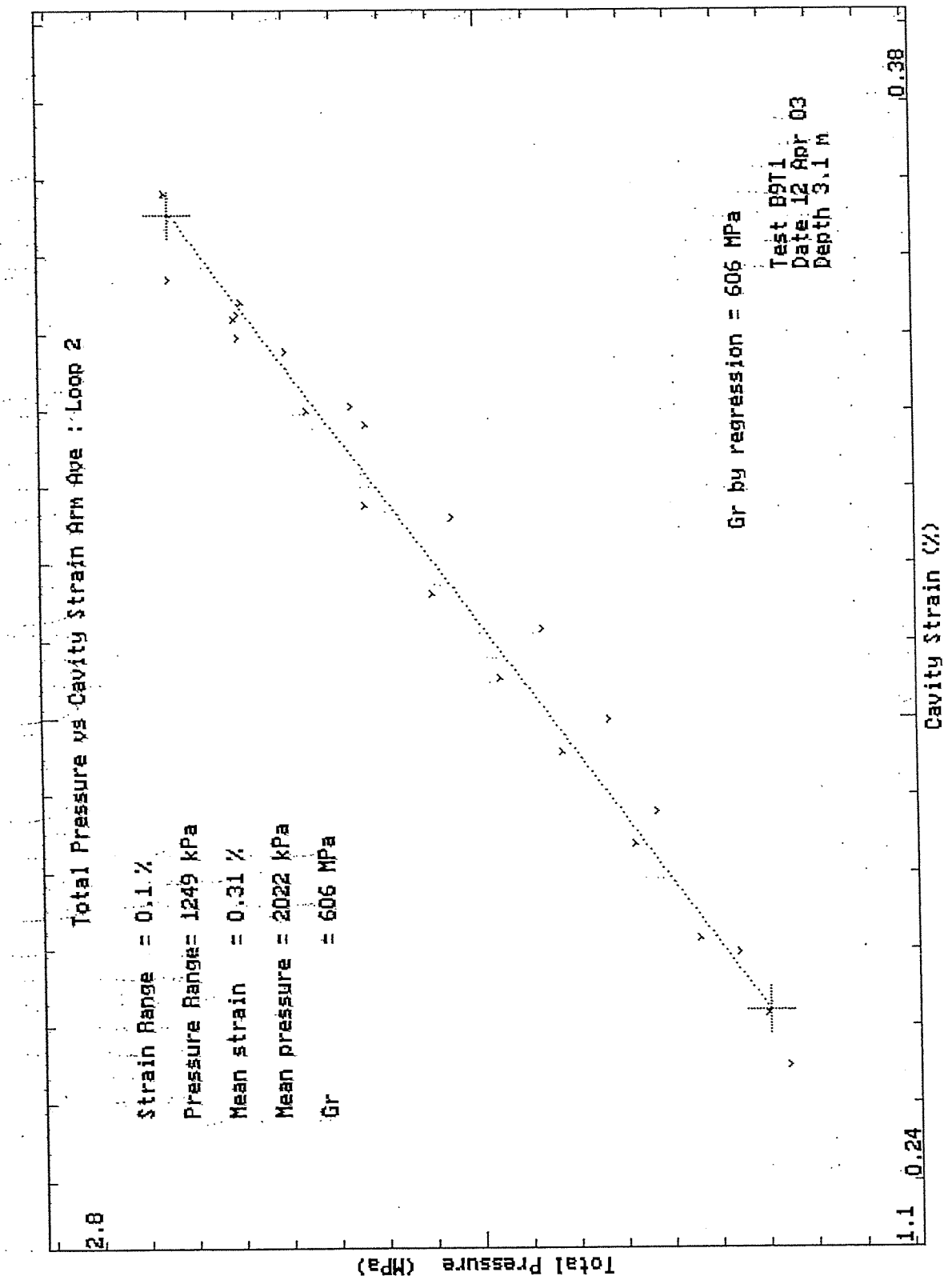
Total Pressure vs Cavity Strain Arm Ave : Loop 2
Strain Range = 0.1 %
Pressure Range= 1249 kPa
Mean strain = 0.31 %
Mean pressure = 2022 kPa
Gr = 606 MPa
Gr by regression = 606 MPa
Test B9T1
Date 12 Apr 03
Depth 3.1 m
Total Pressure (MPa)
Cavity Strain (%)
2.8
1.1
0.24
0.38

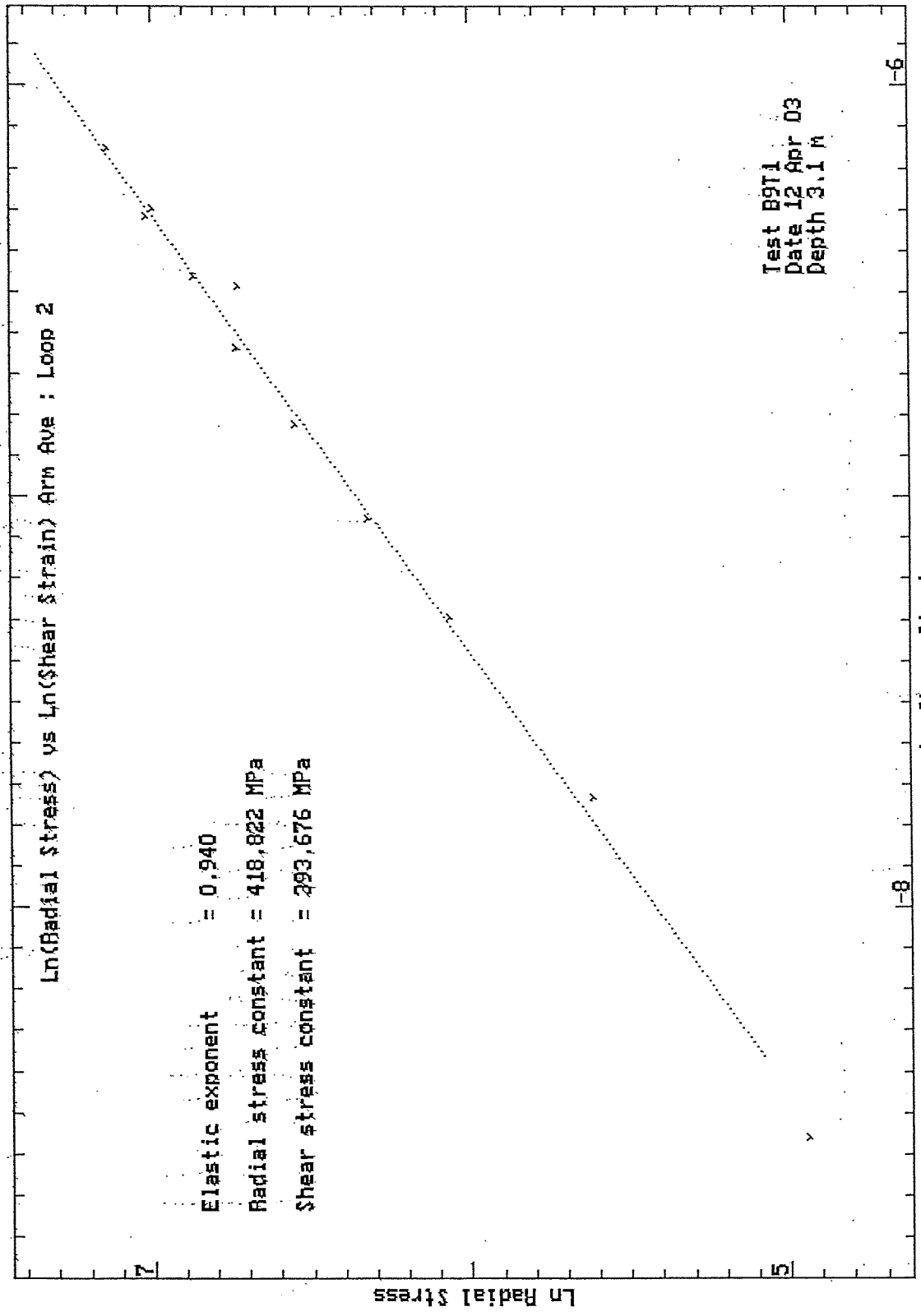
Ln(Radial Stress) vs Ln(Shear Strain) Arm Ave : Loop 2
Test B9T1
Date 12 Apr 03
Depth 3.1 m
Elastic exponent = 0.940
Radial stress constant = 418.822 MPa
Shear stress constant = 293.676 MPa
Ln Radial Stress
Ln Shear Strain
7
5
-8
-6

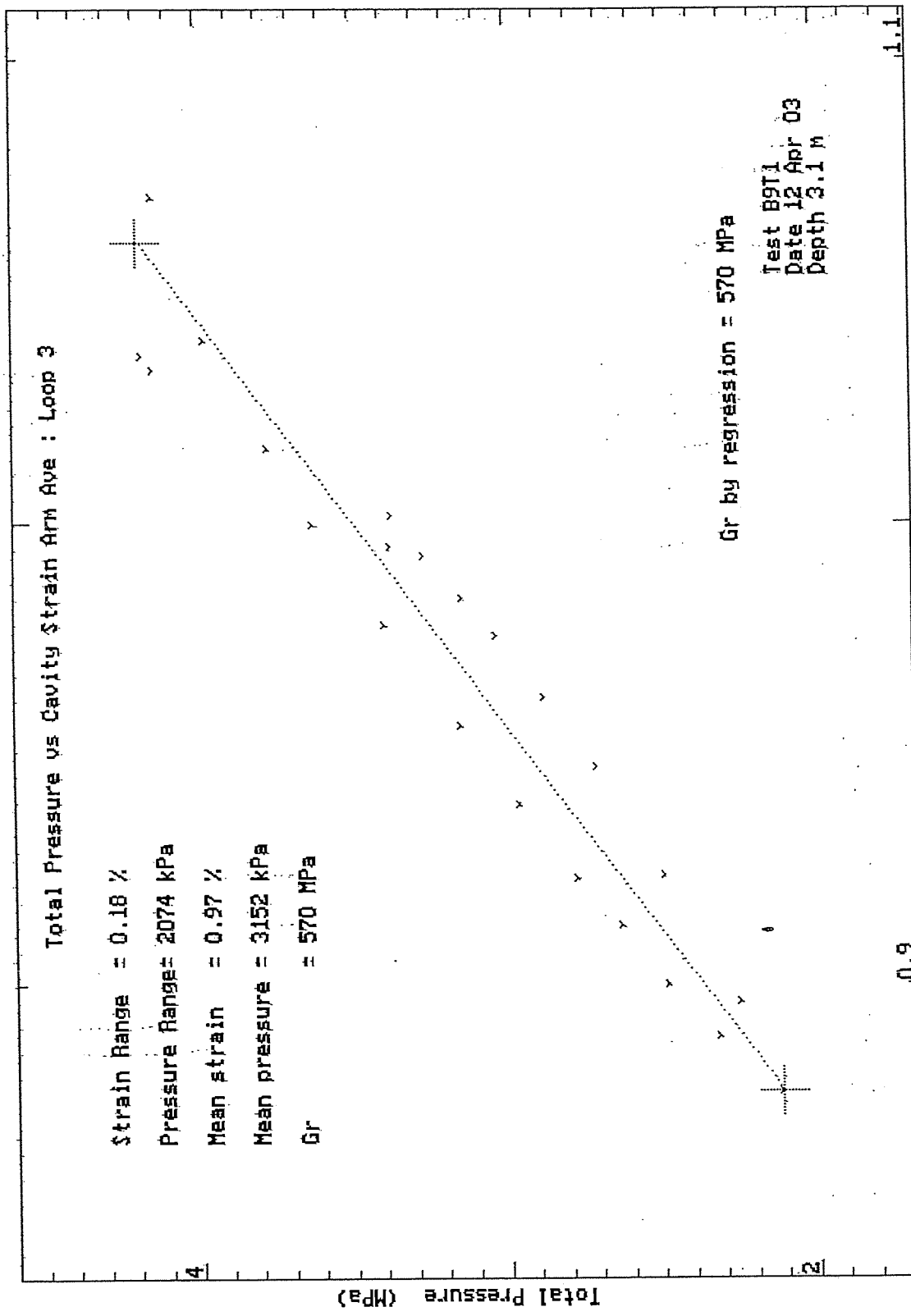
Total Pressure vs Cavity Strain Arm Ave : Loop 3
Strain Range = 0.18 %
Pressure Range= 2074 kPa
Mean strain = 0.97 %
Mean pressure = 3152 kPa
Gr = 570 MPa
Gr by regression = 570 MPa
Test B9T1
Date 12 Apr 03
Depth 3.1 m
Total Pressure (MPa)
Cavity Strain (%)
4
2
0.9
1.1

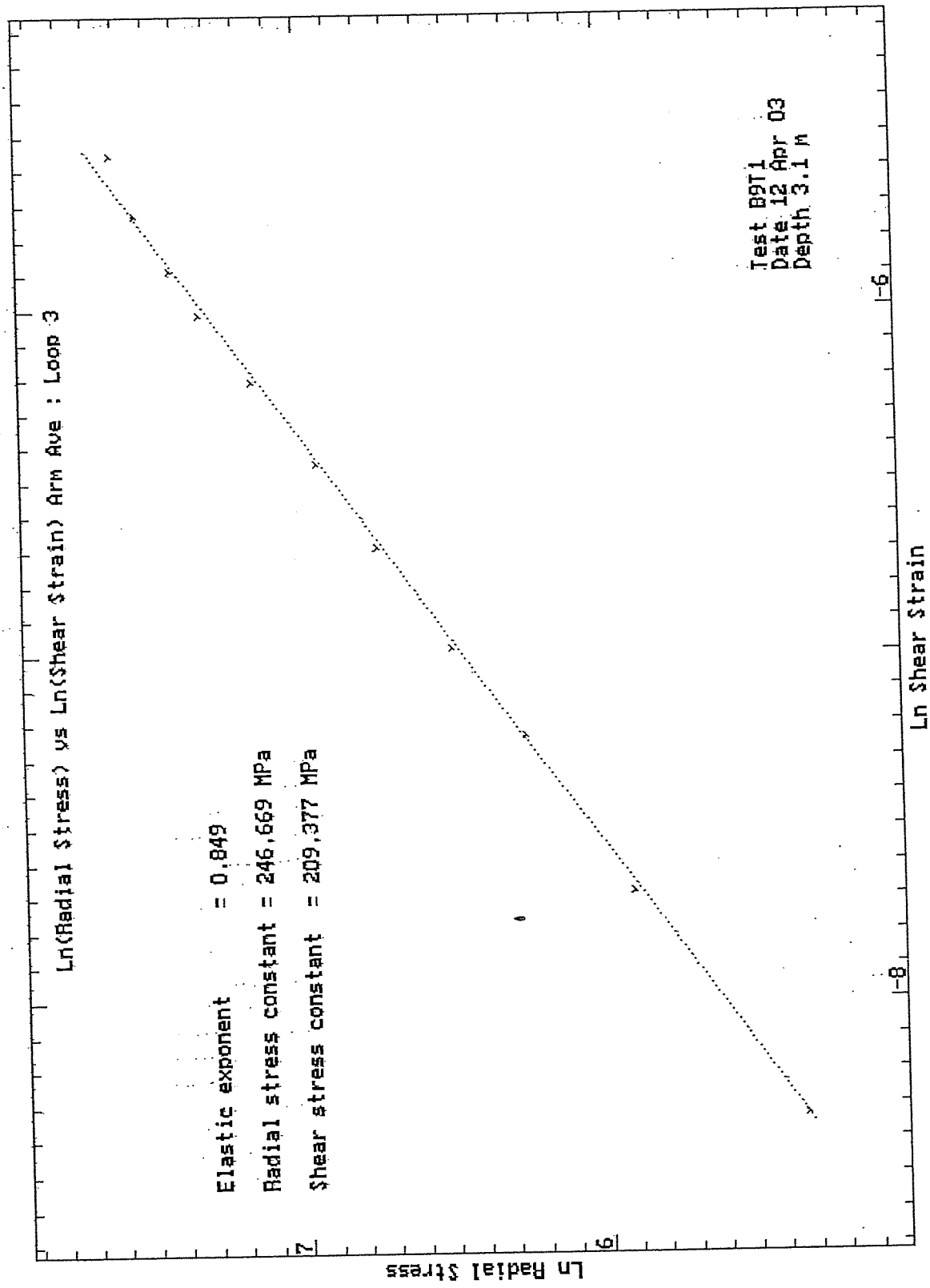
Ln(Radial $tress) vs Ln($hear $train) Arm Ave : Loop 3
Test B9T1
Date 12 Apr 03
Depth 3.1 m
Elastic exponent = 0.849
Radial stress constant = 246.669 MPa
$hear stress constant = 209.377 MPa
Ln Radial $tress
Ln $hear $train
-7
-9
-6
-8

TEST RECORD SHEET - HIGH PRESSURE DILATOMETER

SITE	Date	Day	Borehole	Test No	Depth
HALWICK	13·4·03	SUN	10	1	5·1

Material: SANDSTONE.

Weather	Water Table	Time Now	Drilling End	Orientation	CHL
SUNNY & BREEZY !	SEA CGUEC		17·25		

Drilling	Pocket

Diameter	Distance	Rate	Core Description	Length

Wet/Dry	Rig	Driller	Core Quality	Size
WET	SKANSKA		GOOD	

Pres/Incrmnt	Wait Time	Creep Time	Cycle Time	Disc No.	Operator	Engineer
			10 SEC	3		

ZERO READINGS: TICCY

Machine Diameter 95 mm

Arm 1	Arm 2	Arm 3	Arm 4	Arm 5	Arm 6	T/Press.	Battery
						A: B:	

Calibrations:

Strain Arm Calibration date: 2-10-02 Test No:

Total Pressure Cell Calibration date: 6-3-03 Test No:

Membrane Stiffness Calibration date: 19-3-03 Test No: C999T99

Membrane Compression Calibration date: " Test No: "

New Membrane fitted date: "

Test Comments:

Time	Line No.	Start Test at: 21:00
	71	HOLD ⇒ LOOP (1)
	123	LOOP (2)
	170	LOOP (3)
	265	UNLOAD — FAR ENOUGH
		ARMS MOVING ABOUT A BIT

Test Ends at: 21:50

Max Pressure reached: 10 MPa

General Comments

CAMBRIDGE INSITU, Little Eversden, Cambridge, England CB3 7HE
Telephone: 01223 262 361 Fax:- 01223 263 947

HIGH PRESSURE DILATOMETER RESULTS SUMMARY SHEET

Site:- Bressay Bridge Test :- B10T1 Test Date :- 13th April 2003
Material :- Sandstone Depth (m) :- 5.1 Water depth (m) :- -

Analysis of Insitu Lateral Stress (Po) :-

		Arm Av.
Marsland and Randolph (Iterative Analysis)	kPa	2008
Best Estimate of Po	kPa	2000
Assessed diameter of borehole	mm	99.8

Analysis of Undrained Shear Strength (Cu) :-

Gibson and Anderson	kPa	4425
Failure pressure (Pf)	kPa	3201
Limit Pressure (P_L)	MPa	23

Strength of Sands Analysis (Hughes, Wroth & Windle)

Friction angle at const. vol.	deg	33	(assumed)
Angle of Friction	deg	47	
Angle of Dilation	deg	18	

Analysis of Shear Modulus (G) :-

Initial Modulus (Gi)	MPa	285

Linear Analysis of Reload Loops (Gr) :-

Loop	Value	Co-ordinate		Amplitude	
no.	(MPa)	Strain %	Pressure kPa	Strain %	Pressure kPa
1	599	-0.08	1346	0.05	599
2	800	0.13	2293	0.071	1135
3	697	0.62	3501	0.149	2071

Non-linear Analysis of Reloading data :-

Loop	Linearity exponent	Radial Stress Coeff.	Shear Stress Coeff.
no.	(β)	(MPa)	(MPa)
2	0.95	560	530
3	0.855	320	274

Test Analysed By :- PGH
Date :- 27th May 2003

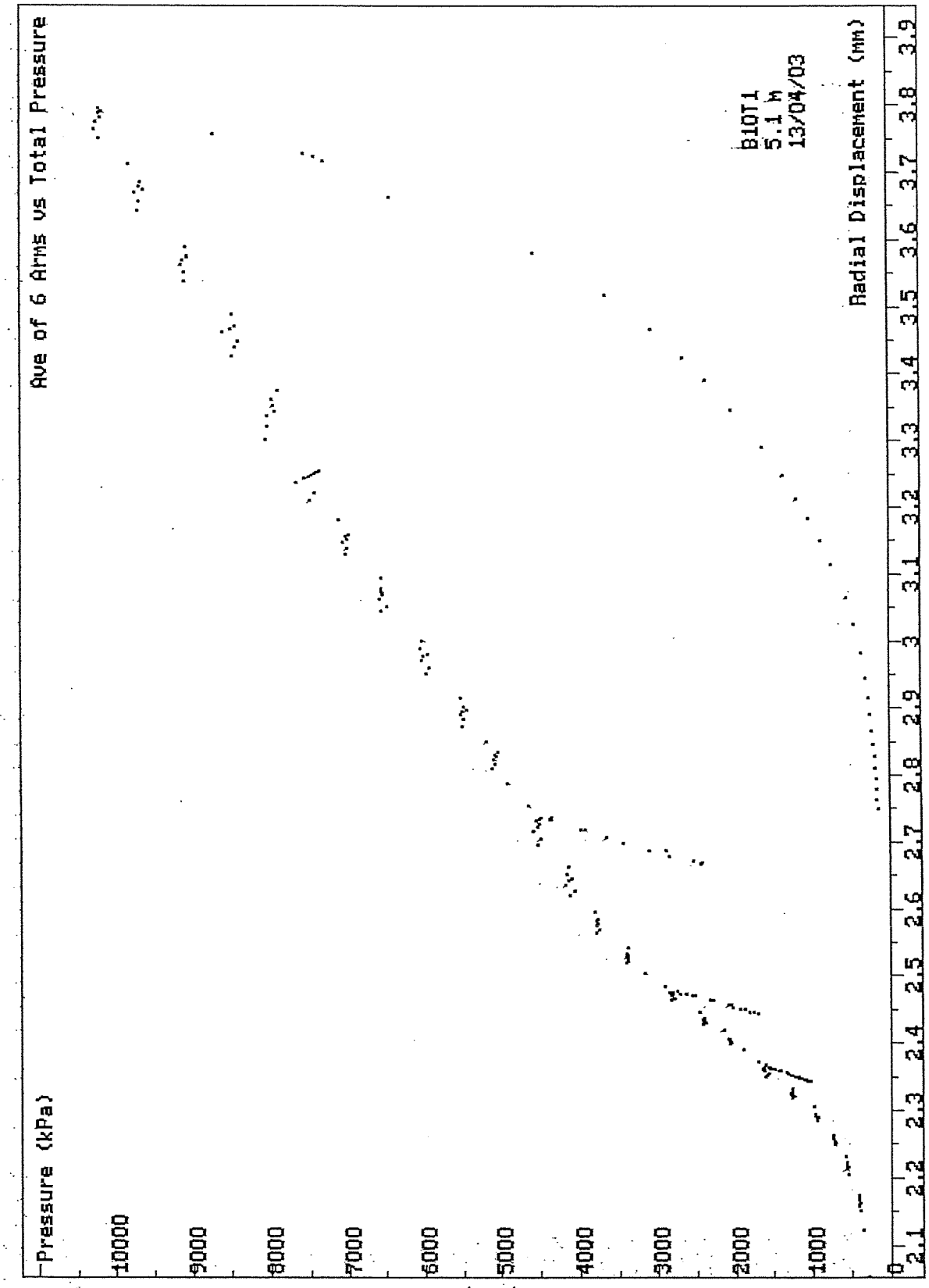

SCREEN DUMP Test: B10T1 Date: 13/04/03 Depth: 5.10m
HPD95 Pressuremeter tests Bressay Bridge Site Investigation
Cambridge Insitu for Seacore April 2003

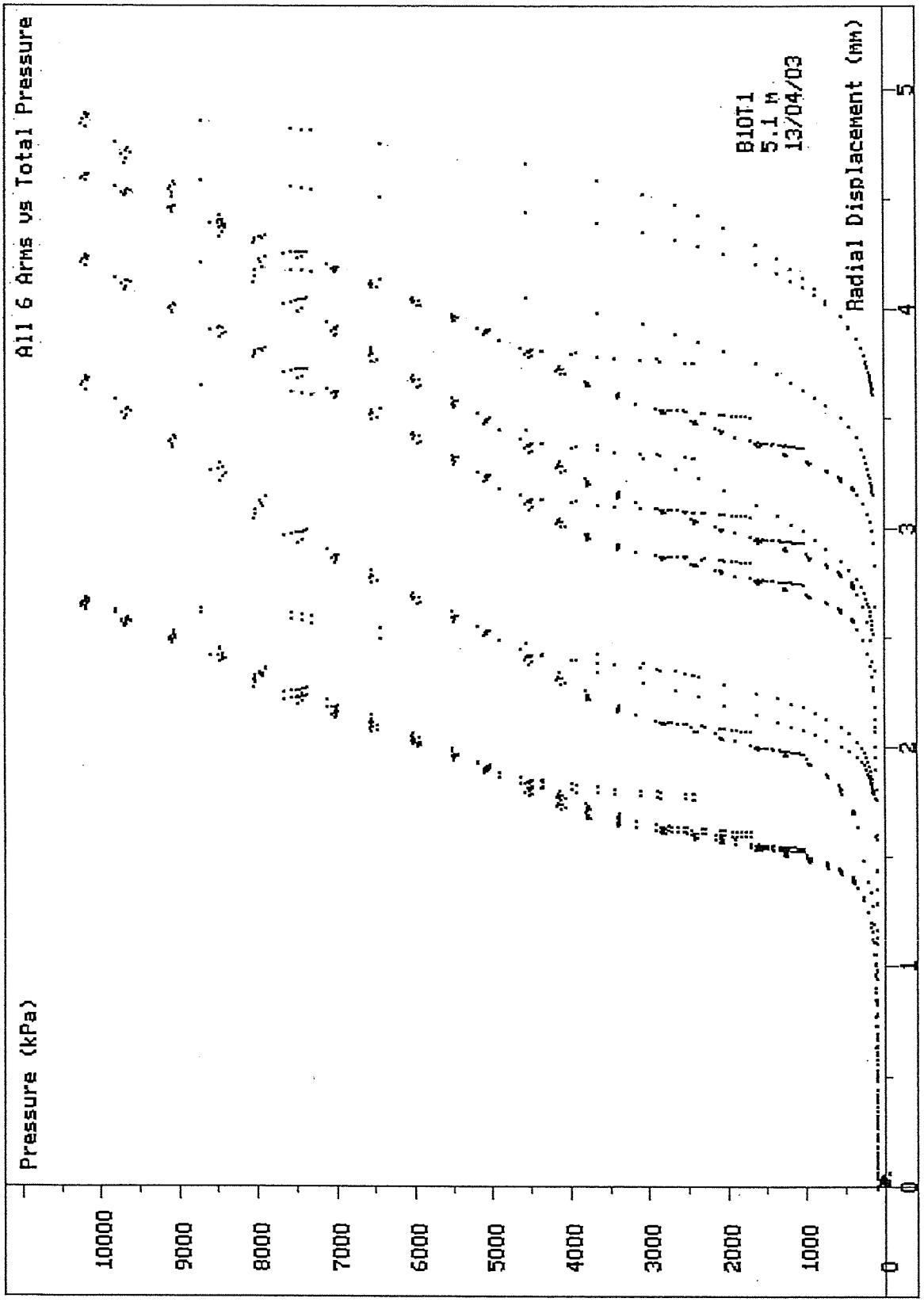

SCREEN DUMP Test: B10T1 Date: 13/04/03 Depth: 5.10m
HPD95 Pressuremeter tests Bressay Bridge Site Investigation
Cambridge Insitu for Seacore April 2003

HPD95 Pressuremeter tests
Cambridge Insitu for Seacore

Bressay Bridge Site Investigation
April 2003

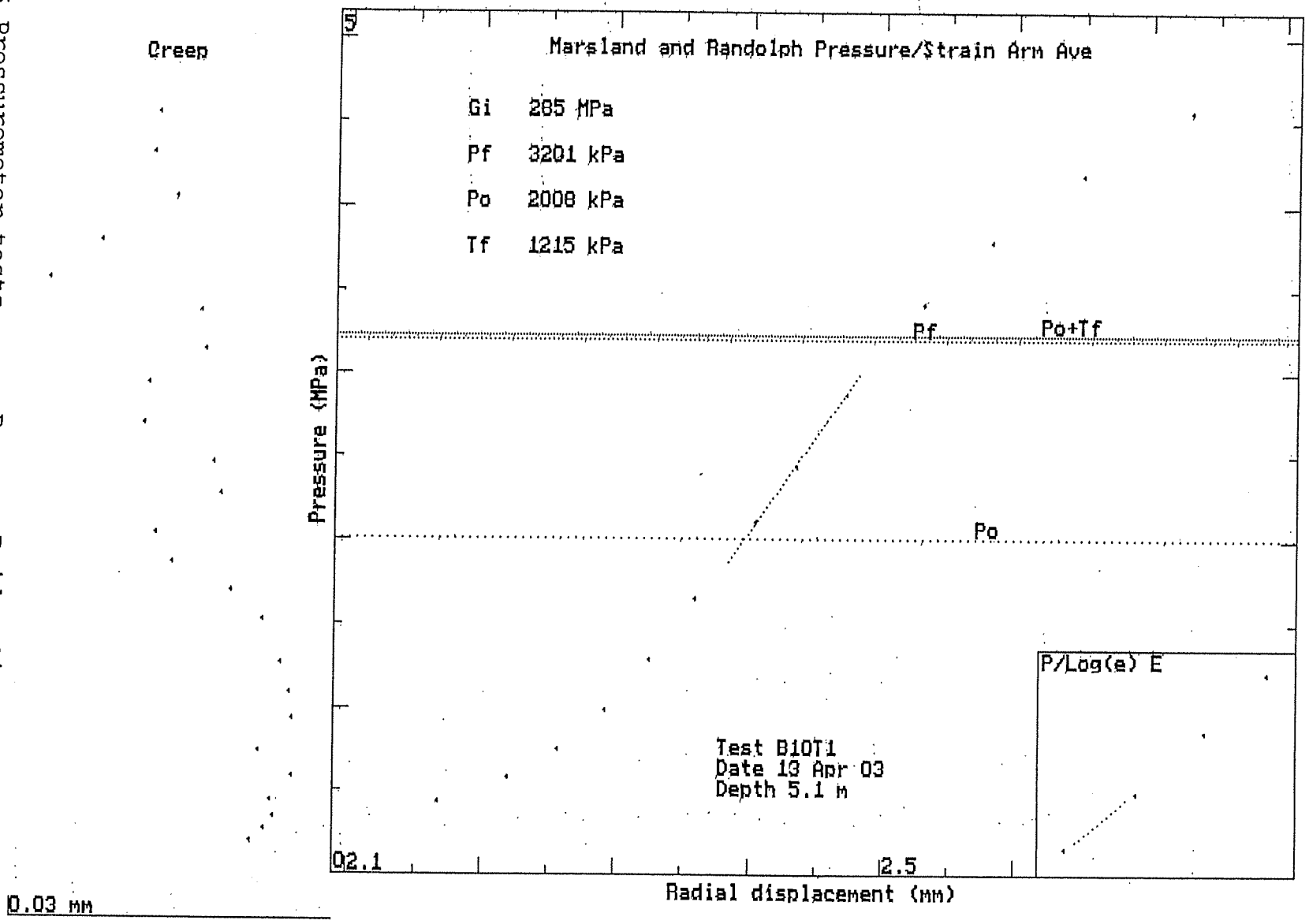

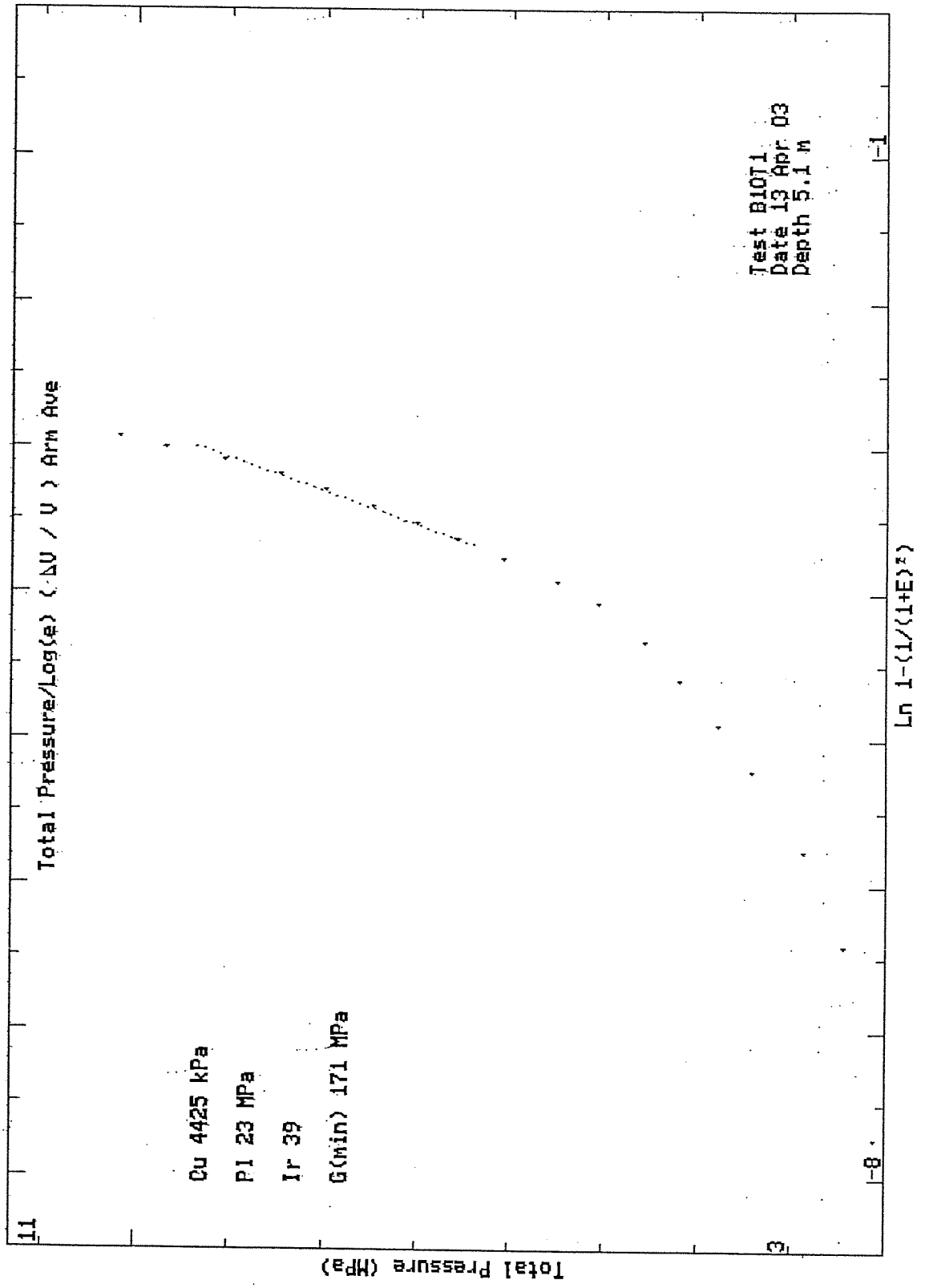

HPD95 Pressuremeter tests
Cambridge Insitu for Seacore

Bressay Bridge Site Investigation
April 2003

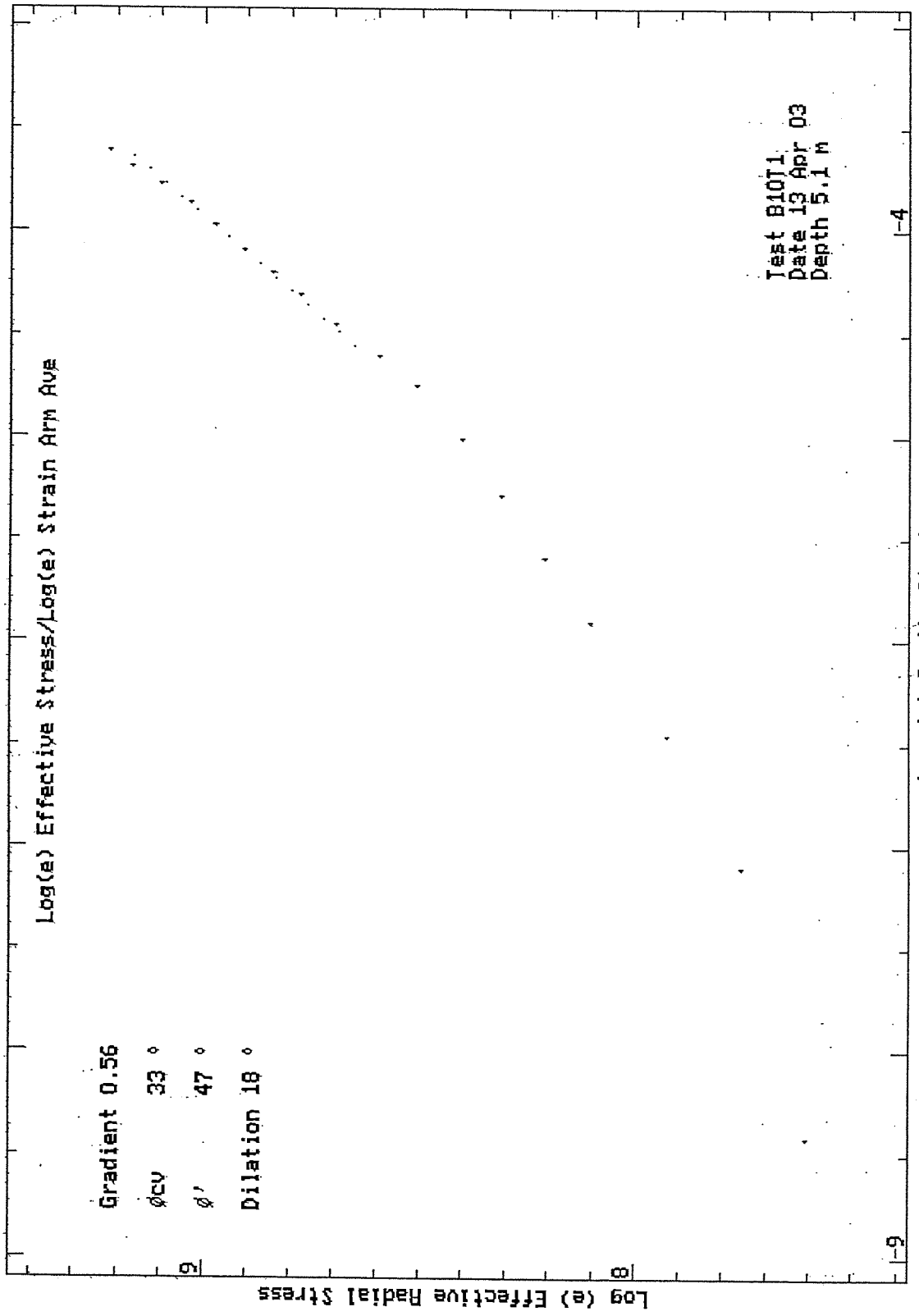
Log(a) Effective Stress/Log(a) Strain Arm Ave
Gradient 0.56
ϕcv 33 °
ϕ' 47 °
Dilation 18 °
Test B10T1
Date 13 Apr 03
Depth 5.1 m
Log (a) Effective Radial Stress
Log (a) Cavity Strain
-9
-8
-4

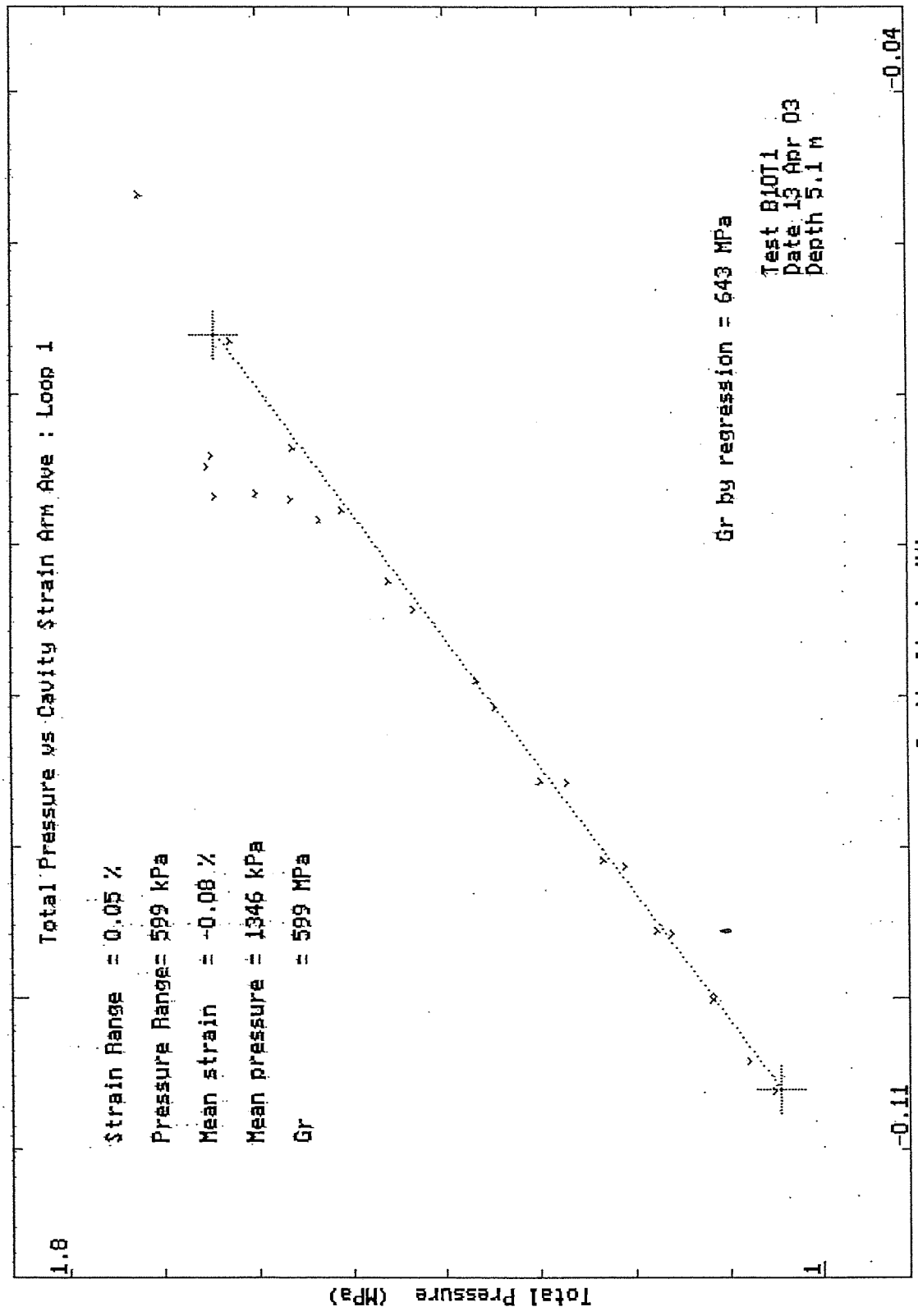
Total Pressure vs Cavity Strain Arm Ave : Loop 1
Strain Range = 0.05 %
Pressure Range= 599 kPa
Mean strain = -0.08 %
Mean pressure = 1346 kPa
Gr = 599 MPa
Gr by regression = 643 MPa
Test B10T1
Date 13 Apr 03
Depth 5.1 m
1.8
1
-0.11
-0.04
Cavity Strain (%)
Total Pressure (MPa)

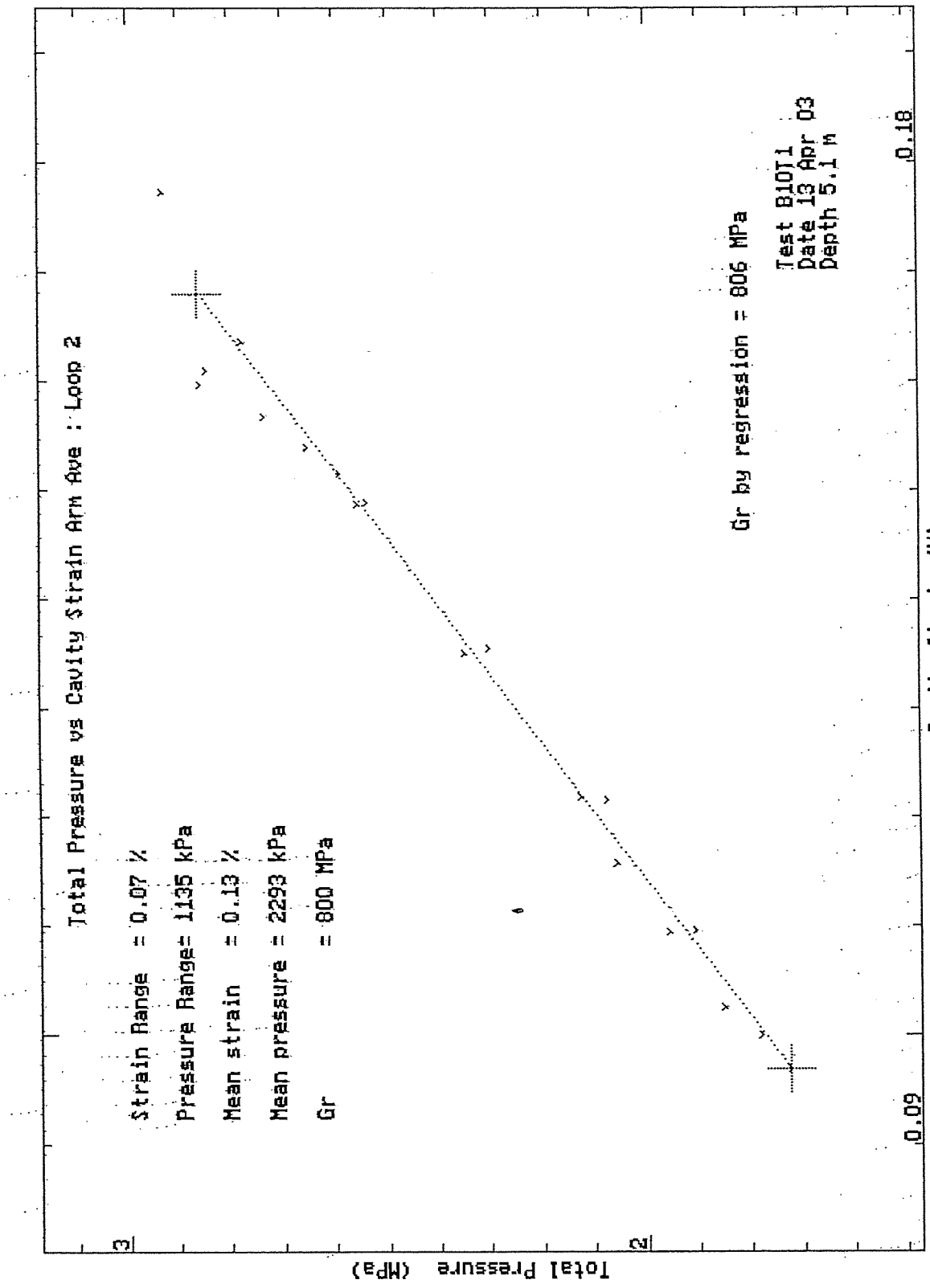
Total Pressure vs Cavity Strain Arm Ave : Loop 2
Strain Range = 0.07 %
Pressure Range= 1135 kPa
Mean strain = 0.13 %
Mean pressure = 2293 kPa
Gr = 800 MPa
Gr by regression = 806 MPa
Test B10T1
Date 13 Apr 03
Depth 5.1 m
Total Pressure (MPa)
Cavity Strain (%)
0.09
0.18
2
3

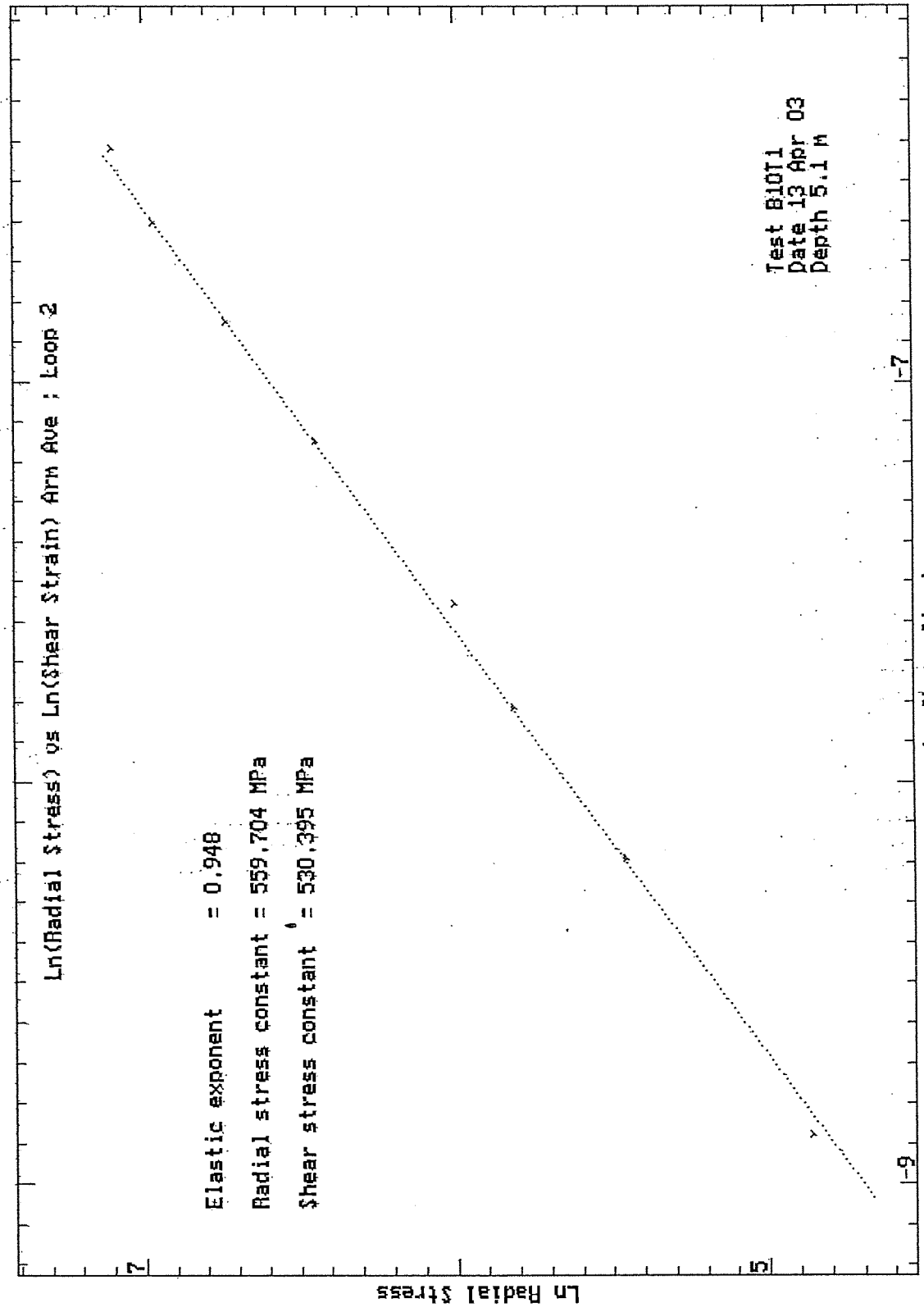
Ln(Radial Stress) vs Ln(Shear Strain) Arm Ave : Loop 2
Elastic exponent = 0,948
Radial stress constant = 559,704 MPa
Shear stress constant = 530,395 MPa
Test B10T1
Date 13 Apr 03
Depth 5,1 m
Ln Radial Stress
Ln Shear Strain
-5
-7
-9

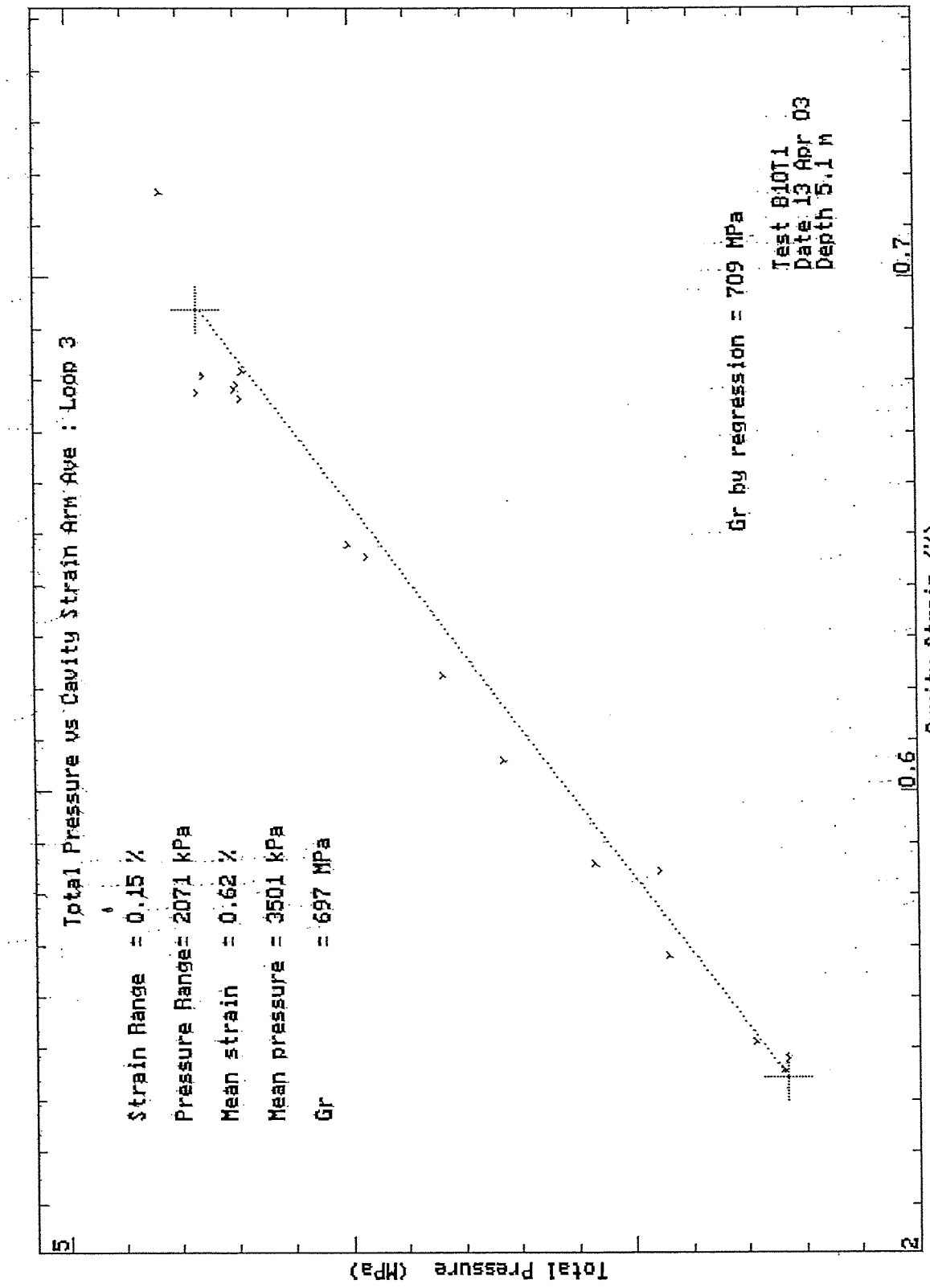
Total Pressure vs Cavity Strain Arm Ave : Loop 3
Strain Range = 0.15 %
Pressure Range= 2071 kPa
Mean strain = 0.62 %
Mean pressure = 3501 kPa
Gr = 697 MPa
Gr by regression = 709 MPa
Test B10T1
Date 13 Apr 03
Depth 5.1 m
Total Pressure (MPa)
Cavity Strain (%)
5
2
0.6
0.7

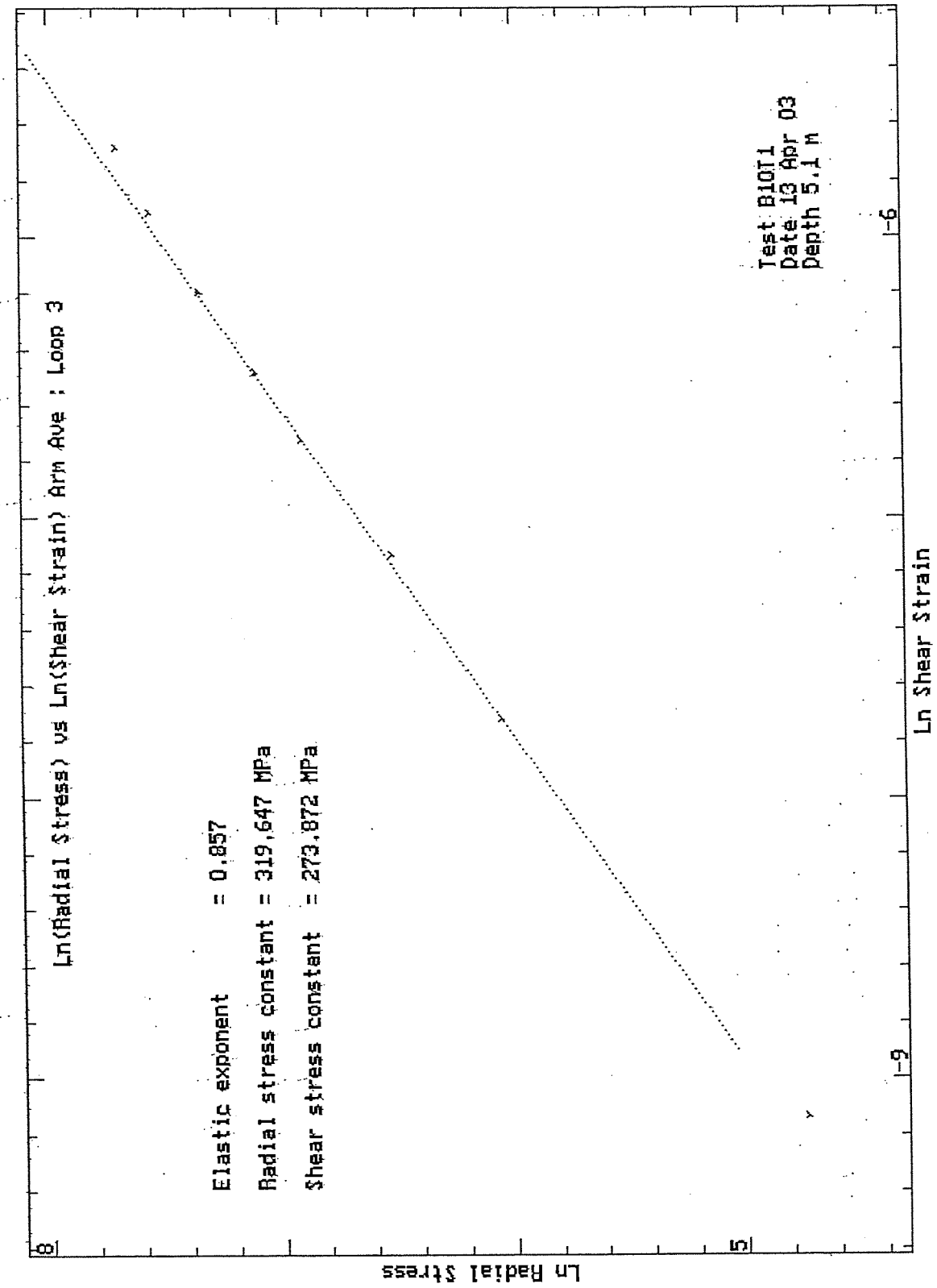
Ln(Radial Stress) vs Ln($hear Strain) Arm Ave : Loop 3
Elastic exponent = 0.857
Radial stress constant = 319.647 MPa
$hear stress constant = 273.872 MPa
Test B1QT1
Date 13 Apr 03
Depth 5.1 m
Ln Radial Stress
Ln Shear Strain
8
5
-9
-6

TEST RECORD SHEET - HIGH PRESSURE DILATOMETER

SITE	Date	Day	Borehole	Test No	Depth
LERWICK	17-4-03	THU	11	1	3.1M

Material: SANDSTONE

Weather	Water Table	Time Now	Drilling End	Orientation	CHL
BEAUTIFUL	SEA LEVEL				✓

Drilling	Pocket

Diameter	Distance	Rate	Core Description	Length

Wet/Dry	Rig	Driller	Core Quality	Size
WET	SKATE 2)			

Pres/Incrmnt	Wait Time	Creep Time	Cycle Time	Disc No.	Operator	Engineer
			10 sec			

ZERO READINGS: TICK

Machine Diameter 95 mm

Arm 1	Arm 2	Arm 3	Arm 4	Arm 5	Arm 6	T/Press.	Battery
AS	FOR	BIRT I				A: B:	

Calibrations:

Strain Arm Calibration date:	2-10-02	Test No:
Total Pressure Cell Calibration date:	6-3-03	Test No:
Membrane Stiffness Calibration date:	19-3-03	Test No: C999T99
Membrane Compression Calibration date:	"	Test No: "
New Membrane fitted date:	"	

Test Comments:

Time	Line No.	Start Test at: 06:12
06:12	50	START PUMPING
	81	HOLD ⇒ Loop (1)
	121	Loop (2)
	159	Loop (3) - BIGGER
	205	Loop (4)
	330	DOWN - LOT of CREEP
		OIL VERY LOW

Test Ends at 07:06

Max. Pressure reached: 10 MPa

General Comments

CAMBRIDGE INSITU, Little Eversden, Cambridge, England CB3 7HE
Telephone: 01223 262 361 Fax:- 01223 263 947

HIGH PRESSURE DILATOMETER RESULTS SUMMARY SHEET

Site:- Bressay Bridge Test :- B11T1 Test Date :- 17th April 2003
Material :- Sandstone Depth (m) :- 3.1 Water depth (m) :- -

Analysis of Insitu Lateral Stress (Po) :-

		Arm Av.
Marsland and Randolph (Iterative Analysis)	kPa	1993
Best Estimate of Po	kPa	2000
Assessed diameter of borehole	mm	99.1

Analysis of Undrained Shear Strength (Cu) :-

Gibson and Anderson	kPa	6058
Failure pressure (Pf)	kPa	6650
Limit Pressure (P_L)	MPa	26

Strength of Sands Analysis (Hughes, Wroth & Windle)

Friction angle at const. vol.	deg	33	(assumed)
Angle of Friction	deg	54	
Angle of Dilation	deg	28	

Analysis of Shear Modulus (G) :-

Initial Modulus (Gi)	MPa	111

Linear Analysis of Reload Loops (Gr) :-

Loop	Value	Co-ordinate		Amplitude	
no.	(MPa)	Strain %	Pressure kPa	Strain %	Pressure kPa
1	576	-0.16	1273	0.043	495
2	573	0.11	1893	0.07	805
3	489	0.49	2365	0.176	1719
4	585	1.11	3567	0.166	1917

Non-linear Analysis of Reloading data :-

Loop	Linearity exponent	Radial Stress Coeff.	Shear Stress Coeff.
no.	(β)	(MPa)	(MPa)
2	0.955	471	449
3	0.855	228	195
4	0.82	216	178

Test Analysed By :- PGH
Date :- 27th May 2003

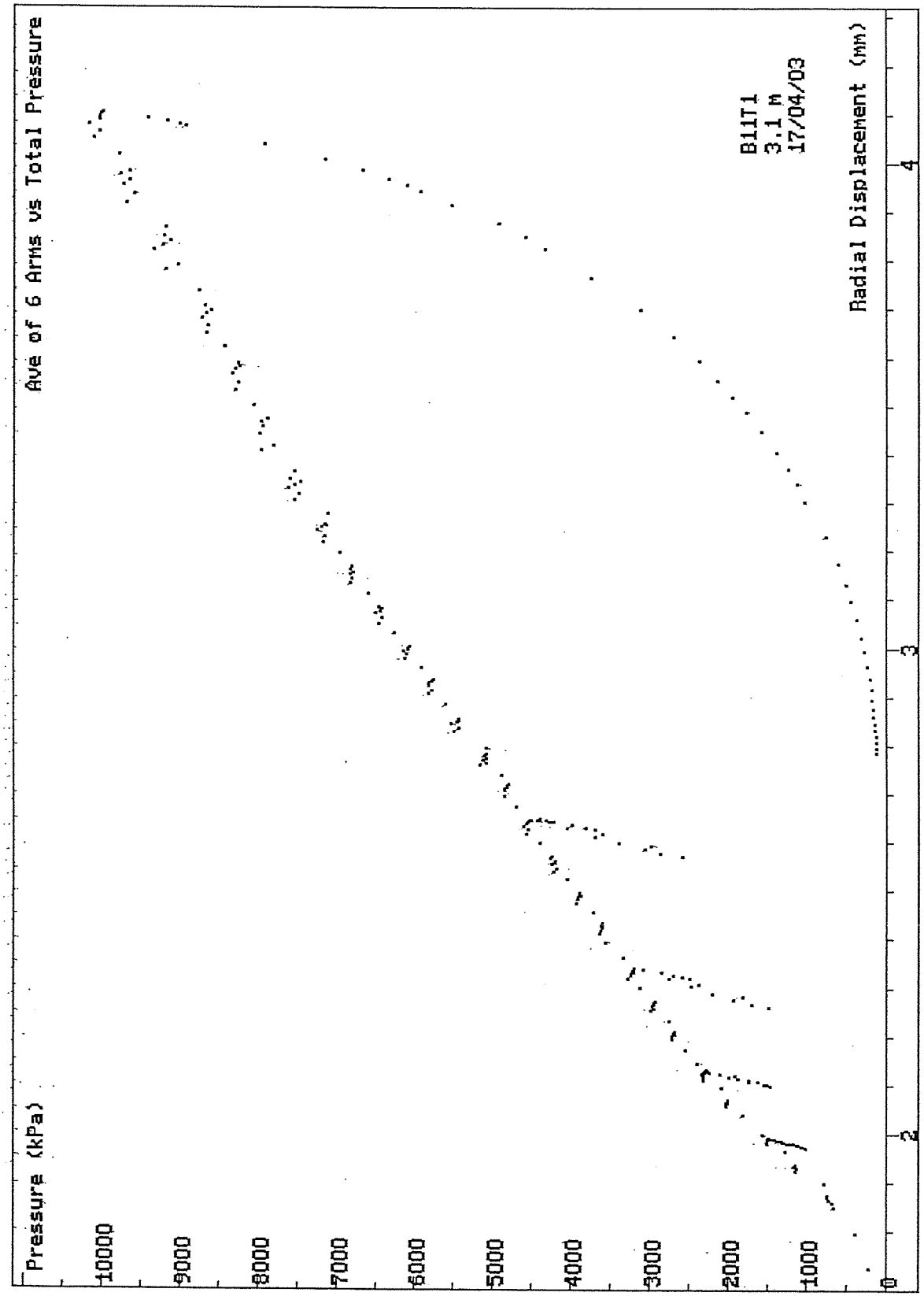

SCREEN DUMP Test: B11T1 Date: 17/04/03 Depth: 3.10m
HPD95 Pressuremeter tests Bressay Bridge Site Investigation
Cambridge Insitu for Seacore April 2003

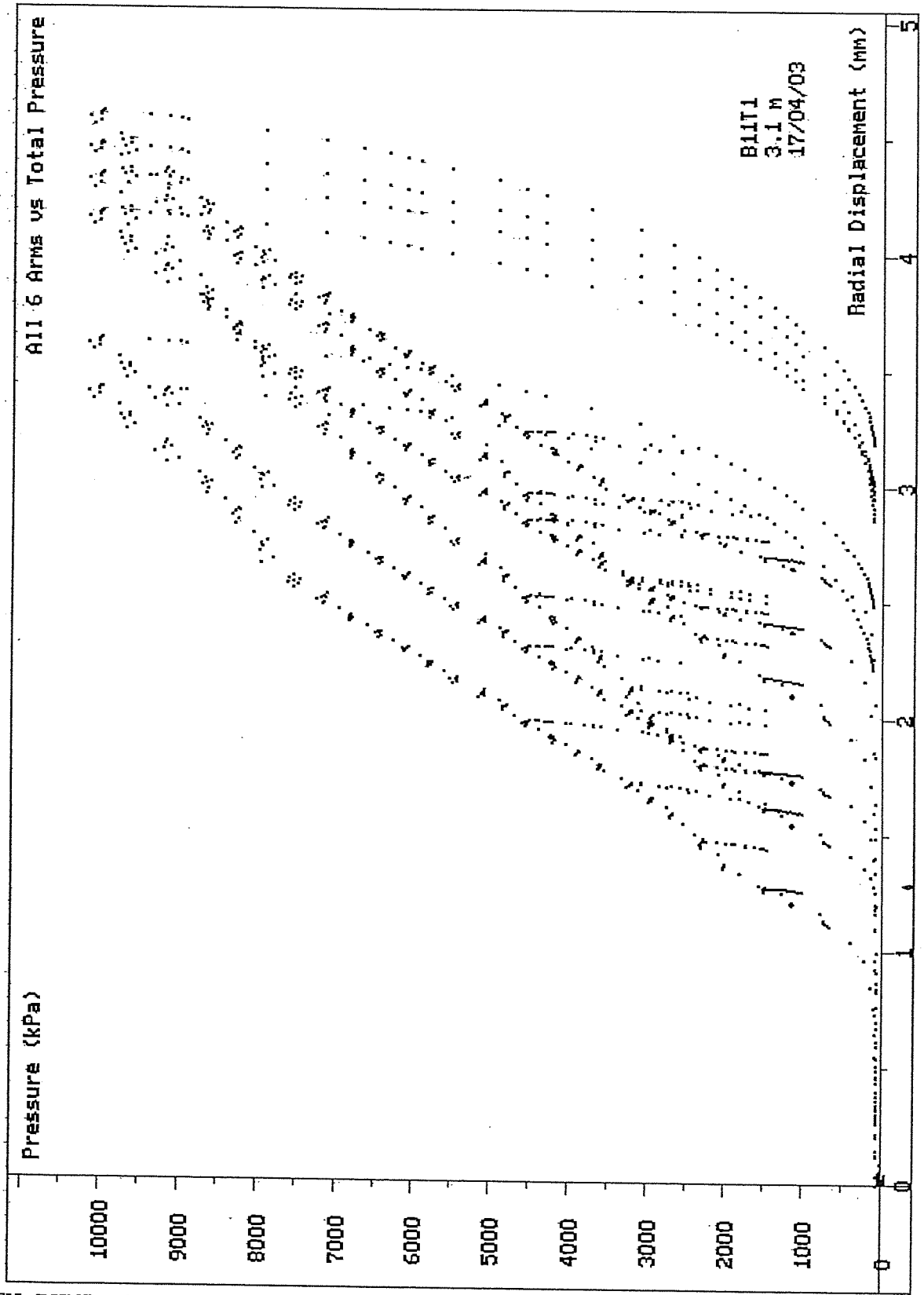

SCREEN DUMP Test: B11T1 Date: 17/04/03 Depth: 3.10m
HPD95 Pressuremeter tests Bressay Bridge Site Investigation
Cambridge Insitu for Seacore April 2003

Marsland and Randolph Pressure/Strain Arm Ave
Gi 111 MPa
Pf 6650 kPa
Po 1993 kPa
Tf 4649 kPa
Pf
Po+Tf
Po
P/Log(e) E
Test B11T1
Date 17 Apr 03
Depth 3.1 m
Pressure (MPa)
Radial displacement (mm)
10
0
2
3
Creep
0.06 mm

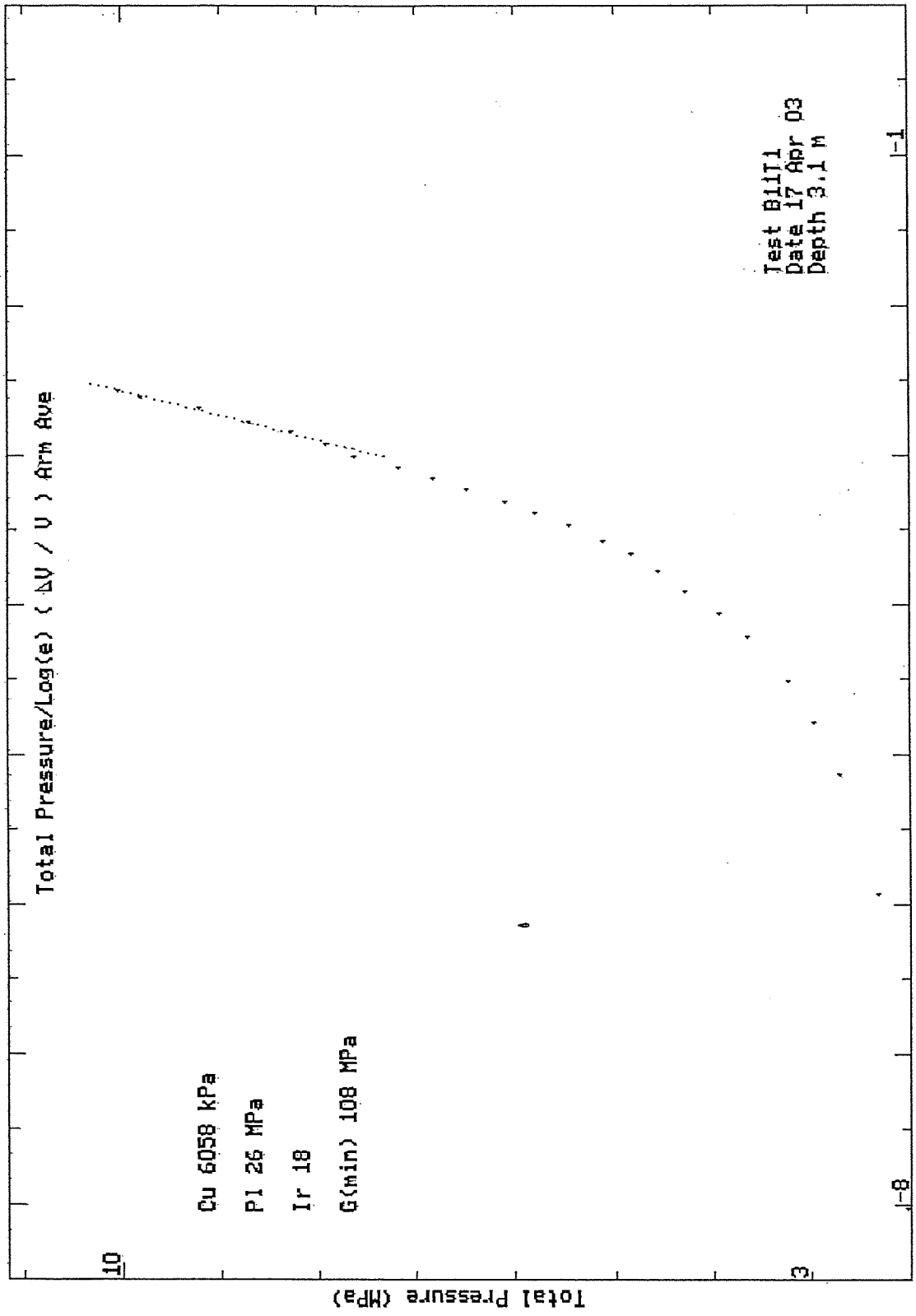
Total Pressure/Log(e) (ΔV / V) Arm Ave
Test B11T1
Date 17 Apr 03
Depth 3.1 m
Cu 6058 kPa
Pl 26 MPa
Ir 18
G(min) 108 MPa
10
3
-8
-1
Total Pressure (MPa)
Ln 1-(1/(1+E)²)

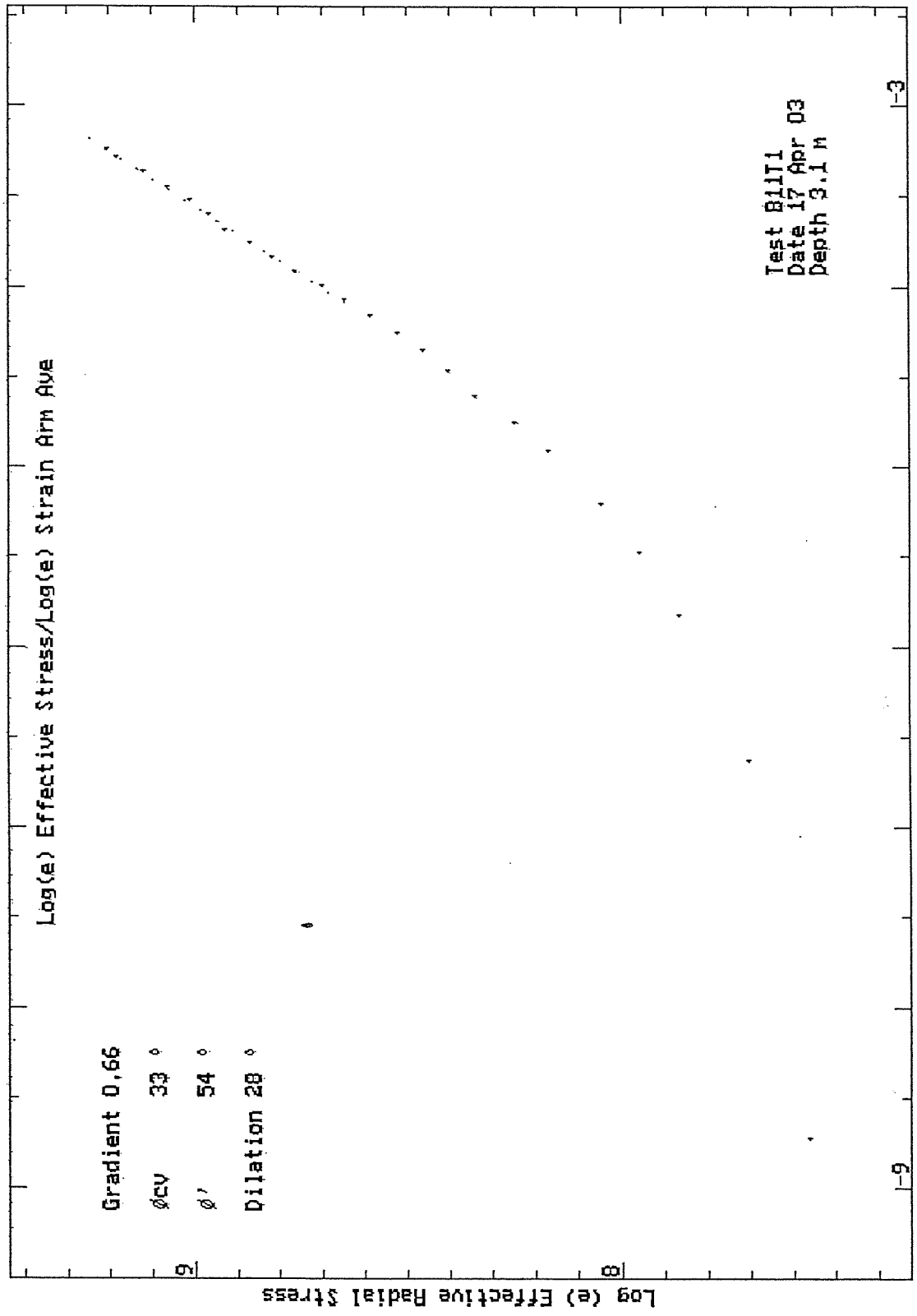
Log(e) Effective Stress/Log(e) Strain Arm Ave
Test B11T1
Date 17 Apr 03
Depth 3.1 m
Gradient 0.66
øcv 33 °
ø' 54 °
Dilation 28 °
Log (e) Effective Radial Stress
Log (e) Cavity Strain
-9
-8
-3

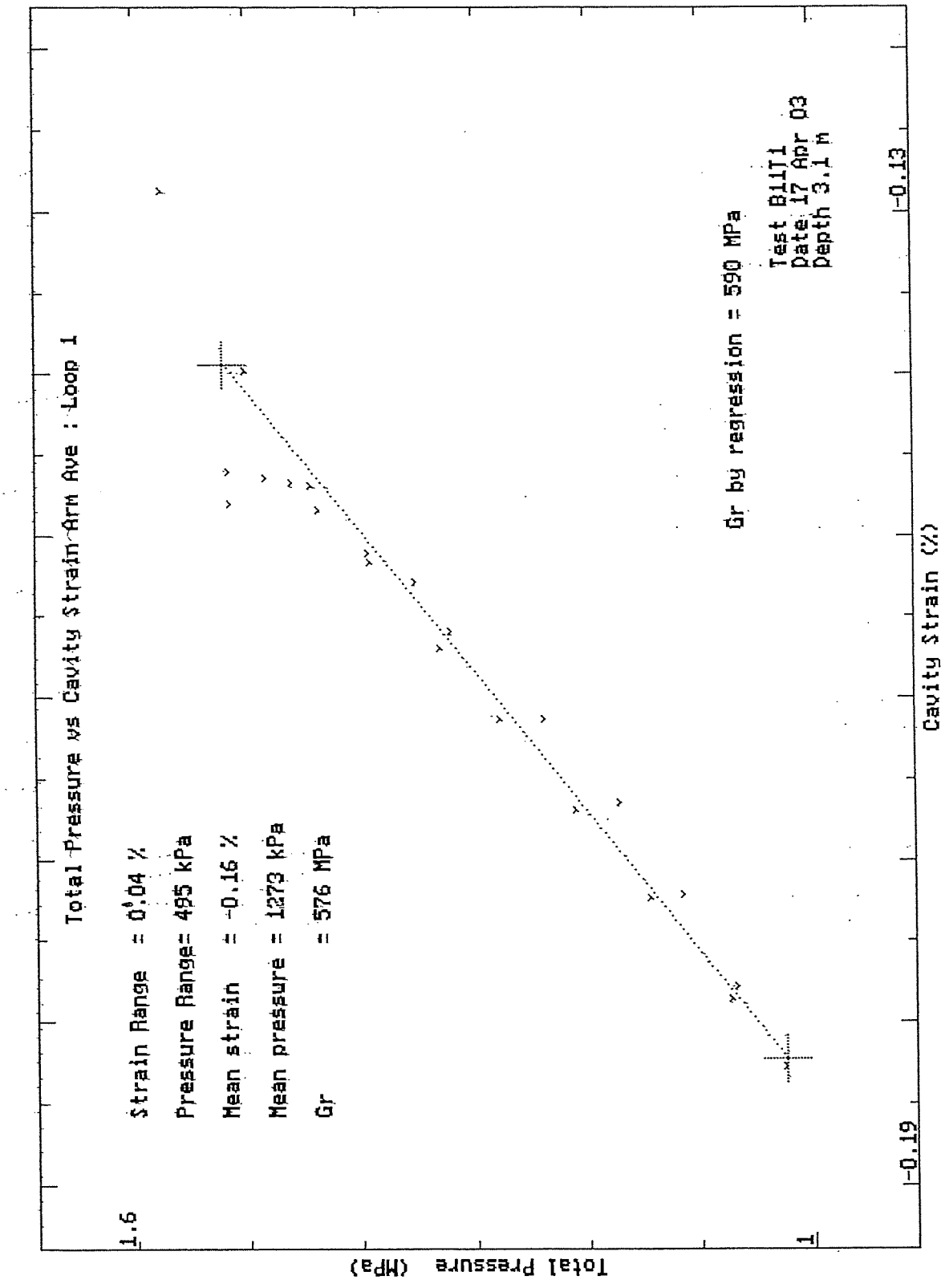
Total Pressure vs Cavity Strain-Arm Ave : Loop 1
Strain Range = 0.04 %
Pressure Range= 495 kPa
Mean strain = -0.16 %
Mean pressure = 1273 kPa
Gr = 576 MPa
Gr by regression = 590 MPa
Test B11T1
Date 17 Apr 03
Depth 3.1 m
1.6
1
-0.19
-0.13
Total Pressure (MPa)
Cavity Strain (%)

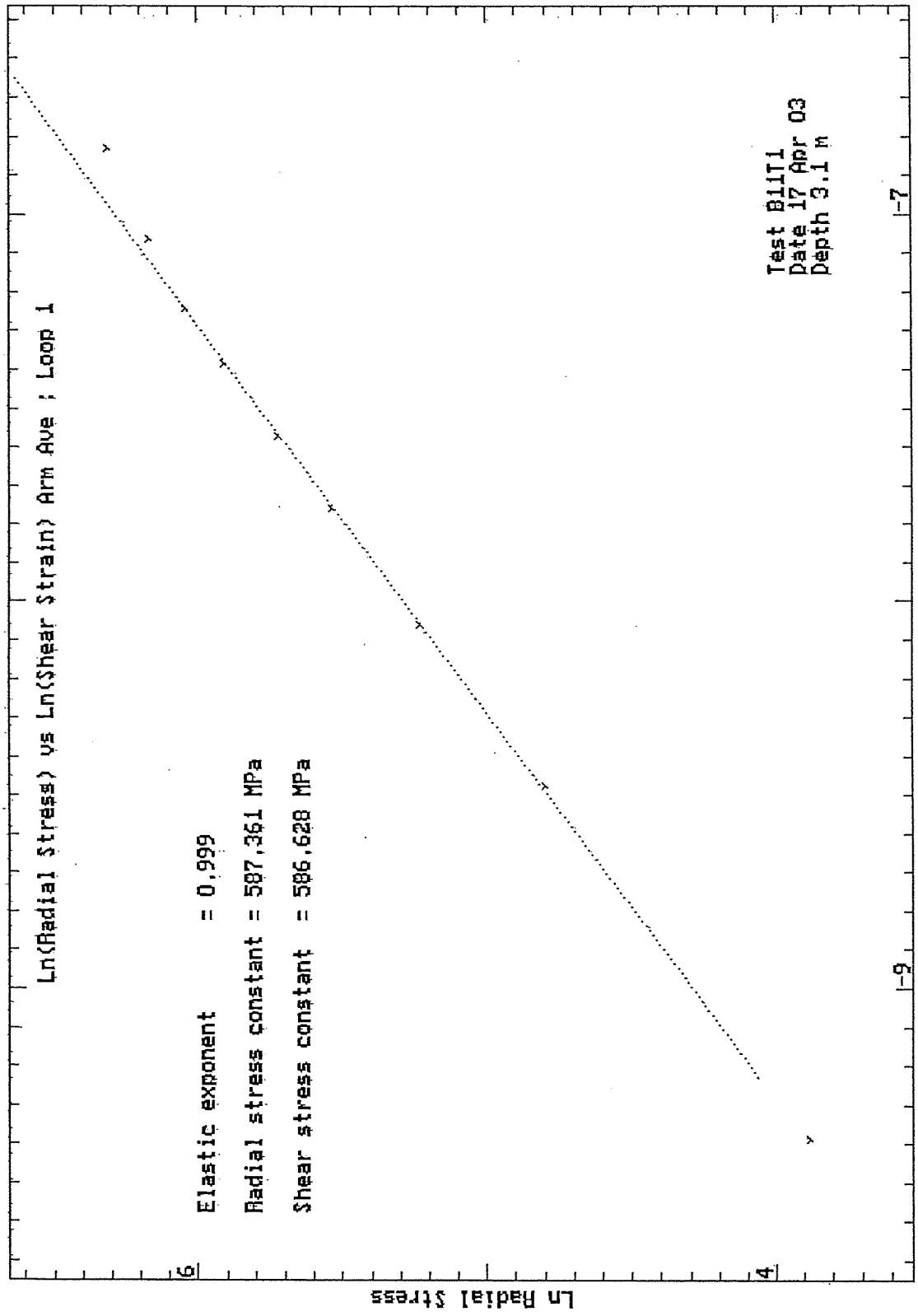
Ln(Radial Stress) vs Ln(Shear Strain) Arm Ave ; Loop 1
Elastic exponent = 0.999
Radial stress constant = 587.361 MPa
Shear stress constant = 586.628 MPa
Test B11T1
Date 17 Apr 03
Depth 3.1 m
Ln Radial Stress
Ln Shear Strain
-6
-4
-9
-7

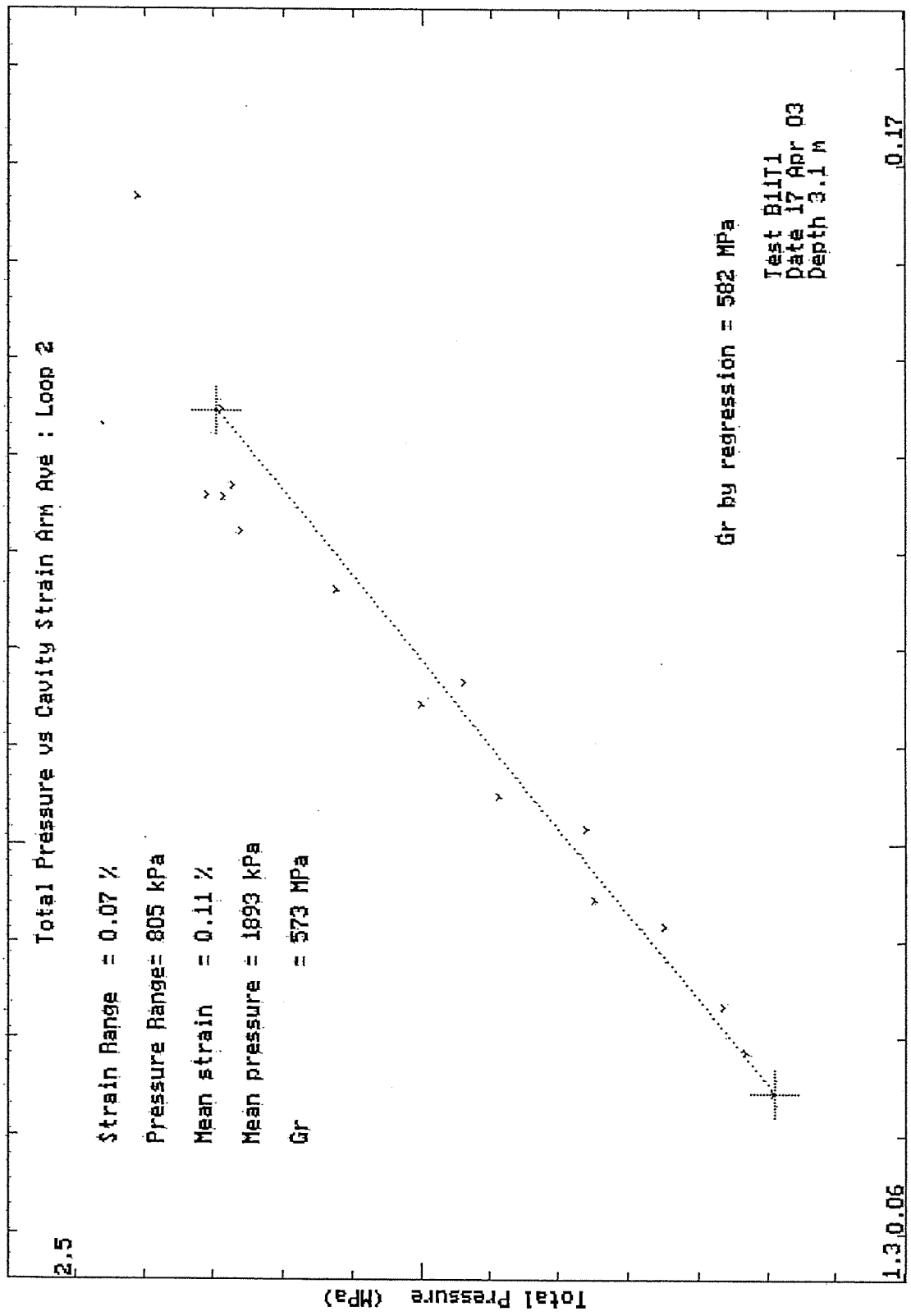
Total Pressure vs Cavity Strain Arm Ave : Loop 2
Strain Range = 0.07 %
Pressure Range= 805 kPa
Mean strain = 0.11 %
Mean pressure = 1893 kPa
Gr = 573 MPa
Gr by regression = 582 MPa
Test B11T1
Date 17 Apr 03
Depth 3.1 m
2.5
1.3
0.06
0.17
Total Pressure (MPa)
Cavity Strain (%)

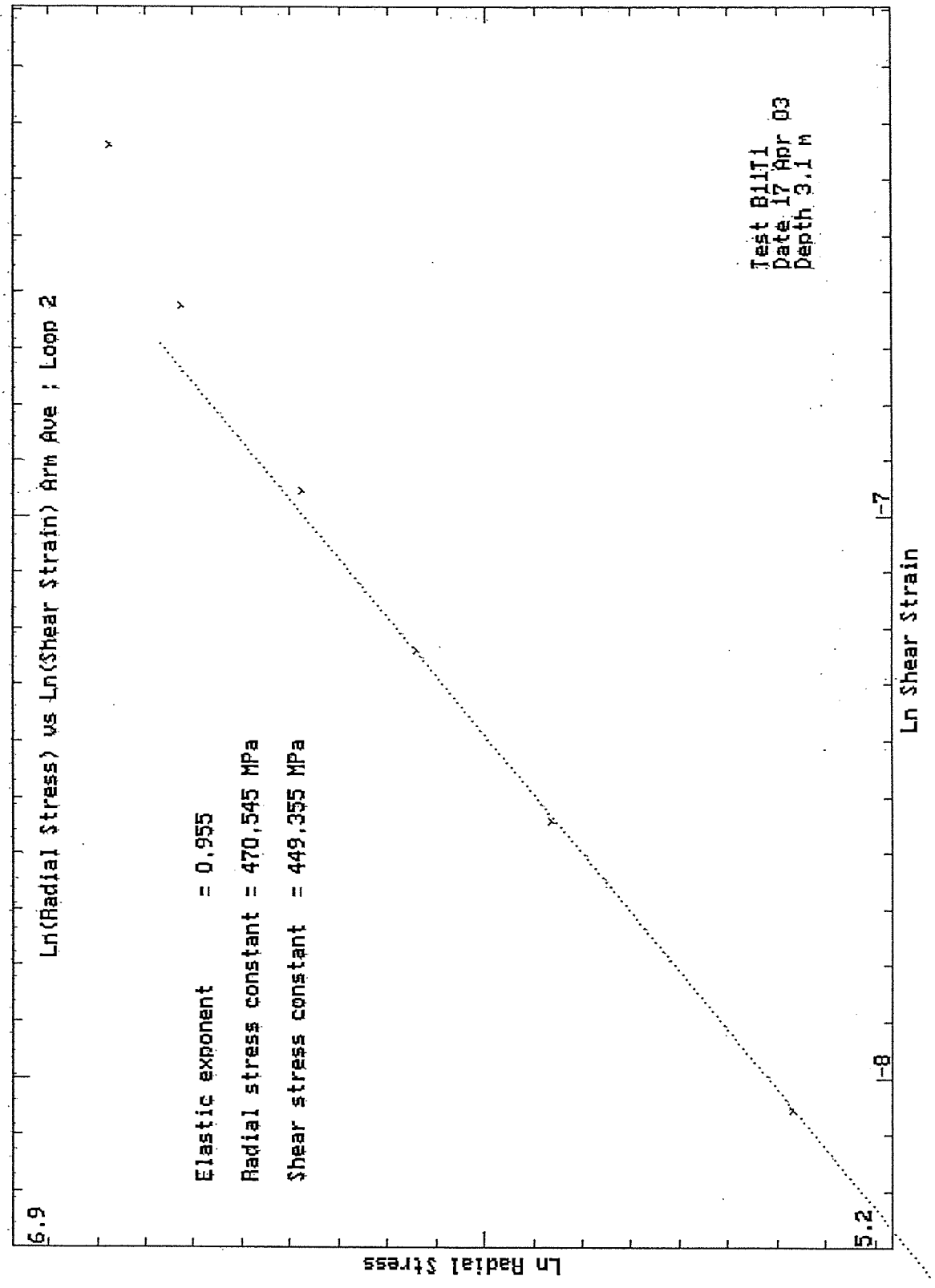
Ln(Radial $tress) vs Ln($hear $train) Arm Ave ; Loop 2
Elastic exponent = 0,955
Radial stress constant = 470,545 MPa
$hear stress constant = 449,355 MPa
Test B11T1
Date 17 Apr 03
Depth 3,1 m
Ln Radial $tress
Ln Shear Strain
6.9
5.2
-7
-8

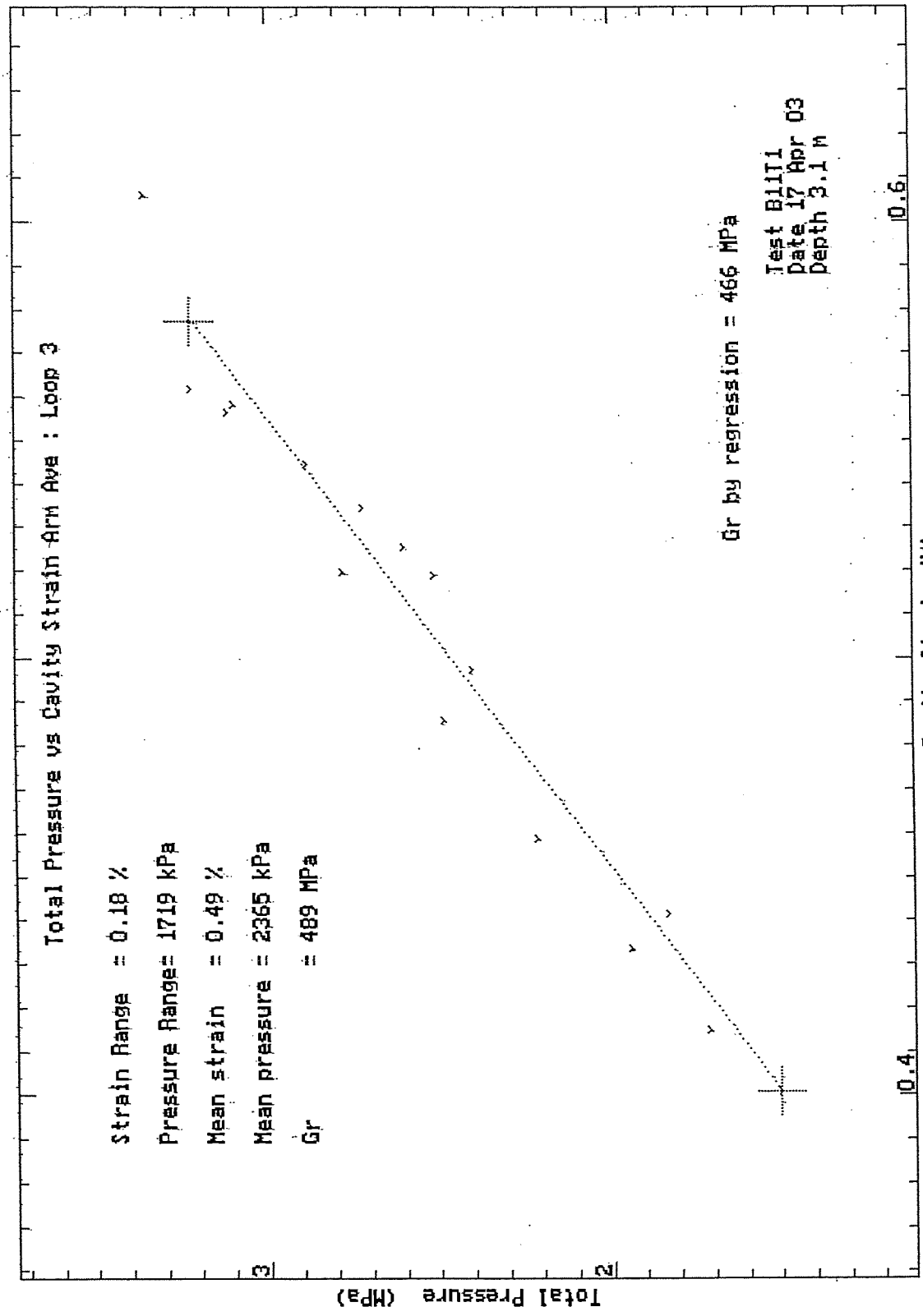
Total Pressure vs Cavity Strain Arm Ave : Loop 3
Strain Range = 0.18 %
Pressure Range= 1719 kPa
Mean strain = 0.49 %
Mean pressure = 2365 kPa
Gr = 489 MPa
Gr by regression = 466 MPa
Test B11T1
Date 17 Apr 03
Depth 3.1 m
Total Pressure (MPa)
Cavity Strain (%)
0.4
0.6
2
3

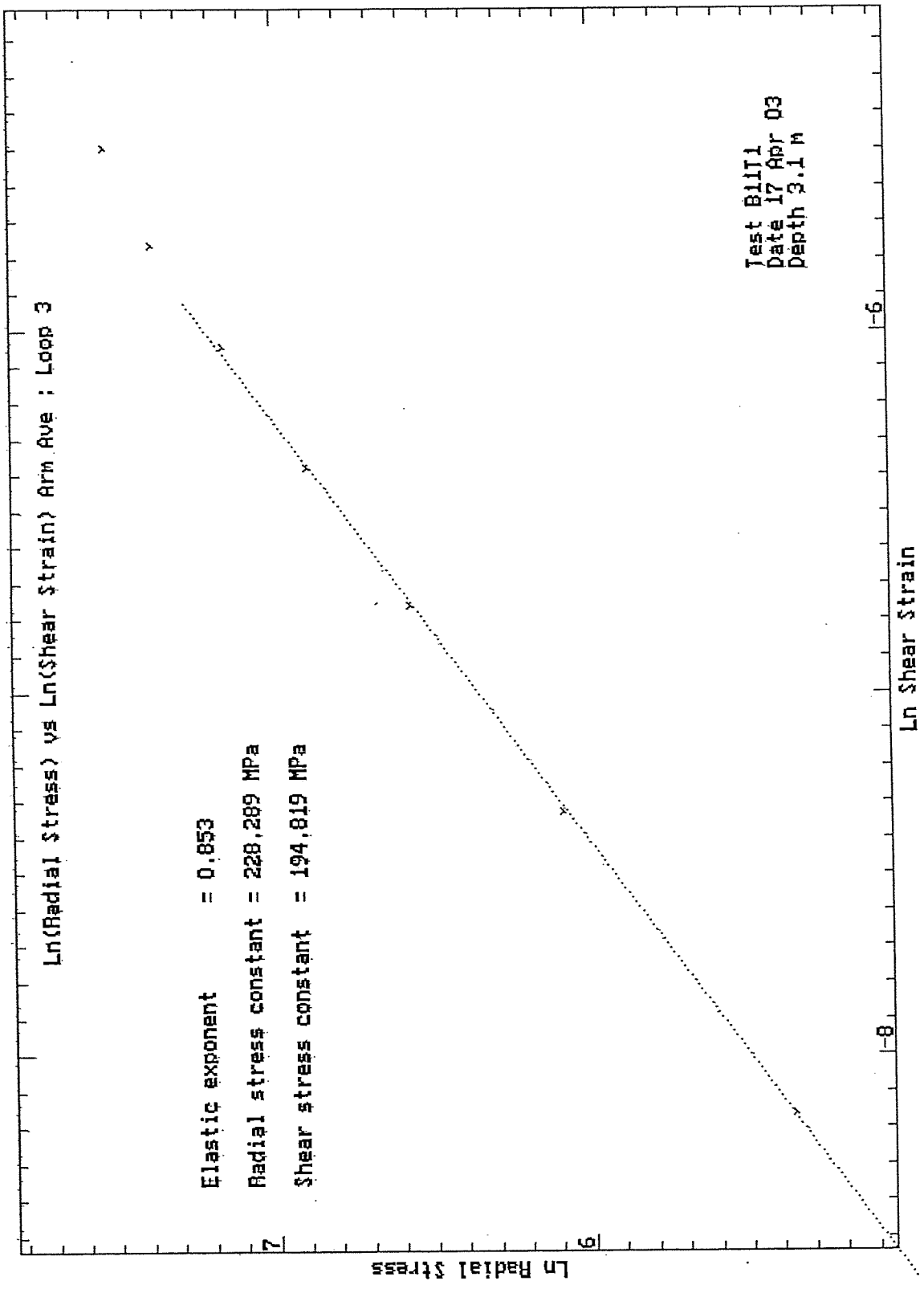
Ln(Radial Stress) vs Ln(Shear Strain) Arm Ave : Loop 3
Elastic exponent = 0.853
Radial stress constant = 228.289 MPa
Shear stress constant = 194.819 MPa
Test B1IT1
Date 17 Apr 03
Depth 3.1 m
Ln Radial Stress
Ln Shear Strain
-7
-6
-8
-6

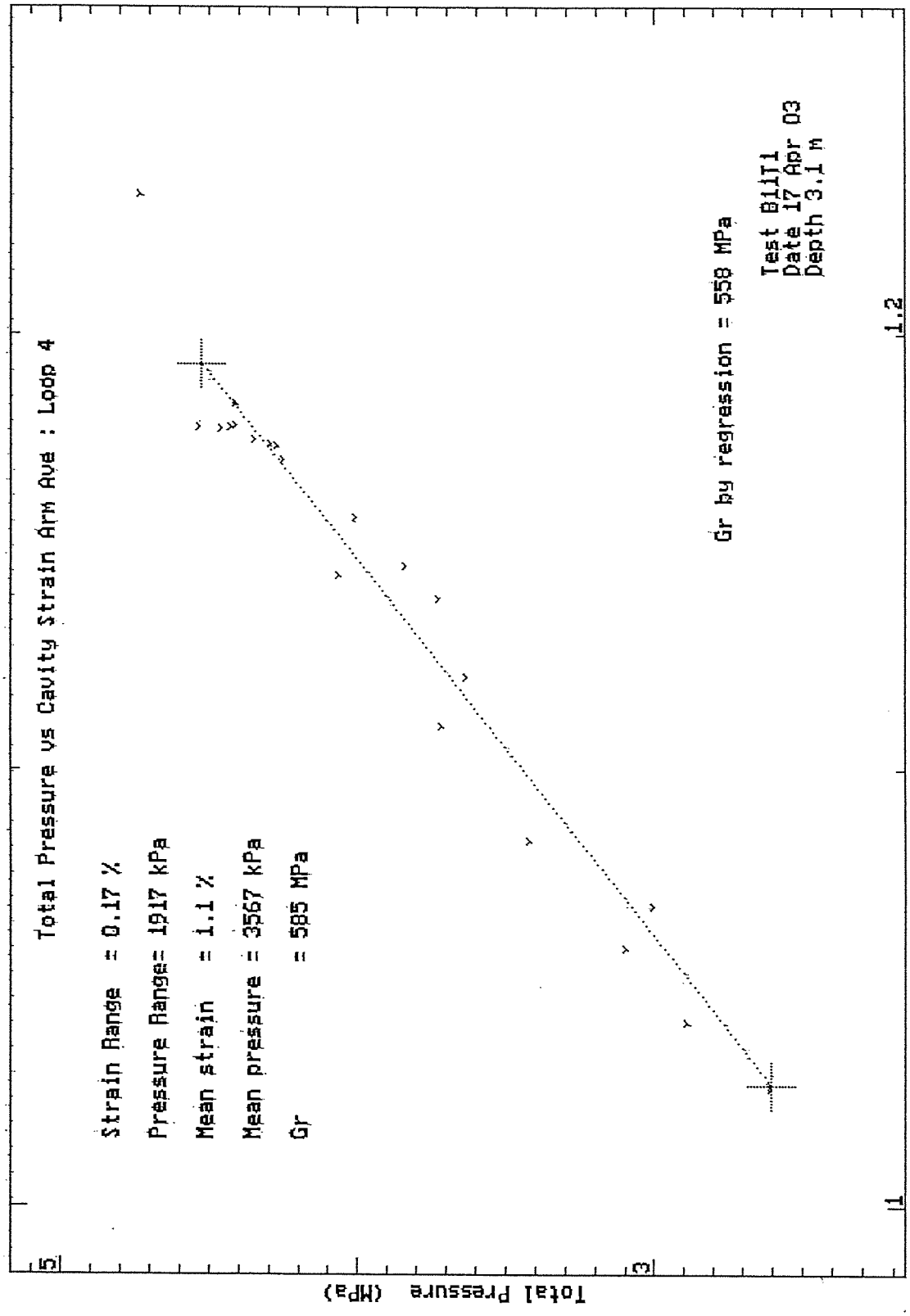
Total Pressure vs Cavity Strain Arm Ave : Loop 4
Strain Range = 0.17 %
Pressure Range= 1917 kPa
Mean strain = 1.1 %
Mean pressure = 3567 kPa
Gr = 585 MPa
Gr by regression = 558 MPa
Test B1IT1
Date 17 Apr 03
Depth 3.1 m
Total Pressure (MPa)
Cavity Strain (%)
5
3
1
1.2

Ln(Radial Stress) vs Ln($hear Strain) Arm Ave : Loop 4
Elastic exponent = 0.822
Radial stress constant = 216,262 MPa
Shear stress constant = 177,773 MPa
Test B11T1
Date 17 Apr 03
Depth 3.1 m
Ln Radial Stress
Ln Shear Strain
-7
-9
-8
-6

TEST RECORD SHEET - HIGH PRESSURE DILATOMETER

Site	Date	Day	Borehole	Test No	Depth
HELWICK	16.4.03	WED	12	1	3.0

Material: CONGLOMERATE

Weather	Water Table	Time Now	Drilling End	Orientation	CHL
FINE & DRY	SGA COVER	18.21	17.15 APP	NK	✓

Drilling	Pocket

Diameter	Distance	Rate	Core Description	Length
			VERY MIXED	

Wet/Dry	Rig	Driller	Core Quality	Size
WET	SKAFE II		POOR	

Pres/Incrmnt	Wait Time	Creep Time	Cycle Time	Disc No.	Operator	Engineer
			10SEC			

ZERO READINGS: TICLY Machine Diameter 95 mm

Arm 1	Arm 2	Arm 3	Arm 4	Arm 5	Arm 6	T/Press.	Battery
1.3887	1.6542	1.5546	1.3735	1.4805	1.5377	A:.0097 B:.0900	12.45

Calibrations:

Strain Arm Calibration date:	2-10-02	Test No:
Total Pressure Cell Calibration date:	6-3-03	Test No:
Membrane Stiffness Calibration date:	10-3-03	Test No: C999 T99
Membrane Compression Calibration date:	"	Test No: "
New Membrane fitted date:		

Test Comments:

Time	Line No.	Start Test at: 1907	
		LOOP 1 @ L 45	900kPa
		LOOP 2 @ L 85	2.1 mPa
		LOOP 3 @ L 125	4 mPa NORM
		LOOP 4 @ L 160	5.4 mPa
		TO UNLOAD L 210	
		Test Ends at:	8.7 mPa
		Max. Pressure reached:	19.45

General Comments: INST IS TINY

CAMBRIDGE INSITU, Little Eversden, Cambridge, England CB3 7HE
Telephone: 01223 262 361 Fax:- 01223 263 947

HIGH PRESSURE DILATOMETER RESULTS SUMMARY SHEET

Site:- Bressay Bridge Test :- B12T1 Test Date :- 16th April 2003
Material :- Conglomerate Depth (m) :- 3.0 Water depth (m) :- -

---

Analysis of Insitu Lateral Stress (Po) :-

		Arm Av.
Marsland and Randolph (Iterative Analysis)	kPa	2000
Interpolation from Initial Modulus	kPa	1268
Best Estimate of Po	kPa	2000
Assessed diameter of borehole	mm	98.6

Analysis of Undrained Shear Strength (Cu) :-

Gibson and Anderson	kPa	3837
Failure pressure (Pf)	kPa	3929
Limit Pressure (P_L)	MPa	23

Strength of Sands Analysis (Hughes, Wroth & Windle)

Friction angle at const. vol.	deg	35	(assumed)
Angle of Friction	deg	49	
Angle of Dilation	deg	19	

Analysis of Shear Modulus (G) :-

Initial Modulus (Gi)	MPa	413

Linear Analysis of Reload Loops (Gr) :-

Loop	Value	Co-ordinate		Amplitude	
no.	(MPa)	Strain %	Pressure kPa	Strain %	Pressure kPa
1	220	-0.23	662	0.077	341
2	561	-0.02	1579	0.111	1247
3	771	0.20	2977	0.139	2138
4	851	0.37	3908	0.175	2965

Non-linear Analysis of Reloading data :-

Loop	Linearity exponent	Radial Stress Coeff.	Shear Stress Coeff.
no.	(β)	(MPa)	(MPa)
3	0.985	773	761
4	0.93	585	544

Test Analysed By :- PGH
Date :- 27th May 2003

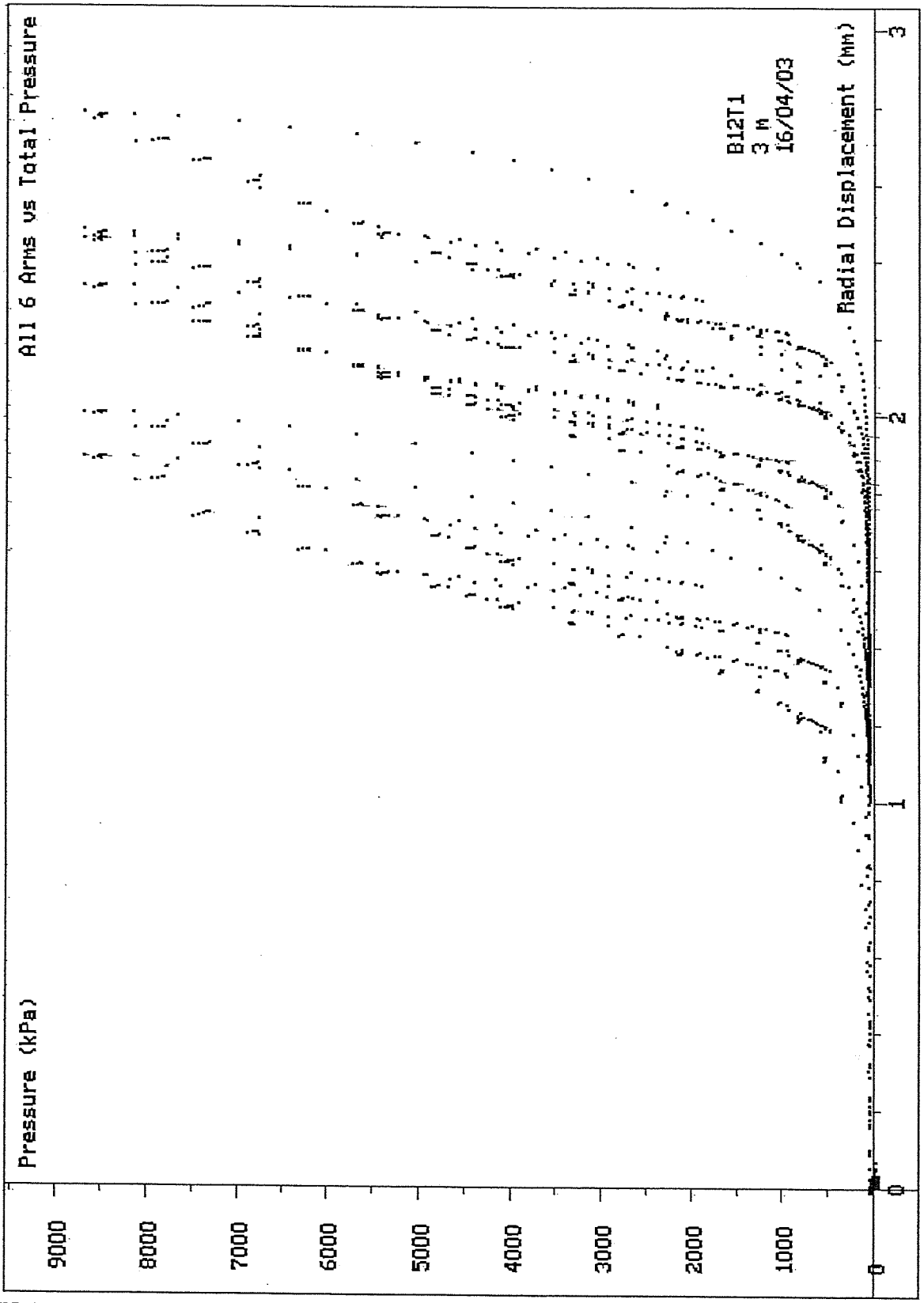

SCREEN DUMP Test: B12T1 Date: 16/04/03 Depth: 3.00m
HPD95 Pressuremeter tests Bressay Bridge Site Investigation
Cambridge Insitu for Seacore April 2003

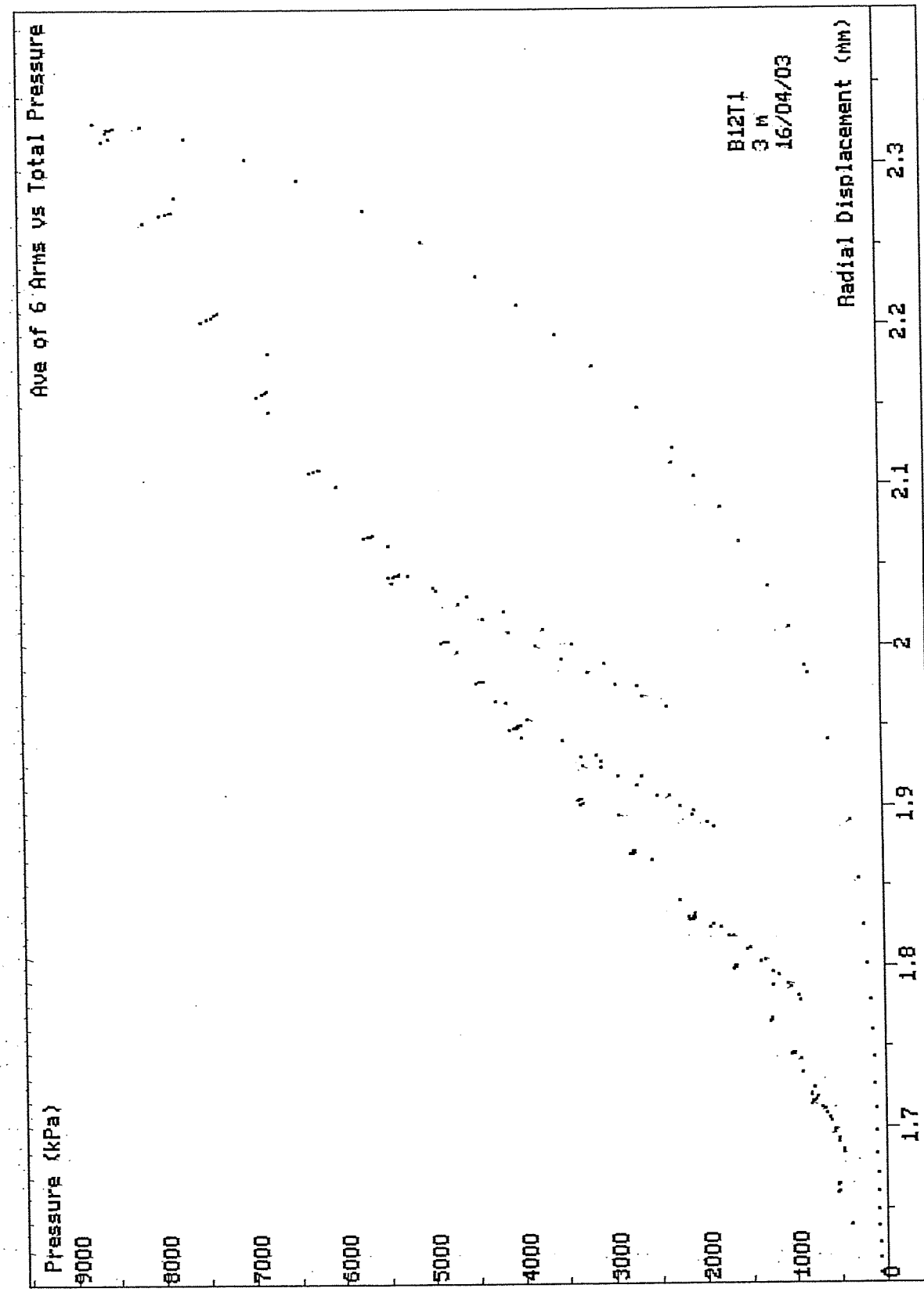

SCREEN DUMP Test: B12T1 Date: 16/04/03 Depth: 3.00m
HPD95 Pressuremeter tests Bressay Bridge Site Investigation
Cambridge Insitu for Seacore April 2003

Marsland and Randolph Pressure/Strain Arm Ave
Gi 413 MPa
Pf 3929 kPa
Po 2000 kPa
Tf 1956 kPa
Pf
Po+Tf
Po
1
P/Log(e) E
Test B12T1
Date 16 Apr 03
Depth 3 m
Pressure (MPa)
6
0
Radial displacement (mm)
Creep
0.01 mm

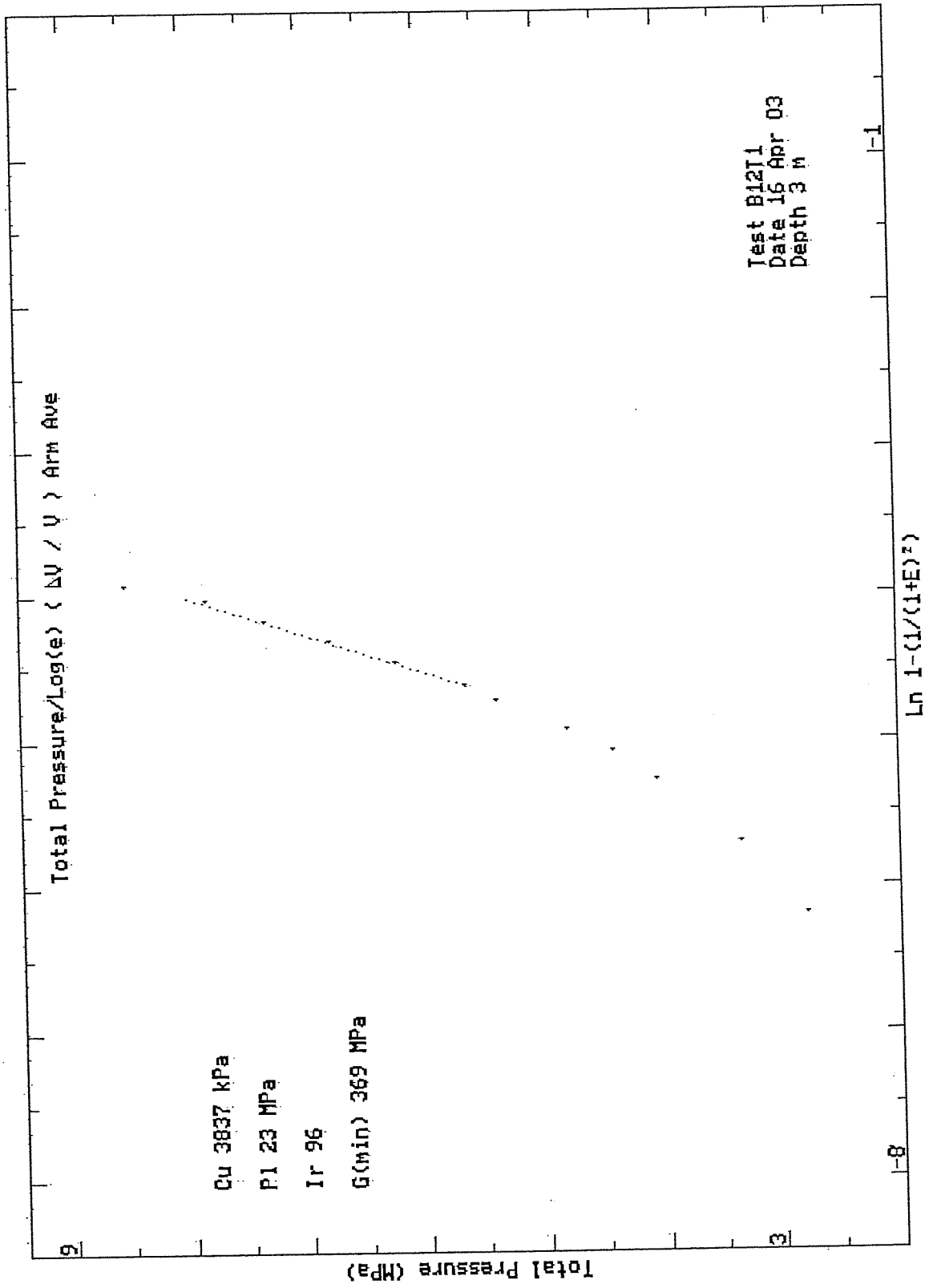

HPD95 Pressuremeter tests
Cambridge Insitu for Seacore

Bressay Bridge Site Investigation
April 2003

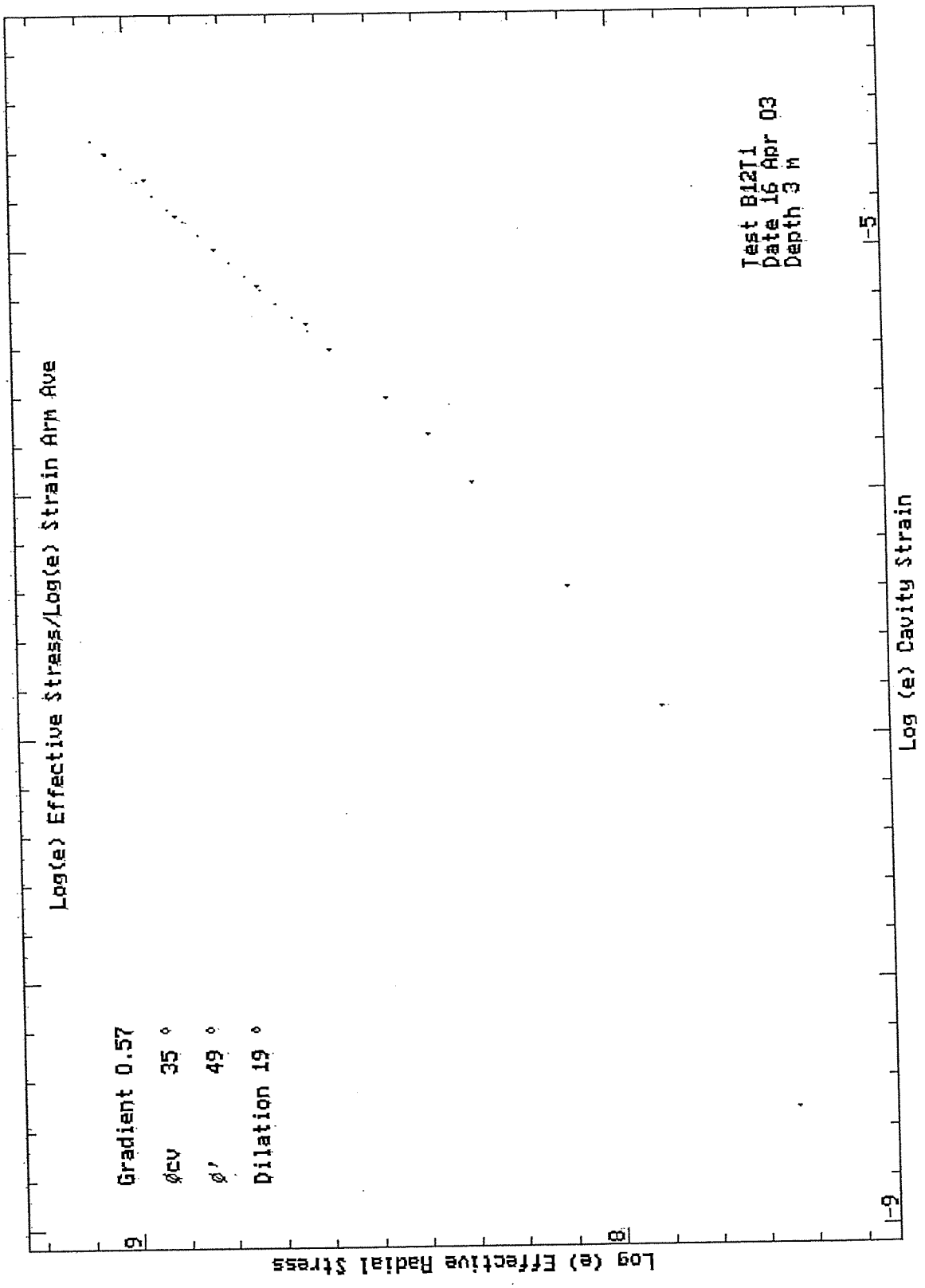
Log(e) Effective Strass/Log(e) Strain Arm Ave
Test B12T1
Date 16 Apr 03
Depth 3 m
Gradient 0.57
φcv 35 °
φ' 49 °
Dilation 19 °
Log (e) Effective Radial Stress
Log (e) Cavity Strain
-9
-8
-5

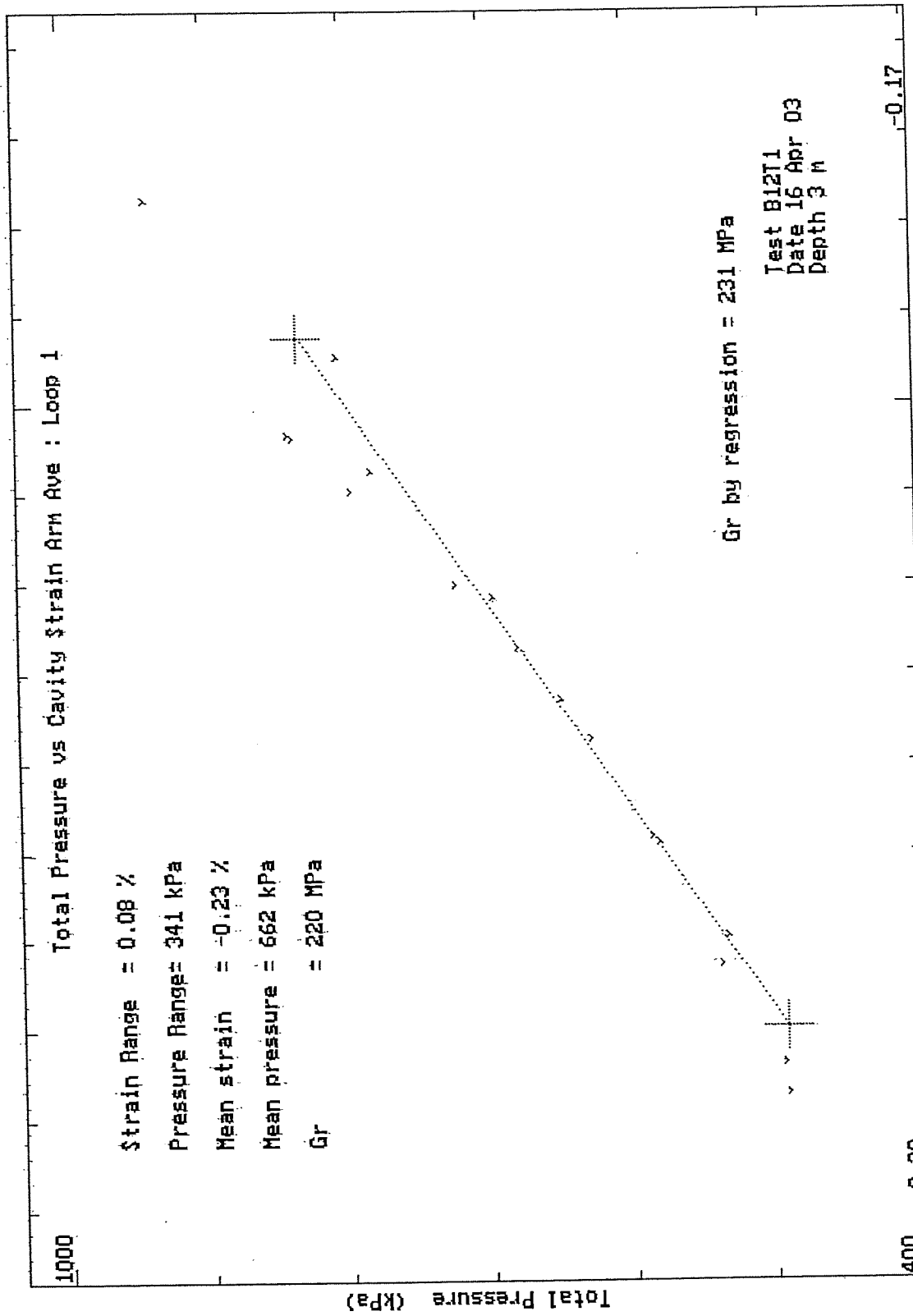
Total Pressure vs Cavity Strain Arm Ave : Loop 1
Strain Range = 0.08 %
Pressure Range= 341 kPa
Mean strain = -0.23 %
Mean pressure = 662 kPa
Gr = 220 MPa
Gr by regression = 231 MPa
Test B12T1
Date 16 Apr 03
Depth 3 m
1000
400
-0.29
-0.17
Total Pressure (kPa)
Cavity Strain (%)

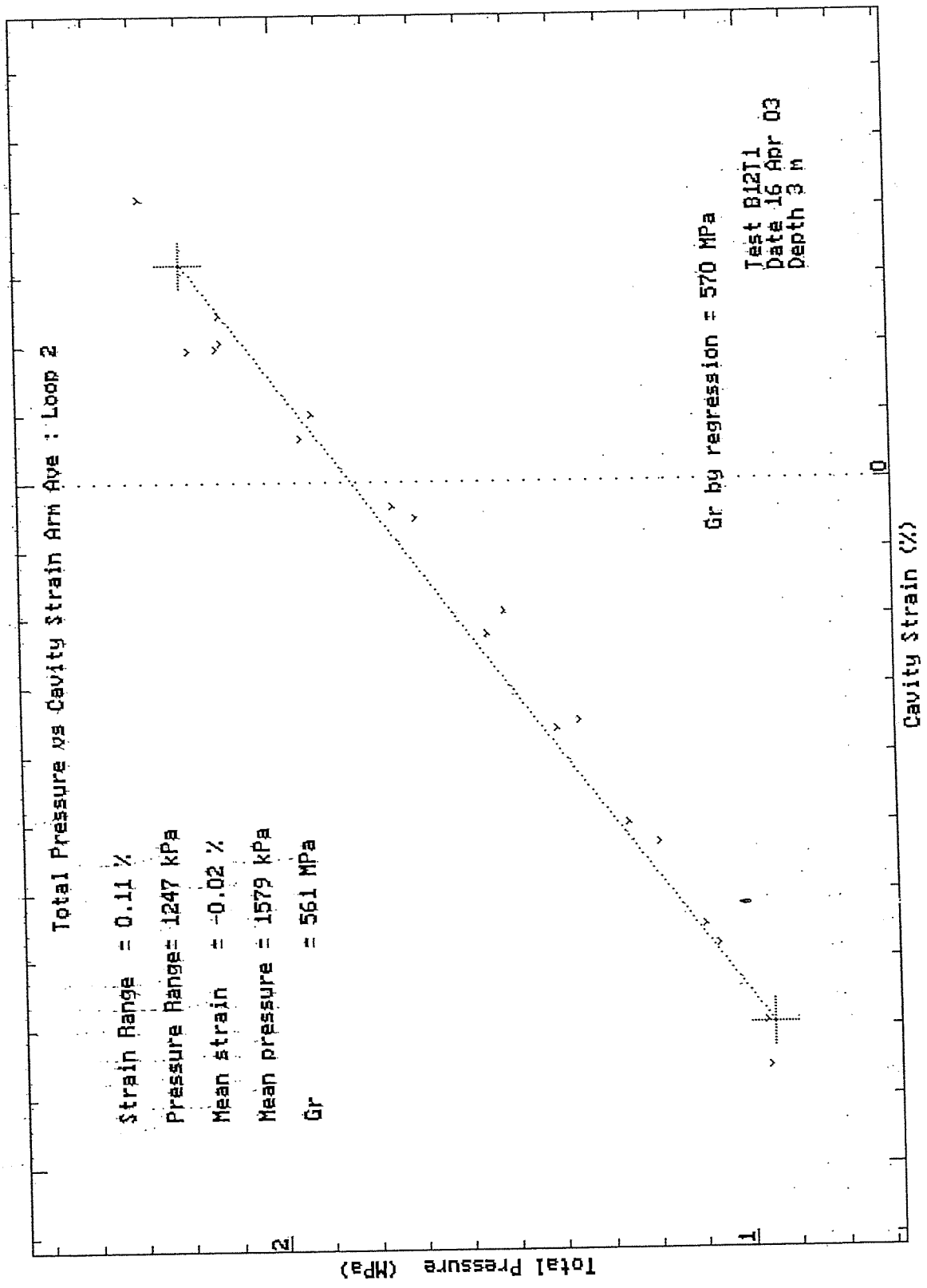

HPD95 Pressuremeter tests
Cambridge Insitu for Seacore

Bressay Bridge Site Investigation
April 2003

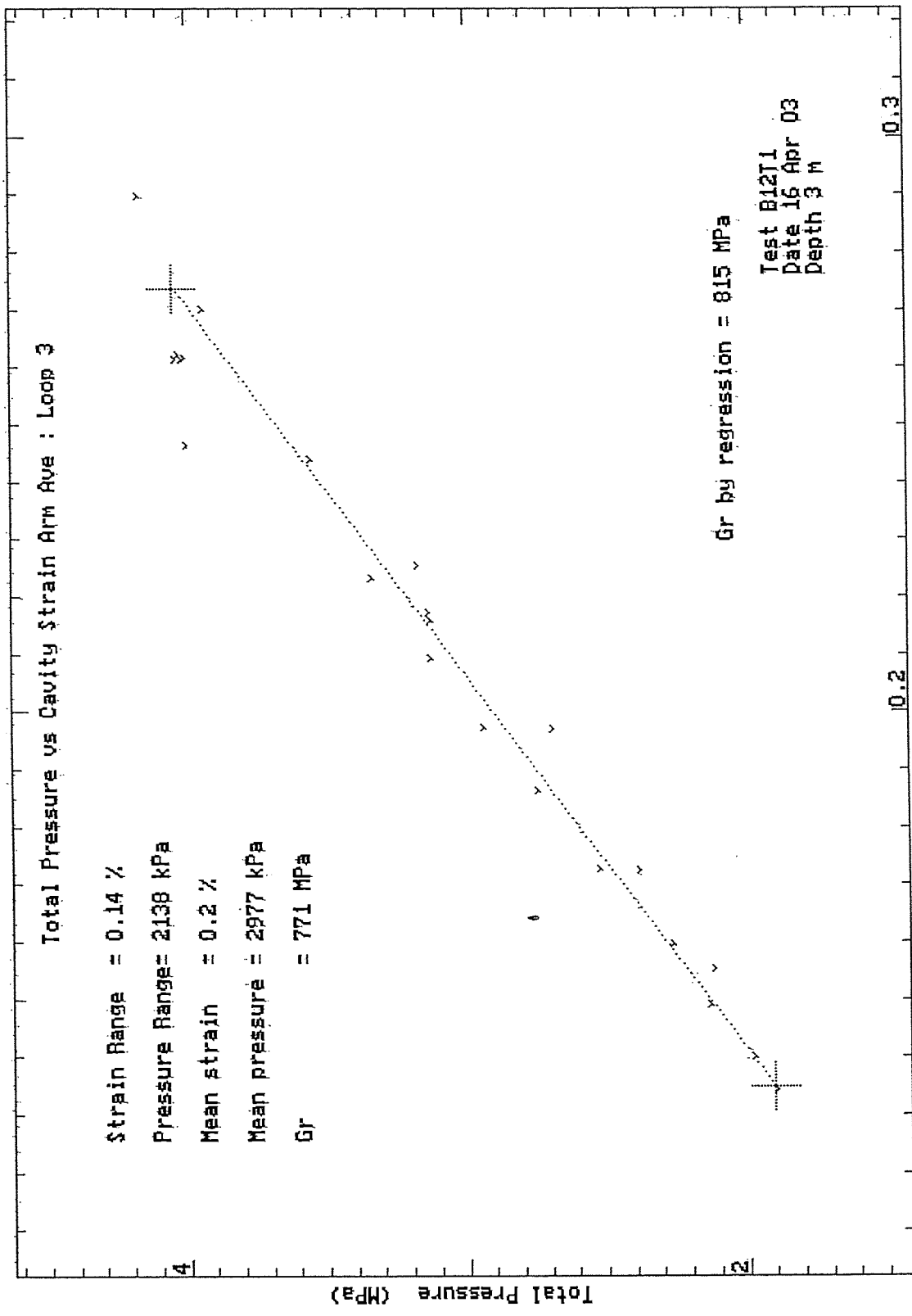
Total Pressure vs Cavity Strain Arm Ave : Loop 3
Strain Range = 0.14 %
Pressure Range= 2138 kPa
Mean strain = 0.2 %
Mean pressure = 2977 kPa
Gr = 771 MPa
Gr by regression = 815 MPa
Test B12T1
Date 16 Apr 03
Depth 3 m
Total Pressure (MPa)
Cavity Strain (%)
4
2
0.2
0.3

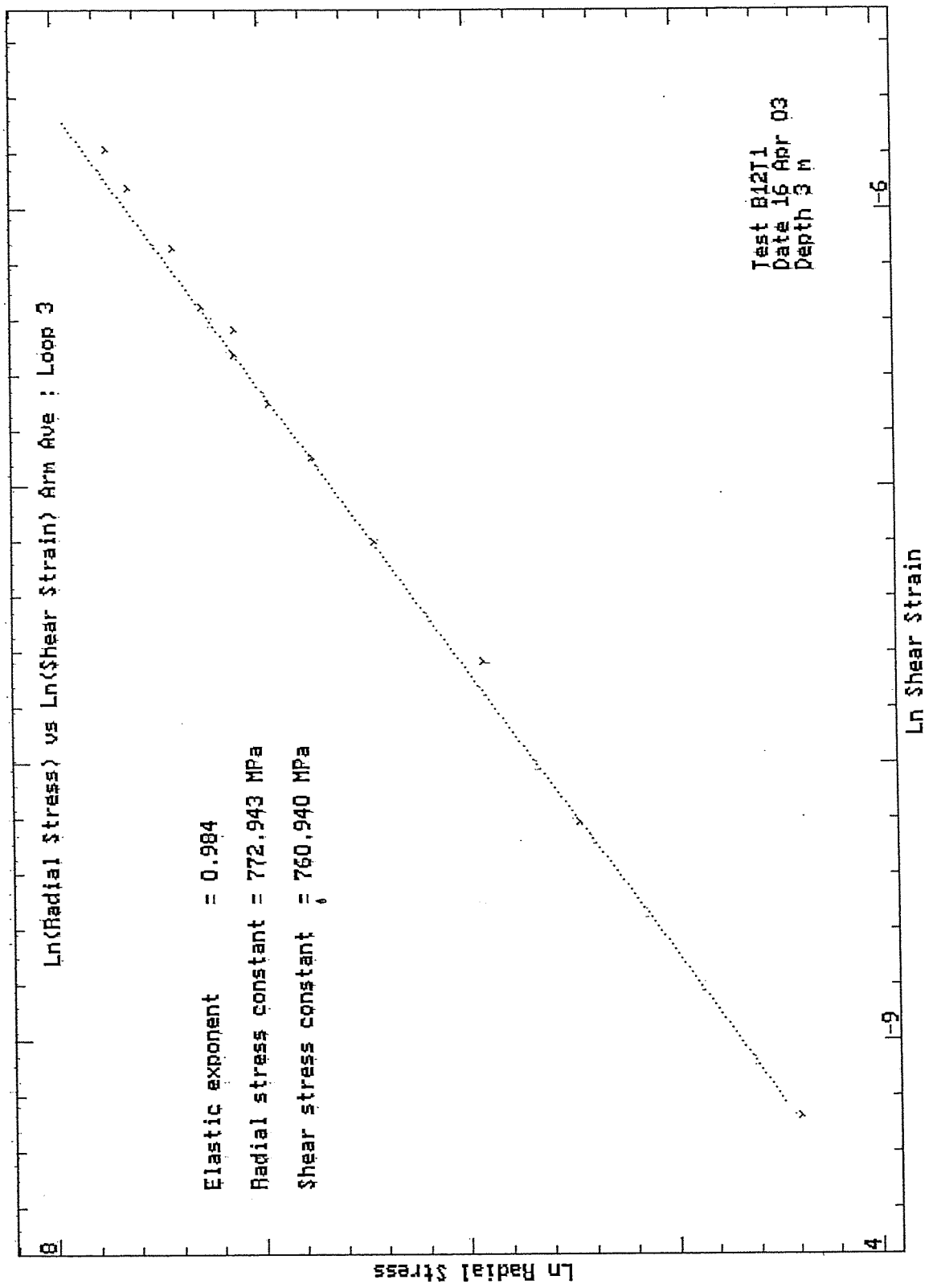
Ln(Radial $tress) vs Ln($hear $train) Arm Ave : Loop 3
Elastic exponent = 0.984
Radial stress constant = 772,943 MPa
$hear stress constant = 760,940 MPa
Test B12T1
Date 16 Apr 03
Depth 3 m
Ln Radial $tress
Ln $hear $train
8
4
-9
-6

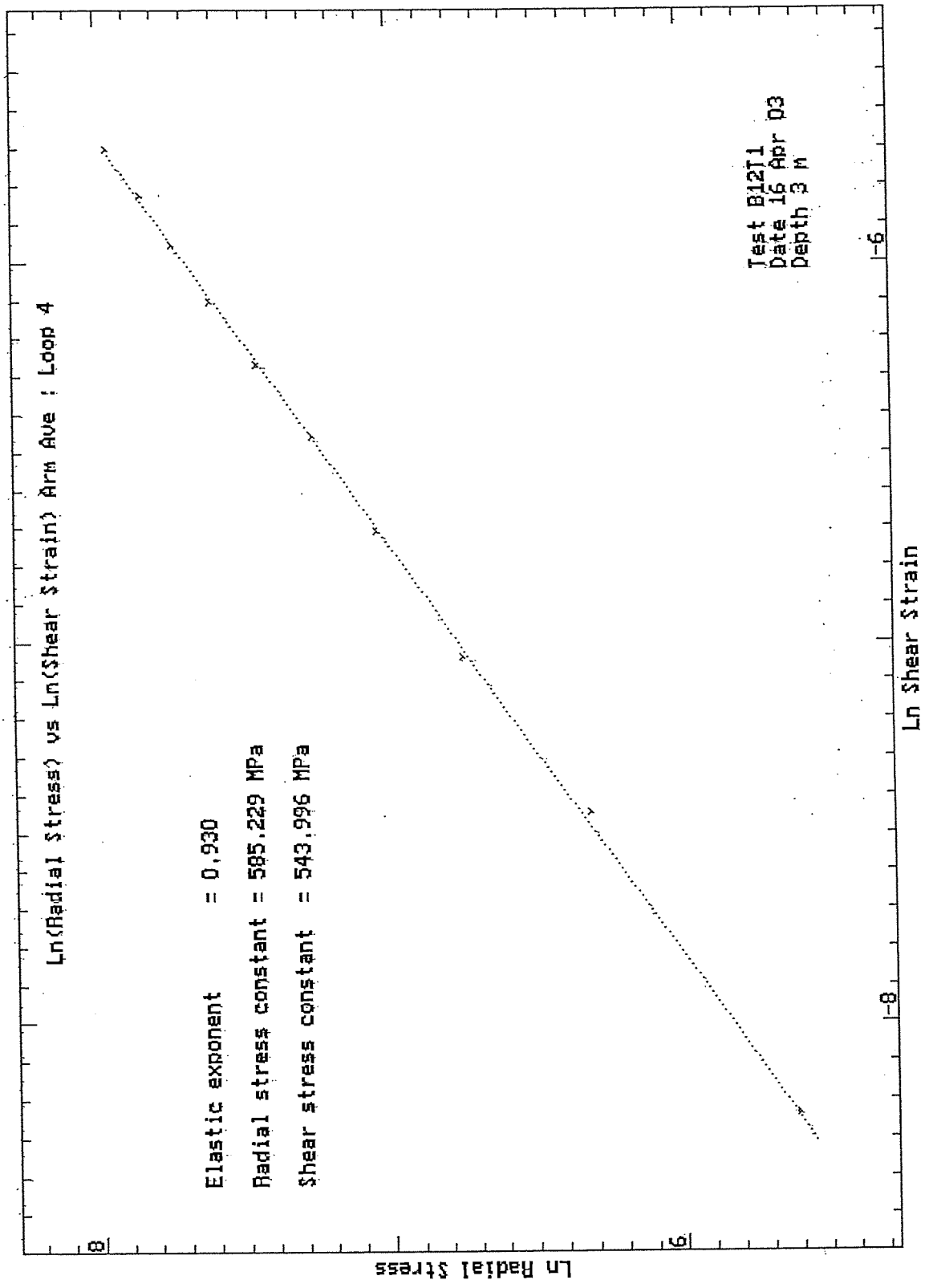
Ln(Radial Stress) vs Ln($hear Strain) Arm Ave : Loop 4
Elastic exponent = 0.930
Radial stress constant = 585.229 MPa
Shear stress constant = 543.996 MPa
Test B12T1
Date 16 Apr 03
Depth 3 m
Ln Radial Stress
Ln Shear Strain
-8
-6
9
8

TEST RECORD SHEET - HIGH PRESSURE DILATOMETER

SITE	Date	Day	Borehole	Test No	Depth
LERWICK	14.4.03	MON	13	1	3.3

Material: PEBBLY SANDSTONE

Weather	Water Table	Time Now	Drilling End	Orientation	CHL
SUNNY / WINDY	SEA LEVEL			NE.	✓

Drilling	Pocket

Diameter	Distance	Rate	Core Description	Length
			V. FRACTURED & MIXED.	

Wet/Dry	Rig	Driller	Core Quality	Size
WET	STRATA II			

Pres/Incrmnt	Wait Time	Creep Time	Cycle Time	Disc No.	Operator	Engineer
			105sec	3		

ZERO READINGS: TILLY — Machine Diameter: 95 mm

Arm 1	Arm 2	Arm 3	Arm 4	Arm 5	Arm 6	T/Press.	Battery
-1.3923	-1.6527	-1.5572	-1.3722	-1.4797	-1.5409	A: .0096 B: .0890	12.26

Calibrations:

Strain Arm Calibration date:	2-10-02	Test No:
Total Pressure Cell Calibration date:	6-3-03	Test No:
Membrane Stiffness Calibration date:	19-3-03	Test No: C999T99
Membrane Compression Calibration date:	"	Test No: "
New Membrane fitted date:		

Test Comments:

Time	Line No.	Start Test at: 0917
		HOLE 1 @ L 70
		HOLE 2 @ L 120
		HOLE 3 @ L 190 1.3 MPa
		HOLE 4 @ L 230
		TO UNLOAD @ L 255
		NO OIL IN RES.

Test Ends at: 10.10 APPROX

Max. Pressure reached: 2.3 MPa

General Comments: 4 HOLES. NOW PRESSURE MEMBRANE BALLOONING

CAMBRIDGE INSITU, Little Eversden, Cambridge, England CB3 7HE
Telephone: 01223 262 361 Fax:- 01223 263 947

HIGH PRESSURE DILATOMETER RESULTS SUMMARY SHEET

Site:- Bressay Bridge Test :- B13T1 Test Date :- 14th April 2003
Material :- Sandstone/pebbles Depth (m) :- 3.3 Water depth (m) :- -

---

Analysis of Insitu Lateral Stress (Po) :-

		Arm Av.
Marsland and Randolph (Iterative Analysis)	kPa	1098
Interpolation from Initial Modulus	kPa	638
Best Estimate of Po	kPa	1100
Assessed diameter of borehole	mm	99.9

Analysis of Undrained Shear Strength (Cu) :-

Gibson and Anderson	kPa	887
Failure pressure (Pf)	kPa	1938
Limit Pressure (P_L)	kPa	6493

Analysis of Shear Modulus (G) :-

Initial Modulus (Gi) MPa 143

Linear Analysis of Reload Loops (Gr) :-

Loop no.	Value (MPa)	Co-ordinate Strain %	Co-ordinate Pressure kPa	Amplitude Strain %	Amplitude Pressure kPa
1	17.1	-1.08	124	0.096	33
2	38.4	-0.71	221	0.153	119
3	270	0	961	0.107	580
4	369	0.25	1497	0.125	916

Non-linear Analysis of Reloading data :-

Loop no.	Linearity exponent (β)	Radial Stress Coeff. (MPa)	Shear Stress Coeff. (MPa)
4	0.88	186	164

Test Analysed By :- PGH
Date :- 27th May 2003

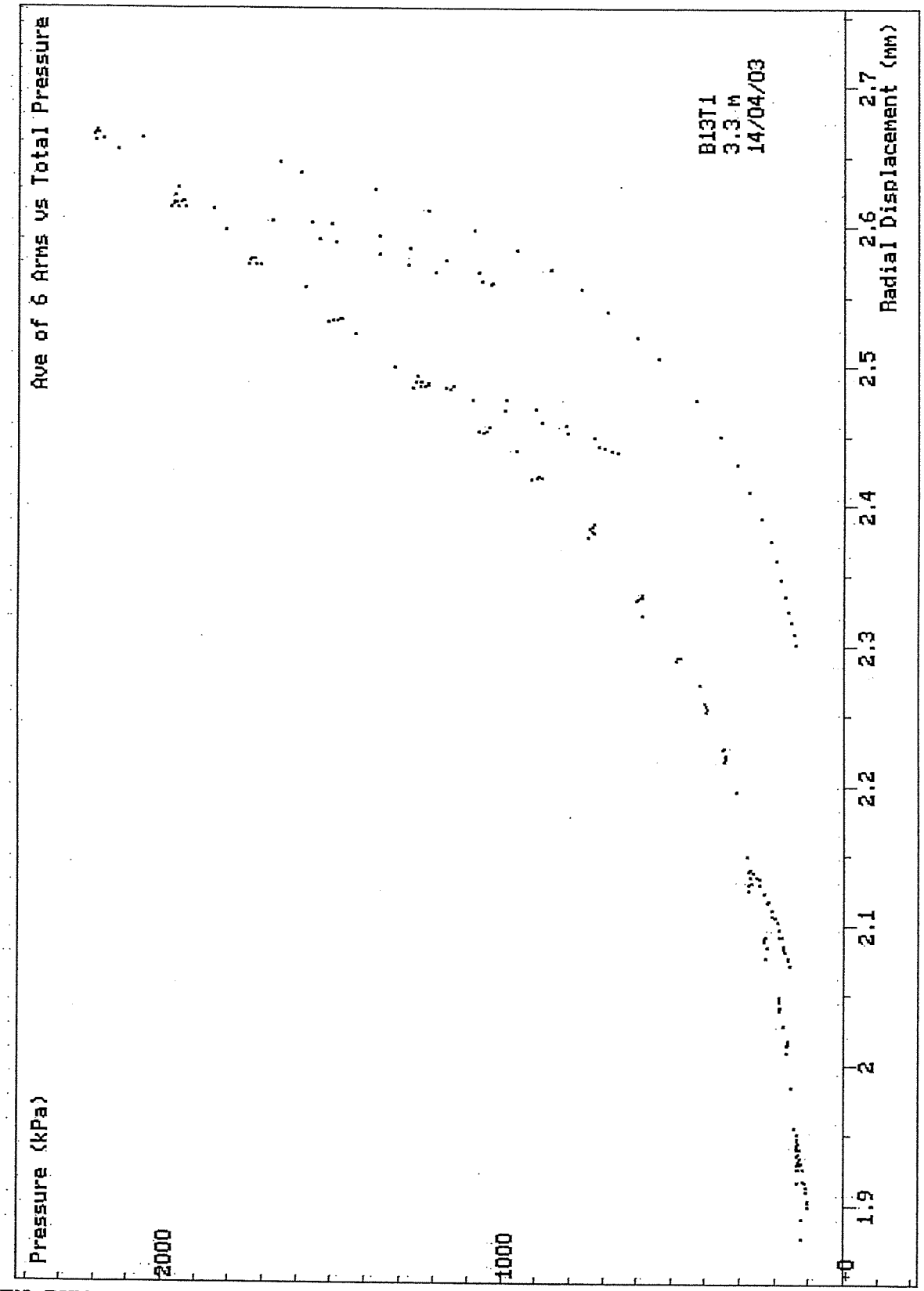

SCREEN DUMP Test: B13T1 Date: 14/04/03 Depth: 3.30m
HPD95 Pressuremeter tests Bressay Bridge Site Investigation
Cambridge Insitu for Seacore April 2003

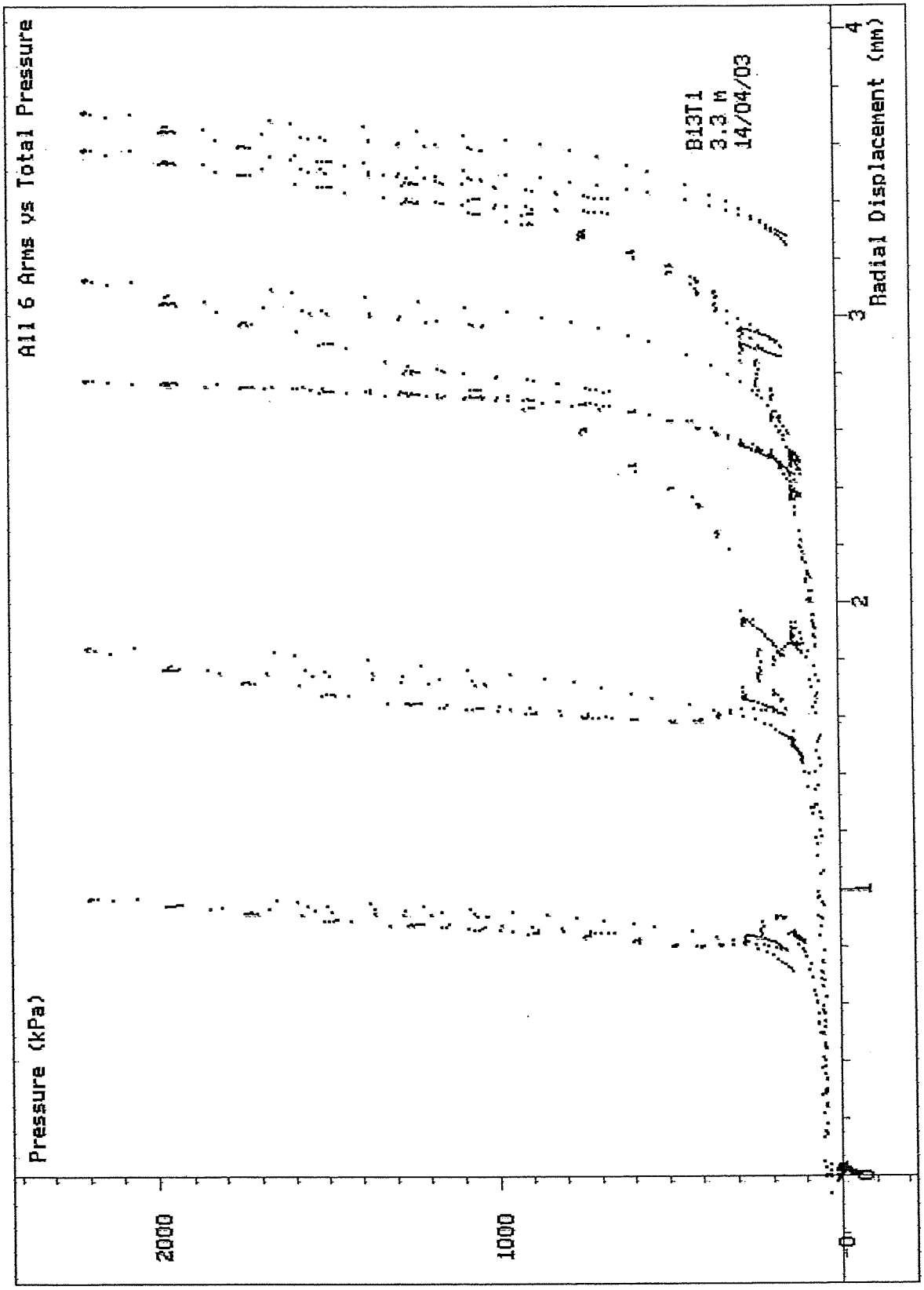

SCREEN DUMP Test: B13T1 Date: 14/04/03 Depth: 3.30m
HPD95 Pressuremeter tests Bressay Bridge Site Investigation
Cambridge Insitu for Seacore April 2003

Marsland and Randolph Pressure/Strain Arm Ave
Gi 143 MPa
Pf 1938 kPa
Po 1098 kPa
Tf 832 kPa
Pf
Po+Tf
Po
P/Log(e) E
Test.B13T1
Date 14 Apr 03
Depth 3.3 m
Pressure (MPa)
Radial displacement (mm)
0
1.8
2.4
2
Creep
0.01 mm

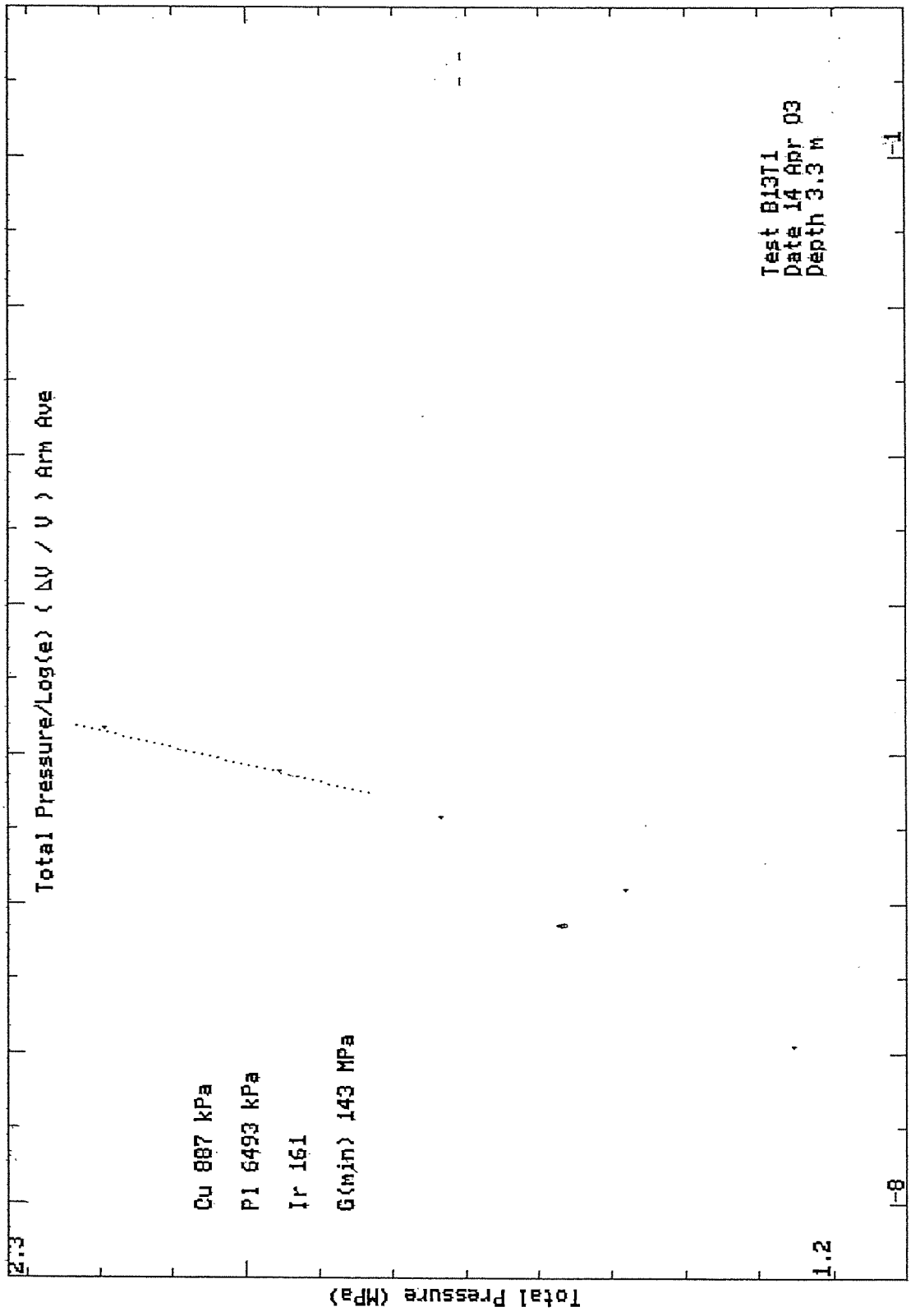
Total Pressure/Log(e) (ΔV / V) Arm Ave
Test B13T1
Date 14 Apr 03
Depth 3.3 m
Cu 887 kPa
Pl 6493 kPa
Ir 161
G(min) 143 MPa
2.3
1.2
-8
-1
Total Pressure (MPa)
Ln 1-(1/(1+E)²)

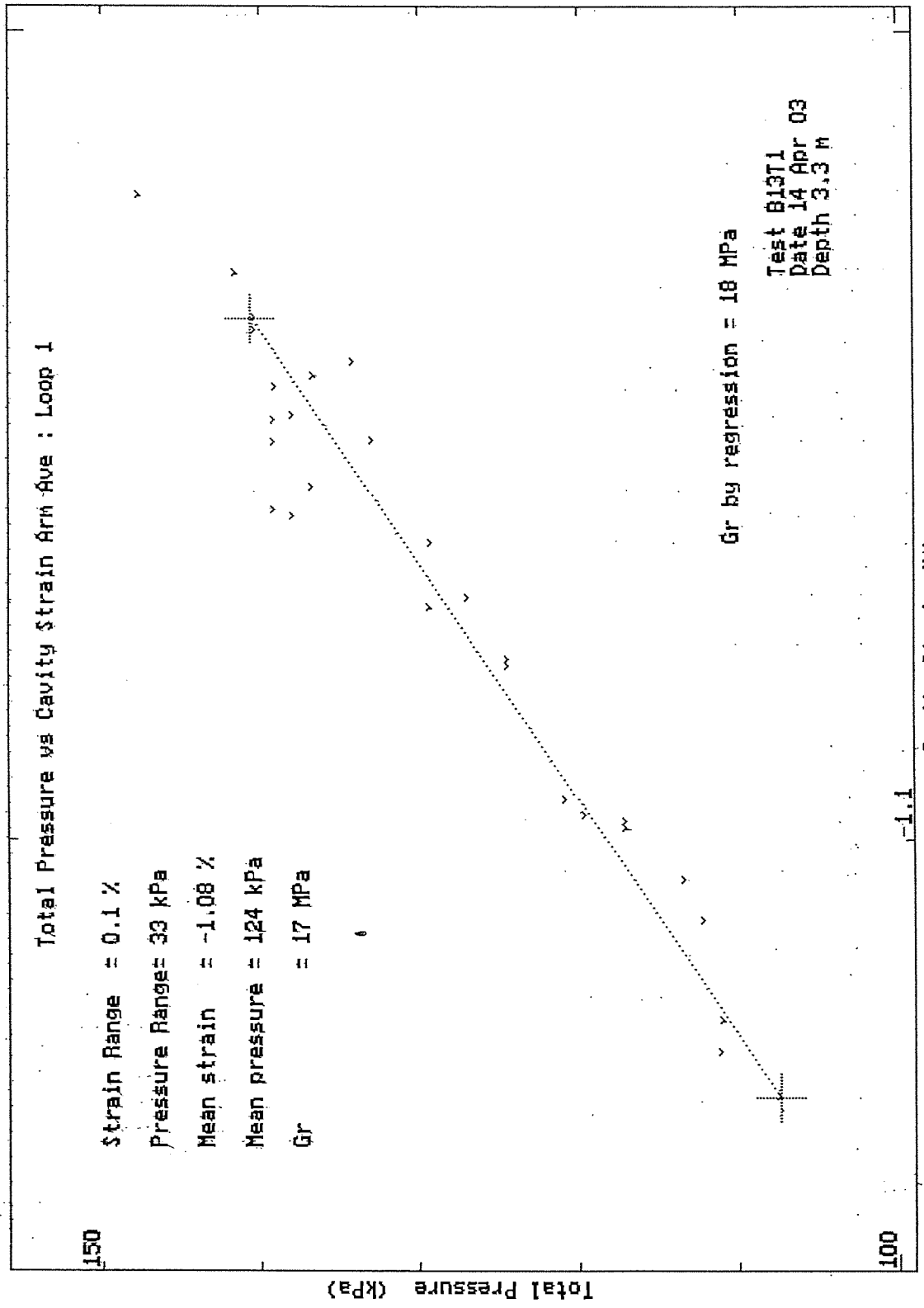
Total Pressure vs Cavity Strain Arm Ave : Loop 1
Strain Range = 0.1 %
Pressure Range= 33 kPa
Mean strain = -1.08 %
Mean pressure = 124 kPa
Gr = 17 MPa
Gr by regression = 18 MPa
Test B13T1
Date 14 Apr 03
Depth 3.3 m
150
100
-1.1
Total Pressure (kPa)
Cavity Strain (%)

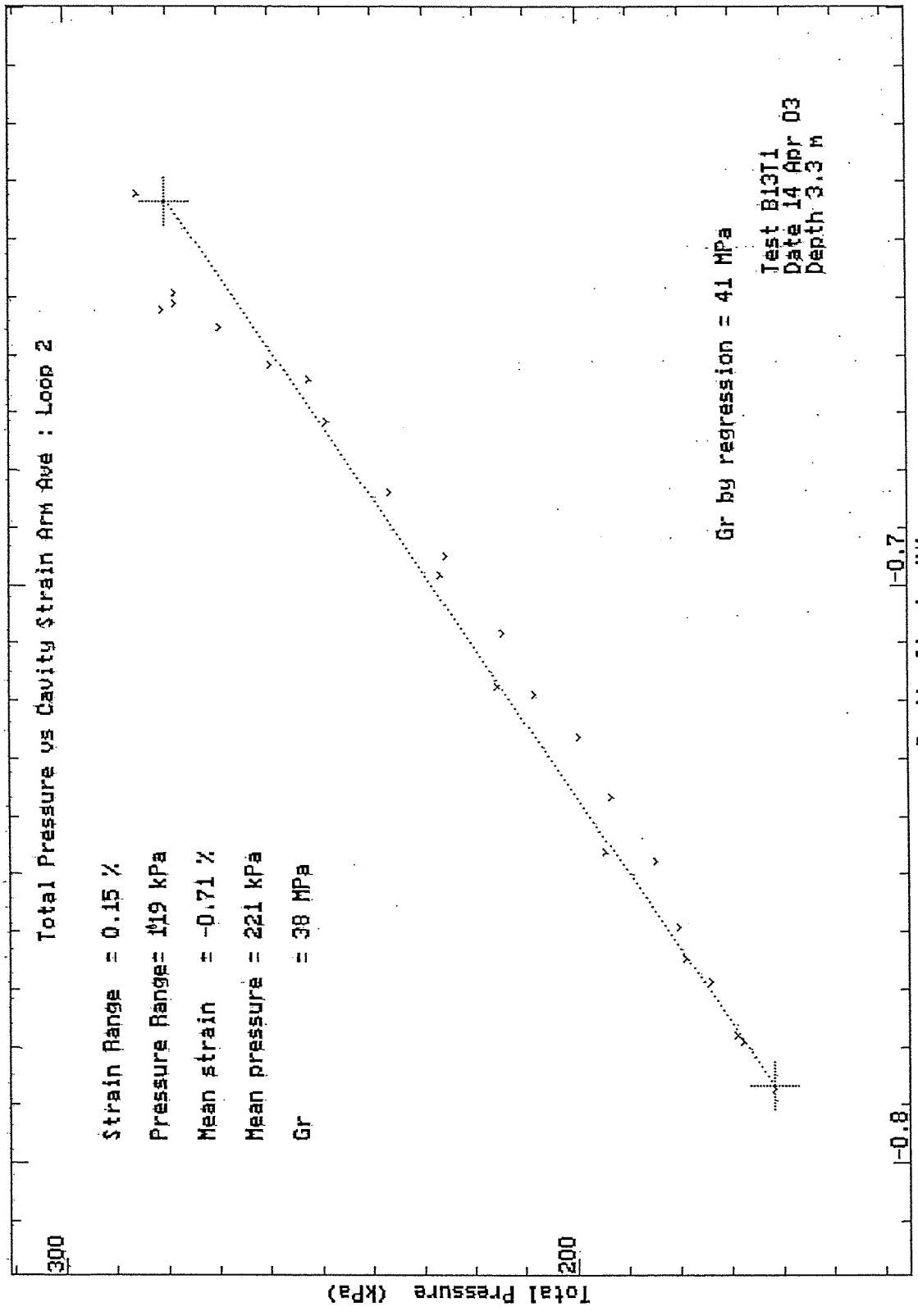
Total Pressure vs Cavity Strain Arm Ave : Loop 2
Strain Range = 0.15 %
Pressure Range= 119 kPa
Mean strain = -0.71 %
Mean pressure = 221 kPa
Gr = 38 MPa
Gr by regression = 41 MPa
Test B13T1
Date 14 Apr 03
Depth 3.3 m
300
200
Total Pressure (kPa)
-0.7
-0.8
Cavity Strain (%)

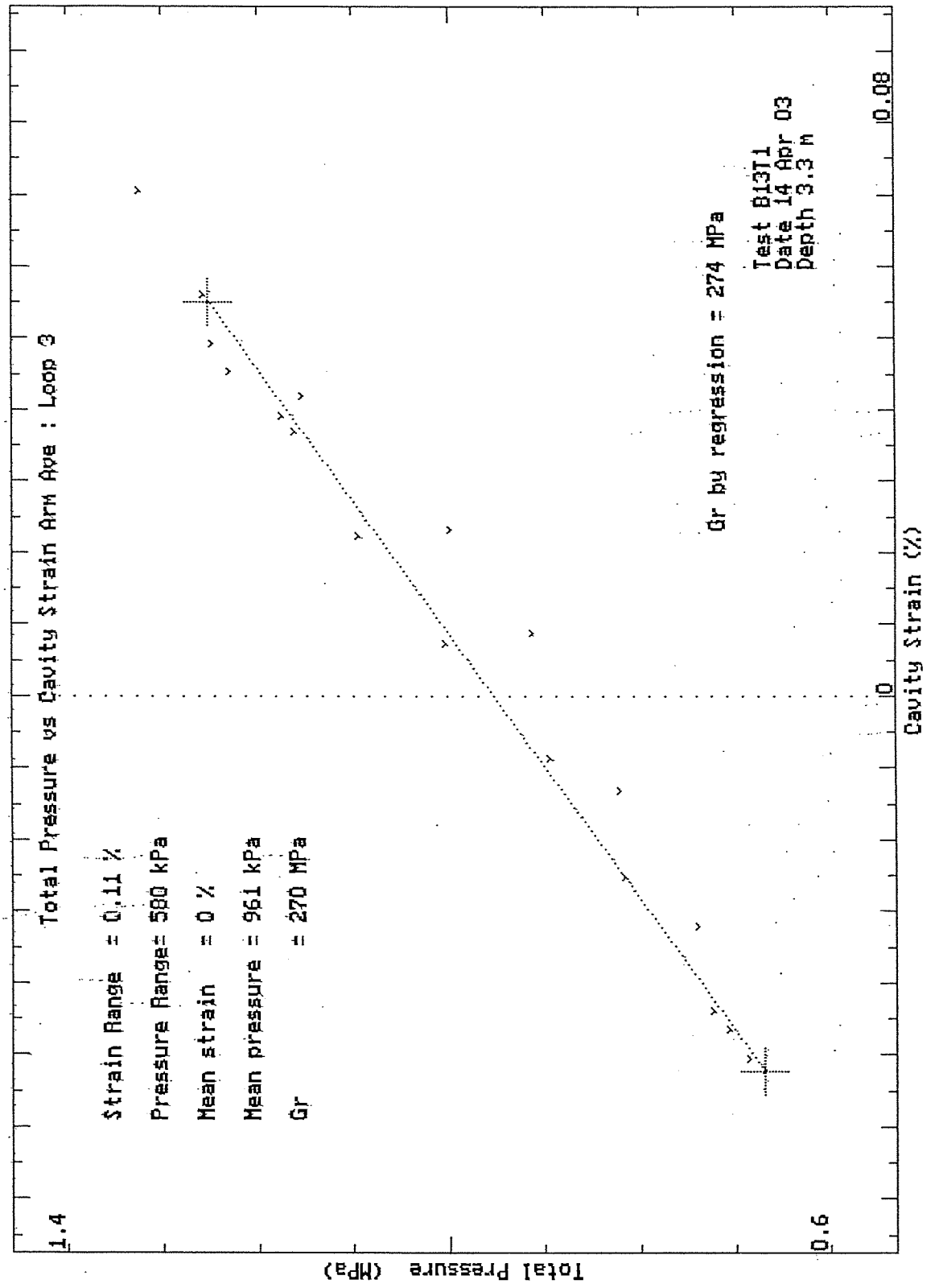
Total Pressure vs Cavity Strain Arm Ave : Loop 3
Strain Range = 0.11 %
Pressure Range= 580 kPa
Mean strain = 0 %
Mean pressure = 961 kPa
Gr = 270 MPa
Gr by regression = 274 MPa
Test B13T1
Date 14 Apr 03
Depth 3.3 m
Total Pressure (MPa)
Cavity Strain (%)
1.4
0.6
0
0.08

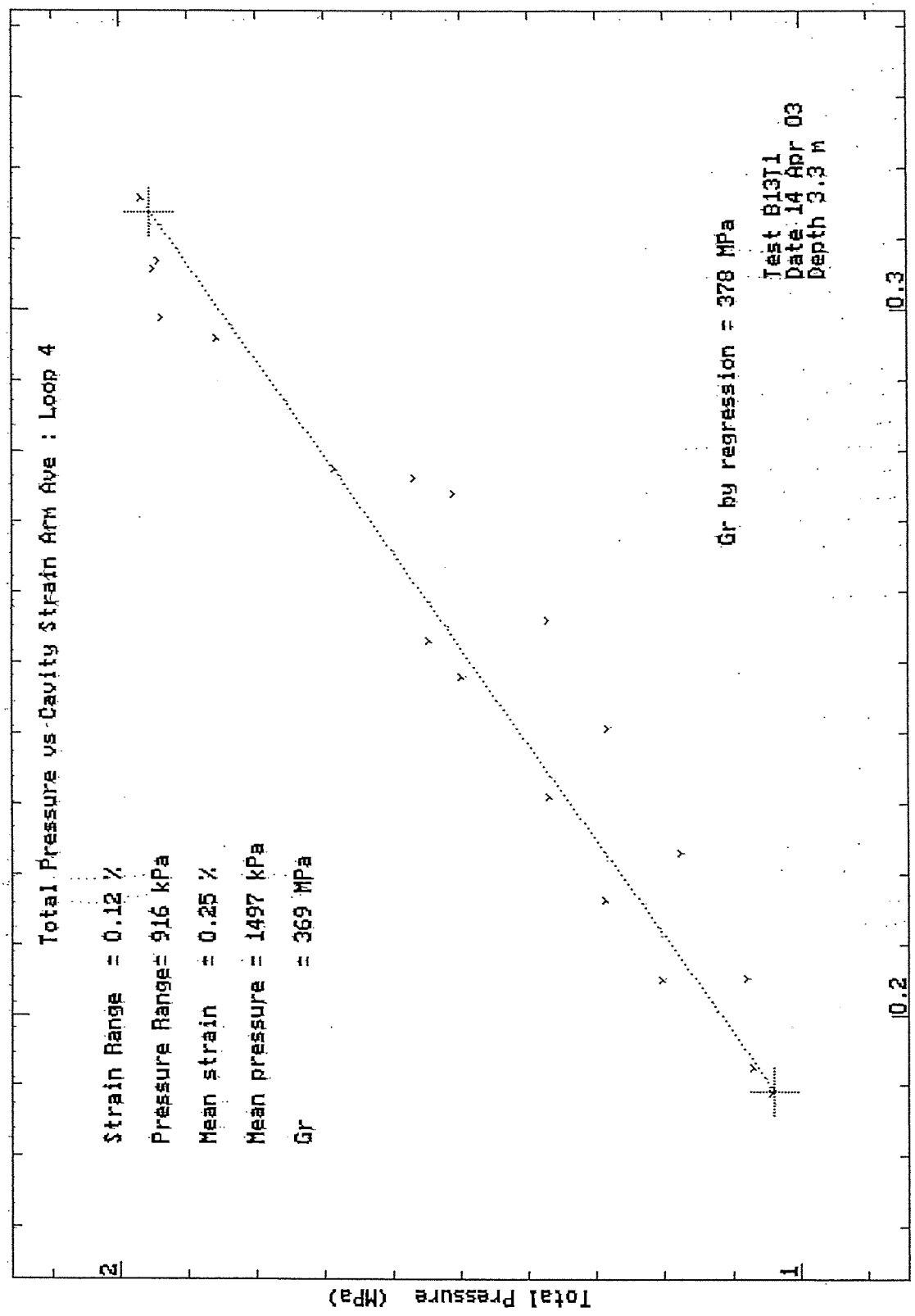
Total Pressure vs Cavity Strain Arm Ave : Loop 4
Strain Range = 0.12 %
Pressure Range= 916 kPa
Mean strain = 0.25 %
Mean pressure = 1497 kPa
Gr = 369 MPa
Gr by regression = 378 MPa
Test B13T1
Date 14 Apr 03
Depth 3.3 m
Total Pressure (MPa)
Cavity Strain (%)
0.2
0.3
1
2

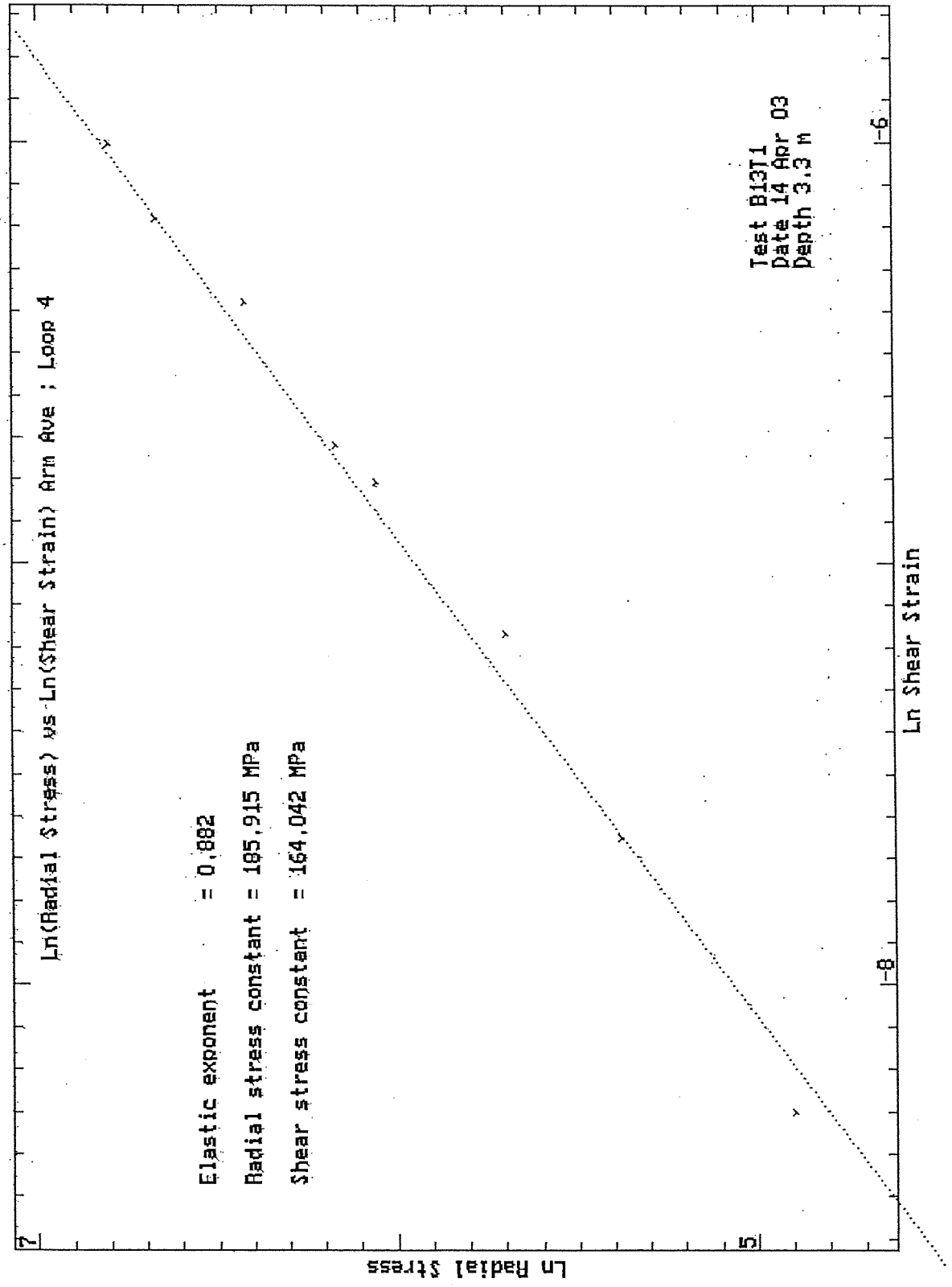
Ln(Radial Stress) vs Ln($hear Strain) Arm Ave ; Loop 4
Elastic exponent = 0,882
Radial stress constant = 185,915 MPa
Shear stress constant = 164,042 MPa
Test B13T1
Date 14 Apr 03
Depth 3,3 m
Ln Radial Stress
Ln Shear Strain
-5
-6
-7
-8

TEST RECORD SHEET - HIGH PRESSURE DILATOMETER

SITE	Date	Day	Borehole	Test No	Depth
LERWICK	16-4-03	WED	14	1	5.4

Material: SANDSTONE

Weather	Water Table	Time Now	Drilling End	Orientation	CHL
CALM	SEA LEVEL				✓

Drilling	Pocket

Diameter	Distance	Rate	Core Description	Length

Wet/Dry	Rig	Driller	Core Quality	Size
WET	SKATE 2)			

Pres/Incrmnt	Wait Time	Creep Time	Cycle Time	Disc No.	Operator	Engineer
~200kPa	20 sec	30 sec	60 sec	4		

ZERO READINGS: TICCY

Machine Diameter 95 mm

Arm 1	Arm 2	Arm 3	Arm 4	Arm 5	Arm 6	T/Press.	Battery
AS FOR BIST 1						A: B:	12.47

Calibrations:

Strain Arm Calibration date:	2-10-02	Test No:
Total Pressure Cell Calibration date:	6-3-03	Test No:
Membrane Stiffness Calibration date:	19-3-03	Test No: C999T99
Membrane Compression Calibration date:	"	Test No: "
New Membrane fitted date:		

Test Comments:

Time	Line No.	Start Test at: 05:35
	75	START PUMPING
	93	HOLD ⇒ LOOP (1)
	154	LOOP (2)
	210	LOOP (3)
	289	LOOP (4)
	370	DOWN — FAR BRANCH
		NEARLY OUT OF OIL

Test Ends at: 06:02

Max. Pressure reached: 7.5 MPa

General Comments:

CAMBRIDGE INSITU, Little Eversden, Cambridge, England CB3 7HE
Telephone: 01223 262 361 Fax:- 01223 263 947

HIGH PRESSURE DILATOMETER RESULTS SUMMARY SHEET

Site:- Bressay Bridge Test :- B14T1 Test Date :- 16th April 2003
Material :- Sandstone Depth (m) :- 5.4 Water depth (m) :- -

Analysis of Insitu Lateral Stress (Po) :-

		Arm Av.
Marsland and Randolph (Iterative Analysis)	kPa	1451
Best Estimate of Po	kPa	1450
Assessed diameter of borehole	mm	102.7

Analysis of Undrained Shear Strength (Cu) :-

Gibson and Anderson	kPa	4170
Failure pressure (Pf)	kPa	2858
Limit Pressure (P_L)	MPa	17

Strength of Sands Analysis (Hughes, Wroth & Windle)

Friction angle at const. vol.	deg	33	(assumed)
Angle of Friction	deg	51	
Angle of Dilation	deg	24	

Analysis of Shear Modulus (G) :-

Initial Modulus (Gi)	MPa	78

Linear Analysis of Reload Loops (Gr) :-

Loop no.	Value (MPa)	Co-ordinate Strain %	Co-ordinate Pressure kPa	Amplitude Strain %	Amplitude Pressure kPa
1	97	-0.58	627	0.168	326
2	186	0.07	1341	0.155	579
3	254	0.88	2364	0.207	1039
4	305	2.25	3662	0.367	2190

Non-linear Analysis of Reloading data :-

Loop no.	Linearity exponent (β)	Radial Stress Coeff. (MPa)	Shear Stress Coeff. (MPa)
3	0.875	138	121
4	0.885	181	160

Test Analysed By :- PGH
Date :- 27th May 2003

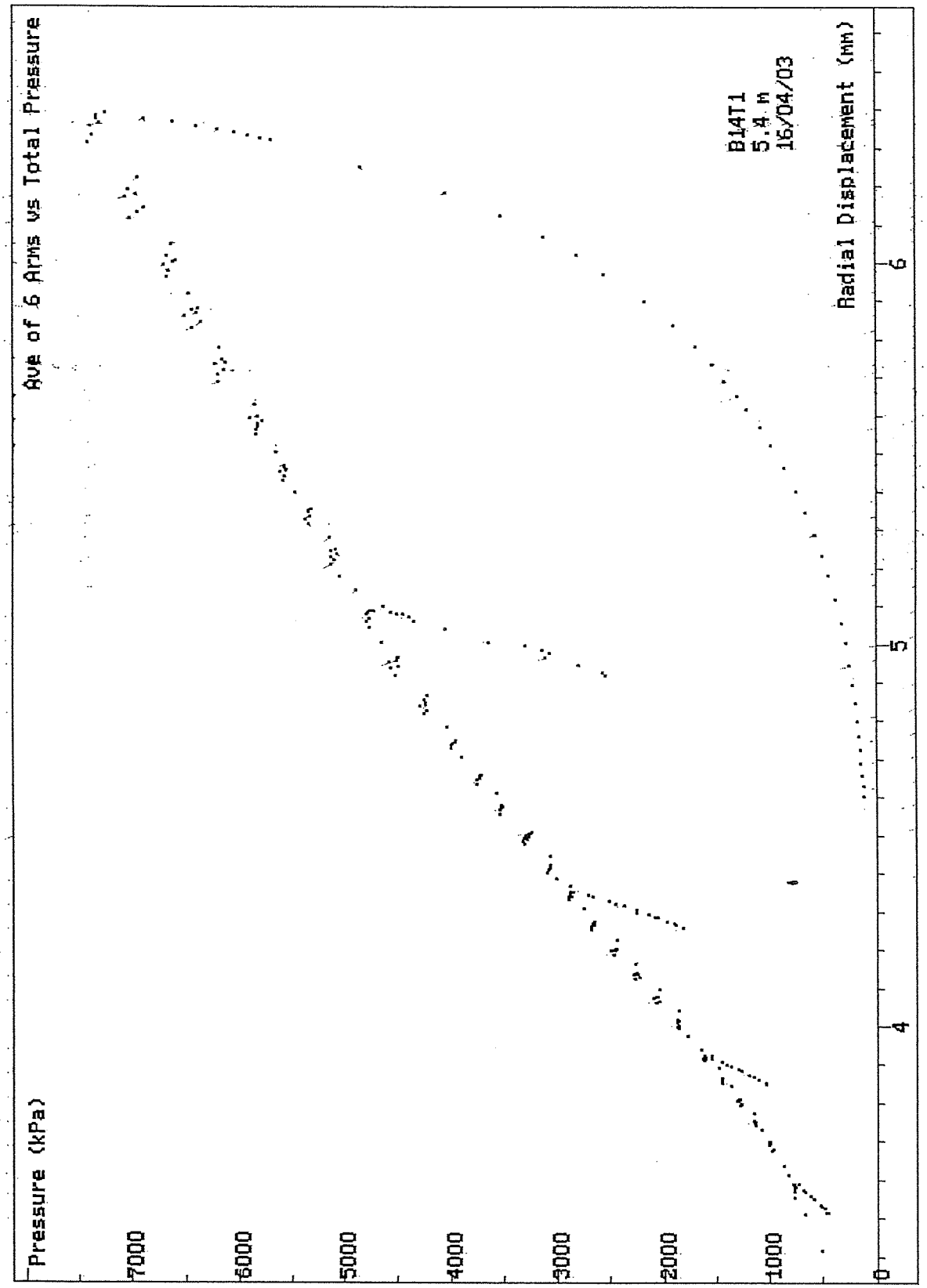

SCREEN DUMP Test: B14T1 Date: 16/04/03 Depth: 5.40m
HPD95 Pressuremeter tests Bressay Bridge Site Investigation
Cambridge Insitu for Seacore April 2003

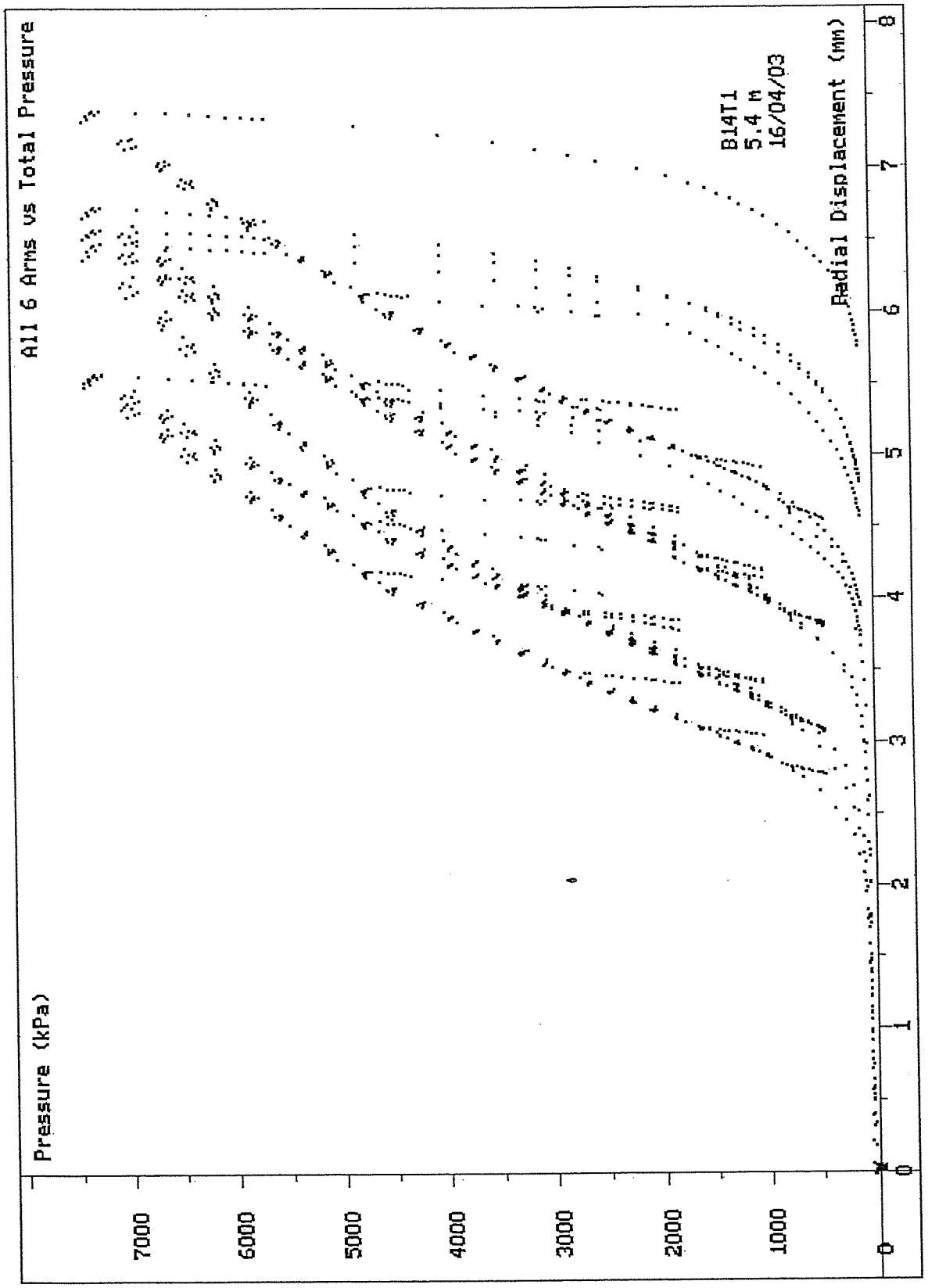

SCREEN DUMP Test: B14T1 Date: 16/04/03 Depth: 5.40m
HPD95 Pressuremeter tests Bressay Bridge Site Investigation
Cambridge Insitu for Seacore April 2003

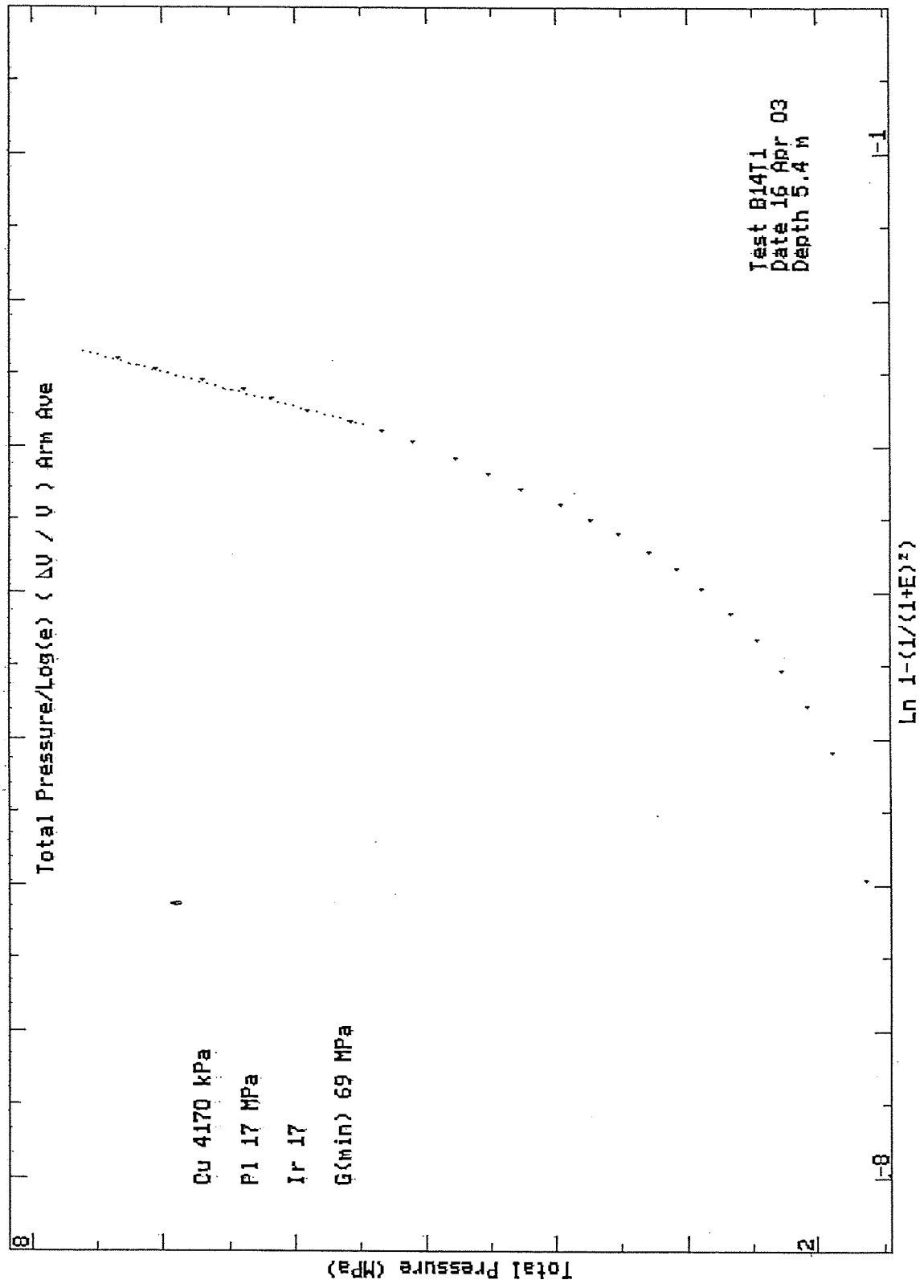

HPD95 Pressuremeter tests
Cambridge Insitu for Seacore

Bressay Bridge Site Investigation
April 2003

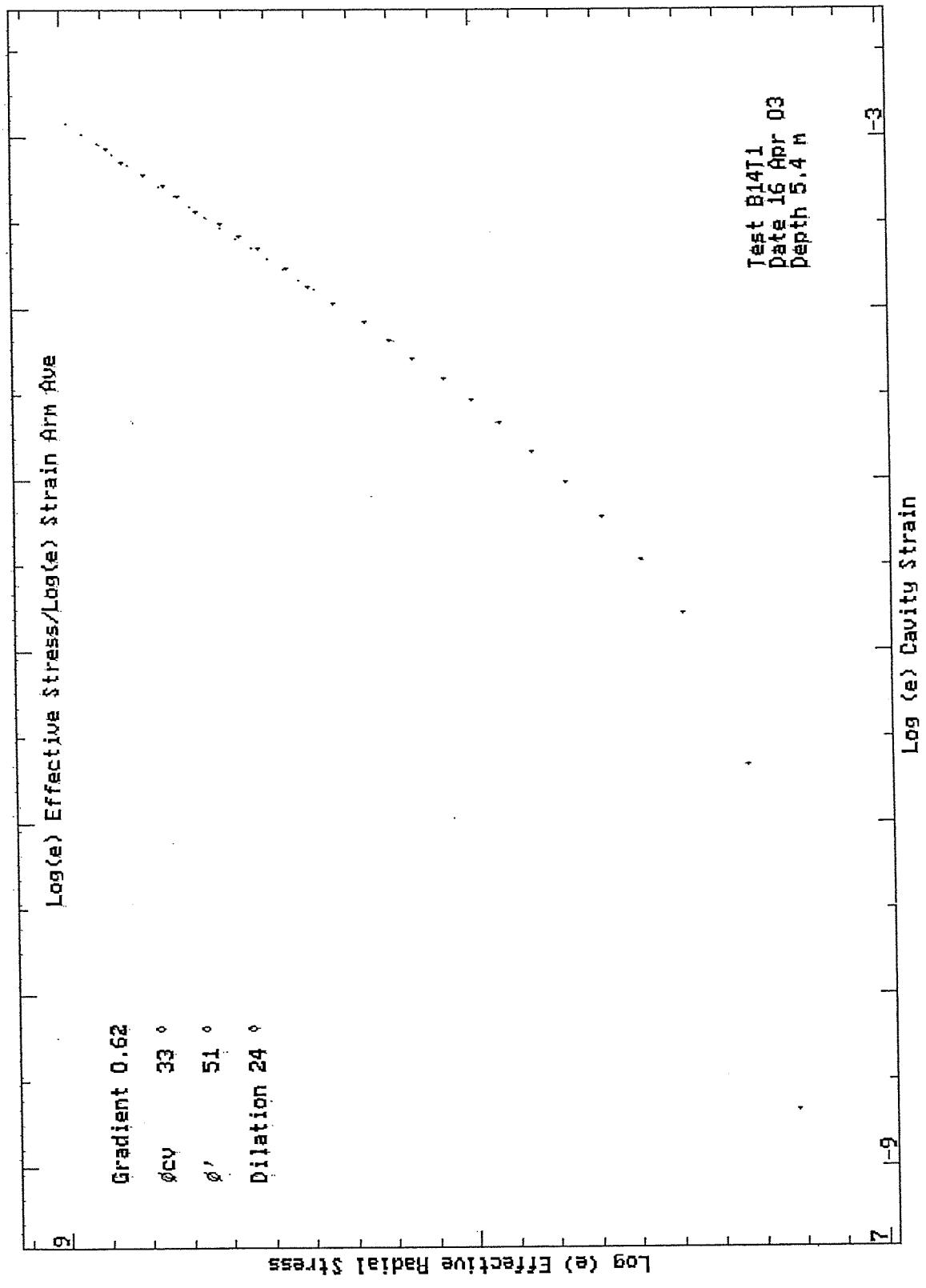
Log(e) Effective Stress/Log(e) Strain Arm Ave
Gradient 0.62
Øcv 33 °
Ø' 51 °
Dilation 24 °
Test B14T1
Date 16 Apr 03
Depth 5.4 m
Log (e) Effective Radial Stress
Log (e) Cavity Strain
-3
-9

Total Pressure vs Cavity Strain Arm Ave : Loop 1
Strain Range = 0.17 %
Pressure Range= 326 kPa
Mean strain = -0.58 %
Mean pressure = 627 kPa
Gr = 97 MPa
Gr by regression = 101 MPa
Test B14T1
Date 16 Apr 03
Depth 5.4 m
800
400
-0.7
-0.5
Total Pressure (kPa)
Cavity Strain (%)

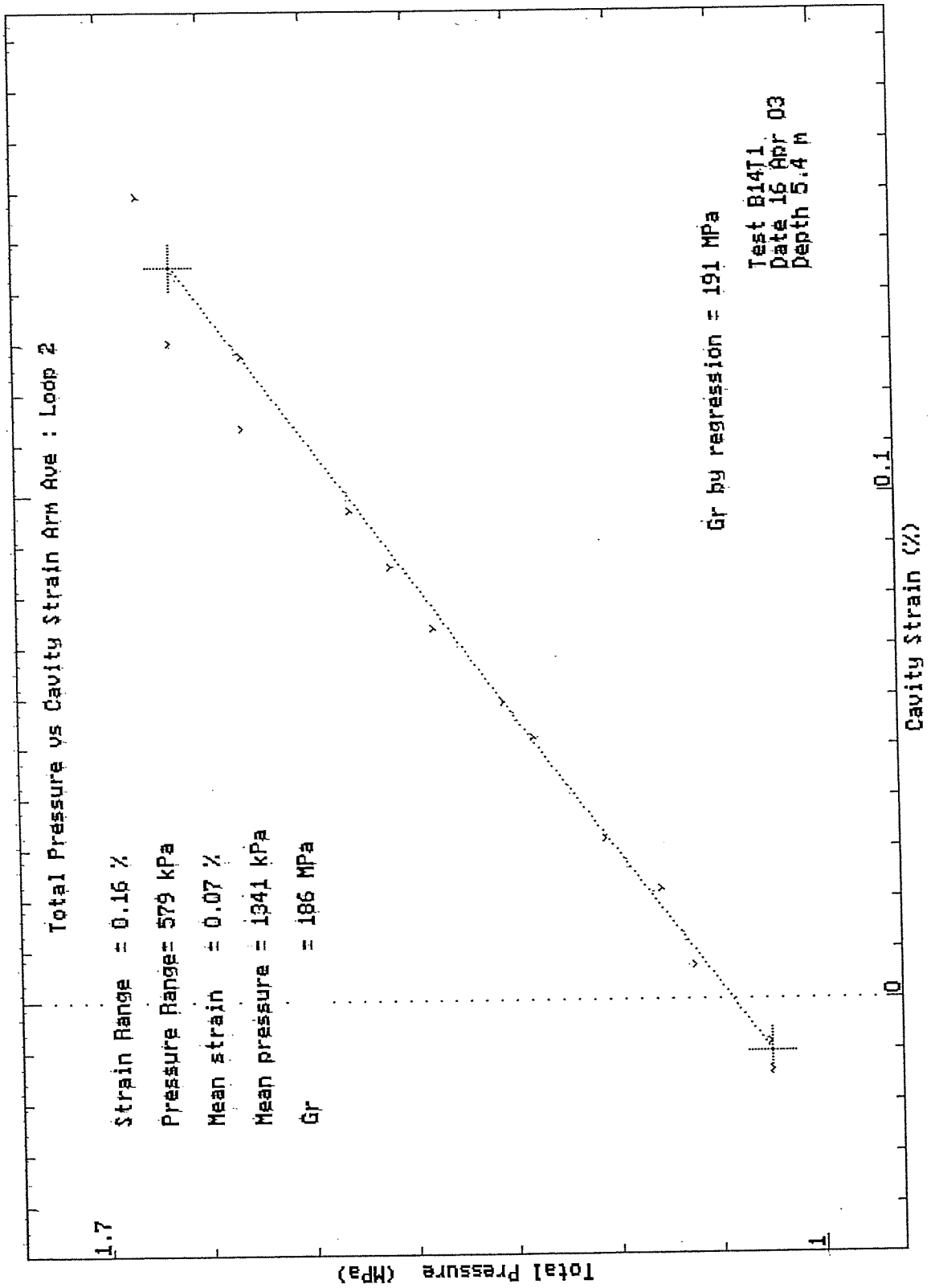
Total Pressure vs Cavity Strain Arm Ave : Loop 2
Strain Range = 0.16 %
Pressure Range= 579 kPa
Mean strain = 0.07 %
Mean pressure = 1341 kPa
Gr = 186 MPa
Gr by regression = 191 MPa
Test B14T1
Date 16 Apr 03
Depth 5.4 m
Total Pressure (MPa)
Cavity Strain (%)
1.7
1
0
0.1

HPD95 Pressuremeter tests
Cambridge Insitu for Seacore

Bressay Bridge Site Investigation
April 2003

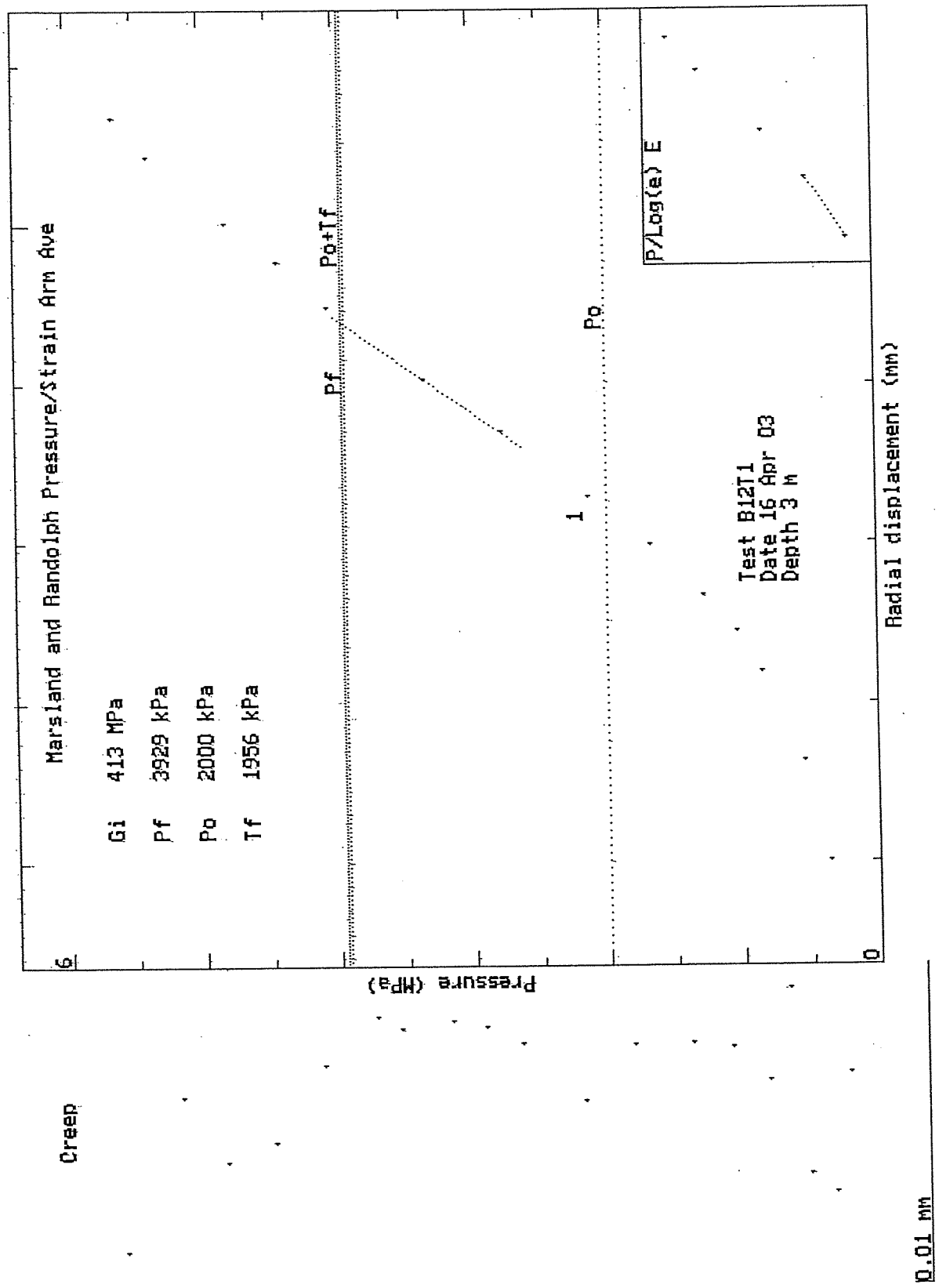
Marsland and Randolph Pressure/Strain Arm Ave
Gi 413 MPa
Pf 3929 kPa
Po 2000 kPa
Tf 1956 kPa
Pf
Po+Tf
Po
1
Test B12T1
Date 16 Apr 03
Depth 3 m
P/Log(e) E
Pressure (MPa)
6
0
Radial displacement (mm)
Creep
0.01 mm

Marsland and Randolph Pressure/Strain Arm Ave
Gi 413 MPa
Pf 3929 kPa
Po 2000 kPa
Tf 1956 kPa
Po+Tf
Pf
Po
1
P/Log(a) E
Test B12T1
Date 16 Apr 03
Depth 3 m
Pressure (MPa)
Radial displacement (mm)
6
0
Creep
0.01 mm

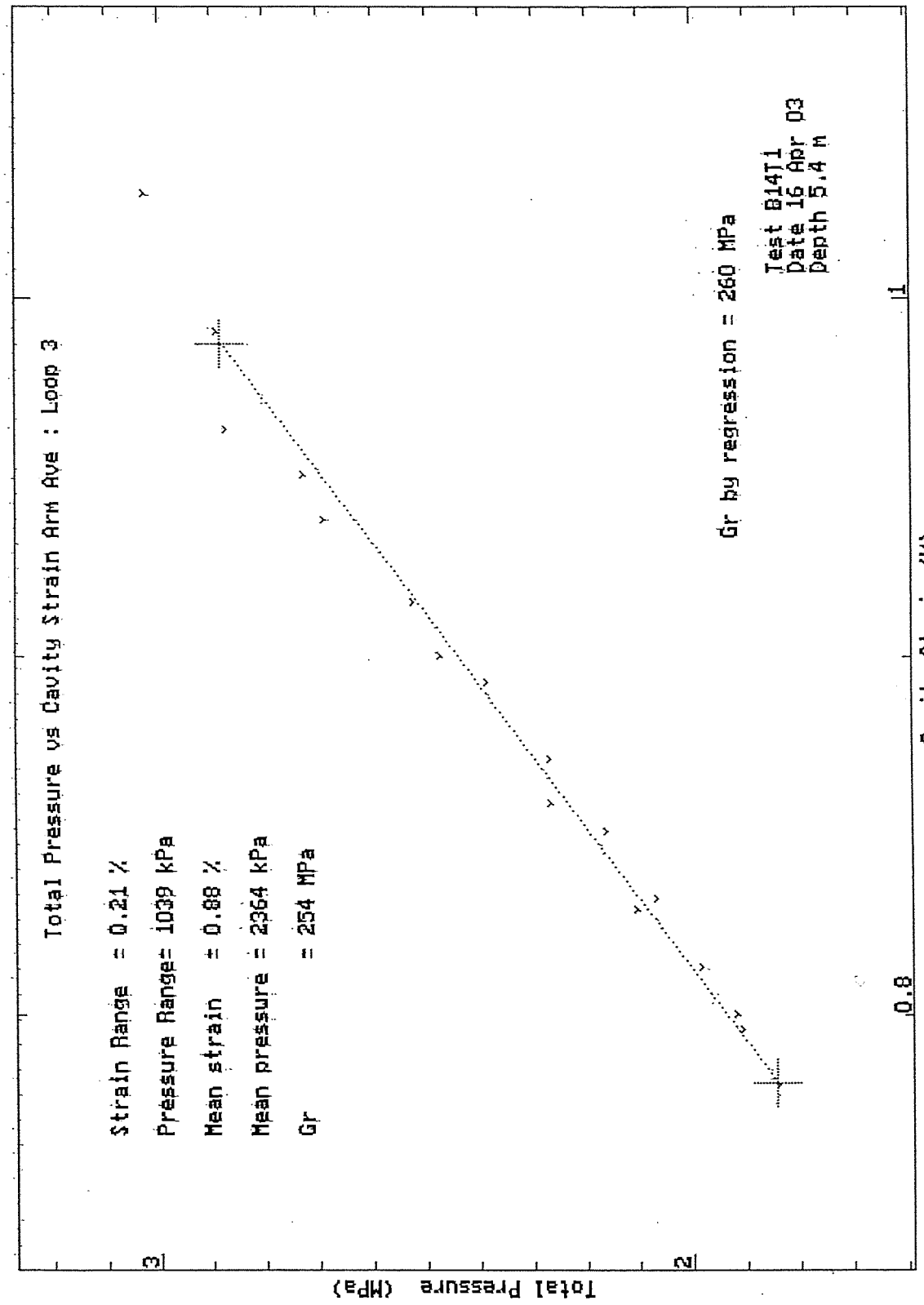
Total Pressure vs Cavity Strain Arm Ave : Loop 3
Strain Range = 0.21 %
Pressure Range= 1039 kPa
Mean strain = 0.88 %
Mean pressure = 2364 kPa
Gr = 254 MPa
Gr by regression = 260 MPa
Test B14T1
Date 16 Apr 03
Depth 5.4 m
Total Pressure (MPa)
Cavity Strain (%)
3
2
1
0.8

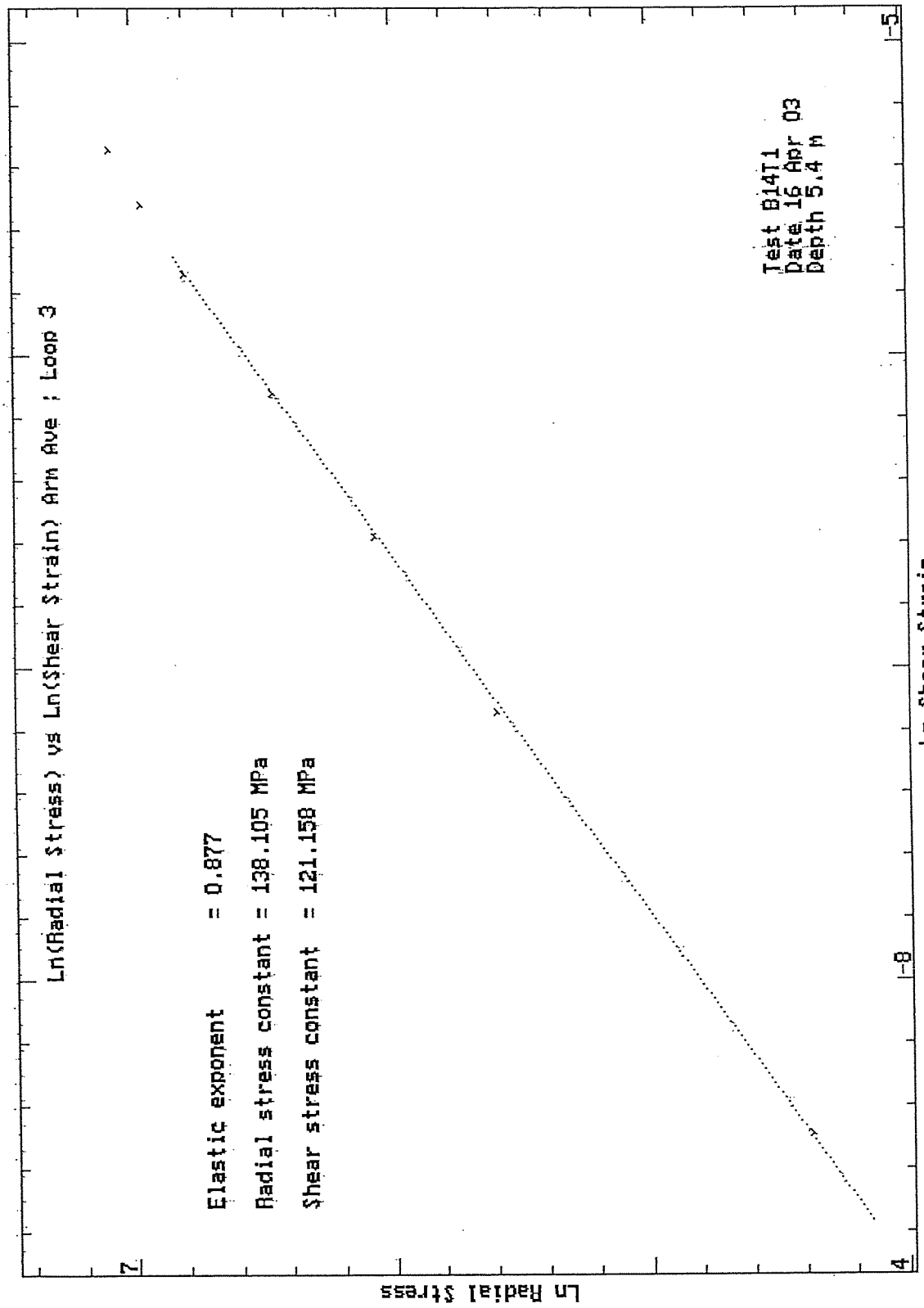
Ln(Radial $tress) vs Ln($hear $train) Arm Ave ; Loop 3
Elastic exponent = 0.877
Radial stress constant = 138.105 MPa
$hear stress constant = 121.158 MPa
Test B14T1
Date 16 Apr 03
Depth 5.4 m
Ln Radial $tress
Ln $hear $train
-7
-8
-5

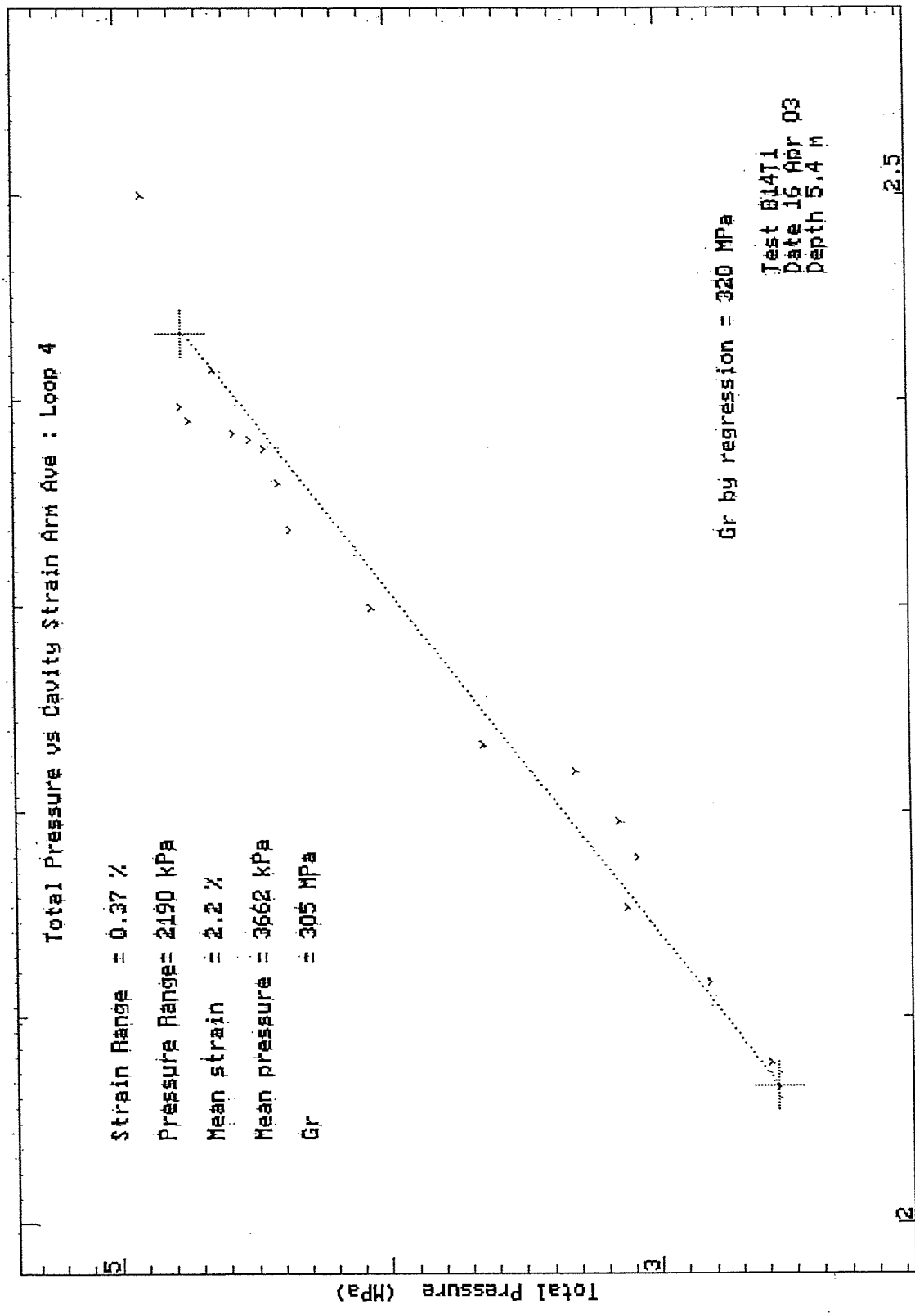
Total Pressure vs Cavity Strain Arm Ave : Loop 4
Strain Range = 0.37 %
Pressure Range= 2190 kPa
Mean strain = 2.2 %
Mean pressure = 3662 kPa
Gr = 305 MPa
Gr by regression = 320 MPa
Test B14T1
Date 16 Apr 03
Depth 5.4 m
Total Pressure (MPa)
Cavity Strain (%)
5
3
2
2.5

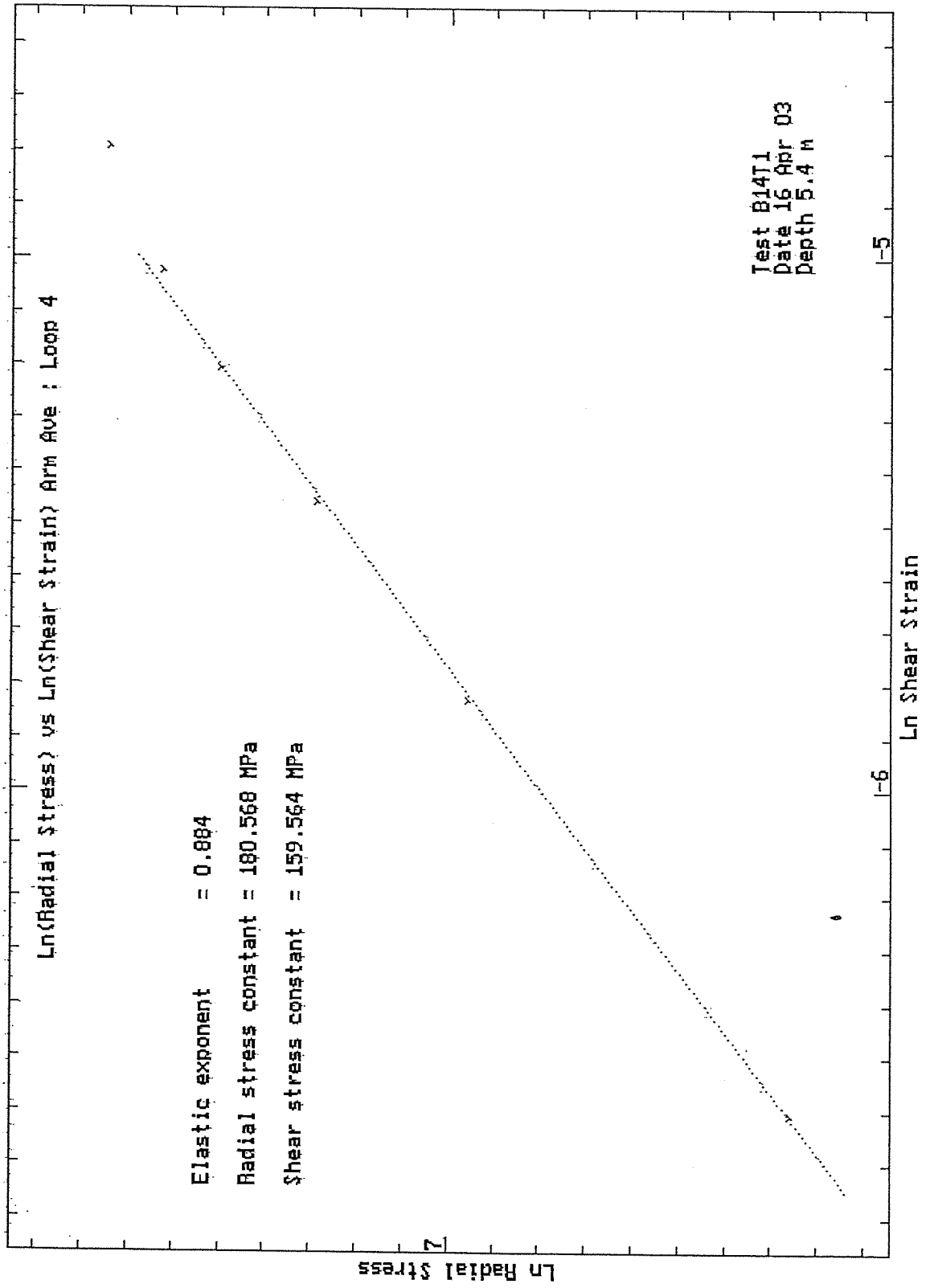
Ln(Radial Stress) vs Ln(Shear Strain) Arm Ave : Loop 4
Elastic exponent = 0.884
Radial stress constant = 180.568 MPa
Shear stress constant = 159.564 MPa
Test B14T1
Date 16 Apr 03
Depth 5.4 m
Ln Radial Stress
Ln Shear Strain
-7
-6
-5

APPENDIX A. DESCRIPTION OF THE EQUIPMENT

Figure 1 The basic HPD-MPX kit

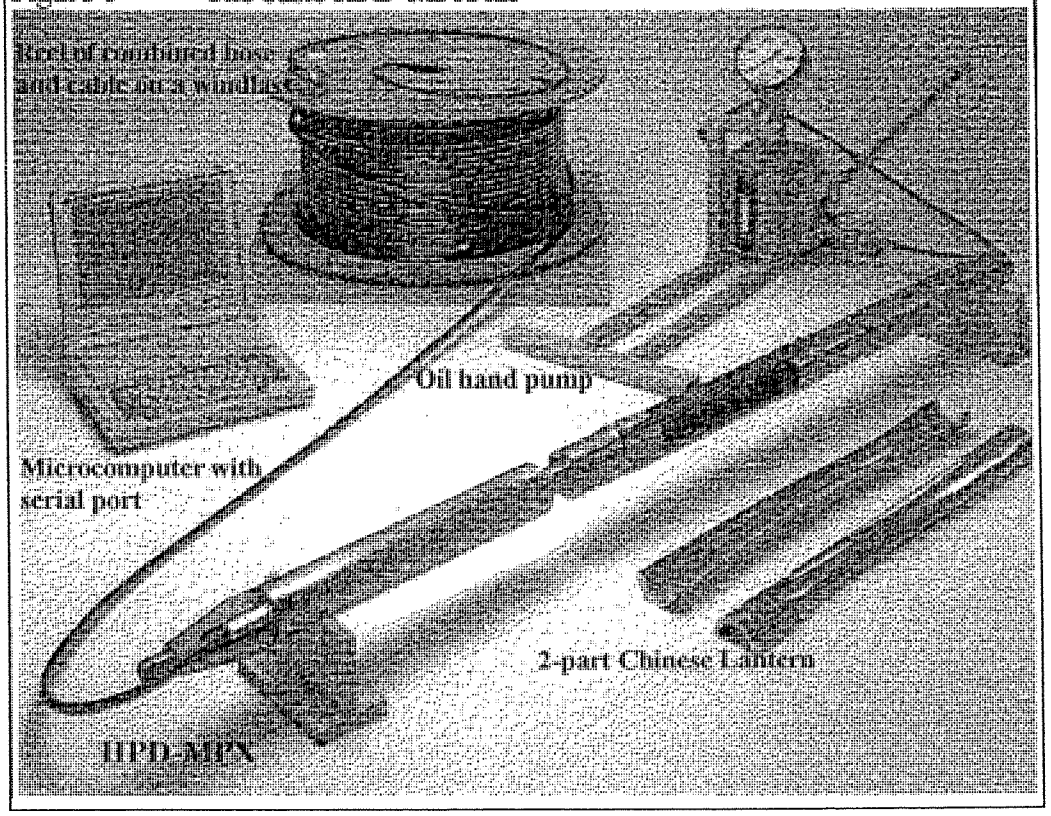

1 OUTLINE

The 95mm High Pressure Dilatometer (95HPD) is a pre-bored hole pressuremeter for testing a 101mm diameter pocket. When a test is required it is lowered into a pocket in the ground conventionally formed by an H size barrel.. On completion of a test it is removed from the borehole which is then extended by conventional drilling techniques.

The instrument is 95 mm in diameter and has an overall length of about 2 metres. The central third of the instrument is covered by a tough rubber membrane about 6mm thick; pressure is applied to the inside of the instrument and the membrane expands, pressing against the borehole wall. The radial displacement of the inside boundary of the membrane is measured at six points equally distributed around the centre of the expanding section.

This displacement, and the pressure necessary to cause the movement, are continously monitored by strain gauged transducers contained within the instrument. Also within the instrument is the analogue and digital electronic circuitry necessary to condition the signals from the transducers. Every ten seconds a set of readings from all the measuring circuits are transmitted to the surface as an RS232 data stream which may be connected directly to the serial port of a microcomputer. Plotting these readings of displacement against pressure produces a loading curve for the material being tested. A number of mathematical analyses are available for translating this loading curve to fundamental strength and stiffness parameters for the ground.

Because the instrument has six strain arms there is some redundancy in the measurement of strain, and this enables the user to carry out a successful test even if one of the arms are defective. In order to give a similar level of reliability to the pressure measuring system a second pressure cell is included in the HPD-MPX, and its readings provide a check of the performance of the first transducer.

The HPD can apply up to 30MPa of pressure to the ground, and can expand from an initial diameter of 95mm to nearly 150mm. It will resolve movements of less than 1 micron and pressure changes of less than 1kPa. Hence although it was developed to test weak rock it can make a test at two extremes of ground conditions - stiff clays, which yield at pressures below 1MPa, and weak rock with a shear modulus greater than 4GPa.

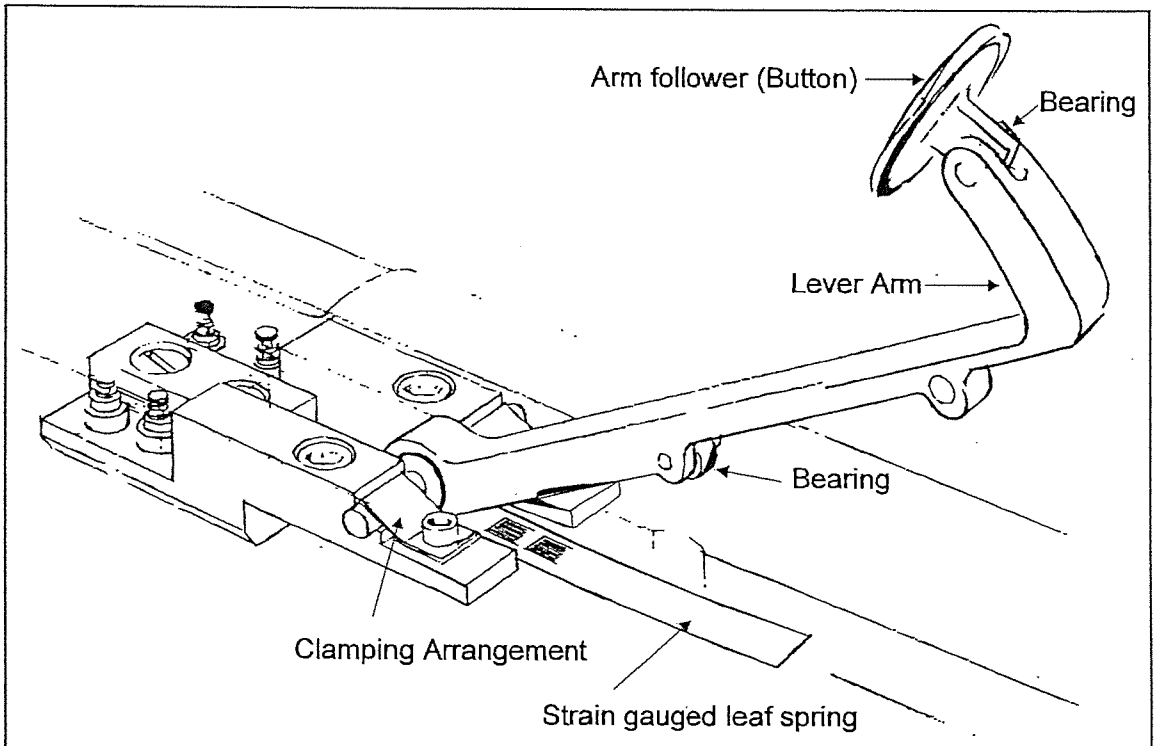

Figure 2 Displacement sensor of the 95mm HPD

The instrument is based on a smaller device (the 73mm HPD) that has had a long and successful history of site work and has been used worldwide. It is a development of an instrument invented by Dr J.M.O. Hughes in 1978. Although internally complex by the standards normally applied to instrumentation of this kind, it is reliable and robust, and the routine maintenance is straightforward. Because all the signal conditioning electronics is contained in the probe itself , the instrument is unaffected by external changes such as replacing the cable.

An additional feature of this pressuremeter is a special electronic compass module fitted to the foot of the instrument. This gives a continuous reading of the orientation of a fixed reference on the instrument with respect to magnetic North. The compass consists of two flux gate magnetometer sensors at right angles to each other. The output of the compass therefore is two signals which are the sine and cosine of the angle made with the Earth's magnetic field. The quotient of these gives an unambiguous direction.

Like all expansion pressuremeters in commercial use the HPD has one fundamental limitation- the loading curve which it produces is derived from following the movement of the *inside* boundary of an elastic membrane. This is different from the movements of the *outside* boundary of the membrane, and hence the movements in the material itself. For the majority of the tests for which the HPD is used, this uncertainty is not significant. However for a small number of tests it is critical; for this reason the calibration procedure described in Appendix B necessarily is complex in order to reduce the margin of uncertainty and set limits to it.

The instrument and all associated electronics for capturing the data are powered from a 12volt vehicle battery.

2 THE MEMBRANE

The membrane itself is a nitrile rubber sleeve. Because the behaviour of the membrane has an influence on the derived displacements it is kept relatively thin (6mm for the standard probe) so that its contribution is small. By its very nature there is a gap between the instrument and the borehole and steps have to be taken to prevent the membrane extruding axially. This is achieved by stiffening the ends of the membrane with rings of stainless steel fingers known because of their appearance as 'Christmas Trees'.

There is a version of the membrane which carries local reinforcement at the ends consisting of kevlar strands. When the applied pressures are fairly modest (no more than about 50% of the available range) then this membrane can be used without Christmas trees.

The entire length of the of rubber membrane is covered with a sheath of eighteen stainless steel strips which are axially stiff but free to expand radially. This sheath protects the membrane from sharp edges, and is known as a 'Chinese Lantern'. The individual strips do not overlap in the closed position.

3 THE PRESSURISING SYSTEM

The instrument is inflated by oil or gas. A strong hose connects the instrument to the pressure source, either a manually operated hydraulic pump or a pneumatic control system. The passage down the centre of the hose is large enough to incorporate a steel logging cable with four electrical conductors. Three of these conductors are used; one carries the digital signals output by the instrument, and two carry power to the instrument from a conventional 12 volt vehicle battery. The power consumption of the pressuremeter is small; up to 500 metres of hose and cable could be connected to the instrument with only minor modification.

The advantages of the oil inflation are that it is inherently safe, requires very little equipment and because it is re-cycled the consumable costs are low. However if the instrument is on a long cable it takes time for the oil to return to the surface and in a dry hole it will never return.

When working offshore, it is normal to use oil, giving the added advantage that should the membrane become punctured the oil will keep the water out of the probe.

4 ELECTRONIC INTERFACE UNIT (EIU)

All pressuremeter hardware is powered by a single 12 volt vehicle battery. The battery is connected to the EIU, which introduces some protection and distributes the power to a number of outlets, including one for the pressuremeter. The returning signals from the pressuremeter connect to the same socket. The digital signals pass through an opto-isolation circuit and are then made available on two identical sockets for connection to the serial port of a computer. There is also an analogue signal which represents the output of TPC A.

The unit has a panel meter which can be switched either to read the battery volts or to read the analogue signal.

5 DATA LOGGING / ANALYSIS SOFTWARE

Software developed by Cambridge Insitu is used to log the data during the test, and for analysing the results subsequently.

The logging software stores the incoming data, displays the pressure/expansion curve in real time, and provides a text file output of the test data in engineering units. This file is read directly by the analysis program, but can also be read by any of the common spreadsheet programs.

The analysis software provides routines which implement a number of standard analyses. The analyses tend to be graphically driven, meaning that the analyst identifies and marks significant parts of the curve, either for breakpoints or slope. The final screen for the analysis is then output as hardcopy backup for the decisions made.

APPENDIX B THE CALIBRATION PROCEDURES

After presenting the background to the calibration procedures the actual calibrations used on this contract are summarised.

1. Scale Factors

The transducers in the probes are based on full bridge strain gauge circuits. Any such transducer produces an output dependent on the voltage being applied to it, the stress deflecting it and the amplification or buffering between it and the recording system.

The instruments contain electronic devices that provide a regulated voltage to the transducers and amplification of the resulting output signals. Because this electronic conditioning is a fixed part of the system it is not mentioned when presenting calibrations. The electrical output of the transducer, in volts, is quoted only as a function of the deflecting stress. This function is termed 'sensitivity' and gives the scale factor for deriving pressure or displacement from the transducer electrical output.

Although the output of the transducers is quoted in volts, the true output of the system is a digital data stream of ASCII encoded numbers representing volts. This signal can be connected directly to the serial port of a small computer. All variables associated with producing the final digital output from the strain gauge signals are a function of the pressuremeter itself, and are independent of external changes such as replacing the cable.

When using the sensitivity calibrations to convert readings from volts into engineering units we make two important assumptions about this output; that it is linear and that the hysteresis is negligible. The calibration procedure needs to provide evidence that these assumptions are reasonable.

2. The Displacement Measuring System

The displacement measuring devices used on the HPD are often referred to as 'the arms'. The arms are calibrated by mounting a micrometer above each in turn and recording the output for a given deflection. When calibrating the instrument it is necessary to plot these readings for both an increasing and reducing deflection. The difference at a given point between increasing readings and reducing readings is a measure of the hysteresis. The worst case figure is noted, and corrective action is taken if the hysteresis is outside an acceptable limit - normally 0.5% of the sensitivity.

The slope of the best fit straight line through all the points is used to quote the arm sensitivity - as an output for a given deflection in units of millivolts per millimetre (mV/mm). A typical figure is 120mV/mm for a 95mm HPD. The arms have a range of 24mm so the output swing is about 3 volts.

3. Pressure Measuring Transducers

For pressure measuring circuits the maximum possible sensitivity is desirable, the only requirement is that the sensitivity be known and be linear and stable.

The sensitivity of internal pressure transducers is determined by placing a large metal cylinder over the probe and applying a known pressure to the inside of the instrument. The pressure being applied is measured by a standard test gauge. As with the arms, readings are plotted, the hysteresis noted, and the best fit straight line drawn through the plotted points.

Pressure sensitivities are quoted in units of millivolts per MegaPascal and a typical figure for the 95mm HPD is 80mV/MPa.

4. Reference ('zero') outputs

The other parameter that the transducers have is a known output for an 'at rest' position. This is the value of the outputs produced by the circuits with atmospheric pressure both inside and outside the instrument, and any displacement measuring system at the initial radius position. This is called a little misleadingly 'zero'.

The absolute value of this figure is normally unimportant - it is not necessary that the figure be zero volts for zero displacement or stress, just that it be known. For practical purposes, as the analogue to digital converter outputs a number between –3.2767 and +3.2767 volts, the 'at rest' readings for the arms are set to be about -2 volts to allow a large output range with a margin for error.

A similar situation applies to the pressure cells – the absolute value of the 'zero' output is unimportant provided it allows the full pressure of the system to be resolved. However an exception is made for cell A. It is convenient to have an analogue representation of the pressure and a buffered output from cell A is taken to the surface via a spare way in the cable. Interpreting the output is easier if zero pressure reads as zero volts and this is arranged in the probe. This output is primarily used when making maintained load tests in softer ground where the resolution of a test gauge is not sufficient to see if the pressure is changing.

Adjustment positions using 1% metal film resistors are provided in the instruments for setting all 'zero' outputs.

It is normal to take zero readings both at ground level and also immediately prior to carrying out a test. A significant change between zero readings must be investigated. 'Significant' would mean a change of 30 millivolts from the last set of zero readings. It is not unusual for shifts of a few millivolts to occur from day to day. It is important that the zero readings be stable when viewed over a period of a few minutes.

Note that when using oil to inflate the probe, ground level readings are the preferred reference because once in the borehole the pressure transducers will read the head of oil. For gas inflation it is probably better to use the zero readings when the probe is in place in the borehole, because it will then be at the temperature most applicable to the test.

5. Membrane stiffness

The membrane that is expanded by the HPD has its own initial tension requiring a finite pressure to move it. The readings measured by the stress cells need to be reduced by this pressure in order to determine the net stress being applied to the ground.

The membrane correction has two components - the pressure to move the membrane from its position at rest on the instrument, and a second component dependent on the radial expansion.

The technique for obtaining the correction data is to pressurise the instrument in free air, ideally using the same rate of expansion as would be applied during a test. For preference, 'free air' is actually inside a large cylinder that fits closely at the ends of the membrane but allows a large expansion elsewhere. This is partly for safety, but also because the ends of the membrane are reinforced by the Christmas trees and it is important that these are not over extended.

The slope and the intercept on the pressure axis of the graph produced by this test give the membrane correction information for each arm.

Knowing that the membrane does not necessarily possess isotropic properties, it has been customary to derive a different set of figures for each arm position. However recent work indicates that an unconfined inflation in air exaggerates any variation in membrane properties; an average correction factor is more appropriate.

The membrane correction data is quoted as a pressure in kPa to move the membrane from its rest position together with a second pressure in units of kPa/mm representing the pressure increase necessary to maintain the inflation. Typical correction figures might be 30kPa and 10kPa/mm.

6. Instrument compliance

The instrument will deform as a consequence of the pressure being internally applied. Put simply, the instrument stretches. Because the displacement measuring system uses the body of the instrument as a reference, movements of the body are seen as apparent displacements of the membrane; some ingenuity is needed to immunise the displacement measuring system from this problem. This system compliance has implications for the measurement of shear modulus, and it can become a significant source of error when measuring very high modulus values.

There are a number of effects to consider but they are collectively determined using a single procedure. The correction figure which results is known somewhat inappropriately as 'membrane compression'.

The procedure normally suggested to obtain correction data for 'membrane compression' is to inflate the pressuremeter inside a number of cylinders of different bores; by comparing these known bores with the displacements actually obtained from the pressuremeter then a correction curve can be obtained. Because the correction has been assumed to be a function of membrane thickness, then it is expected that the effect reduces as the membrane thins. In other words, it is treated as a strain dependent variable, and a change in membrane means a new correction curve must be derived.

For the Cambridge family of pressuremeters real membrane compression, that is the membrane changing in thickness as a direct result of the pressure differential across it, is almost too small to be measurable. There are a number of other factors to consider of significantly greater magnitude than membrane compression.

Inflating the instrument inside a metal cylinder will in theory provide data on the magnitude of these effects. However a separate source of error, which is a function of the calibration procedure itself, then becomes apparent. The membrane is able to expand axially by a small amount, and as a result experiences a change in thickness which may not occur in the ground. Although steps can be taken to keep this axial movement to a minimum, it cannot be easily eliminated.

As a consequence of the poor fit of a calibration cylinder, and also of the relatively low coefficient of friction between the membrane and the steel by comparison with the membrane and the ground, the instrument will move about in the cylinder - its centre will not be the same as the centre of the cylinder. Only average radial movement can be derived from this calibration process, and it is not possible to obtain good data for each arm.

There is evidence that much of the correction is due to the Chinese lantern strips taking up the form of the cylinder, a process that would only occur in the ground if the material was good rock. This is the explanation for much of the initial curvature that occurs when an assembled probe is inflated inside a metal sleeve - it is a serious error to attempt to derive a correction factor from this part of the loading.

Taking account of all the above, the following method is used to calibrate the 95mm HPD. The Chinese lantern is removed, and an aluminium cylinder of known properties with close fitting ends is placed over the membrane of the instrument. It is the same cylinder as is used to do membrane correction tests, and in fact a single test can be used to obtain all membrane parameters. The instrument is inflated slowly until the membrane contacts the wall of the cylinder. This data are used for membrane correction. Now the test continues in steps of 10 bars. Each step is held briefly to ensure maximum accuracy. The probe is pressurised to 200 bars, its safe maximum working pressure. The pressure is then reduced, also in steps of 10 bars. Some users prefer the unloading should be down to 20 bars, then the probe should be reloaded again to maximum pressure and unloaded to zero, in effect doing a large unload/reload cycle. In a good calibration, all loading and unloading slopes will be similar, but it sometimes happens that the probe moves with respect to the cylinder and this will affect the data. In this event doing the second reloading will probably give the best correction information.

The calibration is obtained by plotting the pressure/displacement data on a large scale, and finding the best fit slope through the points. The slope ought to be the known expansion of the cylinder for a change of 200 bars. In practice it is always a little more, the difference being the 'membrane compression' figure. We quote the figure in terms of 'mm/GPa' a typical compression being 3mm/GPa. The cylinder normally used to carry out the compression test has an elastic slope of 2.7mm/GPa.

Quoting the compression in this manner allows the software to calculate the appropriate error for every step of pressure and to make the necessary adjustment to the measured displacements.
To put the correction in context, a slope of 5mm/GPa (a relatively large correction) is equivalent to a modulus greater than 4GPa

7. Membrane thinning

During a test the pressuremeter membrane changes in thickness as a consequence of being stretched. This change in thickness can be calculated by assuming to a first approximation that the cross-section area of the membrane remains constant. The calculation is incorporated into the program that converts raw data into engineering units.

Note that the term 'membrane' includes the stainless steel protective sheath, and that the measurement made by the arms is the radial distance to the inside of the membrane.

Definition of Terms

a	is the internal radius of the membrane at rest
b	is the external radius of the membrane at rest
c	is the internal radius of the membrane expanded
r	is the external radius of the membrane expanded
t	is the thickness of the stainless steel sheath strips
d	is the measured movement of the strain arm
E	is the actual expansion of the membrane

Calculation

At rest the cross-section area of rubber $= \pi(b-t)^2 - \pi a^2$

The expanded cross-section area of rubber $= \pi(r-t)^2 - \pi c^2$

Because the rubber is incompressible, these must be equal:-

therefore $(b-t)^2 - a^2 = (r-t)^2 - c^2$

Now:- $c = a + d$

and:- $r = b + E$

therefore $(b-t)^2 - a^2 = [(b+E)-t]^2 - (a+d)^2$

$$\therefore [(b-t)+E]^2 = (b-t)^2 - a^2 + (a+d)^2$$

$$= (b-t)^2 + d(2a+d)$$

$$\sqrt{(b-t)+E} = \sqrt{[(b-t)^2 + d(2a+d)]}$$

$$E = \sqrt{[(b-t)^2 + d(2a+d)]} - (b-t)$$

This is the form in which the calculation is commonly applied to the data, with $\mathbf{2a}$, $\mathbf{2b}$ and $\boldsymbol{t}$ being known from the manufacturer's data, and $\boldsymbol{d}$ being the measurement made by the displacement sensors during the test.

For a 95mm High Pressure Dilatometer fitted with a 6mm nitrile rubber membrane and Chinese lantern:-

$2a$	=	82.0 mm
$2b$	=	95.0 mm
t	=	0.53 mm

To apply the correction at a given expansion the *average* radius of the expanding membrane is calculated. This average is then entered into the equation and the ratio between the corrected

average and the raw average is expressed as a scale factor (it turns out to be about 0.90 for a 95mm HPD at all expansions). The scale factor is then applied to the individual arm displacement outputs.

8. Repeatability (or how much effort should be devoted to calibrations)

Although it is important regularly to check the sensitivities of the strain gauge circuits, it is unusual for them to change markedly. Indeed it is common for the hysteresis to improve with use. 80% of the performance of a strain gauge bridge application can be predicted from its design; the calibration removes the uncertainty due to manufacturing tolerances, and can give early warning of impending problems in a particular circuit.

The expansion test for example is concerned with making relative measurements, not absolute measurements. The HPD displacement measuring system will resolve movements of less than 0.5 microns over a range of 24 millimetres; the pressure measuring system will resolve changes of 0.5 kPa over a range of 20MPa. This resolution is considerably higher than can be seen with a standard micrometer or test gauge. To put it into context, 0.5 microns is approximately the wavelength of ultraviolet light. Obviously there is no practical possibility of checking by measurement a movement so small.

Hence the term 'calibrating' is inappropriate. What is done in practice is to check that the various sensors are linear over a number of relatively coarse steps or intervals. We assume that this linear behaviour will be true for very much smaller changes.

For this reason alone, without considering additional sources of error such as the skill of the operator carrying out the calibration, the accuracy of the standard used to derive this linearity is of secondary importance. We expect successive calibrations on the same sensor to be within 2% and investigate a difference greater than 3%.

We also ignore secondary sources of error in this assumption of linearity, such as temperature change. The full bridge configuration is relatively insensitive to temperature variation provided the strain gauges used are matched to the characteristics of the surface to which they are bonded. When critical measurements are being made during a test, for example when taking a reload loop, it is reasonable to assume the temperature remains constant. The ground is usually at a constant temperature whenever a test is carried out, but sometimes there are problems - the temperature of the gas being supplied to the downhole tool can have an influence especially if the gas bottle reservoir is lying outside in direct sunlight.

Using spreadsheet software to present the results of the calibrations for sensitivity has become common practice. One benefit of this is that gradients can be calculated by linear regression routines; this ensures different operators given the same set of data will derive identical calibration factors. The calibrations are presented as a tabulation of transducer output against a known reference, with the linearity and hysteresis quoted for each calibration step.

The membrane correction of the HPD seldom changes greatly and the type of material it is used to test means that for the most part any errors in the magnitude of the correction are of minor importance. The total contribution of the correction is less than 200kPa to a typical test.

In general, if the material is weak (shear strength less than 100kPa) then membrane stiffness is important. If the material is extremely stiff (shear modulus greater than 1GPa) then correcting for instrument compliance is important. In between these two extremes the influence of the imperfections of the machine on the derived parameters is negligible.

9 ORIENTATION

The electronics module fitted at the lower end of the instrument contains an electronic compass that can be used to identify the orientation of the probe with respect to magnetic north.The compass consists of two sensors whose output is proportional to the Earth's magnetic field. The sensors are fitted at right angles to each other, each giving a maximum output when that sensor is in line with magnetic north. The consequence is that that at any time the sensors give the sine and cosine of the angle made with magnetic north, permitting an unambiguous direction to be inferred.

The calculation of direction is implemented in the logging software package.

To calibrate the sensors, the instrument is rotated slowly through 360 degrees whilst the output of the sensors are logged. From this, the maximum and minimum output of each sensor is derived and is stored. Thereafter, selecting an option 'Heading' in the logging software uses the derived maximum and minimum values and the current data line to determine a direction.

Because the magnitude of the output is affected by the dip angle made with magnetic north, it is best if such a procedure is carried out in the ground immediately above the test pocket.

The sensors are hidden inside the electronics module container. A brass stud on the outside indicates the position of the Cos sensor, and the electronics module fits to the instrument so that this stud is in line with arm 1. The direction that the compass produces, therefore, is the angle of arm 1 with respect to magnetic north.

10. Tables of measured scalar values

Date	Arm 1	Arm 2	Arm 3	Arm 4	Arm 5	Arm 6	TPC A	TPC B
Tilly	mV/mm	mV/mm	mV/mm	mV/mm	mV/mm	mV/mm	mV/MPa	mV/MPa
05/07/00	123.3	129.2	117.7	117.3	115.0	122.2	80.5	-
13/06/02	122.1	127.2	117.3	116.9	114.4	120.9	80.3	-
07/08/02	122.2	127.3	117.6	117.2	114.7	120.7	81.0	-
02/10/02	122.3	127.3	117.5	117.3	114.2	121.0	80.7	-
06/03/03	-	-	-	-	-	-	80.9	89.5
8-9/05/03	122.0	127.2	117.7	117.4	114.8	120.9	81.3	90.1
Scotty								
26/07/01	120.4	120.0	120.6	120.5	118.8	120.1	78.6	80.8
16/08/01	120.5	120.0	120.5	120.3	118.9	120.0	78.9	81.2
27/11/01	120.3	120.0	120.5	120.0	118.8	120.4	78.7	81.0
01/02/02	120.0	120.0	120.7	120.4	118.9	120.1	77.2	-
12/06/02	120.5	120.0	120.6	120.5	119.0	120.1	78.8	81.0
20/03/03	120.4	119.9	120.5	120.2	118.6	120.3	-	-
24/03/03	-	-	-	-	-	-	78.7	81.0

11. Table of membrane calibrations for HPD tests

Test	Probe	Zero	Slope	Compression
		(kPa)	(kPa/mm)	(mm/GPa)
C999T99	Tilly	48	10	3
C499T99	Scotty	49	9.7	2.5

Plots of these calibrations follow.

95mm HPD		Tilly							
Arm calibration		5th July 2000							
mm	Arm 1	Linearity	Hysteresis	Arm 2	Linearity	Hysteresis	Arm 3	Linearity	Hysteresis
	(mV)	(%)	(%)	(mV)	(%)	(%)	(mV)	(%)	(%)
0	-1385.5	100.1	0.30	-1692.1	102.7	-0.01	-1563.7	93.5	-0.09
2	-1138.8	101.5	0.39	-1426.8	101.3	0.30	-1343.7	103.3	0.09
4	-888.5	99.7	-0.10	-1165.0	101.1	0.33	-1100.5	101.1	0.04
6	-642.6	99.4	-0.08	-903.7	98.8	0.41	-862.5	100.4	-0.05
8	-397.5	98.7	-0.17	-648.3	97.9	0.34	-626.2	99.1	0.11
10	-154.2	97.9	-0.10	-395.4	96.8	0.17	-393.0	99.4	0.02
12	87.1	-97.3		-145.2	-97.8		-159.0	-99.6	
10	-152.7	-98.3		-398.0	-98.9		-393.3	-99.6	
8	-395.0	-99.9		-653.6	-99.2		-627.8	-99.4	
6	-641.4	-99.6		-910.0	-100.7		-861.8	-101.7	
4	-887.0	-104.4		-1170.1	-101.2		-1101.1	-103.6	
2	-1144.5	-99.5		-1431.5	-100.8		-1344.9	-92.5	
0	-1389.9			-1692.0			-1562.5		
Zero	-1385.0	mV		-1687.2	mV		-1570.2	mV	
Slope	123.3	mV/mm		129.2	mV/mm		117.7	mV/mm	
mm	Arm 4	Linearity	Hysteresis	Arm 5	Linearity	Hysteresis	Arm 6	Linearity	Hysteresis
	(mV)	(%)	(%)	(mV)	(%)	(%)	(mV)	(%)	(%)
0	-1378.0	91.0	-0.01	-1475.6	100.4	0.05	-1544.3	102.5	-0.03
2	-1164.4	103.5	-0.09	-1244.7	101.9	0.23	-1293.8	101.8	0.14
4	-921.5	101.6	-0.09	-1010.2	100.1	0.07	-1045.1	100.2	0.15
6	-683.2	100.6	-0.03	-779.9	98.6	0.04	-800.2	98.6	0.07
8	-447.3	99.6	0.06	-553.1	99.0	0.02	-559.3	98.3	0.10
10	-213.6	99.7	-0.08	-325.3	99.1	-0.06	-319.1	98.2	-0.10
12	20.4	-99.3		-97.3	-98.8		-79.2	-97.6	
10	-212.5	-100.4		-324.5	-99.5		-317.7	-99.5	
8	-448.1	-100.0		-553.4	-98.7		-560.8	-98.4	
6	-682.8	-101.2		-780.5	-100.2		-801.2	-100.7	
4	-920.2	-103.5		-1011.1	-102.9		-1047.3	-101.7	
2	-1163.1	-91.5		-1247.9	-99.3		-1295.8	-101.5	
0	-1377.8			-1476.3			-1543.8		
Zero	-1387.5	mV		-1474.0	mV		-1539.0	mV	
Slope	117.3	mV/mm		115.0	mV/mm		122.2	mV/mm	
Pressure cell calibration			5th July 2000		0-250 bar gauge s/n 12574638				
bar	TPC	Linearity	Hysteresis						
	(mV)	(%)	(%)						
0	6.0	91.1	-0.23						
10	79.3	99.5	-0.72						
20	159.4	99.7	-0.69						
30	239.6	99.5	-0.47						
40	319.7	102.2	-0.30						
50	401.9	97.1	-0.11						
60	480.0	102.8	-0.75						
70	562.7	102.0	-0.56						
80	644.8	-97.6							
70	566.3	-101.3							
60	484.8	-102.2							
50	402.6	-100.7							
40	321.6	-98.2							
30	242.6	-97.9							
20	163.8	-99.3							
10	83.90	-94.9							
0	7.5								
Zero	0.2	mV							
Slope	8.0	mV/bar							
Sensitivity	80.5	mV/Mpa							

95mm HPD		Tilly								
Arm calibration		13th June 2002								
mm	Arm 1	Linearity	Hysteresis	Arm 2	Linearity	Hysteresis	Arm 3	Linearity	Hysteresis	
	(mV)	(%)	(%)	(mV)	(%)	(%)	(mV)	(%)	(%)	
0	-1381.1	99.6	-0.02	-1680.0	102.9	-0.03	-1558.0	94.9	-0.07	
2	-1137.8	103.0	-0.05	-1418.2	103.3	0.10	-1335.3	103.9	-0.10	
4	-886.3	101.0	-0.13	-1155.4	102.4	0.19	-1091.6	102.1	-0.18	
6	-639.6	100.2	-0.19	-895.0	100.5	0.22	-852.1	100.2	-0.25	
8	-395.0	100.0	-0.24	-639.3	99.8	0.24	-617.0	99.8	-0.32	
10	-150.9	99.4	-0.25	-385.5	99.1	0.27	-382.8	99.5	-0.32	
12	91.9	99.3	-0.23	-133.5	98.9	0.24	-149.4	98.9	-0.32	
14	334.3	98.9	-0.20	118.0	98.1	0.24	82.7	99.2	-0.26	
16	575.8	98.0	-0.16	367.5	97.5	0.16	315.4	99.2	-0.21	
18	815.2	99.4	-0.19	615.4	97.7	0.12	548.0	99.6	-0.11	
20	1058.0	-97.6		864.0	-98.9		781.7	-98.6		
18	819.8	-98.3		612.3	-97.8		550.5	-98.1		
16	579.7	-98.5		363.4	-98.9		320.3	-98.7		
14	339.2	-99.0		111.8	-98.9		88.8	-98.3		
12	97.5	-99.2		-139.7	-99.3		-141.8	-99.5		
10	-144.7	-100.1		-392.3	-99.5		-375.2	-99.9		
8	-389.2	-100.7		-645.5	-100.2		-609.5	-100.9		
6	-635.0	-101.7		-900.5	-102.1		-846.3	-102.8		
4	-883.2	-103.8		-1160.2	-102.4		-1087.4	-104.7		
2	-1136.7	-99.9		-1420.7	-101.6		-1332.9	-95.3		
0	-1380.7			-1679.2			-1556.4			
Zero	-1374.6	mV		-1668.1	mV		-1557.5	mV		
Slope	122.1	mV/mm		127.2	mV/mm		117.3	mV/mm		
mm	Arm 4	Linearity	Hysteresis	Arm 5	Linearity	Hysteresis	Arm 6	Linearity	Hysteresis	
	(mV)	(%)	(%)	(mV)	(%)	(%)	(mV)	(%)	(%)	
0	-1374.0	96.6	-0.06	-1466.4	99.7	-0.06	-1538.2	102.9	-0.03	
2	-1148.1	103.4	-0.08	-1238.2	103.0	-0.04	-1289.5	103.6	-0.19	
4	-906.4	101.7	-0.18	-1002.6	100.7	-0.15	-1039.0	101.2	-0.26	
6	-668.6	100.6	-0.25	-772.1	99.6	-0.30	-794.4	100.2	-0.34	
8	-433.4	100.0	-0.33	-544.1	99.7	-0.40	-552.1	99.5	-0.40	
10	-199.6	99.6	-0.36	-315.9	99.5	-0.44	-311.7	99.2	-0.45	
12	33.2	99.1	-0.31	-88.3	99.4	-0.44	-72.0	98.2	-0.43	
14	264.9	98.3	-0.25	139.2	99.9	-0.38	165.4	98.7	-0.45	
16	494.8	99.1	-0.29	367.8	99.0	-0.24	403.9	98.6	-0.36	
18	726.5	98.9	-0.10	594.3	97.2	-0.13	642.2	98.3	-0.24	
20	957.8	-97.9		816.8	-96.0		879.8	-95.9		
18	728.8	-97.2		597.2	-97.9		648.0	-97.4		
16	501.5	-98.7		373.2	-98.5		412.7	-97.8		
14	270.8	-98.5		147.9	-98.9		176.2	-98.4		
12	40.5	-99.1		-78.3	-99.5		-61.6	-99.0		
10	-191.2	-100.3		-305.9	-100.1		-300.8	-100.0		
8	-425.8	-101.4		-535.0	-100.6		-542.5	-100.8		
6	-662.8	-102.4		-765.2	-102.3		-786.1	-102.0		
4	-902.2	-104.4		-999.2	-104.1		-1032.6	-104.3		
2	-1146.3	-96.8		-1237.3	-99.5		-1284.8	-104.5		
0	-1372.6			-1465.0			-1537.5			
Zero	-1371.1	mV		-1459.9	mV		-1523.1	mV		
Slope	116.9	mV/mm		114.4	mV/mm		120.9	mV/mm		
Pressure cell calibration			13th June 2002		Budenberg gauge s/n 12394260					
bar	TPC	Linearity	Hysteresis							
	(mV)	(%)	(%)							
0	2.0	104.7	-0.21							
20	170.0	99.1	-0.14							
40	329.1	99.7	0.12							
60	489.2	100.2	0.06							
80	650.0	101.5	-0.19							
100	813.0	-100.6								
80	651.5	-101.4								
60	488.7	-100.0								
40	328.1	-97.8								
20	171.1	-104.3								
0	3.7									
Zero	8.6	mV								
Slope	8.0	mV/bar								
Sensitivity	80.3	mV/Mpa								

95mm HPD		Tilly							
Arm calibration		7th August 2002							
mm	Arm 1	Linearity	Hysteresis	Arm 2	Linearity	Hysteresis	Arm 3	Linearity	Hysteresis
	(mV)	(%)	(%)	(mV)	(%)	(%)	(mV)	(%)	(%)
0	-1376.7	100.3	-0.07	-1675.4	100.4	0.04	-1561.5	98.0	0.01
2	-1131.6	103.1	-0.06	-1419.7	104.0	0.19	-1331.0	103.6	-0.06
4	-879.6	101.2	-0.14	-1154.8	102.2	0.25	-1087.2	101.7	-0.16
6	-632.2	100.6	-0.16	-894.4	100.4	0.27	-848.0	100.2	-0.26
8	-386.3	99.7	-0.18	-638.6	99.6	0.31	-612.3	99.7	-0.31
10	-142.7	99.4	-0.23	-384.9	99.3	0.31	-377.6	97.5	-0.35
12	100.2	98.4	-0.22	-131.9	98.8	0.26	-148.2	100.2	-0.41
14	340.7	99.0	-0.25	119.8	98.0	0.23	87.5	99.3	-0.34
16	582.7	98.5	-0.19	369.5	97.5	0.16	321.2	99.5	-0.28
18	823.4	98.9	-0.16	617.8	97.8	0.02	555.4	98.6	-0.10
20	1065.1	-97.3		866.9	-98.0		787.3	-97.6	
18	827.3	-98.2		617.2	-98.8		557.7	-97.7	
16	587.3	-98.5		365.5	-98.6		327.8	-98.8	
14	346.7	-98.7		114.0	-99.2		95.4	-99.5	
12	105.6	-99.4		-138.6	-99.8		-138.6	-98.0	
10	-137.2	-100.1		-392.8	-99.6		-369.3	-100.2	
8	-381.9	-100.8		-646.4	-100.1		-605.0	-100.7	
6	-628.2	-101.5		-901.4	-102.0		-842.0	-102.6	
4	-876.2	-103.9		-1161.1	-103.4		-1083.4	-104.6	
2	-1130.1	-100.3		-1424.5	-98.9		-1329.6	-98.7	
0	-1375.1			-1676.5			-1561.8		
Zero	-1368.3	mV		-1668.5	mV		-1556.8	mV	
Slope	122.2	mV/mm		127.3	mV/mm		117.6	mV/mm	

mm	Arm 4	Linearity	Hysteresis	Arm 5	Linearity	Hysteresis	Arm 6	Linearity	Hysteresis
	(mV)	(%)	(%)	(mV)	(%)	(%)	(mV)	(%)	(%)
0	-1380.1	100.2	-0.09	-1467.3	103.9	-0.27	-1536.0	99.0	-0.02
2	-1145.2	103.9	-0.13	-1229.0	101.5	0.08	-1297.1	103.4	0.12
4	-901.8	101.6	-0.21	-996.1	101.3	-0.06	-1047.6	101.1	0.16
6	-663.7	100.7	-0.29	-763.8	99.5	-0.21	-803.5	99.4	-0.09
8	-427.8	99.8	-0.34	-535.5	100.0	-0.31	-563.7	99.6	-0.29
10	-194.0	98.8	-0.37	-306.0	99.3	-0.31	-323.2	99.4	-0.38
12	37.6	98.9	-0.33	-78.3	99.7	-0.34	-83.2	99.7	-0.39
14	269.3	99.3	-0.35	150.5	98.9	-0.29	157.4	98.2	-0.31
16	502.0	97.9	-0.23	377.4	97.8	-0.28	394.5	99.3	-0.32
18	731.4	97.3	-0.09	601.8	97.5	-0.20	634.1	98.1	-0.11
20	959.3	-96.4		825.5	-95.6		870.9	-97.0	
18	733.4	-96.4		606.3	-96.9		636.8	-97.2	
16	507.5	-98.1		383.9	-98.8		402.2	-98.3	
14	277.5	-99.0		157.2	-99.3		165.0	-99.0	
12	45.4	-98.5		-70.6	-99.6		-73.9	-99.5	
10	-185.4	-100.1		-299.0	-100.0		-314.0	-100.6	
8	-419.9	-101.2		-528.5	-100.4		-556.8	-101.3	
6	-657.0	-102.3		-758.9	-102.8		-801.3	-103.6	
4	-896.8	-104.7		-994.8	-102.9		-1051.4	-103.0	
2	-1142.2	-100.6		-1230.9	-100.3		-1300.0	-97.6	
0	-1378.0			-1461.1			-1535.5		
Zero	-1369.6	mV		-1455.1	mV		-1531.5	mV	
Slope	117.2	mV/mm		114.7	mV/mm		120.7	mV/mm	

Pressure cell calibration			7th August 2002	Budenberg gauge s/n 12394260
bar	TPC A	Linearity	Hysteresis	
	(mV)	(%)	(%)	
0	10.2	103.7	0.00	
20	178.3	97.5	-0.17	
40	336.3	99.6	-0.20	
60	497.7	98.8	-0.17	
80	657.9	99.3	-0.21	
100	818.8	100.4	-0.22	
120	981.5	101.3	-0.31	
140	1145.7	101.5	-0.11	
160	1310.2	100.8	-0.12	
180	1473.5	101.2	-0.04	
200	1637.5	-100.8		
180	1474.1	-99.9		
160	1312.2	-101.6		
140	1147.5	-99.3		
120	986.5	-101.3		
100	822.3	-99.3		
80	661.3	-99.3		
60	500.4	-99.2		
40	339.6	-97.8		
20	181.10	-105.4		
0	10.2			
Zero	13.5	mV		
Slope	8.1	mV/bar		
Sensitivity	81.0	mV/Mpa		

Calibration summary, our 95mm HPD (TILLY), 2nd Oct 2002																		
mm	Arm 1	Linearity	Hysteresis	Arm 2	Linearity	Hysteresis	Arm 3	Linearity	Hysteresis	Arm 4	Linearity	Hysteresis	Arm 5	Linearity	Hysteresis	Arm 6	Linearity	Hysteresis
	(mV)	(%)	(%)	(mV)	(%)	(%)	(mV)	(%)	(%)	(mV)	(%)	(%)	(mV)	(%)	(%)	(mV)	(%)	(%)
0	-1388.2	102.9	0.00	-1668.4	102.8	0.02	-1558.7	98.3	-0.09	-1380.2	102.4	-0.12	-1468.9	100.0	-0.04	-1535.5	103.8	0.01
2	-1136.5	103.2	-0.09	-1406.5	103.2	0.13	-1327.6	103.5	-0.09	-1140.1	103.8	-0.14	-1240.4	103.4	-0.07	-1284.3	103.1	-0.13
4	-884.0	102.1	-0.16	-1143.7	102.5	0.22	-1084.3	101.6	-0.19	-896.7	101.3	-0.21	-1004.2	101.3	-0.12	-1034.8	101.6	-0.24
6	-634.3	99.5	-0.21	-882.6	100.3	0.25	-845.5	100.0	-0.29	-659.1	100.3	-0.31	-772.8	100.2	-0.21	-789.1	99.6	-0.33
8	-390.8	99.7	-0.26	-627.1	99.6	0.27	-610.4	99.4	-0.37	-423.8	99.9	-0.37	-543.8	100.1	-0.26	-548.1	99.6	-0.42
10	-146.8	99.1	-0.29	-373.4	99.6	0.26	-376.7	98.8	-0.39	-189.4	98.1	-0.41	-315.2	99.9	-0.37	-307.1	99.0	-0.45
12	95.6	99.4	-0.28	-119.8	98.0	0.27	-144.5	99.4	-0.44	40.7	98.7	-0.37	-86.9	99.1	-0.36	-87.5	98.2	-0.42
14	338.8	98.5	-0.23	129.7	97.7	0.20	89.1	99.4	-0.40	272.3	99.5	-0.36	139.4	98.4	-0.33	170.1	98.7	-0.47
16	579.7	97.5	-0.19	378.6	98.2	0.10	322.7	99.5	-0.29	505.8	98.2	-0.27	364.1	97.7	-0.33	409.0	99.0	-0.37
18	818.2	96.5	-0.27	628.8	97.9	0.01	556.7	99.0	-0.12	736.1	98.8	-0.12	587.4	95.2	-0.24	648.4	98.0	-0.18
20	1054.3	-93.8		878.0	-98.0		789.4	-97.8		967.8	-97.6		805.0	-92.9		885.5	-96.2	
18	824.8	-98.3		628.5	-99.1		559.6	-97.9		738.9	-96.7		592.8	-96.8		652.8	-97.1	
16	584.4	-98.1		376.1	-98.8		329.5	-98.2		512.1	-98.6		371.6	-98.3		418.0	-97.8	
14	344.5	-99.0		124.6	-98.7		98.6	-99.0		280.7	-98.6		147.0	-98.8		181.4	-98.7	
12	102.4	-99.0		-126.8	-99.4		-134.1	-99.3		49.5	-97.8		-78.8	-99.8		-57.3	-98.7	
10	-139.7	-100.1		-379.9	-99.7		-367.5	-99.6		-179.8	-100.3		-306.9	-101.2		-296.1	-100.0	
8	-384.5	-100.0		-633.9	-100.2		-601.7	-100.9		-415.1	-100.9		-538.0	-100.7		-538.0	-100.5	
6	-629.2	-102.6		-889.0	-102.2		-838.8	-102.6		-651.9	-102.2		-768.1	-102.1		-781.1	-102.5	
4	-880.1	-103.9		-1149.4	-102.3		-1079.9	-104.4		-891.7	-104.4		-1001.4	-103.9		-1029.0	-104.2	
2	-1134.2	-103.8		-1409.9	-101.7		-1325.4	-98.3		-1136.7	-102.6		-1238.8	-100.4		-1281.1	-105.2	
0	-1388.2			-1668.8			-1556.5			-1377.3			-1468.1			-1535.7		
Intercept	-1374.2	mV		-1657.2	mV		-1553.0	mV		-1366.4	mV		-1460.6	mV		-1519.7	mV	
Slope	122.3	mV/mm		127.3	mV/mm		117.5	mV/mm		117.3	mV/mm		114.2	mV/mm		121.0	mV/mm	

	New TPC calibrations done as C999T99 6th March 2003					
MPa	TPC A	Linearity	Hysteresis	TPC B	Linearity	Hysteresis
	(Volts)	(%)	(%)	(Volts)	(%)	(%)
0	5.6	101.7	-0.04	80.9	108.7	-0.30
20	170.1	97.6	-0.37	275.6	103.1	-1.58
40	328.0	101.9	-0.56	460.2	103.2	-1.54
60	492.8	100.1	-0.27	645.0	100.9	-1.51
80	654.7	99.0	-0.62	825.6	97.1	-1.59
100	814.8	96.4	-0.39	999.4	101.9	-1.49
120	970.7	103.1	-0.66	1181.8	94.6	-0.95
140	1137.4	98.4	-0.44	1351.1	99.3	-1.23
160	1296.6	100.4	-0.48	1528.8	95.7	-0.90
180	1458.9	103.6	-0.95	1700.1	106.2	-1.36
200	1626.5	-94.1		1890.3	-92.5	
180	1474.3	-105.1		1724.7	-100.4	
160	1304.4	-98.9		1545.0	-95.9	
140	1144.5	-100.9		1373.3	-97.4	
120	981.4	-99.1		1198.9	-96.4	
100	821.1	-96.7		1026.3	-96.1	
80	664.8	-103.6		854.3	-101.6	
60	497.2	-99.0		672.4	-102.9	
40	337.1	-99.6		488.1	-102.7	
20	176.1	-105.1		304.2	-121.7	
0	6.2			86.3		
Intercept	9.1	mVolts		109.9	mVolts	
Slope	8.086	mV/Bars		8.952	mV/Bars	
Slope	80.9	mV/MPa		89.5	mV/MPa	

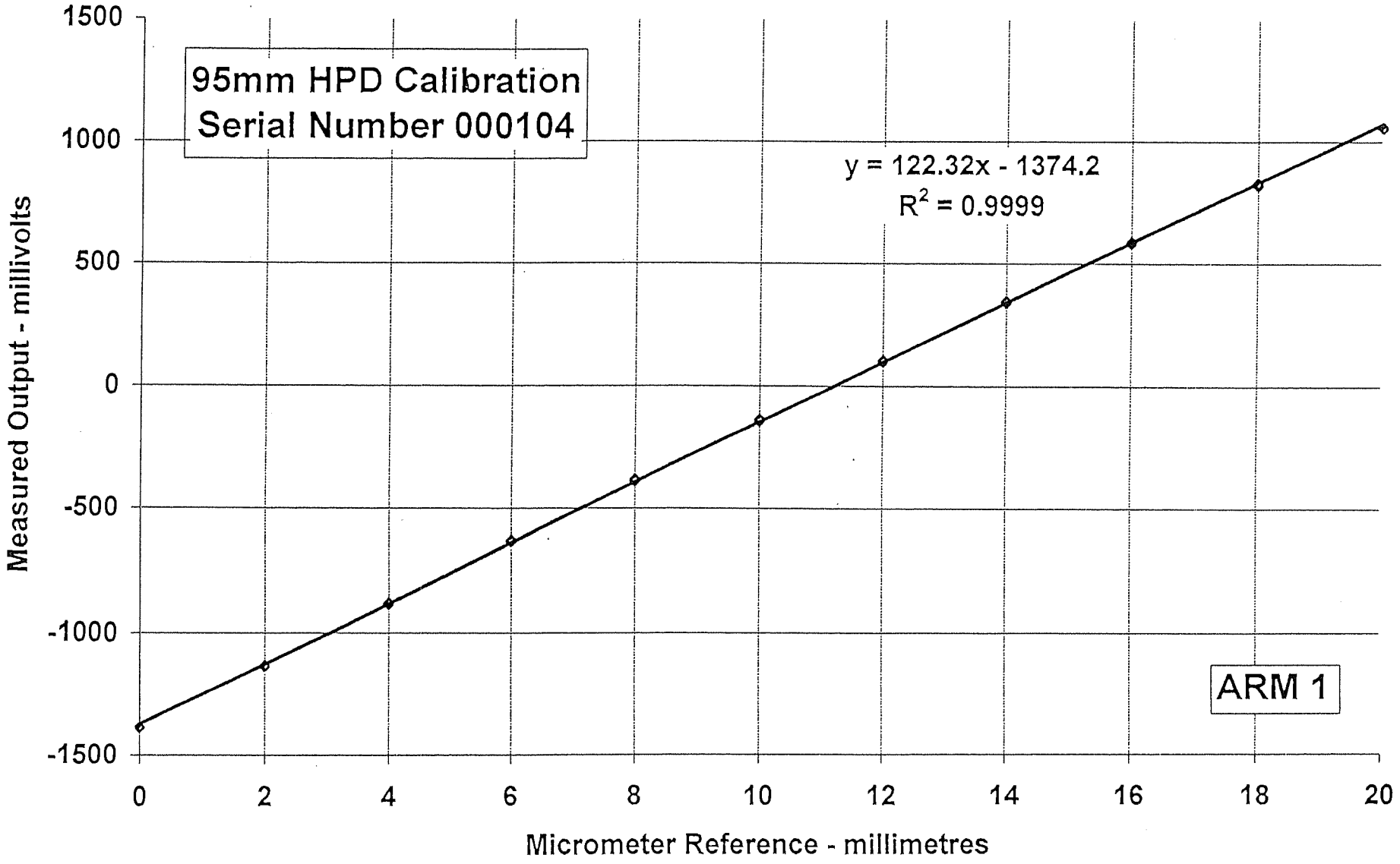
95mm HPD Calibration
Serial Number 000104
y = 122.32x - 1374.2
R2 = 0.9999
ARM 1
Measured Output - millivolts
1500
1000
500
0
-500
-1000
-1500
0
2
4
6
8
10
12
14
16
18
20
Micrometer Reference - millimetres

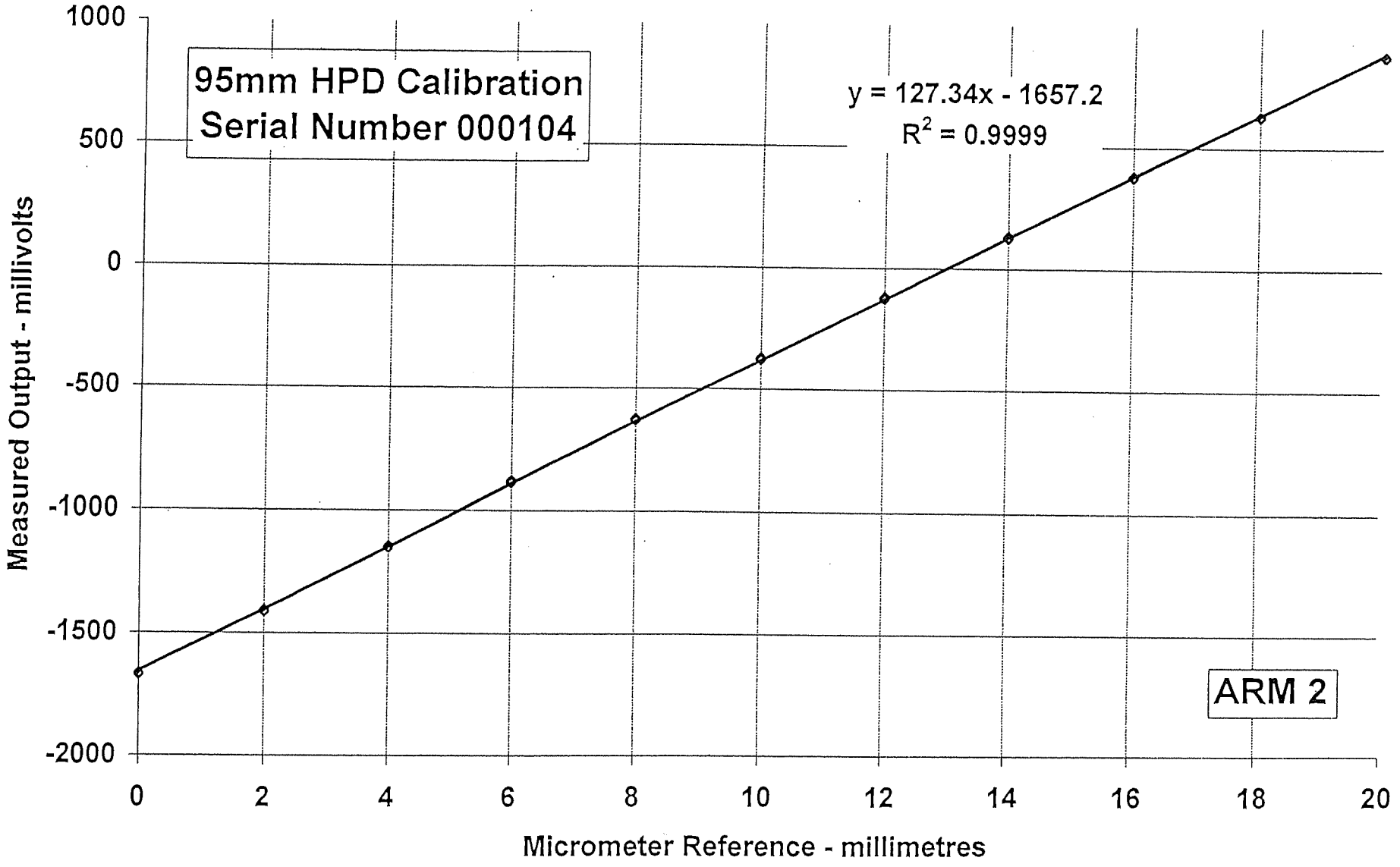
95mm HPD Calibration
Serial Number 000104
y = 127.34x - 1657.2
R2 = 0.9999
ARM 2
Measured Output - millivolts
1000
500
0
-500
-1000
-1500
-2000
0
2
4
6
8
10
12
14
16
18
20
Micrometer Reference - millimetres

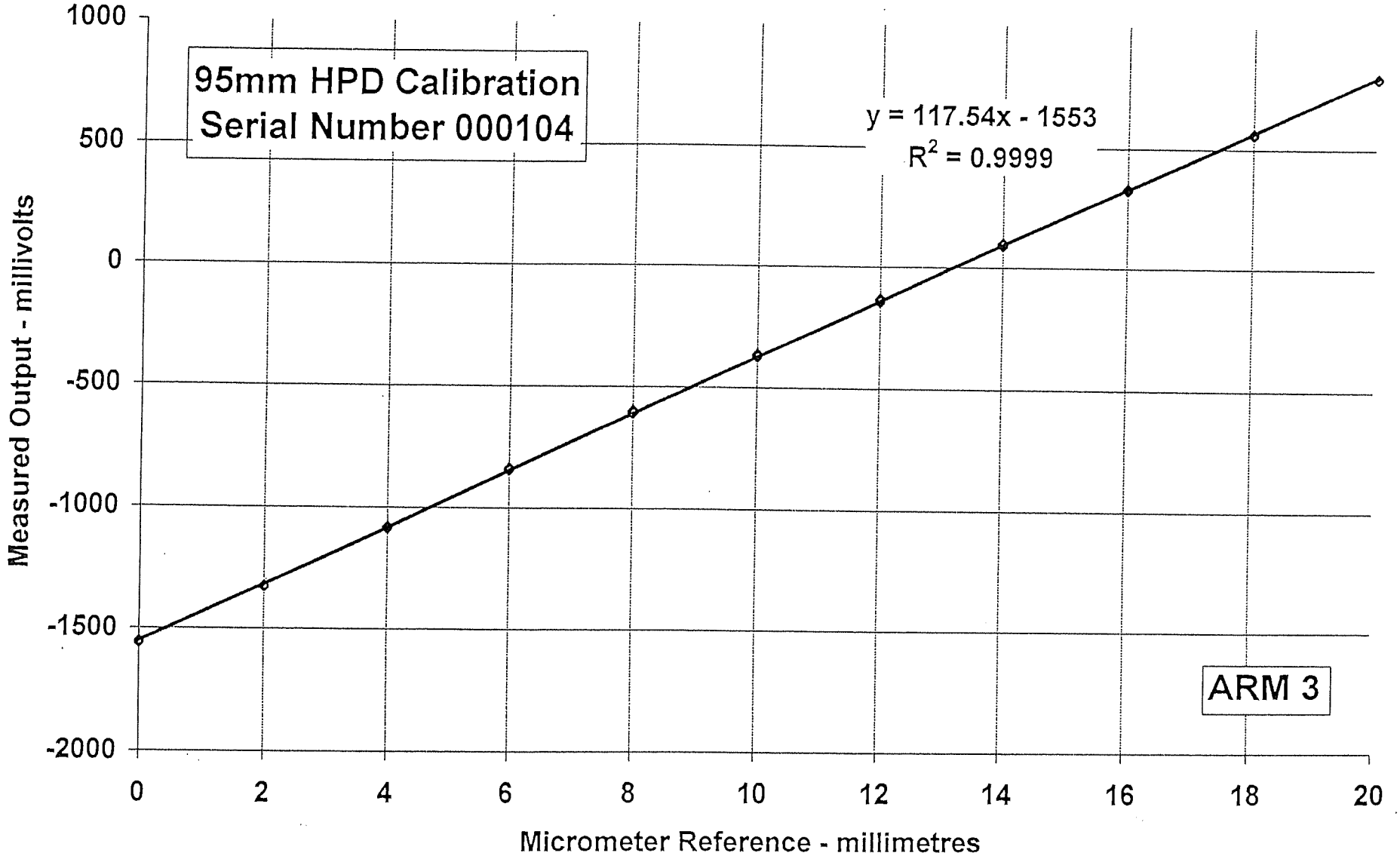
95mm HPD Calibration
Serial Number 000104
y = 117.54x - 1553
R2 = 0.9999
ARM 3
Measured Output - millivolts
1000
500
0
-500
-1000
-1500
-2000
0
2
4
6
8
10
12
14
16
18
20
Micrometer Reference - millimetres

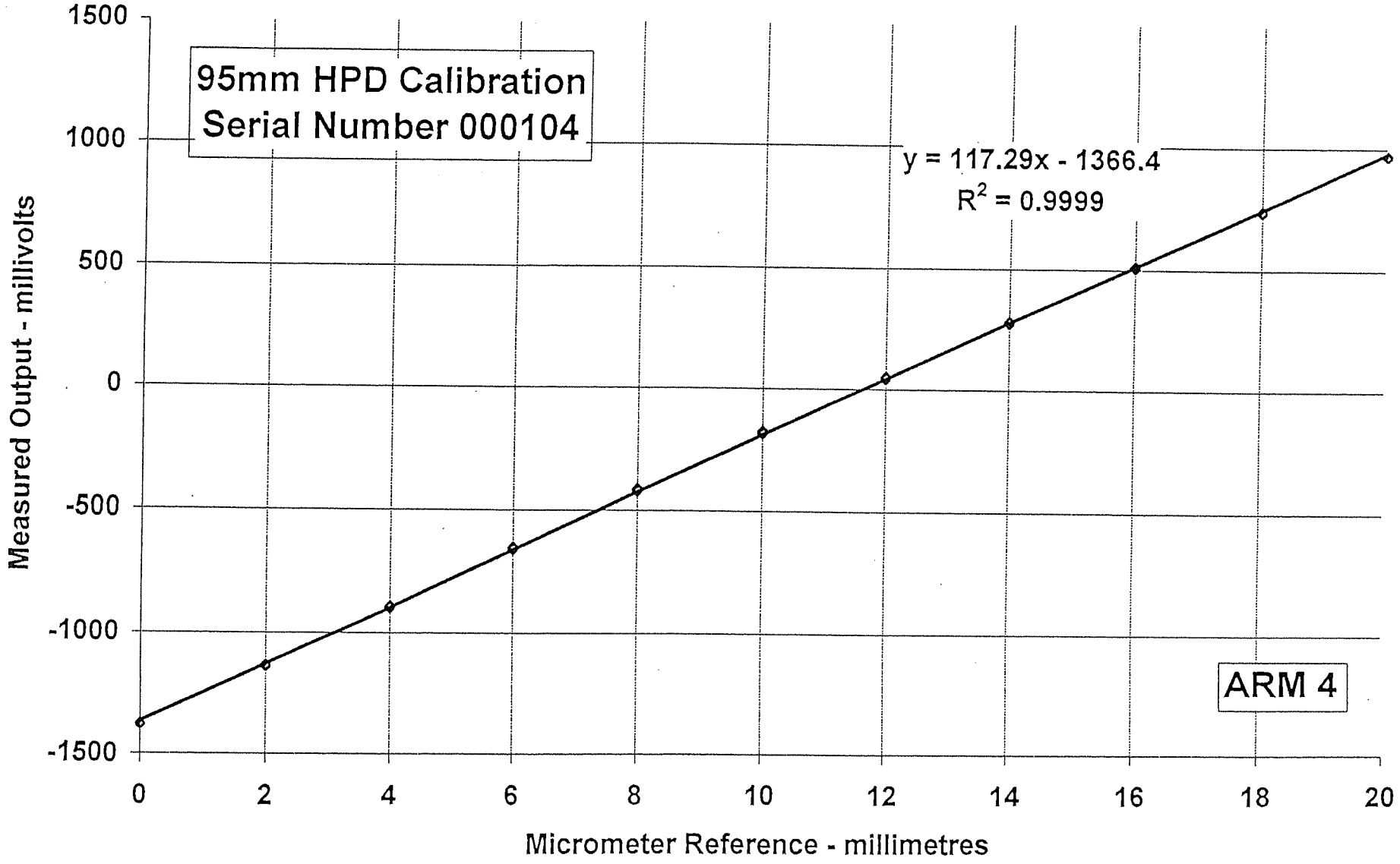
95mm HPD Calibration
Serial Number 000104
y = 117.29x - 1366.4
R2 = 0.9999
ARM 4
Measured Output - millivolts
1500
1000
500
0
-500
-1000
-1500
0
2
4
6
8
10
12
14
16
18
20
Micrometer Reference - millimetres

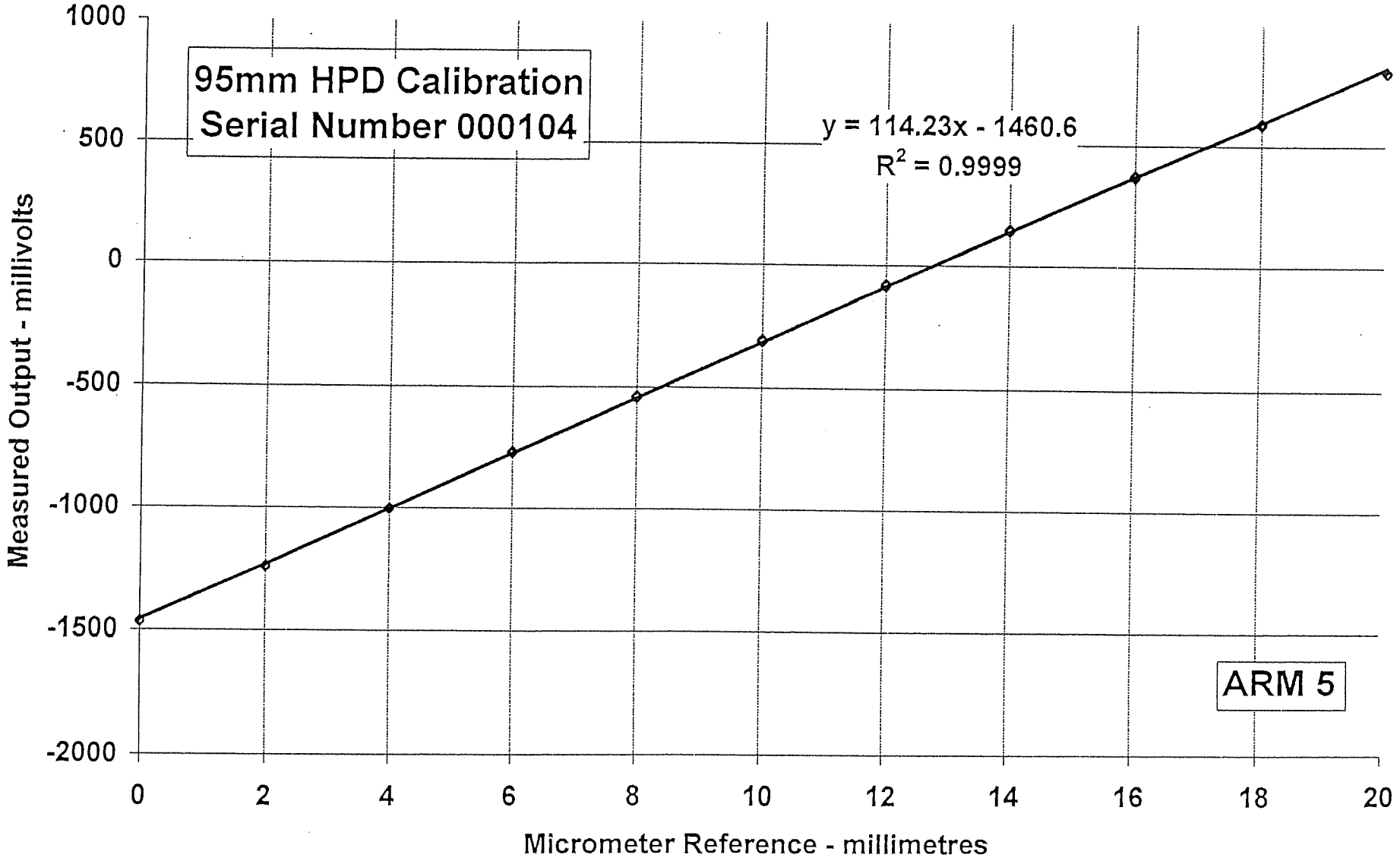
95mm HPD Calibration
Serial Number 000104
y = 114.23x - 1460.6
R2 = 0.9999
ARM 5
Measured Output - millivolts
1000
500
0
-500
-1000
-1500
-2000
0
2
4
6
8
10
12
14
16
18
20
Micrometer Reference - millimetres

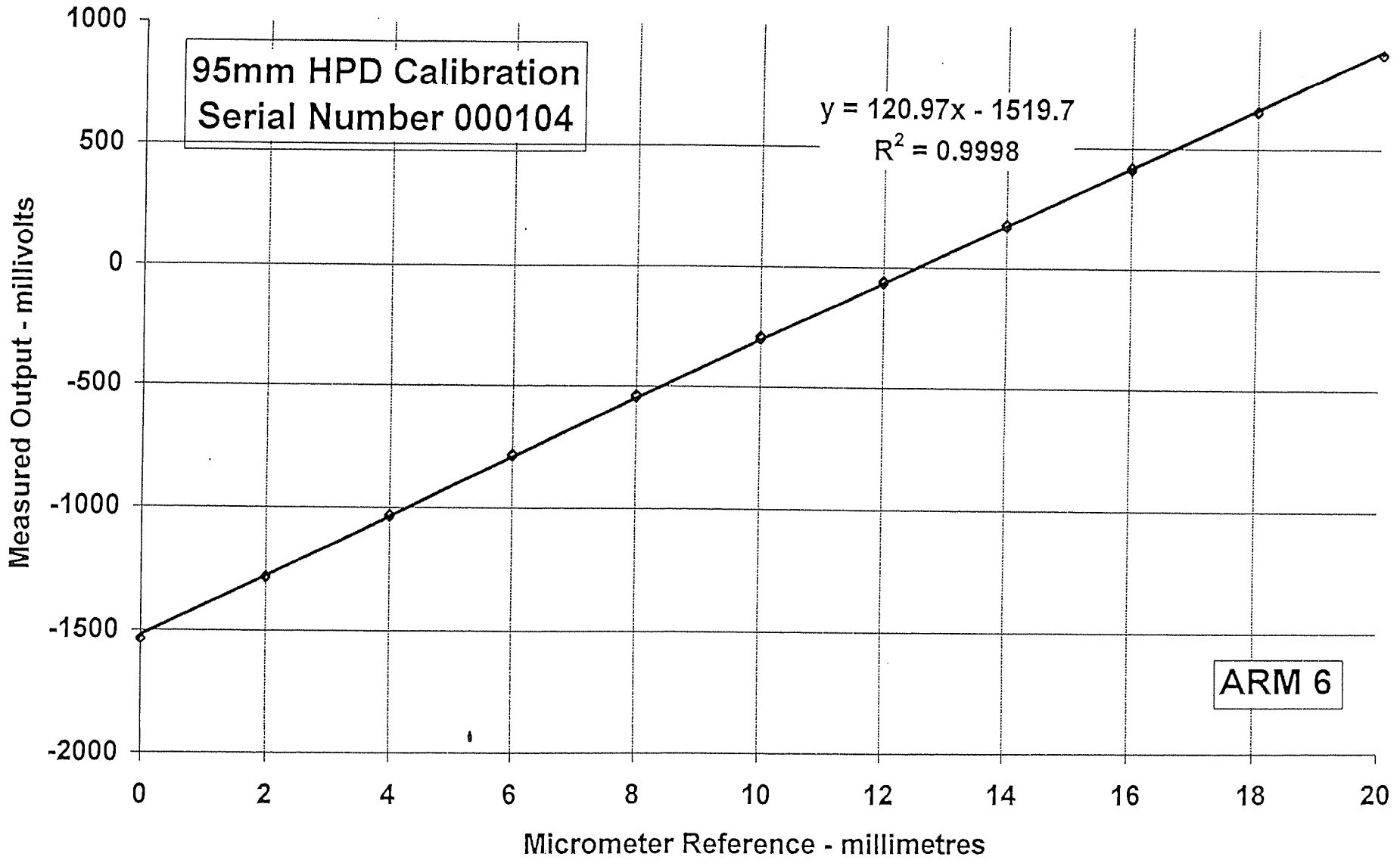
95mm HPD Calibration
Serial Number 000104
y = 120.97x - 1519.7
R2 = 0.9998
ARM 6
Measured Output - millivolts
1000
500
0
-500
-1000
-1500
-2000
0
2
4
6
8
10
12
14
16
18
20
Micrometer Reference - millimetres

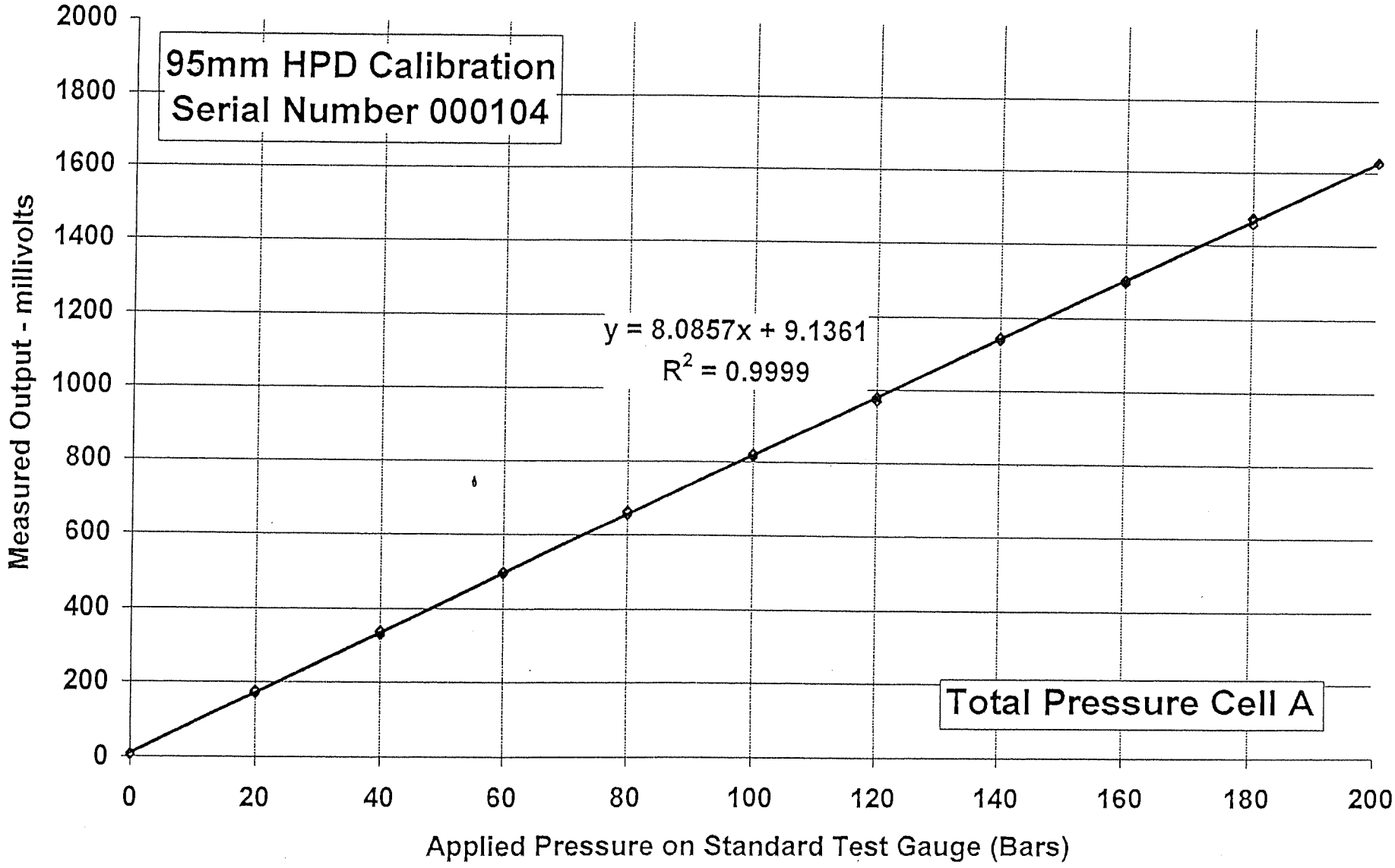
95mm HPD Calibration
Serial Number 000104
y = 8.0857x + 9.1361
R2 = 0.9999
Total Pressure Cell A
Measured Output - millivolts
Applied Pressure on Standard Test Gauge (Bars)
0
200
400
600
800
1000
1200
1400
1600
1800
2000
0
20
40
60
80
100
120
140
160
180
200

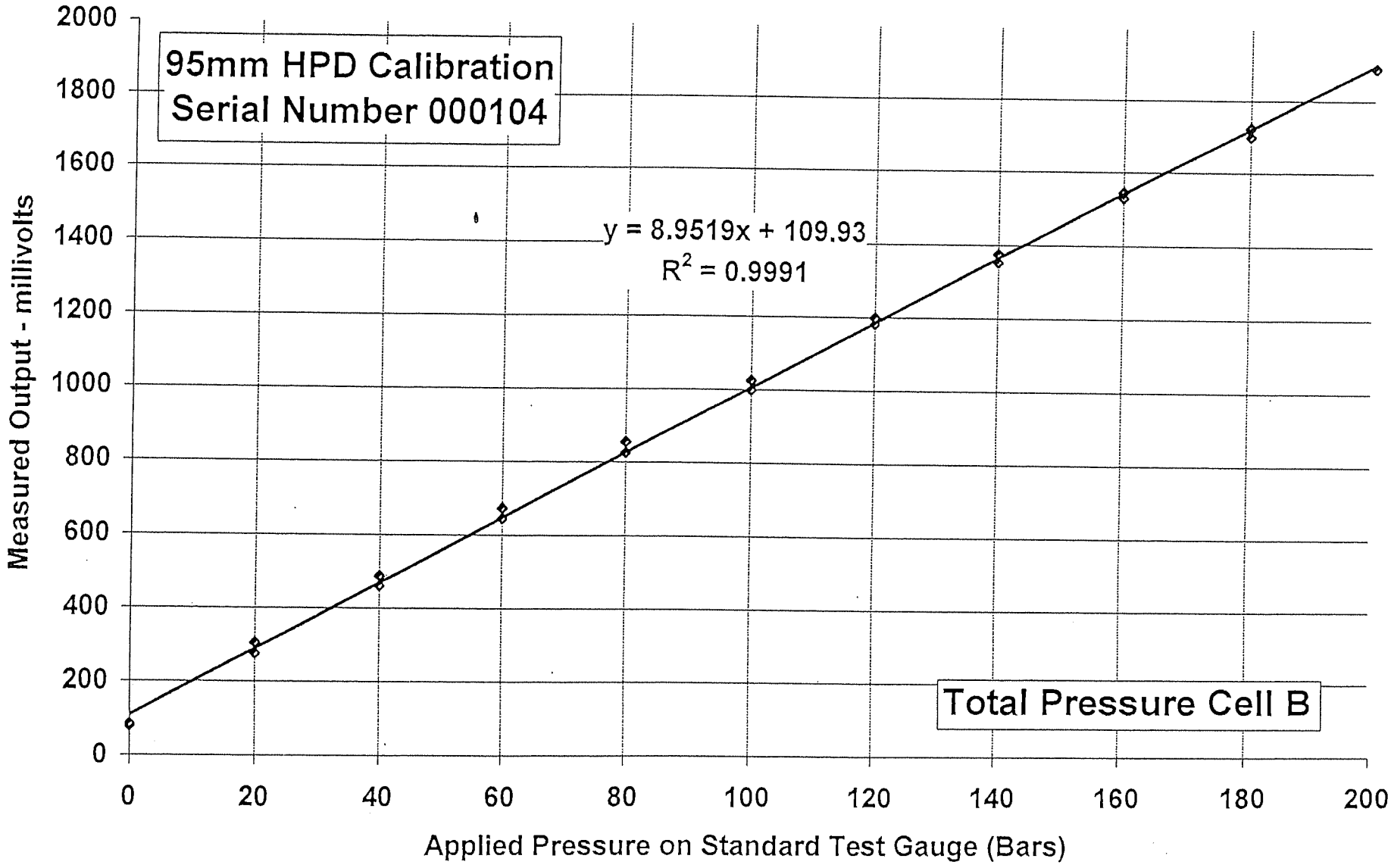
95mm HPD Calibration
Serial Number 000104
y = 8.9519x + 109.93
R2 = 0.9991
Total Pressure Cell B
Measured Output - millivolts
Applied Pressure on Standard Test Gauge (Bars)
0
200
400
600
800
1000
1200
1400
1600
1800
2000
0
20
40
60
80
100
120
140
160
180
200

Calibration summary, our 95mm HPD (TILLY), 8th/9th May 2003																		
Arm calibrations done 9-5-03																		
mm	Arm 1	Linearity	Hysteresis	Arm 2	Linearity	Hysteresis	Arm 3	Linearity	Hysteresis	Arm 4	Linearity	Hysteresis	Arm 5	Linearity	Hysteresis	Arm 6	Linearity	Hysteresis
	(mV)	(%)	(%)	(mV)	(%)	(%)	(mV)	(%)	(%)	(mV)	(%)	(%)	(mV)	(%)	(%)	(mV)	(%)	(%)
0	-1376.3	103.3	-0.08	-1655.0	103.8	0.15	-1556.7	98.9	0.05	-1376.6	101.3	-0.03	-1467.7	103.4	0.00	-1534.9	102.7	-0.12
2	-1124.2	102.7	-0.14	-1390.8	103.8	0.20	-1323.9	103.1	-0.12	-1138.8	103.0	-0.06	-1230.2	103.3	-0.04	-1286.5	102.7	0.02
4	-873.5	101.1	-0.19	-1126.7	102.4	0.29	-1081.1	101.9	-0.24	-897.0	101.4	-0.17	-993.0	100.1	-0.10	-1038.2	100.8	-0.18
6	-626.8	100.4	-0.30	-866.1	100.0	0.30	-841.1	99.8	-0.29	-658.9	100.4	-0.24	-763.2	99.7	-0.25	-794.5	100.4	-0.33
8	-381.7	99.8	-0.31	-611.6	99.4	0.32	-606.0	99.5	-0.35	-423.2	99.5	-0.29	-534.2	100.1	-0.34	-551.7	99.7	-0.38
10	-138.1	99.2	-0.30	-358.7	98.9	0.28	-371.8	99.3	-0.40	-189.6	99.1	-0.37	-304.4	99.9	-0.33	-310.7	99.5	-0.40
12	104.0	98.2	-0.27	-107.0	98.5	0.28	-137.9	98.9	-0.39	43.1	98.7	-0.37	-75.1	99.4	-0.37	-70.1	99.3	-0.39
14	343.8	100.0	-0.27	143.6	98.0	0.26	94.9	99.3	-0.37	274.7	99.0	-0.36	153.2	98.7	-0.22	170.0	98.6	-0.34
16	587.8	98.3	-0.18	392.9	98.0	0.16	328.6	99.1	-0.28	507.1	98.9	-0.23	379.9	98.4	-0.18	408.4	98.3	-0.30
18	827.8	96.3	-0.17	642.3	97.1	0.10	562.0	99.1	-0.09	739.2	98.5	-0.06	605.8	93.6	-0.13	646.2	95.8	-0.21
20	1062.9	-94.6		889.3	-98.1		795.3	-98.1		970.5	-97.9		820.8	-92.4		877.9	-93.8	
18	832.0	-98.3		639.8	-98.6		564.2	-97.2		740.7	-97.2		608.7	-97.8		651.2	-97.4	
16	592.1	-99.1		388.9	-99.0		335.3	-98.4		512.4	-97.6		384.1	-98.4		415.7	-98.3	
14	350.3	-98.2		136.9	-98.7		103.7	-98.7		283.2	-98.6		158.3	-98.0		178.1	-98.8	
12	110.6	-98.9		-114.2	-98.9		-128.8	-99.2		51.8	-99.1		-66.6	-100.3		-60.8	-99.4	
10	-130.8	-99.7		-365.9	-99.7		-362.4	-99.9		-180.8	-100.3		-296.9	-100.0		-301.1	-99.8	
8	-374.1	-100.5		-619.7	-99.9		-597.7	-100.5		-416.3	-100.9		-526.5	-100.6		-542.5	-100.9	
6	-619.5	-102.1		-873.8	-102.3		-834.3	-102.4		-653.2	-102.2		-757.5	-101.6		-786.6	-102.2	
4	-868.8	-103.3		-1134.0	-102.9		-1075.5	-104.3		-893.1	-104.0		-990.7	-103.9		-1033.8	-104.8	
2	-1120.9	-103.9		-1395.9	-103.3		-1321.0	-100.6		-1137.3	-101.6		-1229.2	-103.9		-1287.1	-101.2	
0	-1374.4			-1658.7			-1557.8			-1375.9			-1467.7			-1531.9		
Intercept	-1362.2	mV		-1642.4	mV		-1550.4	mV		-1366.4	mV		-1454.8	mV		-1522.1	mV	
Slope	122.0	mV/mm		127.2	mV/mm		117.7	mV/mm		117.4	mV/mm		114.8	mV/mm		120.9	mV/mm	
TPC calibrations done 8-5-03																		
MPa	TPC A	Linearity	Hysteresis	TPC B	Linearity	Hysteresis												
	(Volts)	(%)	(%)	(Volts)	(%)	(%)												
0	10.7	103.2	0.06	89.5	111.4	0.12												
20	178.6	98.4	-0.20	290.2	102.7	-1.51												
40	338.7	99.2	-0.53	475.3	101.8	-1.91												
60	500.1	99.1	-0.13	658.7	99.7	-1.56												
80	661.3	101.4	-0.27	838.4	100.4	-1.28												
100	826.3	98.9	-0.02	1019.2	98.0	-1.10												
120	987.2	98.5	-0.34	1195.7	96.7	-1.17												
140	1147.4	101.1	-0.53	1369.9	98.9	-1.19												
160	1311.9	100.8	-0.37	1548.1	99.2	-1.00												
180	1475.8	102.5	-0.34	1726.9	100.7	-0.74												
200	1642.5	-99.1		1908.3	-93.2													
180	1481.3	-100.4		1740.4	-96.7													
160	1318.0	-99.6		1566.2	-96.9													
140	1156.0	-100.3		1391.6	-97.0													
120	992.8	-102.1		1216.9	-98.6													
100	826.7	-99.0		1039.2	-98.6													
80	665.7	-100.5		861.6	-96.9													
60	502.3	-95.3		687.0	-98.2													
40	347.3	-101.7		510.0	-106.7													
20	181.9	-105.8		317.7	-127.8													
0	9.8			87.4														
Intercept	14.1	mVolts		120.1	mVolts													
Slope	8.133	mV/Bars		9.008	mV/Bars													
Slope	81.3	mV/MPa		90.1	mV/MPa													

95mm HPD		Scotty								
Arm calibration		26th July 2001								
mm	Arm 1	Linearity	Hysteresis	Arm 2	Linearity	Hysteresis	Arm 3	Linearity	Hysteresis	
	(mV)	(%)	(%)	(mV)	(%)	(%)	(mV)	(%)	(%)	
0	-2108.0	103.9	0.01	-1994.6	102.4	0.04	-1840.8	103.9	0.01	
2	-1857.9	103.1	0.01	-1749.0	103.5	-0.05	-1590.1	102.5	-0.07	
4	-1609.8	102.1	-0.02	-1500.7	101.2	-0.06	-1342.7	100.8	-0.15	
6	-1363.9	100.2	-0.02	-1258.0	100.5	-0.12	-1099.5	99.6	-0.22	
8	-1122.7	99.2	-0.09	-1017.0	100.2	-0.18	-859.2	99.7	-0.28	
10	-883.9	99.1	-0.10	-776.6	100.0	-0.21	-618.7	98.9	-0.28	
12	-645.3	97.8	-0.10	-536.7	98.4	-0.24	-380.1	99.5	-0.31	
14	-409.9	98.4	-0.17	-300.7	98.1	-0.28	-140.0	98.1	-0.29	
16	-172.9	99.0	-0.13	-65.3	96.8	-0.23	96.6	99.1	-0.25	
18	65.4	98.5	-0.09	167.0	95.8	-0.14	335.7	100.0	-0.18	
20	302.5	-97.6		396.8	-94.4		577.0	-98.2		
18	67.5	-98.6		170.3	-96.0		340.0	-98.4		
16	-169.8	-98.1		-59.9	-97.6		102.7	-97.7		
14	-405.9	-98.4		-294.0	-98.7		-133.1	-99.3		
12	-642.8	-99.2		-530.9	-100.3		-372.6	-99.2		
10	-881.5	-99.3		-771.5	-100.5		-611.9	-99.7		
8	-1120.6	-100.9		-1012.7	-101.1		-852.5	-100.2		
6	-1363.4	-102.1		-1255.2	-101.7		-1094.3	-101.5		
4	-1609.2	-103.4		-1499.2	-103.7		-1339.2	-103.2		
2	-1858.1	-103.9		-1747.9	-103.2		-1588.3	-104.7		
0	-2108.2			-1995.6			-1841.0			
Zero	-2093.9	mV		-1982.0	mV		-1827.6	mV		
Slope	120.4	mV/mm		120.0	mV/mm		120.6	mV/mm		
mm	Arm 4	Linearity	Hysteresis	Arm 5	Linearity	Hysteresis	Arm 6	Linearity	Hysteresis	
	(mV)	(%)	(%)	(mV)	(%)	(%)	(mV)	(%)	(%)	
0	-1810.1	104.5	-0.04	-1901.1	103.5	-0.01	-1960.1	103.9	0.02	
2	-1558.2	102.5	-0.09	-1655.2	102.7	0.03	-1710.6	103.0	0.01	
4	-1311.2	101.0	-0.15	-1411.3	101.6	-0.09	-1463.2	101.4	-0.02	
6	-1067.7	100.0	-0.22	-1169.9	100.4	-0.19	-1219.7	100.0	-0.06	
8	-826.7	99.6	-0.27	-931.4	99.1	-0.23	-979.6	99.8	-0.10	
10	-586.7	99.5	-0.29	-696.0	99.3	-0.36	-739.9	98.5	-0.04	
12	-347.0	99.3	-0.29	-460.2	99.8	-0.45	-503.3	98.2	-0.13	
14	-107.7	97.4	-0.24	-223.0	99.2	-0.37	-267.5	98.8	-0.19	
16	127.0	99.7	-0.25	12.7	95.9	-0.29	-30.2	99.0	-0.17	
18	367.4	97.4	-0.07	240.5	94.8	-0.17	207.5	98.4	-0.11	
20	602.2	-96.8		465.6	-93.0		443.9	-97.3		
18	369.0	-97.9		244.6	-94.8		210.2	-98.4		
16	133.0	-97.5		19.5	-98.4		-26.2	-98.6		
14	-101.9	-98.8		-214.3	-99.0		-263.0	-98.8		
12	-340.0	-99.5		-449.6	-100.1		-500.2	-99.4		
10	-579.7	-99.8		-687.4	-100.4		-738.9	-99.3		
8	-820.3	-100.5		-925.9	-100.8		-977.3	-100.4		
6	-1062.4	-101.7		-1165.4	-102.6		-1218.3	-101.8		
4	-1307.5	-103.1		-1409.1	-103.8		-1462.3	-103.3		
2	-1556.1	-105.0		-1655.8	-103.1		-1710.8	-104.0		
0	-1808.1			-1900.8			-1960.5			
Zero	-1795.0	mV		-1887.2	mV		-1946.8	mV		
Slope	120.5	mV/mm		118.8	mV/mm		120.1	mV/mm		
Pressure cell calibration			27th July 2001		Budenberg gauge s/n 12394260					
bar	TPC A	Linearity	Hysteresis	TPC B	Linearity	Hysteresis				
	(mV)	(%)	(%)	(mV)	(%)	(%)				
0	-75.2	107.4	-0.37	-91.5	106.3	-0.35				
20	93.6	94.2	-0.39	80.3	97.6	-0.68				
40	241.6	101.9	-0.61	238.1	98.6	-0.78				
60	401.8	102.2	-0.56	397.4	101.5	-0.97				
80	562.4	99.1	-0.09	561.5	102.4	-0.69				
100	718.1	97.9	-0.11	727.0	97.3	-0.24				
120	872.0	100.4	-0.47	884.3	100.4	-0.67				
140	1029.8	101.5	-0.48	1046.5	101.7	-0.65				
160	1189.3	99.9	-0.21	1210.8	100.1	-0.33				
180	1346.4	105.2	-0.57	1372.5	105.3	-0.44				
200	1511.8	-99.5		1542.7	-100.9					
180	1355.4	-103.6		1379.6	-101.1					
160	1192.6	-98.8		1216.2	-98.5					
140	1037.3	-100.5		1057.0	-100.2					
120	879.4	-101.5		895.1	-101.7					
100	719.8	-99.2		730.8	-97.8					
80	563.8	-97.5		572.7	-98.8					
60	410.6	-101.4		413.0	-100.4					
40	251.2	-96.3		250.7	-98.6					
20	99.80	-107.6		91.30	-109.6					
0	-69.4			-85.9						
Zero	-65.4	mV		-78.6	mV					
Slope	7.9	mV/bar		8.1	mV/bar					
Sensitivity	78.6	mV/Mpa		80.8	mV/Mpa					

Calibration summary, our 95mm HPD (SCOTTY), 16th Aug 2001																		
mm	Arm 1	Linearity	Hysteresis	Arm 2	Linearity	Hysteresis	Arm 3	Linearity	Hysteresis	Arm 4	Linearity	Hysteresis	Arm 5	Linearity	Hysteresis	Arm 6	Linearity	Hysteresis
	(mV)	(%)	(%)	(mV)	(%)	(%)	(mV)	(%)	(%)	(mV)	(%)	(%)	(mV)	(%)	(%)	(mV)	(%)	(%)
0	-2101.8	103.7	-0.10	-1992.6	102.7	0.00	-1835.4	102.9	0.10	-1802.7	105.9	0.02	-1900.5	104.9	-0.10	-1970.3	103.2	-0.10
2	-1851.9	103.2	0.00	-1746.3	103.1	-0.11	-1587.5	102.5	-0.11	-1547.8	102.6	-0.07	-1651.0	103.1	-0.10	-1710.6	103.2	0.14
4	-1603.2	102.1	-0.07	-1498.9	101.7	-0.10	-1340.5	100.8	-0.15	-1301.0	101.1	-0.14	-1405.9	101.4	-0.19	-1463.0	100.9	0.15
6	-1357.3	100.2	-0.10	-1254.9	100.4	-0.11	-1097.5	99.9	-0.24	-1057.7	100.0	-0.20	-1164.9	100.2	-0.27	-1220.8	99.9	0.06
8	-1115.8	98.6	-0.05	-1014.1	100.0	-0.14	-856.8	98.8	-0.28	-817.0	99.7	-0.25	-926.6	99.6	-0.32	-981.1	99.2	0.01
10	-878.2	99.9	-0.14	-774.1	100.0	-0.20	-618.7	99.2	-0.30	-577.1	99.4	-0.27	-689.9	99.7	-0.38	-743.0	99.0	-0.06
12	-637.6	98.5	-0.10	-534.1	98.8	-0.22	-379.7	99.7	-0.28	-337.8	98.8	-0.25	-452.9	99.1	-0.37	-505.5	98.5	-0.06
14	-400.2	98.1	-0.07	-297.0	98.1	-0.23	-139.4	99.3	-0.23	-100.0	98.6	-0.22	-217.4	98.6	-0.33	-269.0	98.5	-0.05
16	-163.9	98.7	-0.10	-61.6	96.7	-0.18	99.9	98.6	-0.18	137.3	97.4	-0.14	17.1	96.4	-0.27	-32.7	98.1	-0.02
18	73.8	98.3	-0.10	170.3	95.5	-0.12	337.6	99.5	-0.18	371.6	96.9	-0.14	246.3	95.1	-0.20	202.8	97.1	-0.02
20	310.6	-97.3		399.4	-94.3		577.5	-97.8		604.9	-95.5		472.5	-93.2		435.9	-96.9	
18	76.2	-93.6		173.1	-96.1		341.9	-98.6		375.0	-97.4		251.0	-95.6		203.3	-98.1	
16	-161.4	-98.4		-57.4	-97.6		104.3	-98.8		140.7	-97.9		23.6	-98.0		-32.1	-98.2	
14	-398.5	-98.3		-291.5	-98.9		-133.8	-99.2		-94.8	-98.4		-209.5	-98.7		-267.9	-98.4	
12	-635.3	-99.4		-528.8	-100.2		-372.9	-99.0		-331.7	-99.3		-444.1	-99.6		-504.1	-99.0	
10	-874.9	-99.5		-769.2	-100.7		-611.4	-99.0		-570.6	-99.9		-680.9	-100.1		-741.6	-99.9	
8	-1114.6	-99.8		-1010.8	-100.7		-850.1	-100.3		-810.9	-100.6		-918.9	-100.8		-981.3	-100.4	
6	-1355.0	-102.3		-1252.3	-101.8		-1091.8	-101.7		-1053.0	-101.6		-1158.5	-102.2		-1222.3	-101.7	
4	-1601.6	-103.8		-1496.5	-103.0		-1337.0	-102.9		-1297.6	-103.2		-1401.4	-104.0		-1466.5	-103.1	
2	-1851.8	-102.7		-1743.6	-103.8		-1584.9	-105.0		-1546.0	-106.9		-1648.6	-105.0		-1713.9	-105.9	
0	-2099.3			-1992.7			-1837.9			-1803.2			-1898.2			-1968.0		
Intercept	-2087.4	mV		-1979.4	mV		-1824.5	mV		-1785.0	mV		-1882.5	mV		-1950.1	mV	
Slope	120.5	mV/mm		120.0	mV/mm		120.5	mV/mm		120.3	mV/mm		118.9	mV/mm		120.0	mV/mm	

Bars	TPC A	Linearity	Hysteresis	TPC B	Linearity	Hysteresis
	(Volts)	(%)	(%)	(Volts)	(%)	(%)
0	-76.7	102.4	-0.04	-87.3	105.3	-0.12
20	84.9	98.2	-0.25	83.8	95.0	-0.18
40	240.0	102.2	-0.53	238.1	102.0	-0.87
60	401.4	103.4	-0.28	403.8	101.2	-0.66
80	564.6	96.2	0.22	568.1	99.9	-0.48
100	716.5	90.3	-0.03	730.3	100.2	-0.25
120	859.1	108.8	-0.93	893.1	99.5	-0.14
140	1030.9	100.1	-0.23	1054.7	99.9	-0.34
160	1189.0	102.0	-0.15	1217.0	101.4	-0.26
180	1350.1	100.8	0.23	1381.7	99.7	0.32
200	1509.2	-103.1		1543.7	-102.9	
180	1346.4	-98.2		1376.5	-95.5	
160	1191.3	-99.3		1221.3	-99.2	
140	1034.6	-101.8		1060.2	-101.5	
120	873.9	-99.5		895.4	-99.1	
100	716.9	-98.7		734.4	-97.5	
80	561.1	-98.4		576.0	-99.4	
60	405.8	-99.7		414.5	-99.9	
40	248.4	-101.1		252.3	-102.0	
20	88.8	-104.4		86.7	-106.0	
0	-76.0			-85.4		
Intercept	-72.7	mVolts		-80.2	mVolts	
Slope	78.9	mV/MPa		81.2	mV/MPa	

Gauge used: Budenberg 12394260

95mm HPD		Scotty							
Arm calibration		27th November 2001							
mm	Arm 1	Linearity	Hysteresis	Arm 2	Linearity	Hysteresis	Arm 3	Linearity	Hysteresis
	(mV)	(%)	(%)	(mV)	(%)	(%)	(mV)	(%)	(%)
0	-2110.2	102.2	0.00	-1989.4	102.6	-0.02	-1835.9	102.8	-0.01
2	-1864.3	102.6	-0.02	-1743.2	103.1	-0.02	-1588.3	102.6	-0.07
4	-1617.5	102.5	-0.07	-1495.8	101.6	-0.05	-1341.2	100.7	-0.13
6	-1371.0	100.3	-0.09	-1251.9	100.7	-0.12	-1098.7	99.5	-0.23
8	-1129.8	99.3	-0.12	-1010.3	99.8	-0.17	-859.0	99.2	-0.29
10	-891.0	99.2	-0.15	-770.8	99.0	-0.22	-620.0	99.7	-0.34
12	-652.3	98.7	-0.14	-533.3	100.0	-0.31	-379.7	99.2	-0.32
14	-415.0	98.0	-0.11	-293.3	97.5	-0.19	-140.8	99.1	-0.25
16	-179.3	98.7	-0.16	-59.3	97.1	-0.21	98.0	99.8	-0.22
18	58.1	98.3	-0.12	173.8	96.2	-0.12	338.4	98.5	-0.07
20	294.6	-97.1		404.7	-95.0		575.8	-97.8	
18	61.1	-98.4		176.8	-96.2		340.1	-98.3	
16	-175.5	-98.5		-54.2	-97.7		103.2	-98.7	
14	-412.3	-98.4		-288.8	-98.8		-134.7	-98.5	
12	-648.1	-98.1		-525.3	-98.9		-372.0	-99.5	
10	-887.3	-99.6		-765.6	-100.2		-611.7	-99.8	
8	-1126.9	-100.6		-1006.1	-101.2		-852.1	-100.0	
6	-1368.8	-102.7		-1249.0	-102.3		-1093.1	-101.6	
4	-1615.8	-103.1		-1494.5	-103.4		-1338.0	-103.1	
2	-1863.8	-102.5		-1742.6	-102.7		-1586.5	-103.4	
0	-2110.3			-1989.0			-1835.7		
Zero	-2098.9	mV		-1976.6	mV		-1825.0	mV	
Slope	120.3	mV/mm		120.0	mV/mm		120.5	mV/mm	

mm	Arm 4	Linearity	Hysteresis	Arm 5	Linearity	Hysteresis	Arm 6	Linearity	Hysteresis
	(mV)	(%)	(%)	(mV)	(%)	(%)	(mV)	(%)	(%)
0	-1813.0	98.7	0.01	-1913.0	103.5	-0.03	-1977.7	105.6	-0.01
2	-1576.3	102.7	0.00	-1667.2	103.2	-0.14	-1723.6	102.6	0.08
4	-1329.8	101.0	-0.09	-1422.0	101.3	-0.24	-1476.6	101.5	0.16
6	-1087.4	100.5	-0.19	-1181.3	100.5	-0.34	-1232.3	99.9	0.05
8	-846.3	99.7	-0.22	-942.7	99.9	-0.42	-991.8	99.5	-0.01
10	-607.2	99.7	-0.27	-705.5	99.9	-0.45	-752.2	99.0	-0.02
12	-368.0	99.5	-0.25	-468.2	99.2	-0.41	-513.8	99.4	0.02
14	-129.3	99.2	-0.20	-232.5	97.9	-0.38	-274.6	97.0	0.05
16	108.6	98.4	-0.11	0.1	96.5	-0.39	-41.1	99.2	-0.03
18	344.6	98.2	-0.06	229.2	94.2	-0.23	197.7	98.3	0.00
20	580.3	-97.7		453.0	-91.9		434.4	-98.3	
18	346.0	-97.9		234.7	-94.9		197.8	-98.9	
16	111.2	-98.2		9.3	-98.0		-40.4	-97.7	
14	-124.4	-99.1		-223.5	-98.9		-275.7	-99.1	
12	-362.1	-99.5		-458.4	-99.6		-514.2	-98.6	
10	-600.8	-100.1		-694.9	-100.1		-751.6	-99.7	
8	-841.0	-100.8		-933.7	-101.3		-991.6	-100.4	
6	-1082.8	-102.1		-1173.3	-102.3		-1233.4	-102.6	
4	-1327.7	-103.7		-1416.3	-104.2		-1480.4	-101.9	
2	-1576.4	-98.7		-1663.9	-104.5		-1725.6	-104.6	
0	-1813.3			-1912.2			-1977.4		
Zero	-1808.8	mV		-1896.8	mV		-1962.8	mV	
Slope	120.0	mV/mm		118.8	mV/mm		120.4	mV/mm	

Pressure cell calibration			28th November 2001			STG: 10759918 (0-600psi)
psi	TPC A	Linearity	Hysteresis	TPC B	Linearity	Hysteresis
	(mV)	(%)	(%)	(mV)	(%)	(%)
0	-78.8	98.9	-0.55	-70.5	97.8	-0.09
100	-25.1	101.9	-0.61	-15.9	99.8	-0.18
200	30.2	102.8	-0.25	39.8	101.2	-0.24
300	86.0	99.1	0.21	96.3	99.8	-0.12
400	139.8	99.3	0.09	152.0	100.9	-0.03
500	193.7	97.7	0.09	208.3	97.6	0.06
600	246.7	-98.2		262.8	-98.0	
500	193.4	-99.3		208.1	-100.3	
400	139.5	-99.9		152.1	-99.2	
300	85.3	-100.0		96.7	-100.5	
200	31.0	-99.7		40.6	-100.1	
100	-23.1	-99.3		-15.5	-98.4	
0	-77.0			-70.2		
	-77.9	mV		-70.8	mV	
	0.54	mV/psi		0.56	mV/psi	
	78.7	mV/MPa		81.0	mV/MPa	

95mm HPD		Scotty							
Arm calibration		1st February 2002							
mm	Arm 1	Linearity	Hysteresis	Arm 2	Linearity	Hysteresis	Arm 3	Linearity	Hysteresis
	(mV)	(%)	(%)	(mV)	(%)	(%)	(mV)	(%)	(%)
0	-2112.6	102.0	-0.14	-1994.8	102.5	0.00	-1841.1	102.8	0.19
2	-1867.9	102.9	0.07	-1748.8	103.0	-0.05	-1592.9	102.8	-0.10
4	-1621.1	102.3	0.03	-1501.7	101.8	-0.11	-1344.6	100.8	-0.13
6	-1375.6	100.4	0.00	-1257.5	100.7	-0.15	-1101.3	99.8	-0.21
8	-1134.8	99.4	-0.05	-1015.9	99.8	-0.20	-860.3	99.1	-0.27
10	-896.4	98.7	-0.08	-776.4	98.9	-0.23	-621.1	99.3	-0.32
12	-659.7	98.5	-0.13	-539.0	99.6	-0.30	-381.4	98.5	-0.32
14	-423.5	98.4	-0.18	-300.1	98.1	-0.23	-143.5	99.2	-0.34
16	-187.5	99.0	-0.20	-64.8	97.1	-0.19	95.9	98.9	-0.28
18	49.9	98.7	-0.15	168.2	96.1	-0.13	334.6	100.1	-0.17
20	286.7	-97.2		398.7	-94.8		576.3	-98.5	
18	53.5	-98.4		171.3	-96.5		338.6	-97.8	
16	-182.6	-98.6		-60.3	-97.7		102.6	-98.6	
14	-419.2	-98.9		-294.7	-98.9		-135.4	-98.7	
12	-656.5	-99.2		-531.9	-99.6		-373.7	-99.3	
10	-894.5	-99.7		-770.8	-100.1		-613.4	-99.5	
8	-1133.6	-100.8		-1011.0	-101.3		-853.7	-100.5	
6	-1375.5	-102.7		-1254.0	-102.1		-1096.3	-101.6	
4	-1621.9	-103.2		-1499.1	-103.6		-1341.5	-103.2	
2	-1869.6	-99.9		-1747.6	-103.0		-1590.6	-105.6	
0	-2109.3			-1994.8			-1845.6		
Zero	-2102.0	mV		-1981.9	mV		-1830.0	mV	
Slope	120.0	mV/mm		120.0	mV/mm		120.7	mV/mm	

mm	Arm 4	Linearity	Hysteresis	Arm 5	Linearity	Hysteresis	Arm 6	Linearity	Hysteresis
	(mV)	(%)	(%)	(mV)	(%)	(%)	(mV)	(%)	(%)
0	-1823.3	102.9	-0.07	-1913.5	103.2	-0.08	-1983.4	107.1	-0.16
2	-1575.5	103.2	-0.16	-1668.1	103.2	-0.10	-1726.2	103.0	-0.04
4	-1327.0	100.5	-0.17	-1422.7	101.2	-0.22	-1478.8	101.0	-0.05
6	-1085.0	100.3	-0.27	-1182.2	100.6	-0.32	-1236.1	100.1	-0.14
8	-843.5	99.7	-0.31	-943.0	100.0	-0.38	-995.7	99.5	-0.17
10	-603.5	99.4	-0.34	-705.3	98.6	-0.42	-756.8	99.0	-0.20
12	-364.2	99.4	-0.32	-470.9	99.8	-0.50	-519.0	98.7	-0.21
14	-124.8	98.1	-0.27	-233.7	98.9	-0.46	-281.8	97.5	-0.18
16	111.5	99.1	-0.27	1.4	96.4	-0.37	-47.5	98.7	-0.25
18	350.2	97.7	-0.09	230.5	94.4	-0.22	189.5	98.1	-0.17
20	585.5	-96.8		454.9	-92.2		425.1	-96.4	
18	352.4	-97.4		235.7	-94.8		193.6	-97.9	
16	117.9	-98.1		10.3	-98.0		-41.6	-98.2	
14	-118.3	-98.9		-222.7	-99.4		-277.4	-98.5	
12	-356.4	-99.2		-459.1	-99.4		-513.9	-99.1	
10	-595.3	-100.0		-695.4	-100.4		-751.9	-99.7	
8	-836.0	-100.7		-934.0	-101.2		-991.5	-100.4	
6	-1078.5	-101.5		-1174.5	-102.2		-1232.7	-101.9	
4	-1322.9	-103.3		-1417.5	-104.4		-1477.5	-103.2	
2	-1571.7	-103.8		-1665.8	-103.4		-1725.3	-105.9	
0	-1821.7			-1911.7			-1979.6		
Zero	-1810.1	mV		-1898.1	mV		-1963.4	mV	
Slope	120.4	mV/mm		118.9	mV/mm		120.1	mV/mm	

Pressure cell calibration					Budenberg gauge s/n 12574638 (0 - 250 bar)				
bar	TPC A	Linearity	Hysteresis	TPC B	Linearity	Hysteresis			
	(mV)	(%)	(%)	(mV)	(%)	(%)			
0	-71.8	104.1	-0.04						
10	8.6	95.5	0.46						
20	82.3	99.5	-0.09	Not working properly.					
30	159.1	100.1	0.00						
40	236.4	100.8	-0.20						
50	314.2	99.5	-0.06						
60	391.0	102.8	-0.31						
70	470.4	-100.6							
60	392.7	-101.3							
50	314.5	-99.7							
40	237.5	-101.5							
30	159.1	-98.8							
20	82.8	-99.3							
10	6.10	-100.6							
0	-71.6								
Zero	-71.3	mV							
Slope	7.7	mV/bar							
Sensitivity	77.2	mV/Mpa							

95mm HPD		Scotty								
Arm calibration		12th June 2002								
mm	Arm 1	Linearity	Hysteresis	Arm 2	Linearity	Hysteresis	Arm 3	Linearity	Hysteresis	
	(mV)	(%)	(%)	(mV)	(%)	(%)	(mV)	(%)	(%)	
0	-2118.5	102.6	0.07	-1998.7	102.4	0.10	-1832.8	103.6	-0.01	
2	-1871.4	103.3	0.00	-1753.0	102.5	0.06	-1583.0	102.5	-0.07	
4	-1622.6	101.9	-0.02	-1506.9	101.5	-0.05	-1335.8	100.9	-0.15	
6	-1377.0	100.3	-0.07	-1263.3	100.5	-0.16	-1092.3	99.7	-0.22	
8	-1135.4	99.2	-0.10	-1022.0	100.1	-0.21	-851.7	99.2	-0.29	
10	-896.5	98.9	-0.14	-781.8	98.9	-0.22	-612.5	99.1	-0.35	
12	-658.2	99.0	-0.14	-544.5	99.2	-0.35	-373.5	99.6	-0.34	
14	-419.7	97.8	-0.09	-306.3	98.2	-0.27	-133.2	98.5	-0.27	
16	-184.2	99.0	-0.10	-70.7	98.1	-0.17	104.5	99.5	-0.27	
18	54.4	98.4	-0.09	164.8	96.1	-0.02	344.6	98.7	-0.08	
20	291.5	-97.5		395.5	-95.9		582.8	-98.0		
18	56.5	-98.9		165.3	-96.6		346.5	-97.7		
16	-181.7	-97.9		-66.6	-97.2		110.9	-98.5		
14	-417.5	-98.5		-299.8	-98.4		-126.7	-98.9		
12	-654.9	-98.9		-536.1	-100.2		-365.2	-99.0		
10	-893.2	-99.5		-776.6	-100.2		-604.1	-99.7		
8	-1133.0	-100.6		-1017.0	-101.0		-844.7	-100.4		
6	-1375.3	-102.5		-1259.4	-102.6		-1087.0	-101.6		
4	-1622.2	-103.4		-1505.7	-103.6		-1332.2	-103.3		
2	-1871.3	-103.3		-1754.4	-102.8		-1581.4	-104.1		
0	-2120.1			-2001.1			-1832.6			
Zero	-2106.7	mV		-1987.7	mV		-1820.1	mV		
Slope	120.5	mV/mm		120.0	mV/mm		120.6	mV/mm		

mm	Arm 4	Linearity	Hysteresis	Arm 5	Linearity	Hysteresis	Arm 6	Linearity	Hysteresis
	(mV)	(%)	(%)	(mV)	(%)	(%)	(mV)	(%)	(%)
0	-1823.3	104.1	0.02	-1919.0	103.7	-0.07	-1975.3	105.4	-0.01
2	-1572.3	102.5	-0.09	-1672.2	103.4	-0.08	-1722.2	103.4	-0.04
4	-1325.3	100.8	-0.10	-1426.1	101.3	-0.21	-1473.7	101.1	-0.07
6	-1082.3	100.2	-0.21	-1185.1	100.4	-0.30	-1230.9	100.2	-0.12
8	-840.7	99.5	-0.27	-946.1	100.0	-0.38	-990.3	99.4	-0.15
10	-600.8	99.5	-0.29	-708.2	99.7	-0.42	-751.5	99.2	-0.18
12	-361.0	99.1	-0.27	-470.9	98.9	-0.40	-513.1	98.9	-0.18
14	-122.2	99.0	-0.23	-235.5	98.5	-0.42	-275.6	97.4	-0.14
16	116.4	97.6	-0.14	-1.1	96.5	-0.39	-41.6	98.1	-0.18
18	351.5	97.5	-0.13	228.5	94.2	-0.16	194.1	99.0	-0.14
20	586.5	-96.2		452.6	-92.5		431.8	-97.5	
18	354.6	-97.4		232.4	-94.2		197.5	-97.7	
16	119.8	-98.1		8.3	-98.3		-37.3	-97.8	
14	-116.6	-98.7		-225.6	-99.0		-272.3	-98.4	
12	-354.5	-99.3		-461.3	-99.5		-508.7	-99.3	
10	-593.9	-99.7		-698.2	-100.4		-747.2	-99.7	
8	-834.2	-100.9		-937.1	-101.2		-986.8	-100.4	
6	-1077.3	-101.9		-1177.9	-102.2		-1228.0	-101.6	
4	-1322.8	-102.7		-1421.1	-104.7		-1472.1	-103.7	
2	-1570.2	-105.2		-1670.2	-103.8		-1721.2	-105.7	
0	-1823.7			-1917.3			-1975.0		
Zero	-1809.2	mV		-1902.5	mV		-1958.2	mV	
Slope	120.5	mV/mm		119.0	mV/mm		120.1	mV/mm	

Pressure cell calibration		12th June 2002		Budenberg gauge s/n 12394260		
bar	TPC A	Linearity	Hysteresis	TPC B	Linearity	Hysteresis
	(mV)	(%)	(%)	(mV)	(%)	(%)
0	-74.5	102.3	-0.07	32.4	102.9	-0.13
20	86.6	97.6	-0.04	199.1	98.0	-0.19
40	240.4	97.0	0.01	357.8	96.9	-0.14
60	393.2	99.4	-0.10	514.8	99.8	-0.23
80	549.8	100.7	-0.23	676.5	99.8	-0.30
100	708.4	100.0	-0.09	838.2	100.0	-0.26
120	865.9	100.2	-0.06	1000.2	102.2	-0.23
140	1023.8	102.0	0.02	1165.8	101.0	-0.01
160	1184.5	100.2	-0.06	1329.5	101.5	-0.11
180	1342.3	104.4	-0.15	1494.0	100.9	-0.03
200	1506.7	-102.9		1657.4	-100.6	
180	1344.6	-101.0		1494.5	-100.7	
160	1185.5	-102.8		1331.3	-102.1	
140	1023.5	-99.5		1165.9	-100.0	
120	866.8	-99.7		1003.9	-99.7	
100	709.8	-99.3		842.4	-99.4	
80	553.4	-100.7		681.4	-100.6	
60	394.7	-98.0		518.5	-97.8	
40	240.3	-97.1		360.0	-97.4	
20	87.30	-102.0		202.2	-103.5	
0	-73.4			34.5		
Zero	-76.2	mV		33.3	mV	
Slope	7.9	mV/bar		8.1	mV/bar	
Sensitivity	78.8	mV/Mpa		81.0	mV/Mpa	

Calibrating 95 HPD "Scotty" 20/03/03																		
mm	Arm 1	Linearity	Hysteresis	Arm 2	Linearity	Hysteresis	Arm 3	Linearity	Hysteresis	Arm 4	Linearity	Hysteresis	Arm 5	Linearity	Hysteresis	Arm 6	Linearity	Hysteresis
	(mV)	(%)	(%)	(mV)	(%)	(%)	(mV)	(%)	(%)	(mV)	(%)	(%)	(mV)	(%)	(%)	(mV)	(%)	(%)
0	-2116.5	103.0	0.02	-1993.4	103.5	-0.37	-1821.9	104.1	-0.04	-1811.7	105.1	0.00	-1913.2	103.8	-0.16	-1965.4	106.9	0.26
2	-1868.5	102.6	-0.03	-1745.2	102.6	0.01	-1571.1	102.5	-0.56	-1559.0	101.8	-0.06	-1666.8	103.3	-0.14	-1708.3	102.9	0.00
4	-1621.5	102.3	-0.07	-1499.2	101.9	-0.11	-1324.0	100.4	-0.11	-1314.3	100.5	-0.18	-1421.6	100.9	-0.20	-1460.8	101.2	-0.03
6	-1375.3	100.4	-0.10	-1254.8	100.5	-0.13	-1082.1	99.8	-0.25	-1072.7	100.3	-0.30	-1182.1	100.4	-0.32	-1217.3	99.5	-0.10
8	-1133.7	99.2	-0.11	-1013.9	99.5	-0.19	-841.7	103.8	0.07	-831.7	99.9	-0.32	-943.9	100.0	-0.40	-977.9	99.6	-0.13
10	-895.0	99.0	-0.11	-775.3	100.1	0.22	-591.6	99.0	0.11	-591.6	99.3	-0.29	-706.7	99.8	-0.42	-738.3	98.9	-0.15
12	-656.8	98.7	-0.15	-535.2	98.6	-0.24	-353.0	95.1	0.11	-353.0	99.1	-0.29	-469.8	99.7	-0.41	-500.3	98.4	-0.10
14	-419.2	98.6	-0.17	-298.8	98.6	-0.28	-123.8	102.5	-0.25	-114.9	99.1	-0.25	-233.2	98.4	-0.36	-263.5	98.4	-0.16
16	-181.9	98.4	-0.14	-62.3	97.2	-0.22	123.3	95.3	0.13	123.3	98.0	-0.15	0.4	96.0	-0.33	-26.7	97.8	-0.12
18	55.0	98.1	-0.10	170.8	96.2	-0.11	353.0	99.1	-0.15	358.9	98.1	-0.10	228.3	94.1	-0.16	208.6	97.6	-0.14
20	291.2	-97.1		401.5	-95.1		591.9	-97.6		594.6	-97.1		451.7	-92.6		443.4	-96.2	
18	57.5	-98.0		173.4	-96.1		356.7	-98.2		361.3	-97.5		232.0	-94.4		212.0	-98.1	
16	-178.5	-98.3		-57.1	-98.0		120.1	-98.7		127.0	-98.1		8.1	-98.2		-23.9	-98.0	
14	-415.2	-98.8		-292.0	-99.0		-117.7	-98.7		-108.8	-98.7		-224.8	-99.1		-259.6	-99.0	
12	-653.1	-99.4		-529.4	-104.8		-355.6	-99.0		-346.0	-99.3		-460.0	-99.8		-497.8	-98.4	
10	-892.4	-99.1		-780.6	-95.4		-594.2	-103.4		-584.6	-99.6		-696.8	-100.1		-734.6	-99.8	
8	-1131.0	-100.5		-1009.4	-101.0		-843.3	-96.6		-824.1	-100.5		-934.4	-101.2		-974.7	-99.8	
6	-1373.0	-102.5		-1251.6	-102.2		-1076.1	-101.7		-1065.6	-101.6		-1174.5	-102.2		-1214.9	-101.9	
4	-1619.7	-103.0		-1496.6	-103.8		-1321.3	-98.1		-1309.9	-103.0		-1416.9	-103.9		-1460.0	-103.2	
2	-1867.7	-103.6		-1745.4	-99.8		-1557.6	-109.3		-1557.6	-105.7		-1663.5	-103.6		-1708.3	-109.5	
0	-2117.0			-1984.6			-1821.0			-1811.6			-1909.3			-1971.7		
Intercept	-2104.0	mV		-1978.9	mV		-1807.1	mV		-1796.6	mV		-1896.4	mV		-1947.5	mV	
Slope	120.4	mV/mm		119.9	mV/mm		120.5	mV/mm		120.2	mV/mm		118.6	mV/mm		120.3	mV/mm	

bar	MPa	TPC A	Linearity	Hysteresis	TPC B	Linearity	Hysteresis
		(Volts)	(%)	(%)	(Volts)	(%)	(%)
0	0.0	-68.1	101.6	-0.02	113.5	101.8	-0.03
20	2.0	91.9	97.2	-0.34	278.5	97.6	-0.61
40	4.0	245.0	97.9	-0.37	436.7	97.9	-0.57
60	6.0	399.1	97.9	-0.43	595.4	97.7	-0.65
80	8.0	553.3	102.9	-0.63	753.7	102.9	-0.88
100	10.0	715.4	100.0	-0.37	920.5	100.1	-0.62
120	12.0	872.9	100.3	0.01	1082.8	100.2	-0.42
140	14.0	1030.8	101.8	-0.16	1245.3	105.2	-0.35
160	16.0	1191.1	102.7	-0.13	1415.9	98.0	0.01
180	18.0	1352.9	99.2	-0.14	1574.8	99.1	-0.31
200	20.0	1509.1	-97.8		1735.4	-95.9	
180	18.0	1355.1	-102.9		1579.9	-101.3	
160	16.0	1193.1	-101.4		1415.7	-101.6	
140	14.0	1033.4	-102.0		1251.0	-99.6	
120	12.0	872.8	-96.3		1089.6	-98.1	
100	10.0	721.2	-100.3		930.5	-100.2	
80	8.0	563.3	-99.9		768.0	-99.9	
60	6.0	405.9	-98.4		606.0	-98.7	
40	4.0	250.9	-97.6		446.0	-97.2	
20	2.0	97.2	-104.8		288.4	-107.6	
0	0.0	-67.8			114.0		
	Intercept	-68.10	mVolts		115.8	mVolts	
	Slope	7.874	mV/bar		8.105	mV/bar	
	Slope	78.7	mV/MPa		81.0	mV/MPa	

PRIOR TO BRESSAY

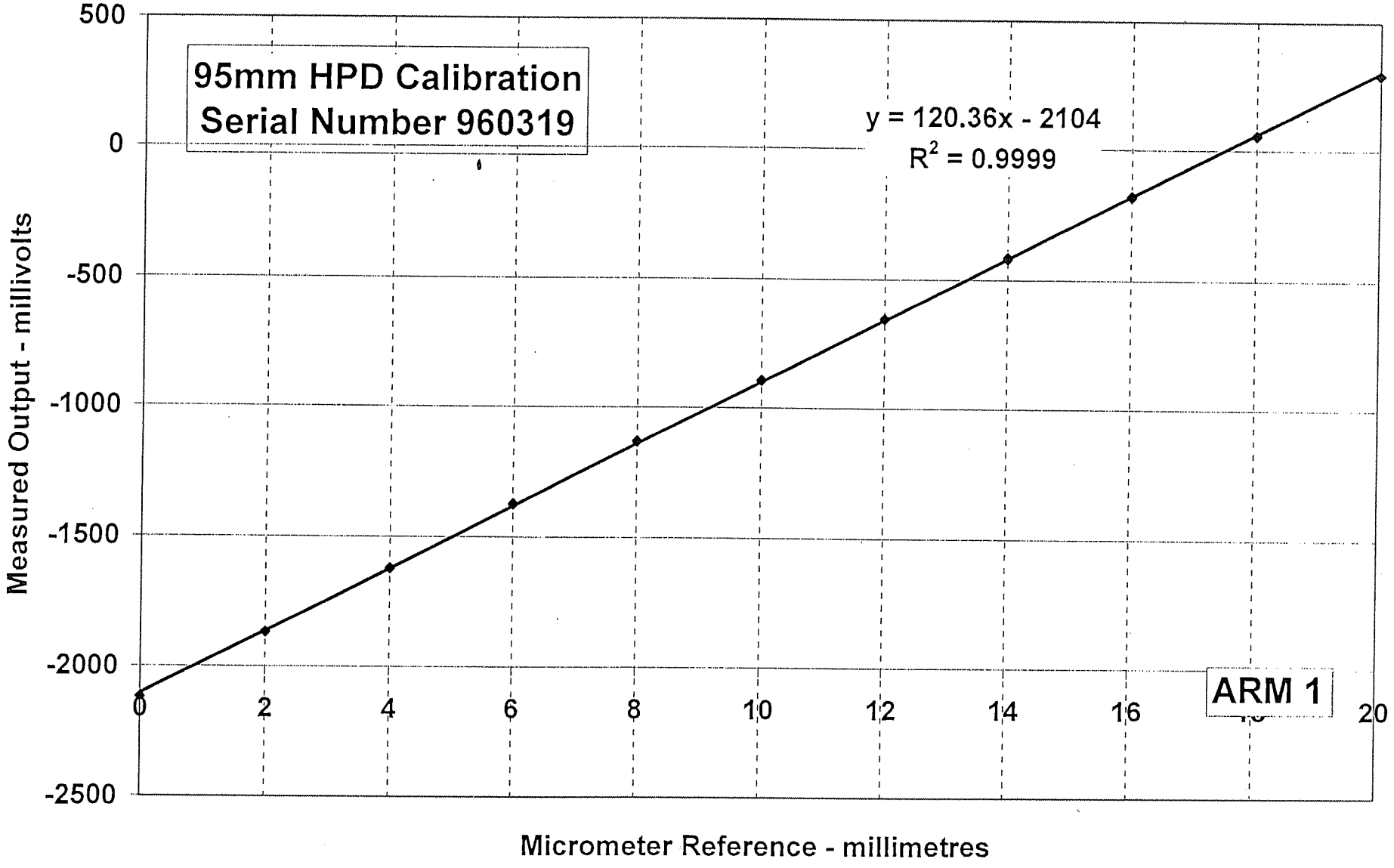
95mm HPD Calibration
Serial Number 960319
y = 120.36x - 2104
R² = 0.9999
ARM 1
Measured Output - millivolts
500
0
-500
-1000
-1500
-2000
-2500
0
2
4
6
8
10
12
14
16
20
Micrometer Reference - millimetres

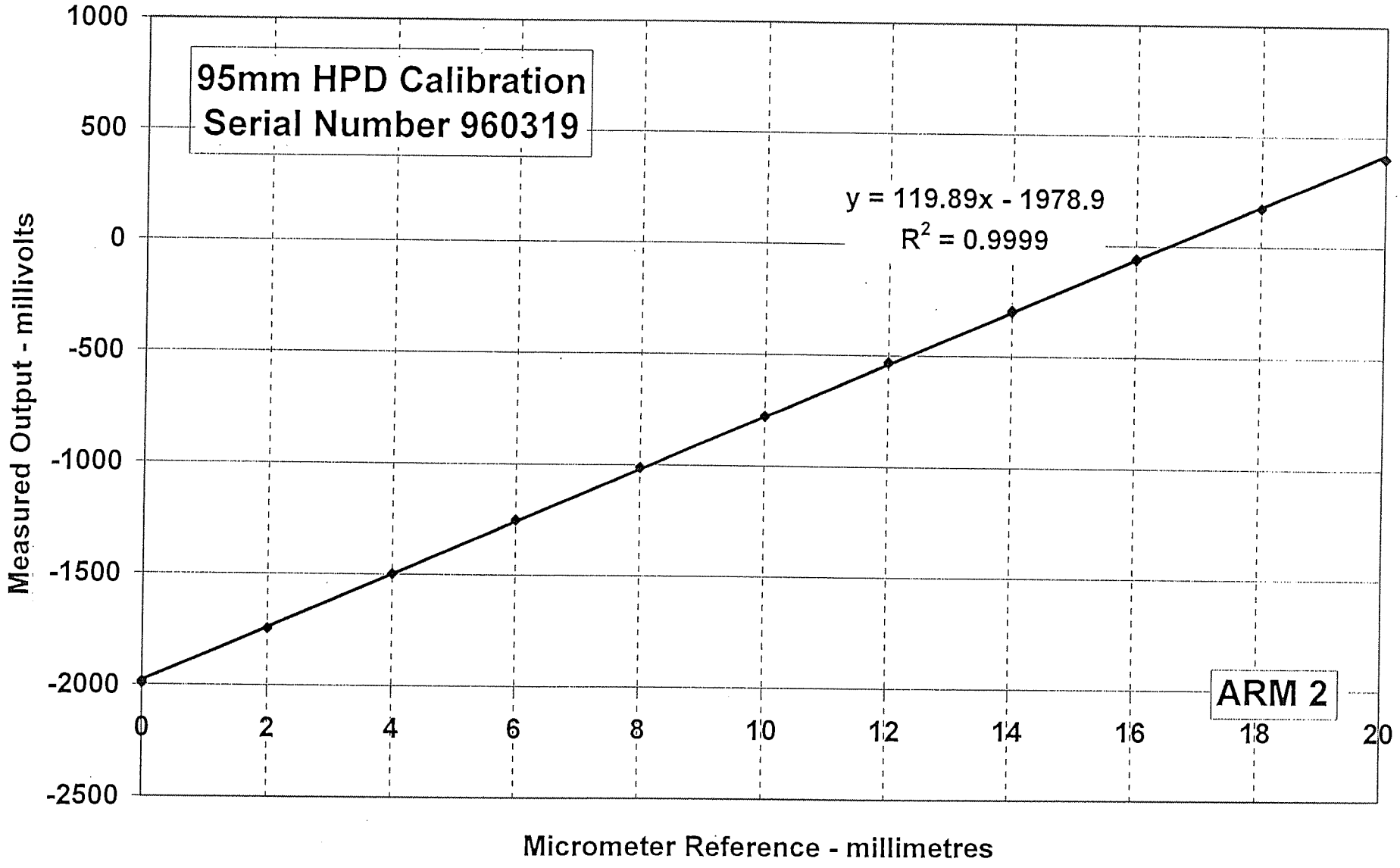
95mm HPD Calibration
Serial Number 960319
y = 119.89x - 1978.9
R2 = 0.9999
ARM 2
Measured Output - millivolts
Micrometer Reference - millimetres
1000
500
0
-500
-1000
-1500
-2000
-2500
0
2
4
6
8
10
12
14
16
18
20

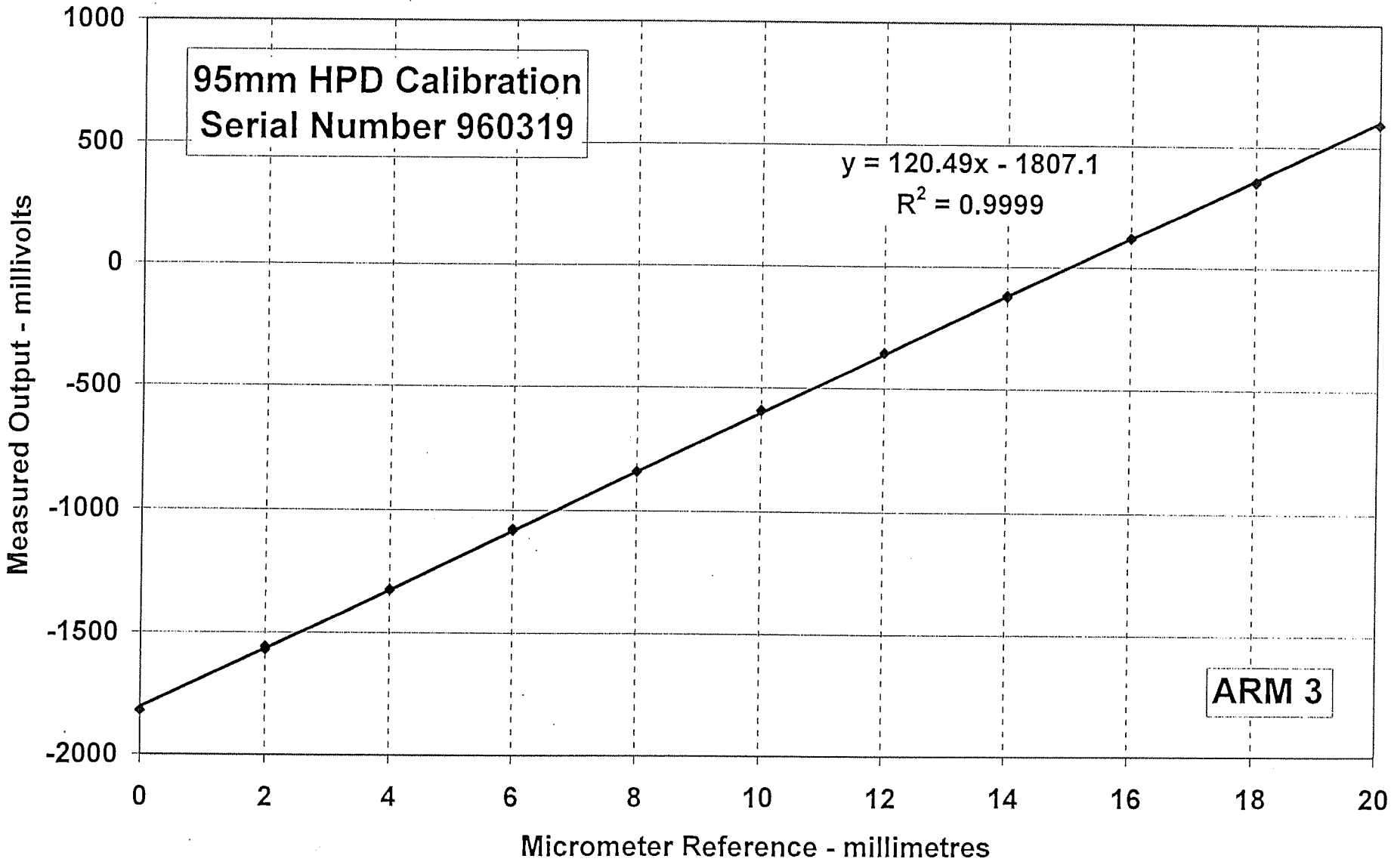
95mm HPD Calibration
Serial Number 960319
y = 120.49x - 1807.1
R2 = 0.9999
ARM 3
Measured Output - millivolts
1000
500
0
-500
-1000
-1500
-2000
0
2
4
6
8
10
12
14
16
18
20
Micrometer Reference - millimetres

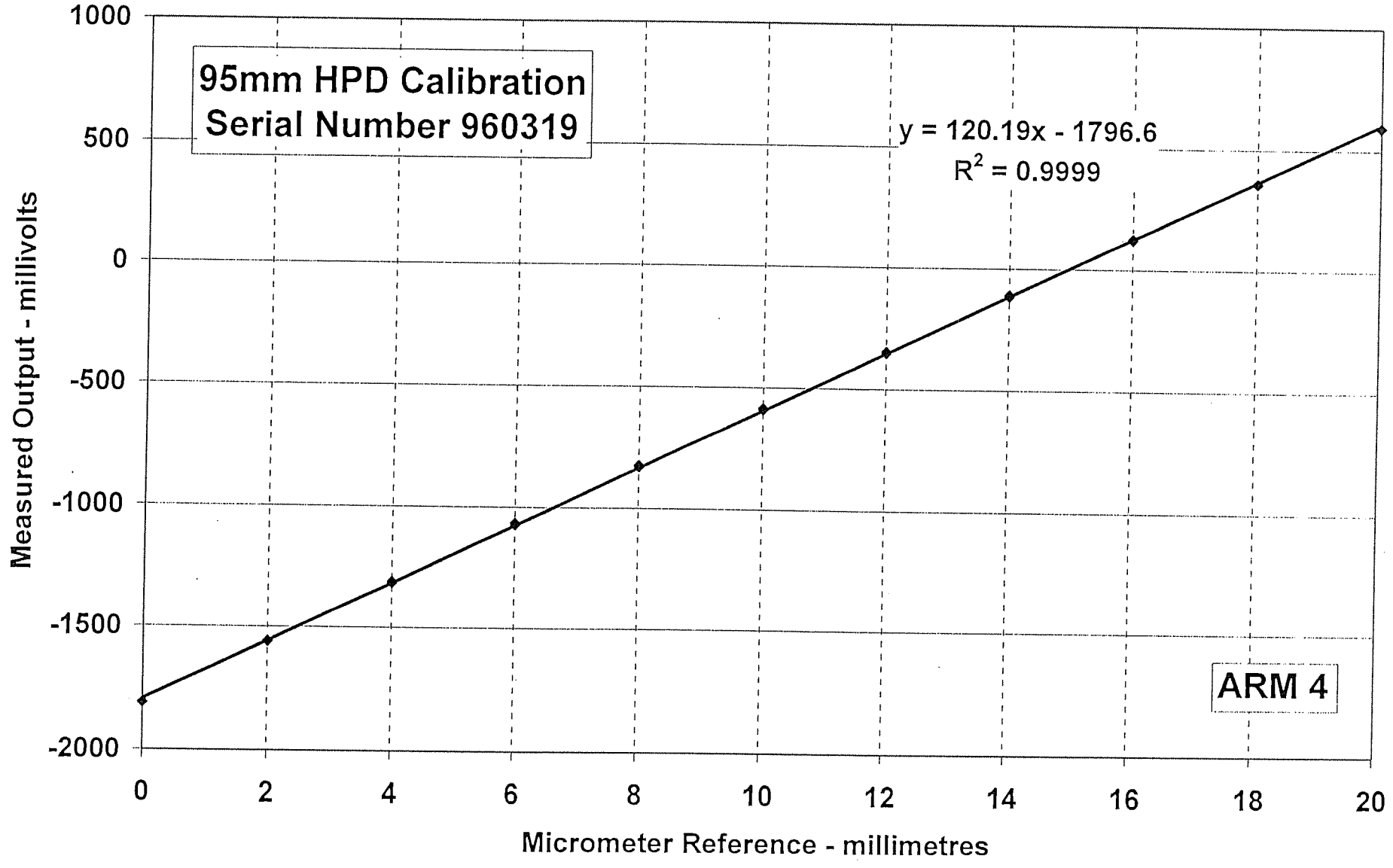
95mm HPD Calibration
Serial Number 960319
y = 120.19x - 1796.6
R2 = 0.9999
ARM 4
Measured Output - millivolts
1000
500
0
-500
-1000
-1500
-2000
0
2
4
6
8
10
12
14
16
18
20
Micrometer Reference - millimetres

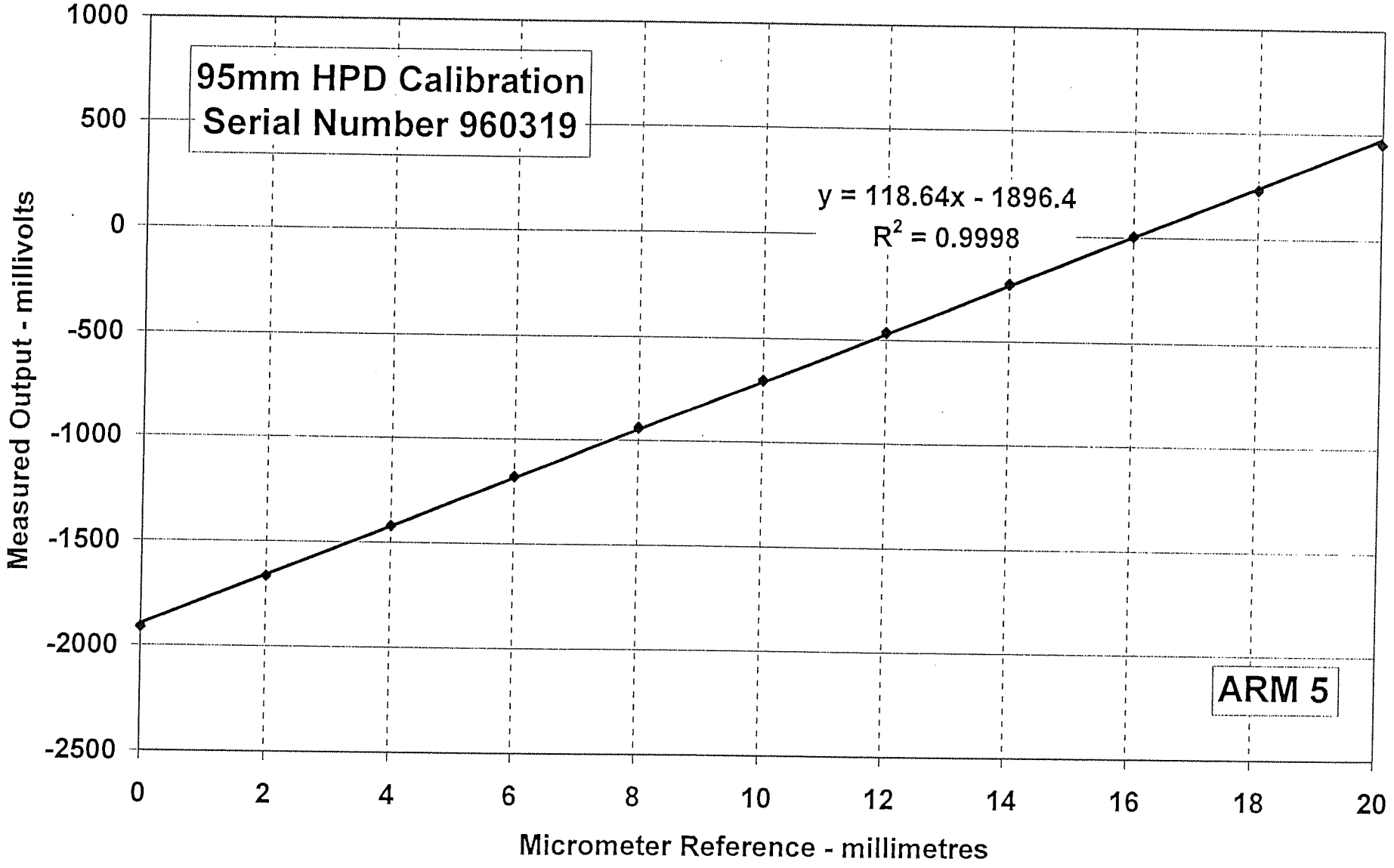
95mm HPD Calibration
Serial Number 960319
y = 118.64x - 1896.4
R² = 0.9998
ARM 5
Measured Output - millivolts
1000
500
0
-500
-1000
-1500
-2000
-2500
0
2
4
6
8
10
12
14
16
18
20
Micrometer Reference - millimetres

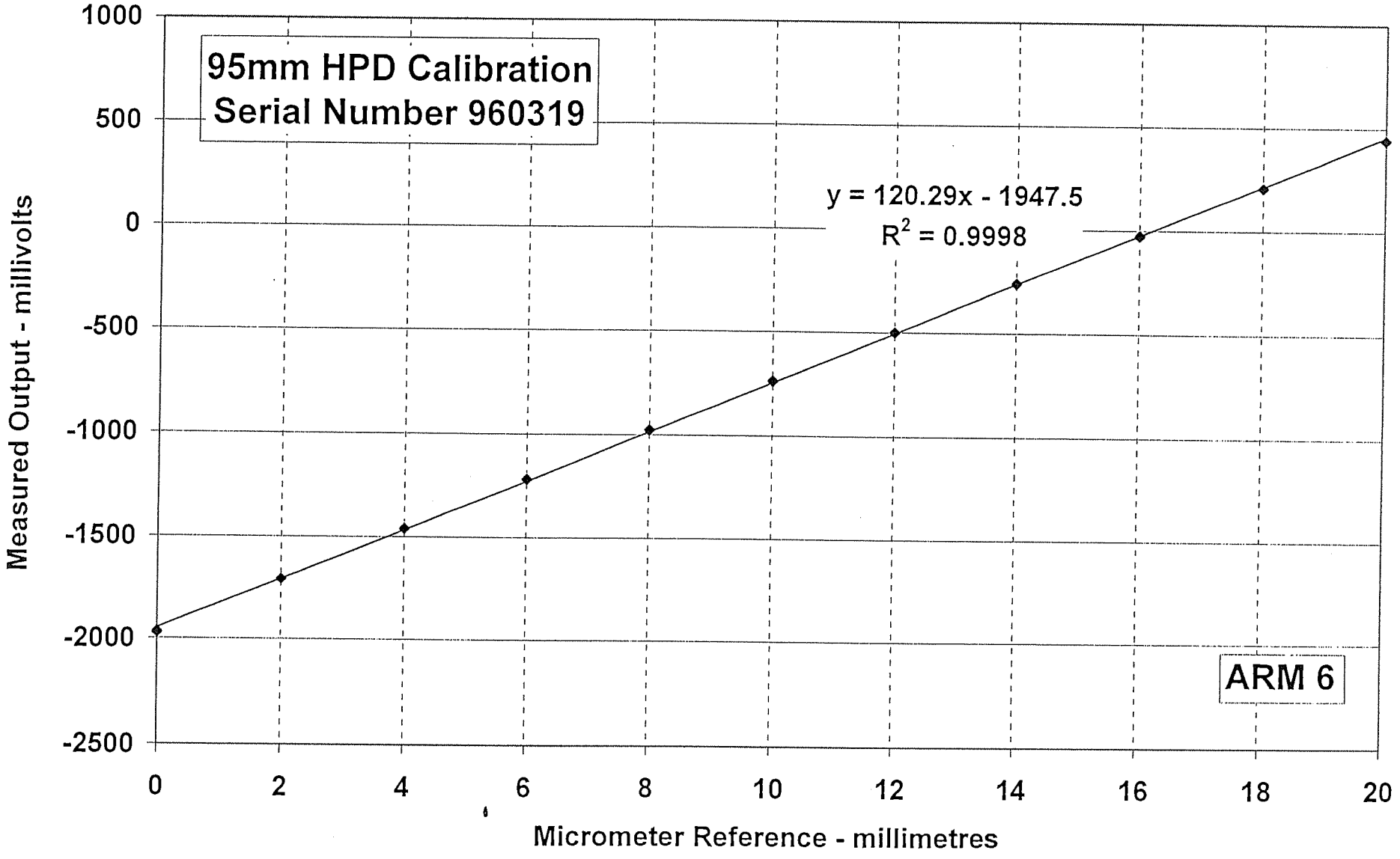
95mm HPD Calibration
Serial Number 960319
y = 120.29x - 1947.5
R2 = 0.9998
ARM 6
Measured Output - millivolts
1000
500
0
-500
-1000
-1500
-2000
-2500
0
2
4
6
8
10
12
14
16
18
20
Micrometer Reference - millimetres

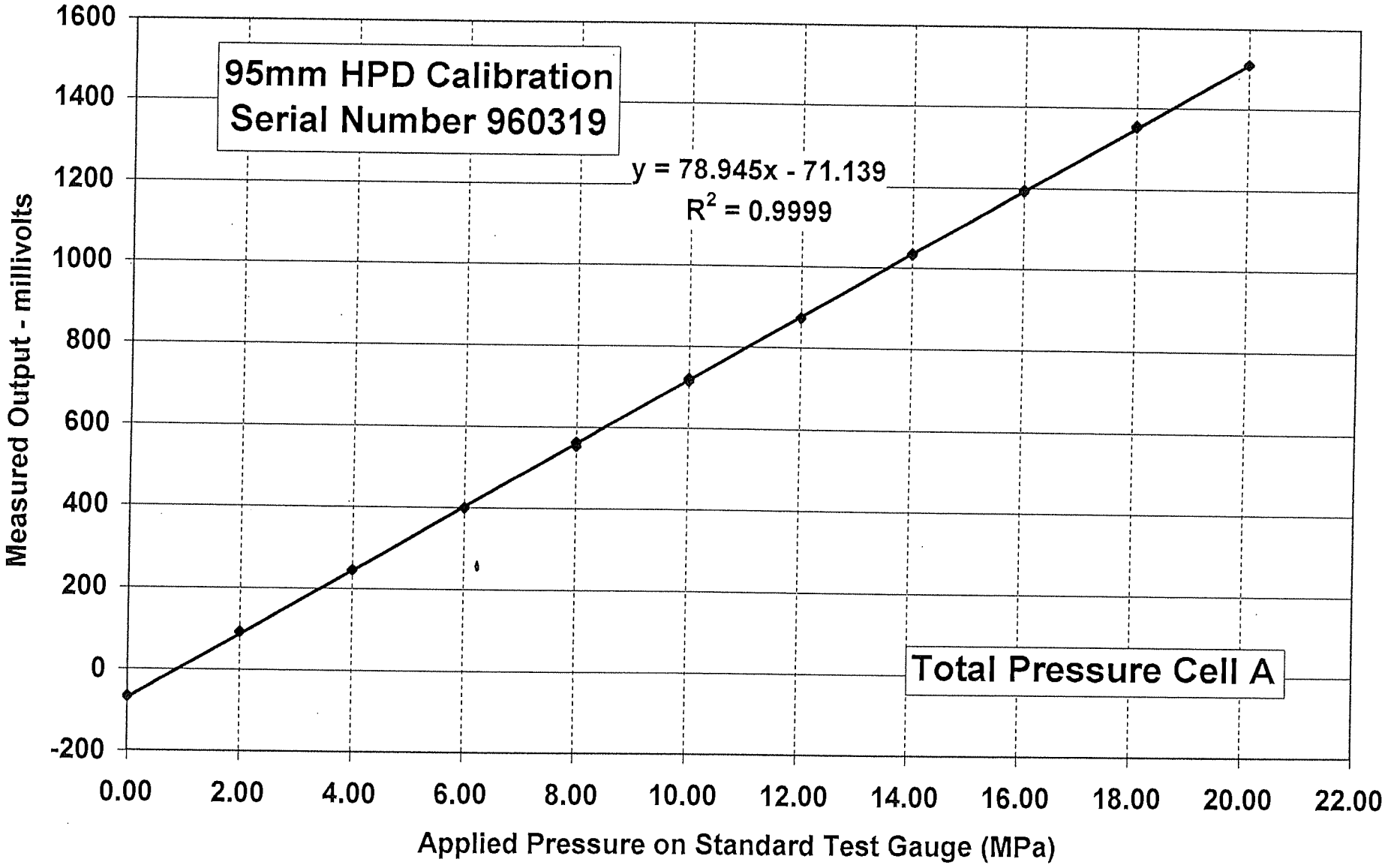
95mm HPD Calibration
Serial Number 960319
y = 78.945x - 71.139
R2 = 0.9999
Total Pressure Cell A
Measured Output - millivolts
1600
1400
1200
1000
800
600
400
200
0
-200
0.00
2.00
4.00
6.00
8.00
10.00
12.00
14.00
16.00
18.00
20.00
22.00
Applied Pressure on Standard Test Gauge (MPa)

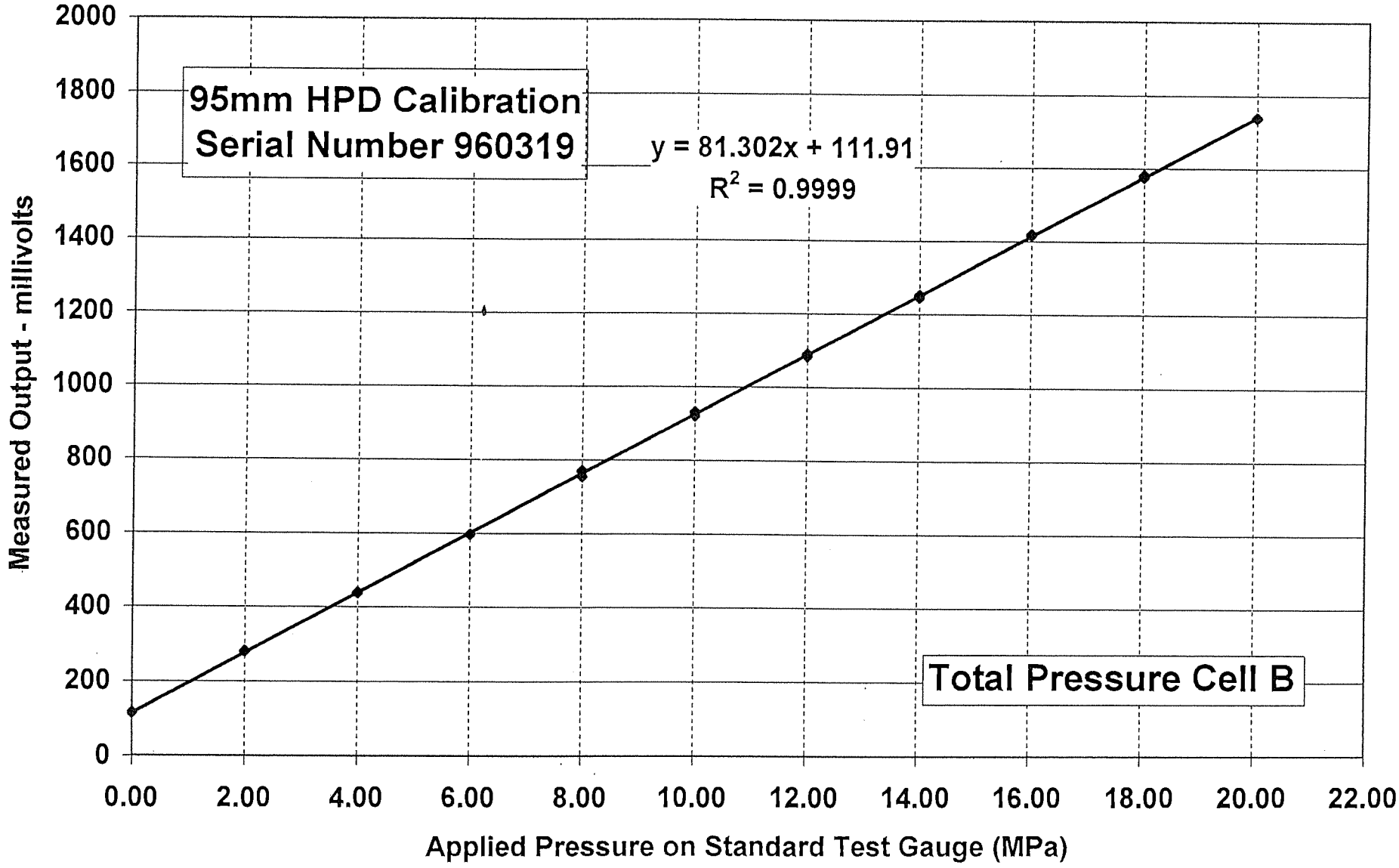
95mm HPD Calibration
Serial Number 960319
y = 81.302x + 111.91
R2 = 0.9999
Total Pressure Cell B
Measured Output - millivolts
Applied Pressure on Standard Test Gauge (MPa)
2000
1800
1600
1400
1200
1000
800
600
400
200
0
0.00
2.00
4.00
6.00
8.00
10.00
12.00
14.00
16.00
18.00
20.00
22.00

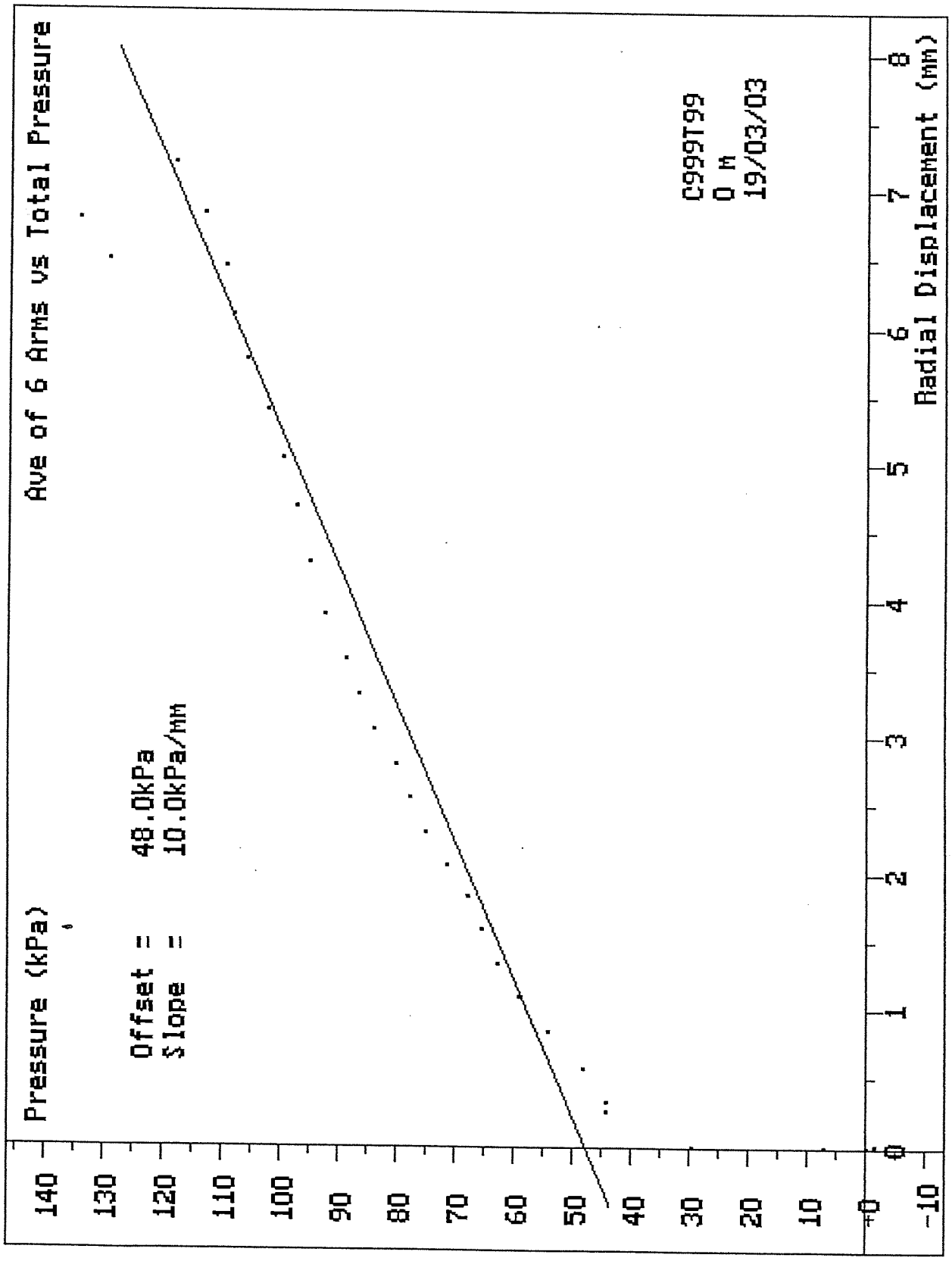

SCREEN DUMP Test: C999T99 Date: 19/03/03 Depth: 0.00m

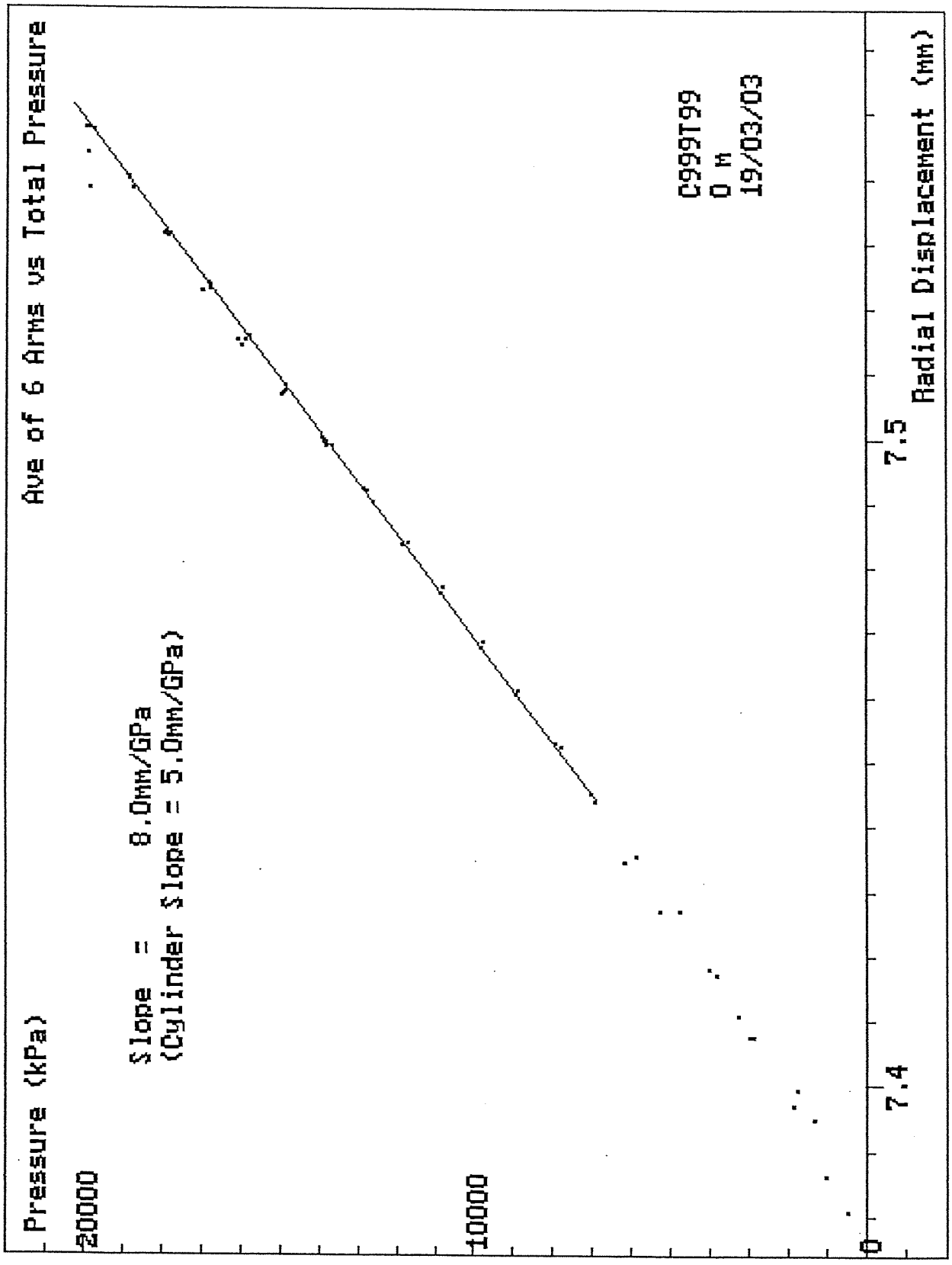

SCREEN DUMP Test: C999T99 Date: 19/03/03 Depth: 0.00m

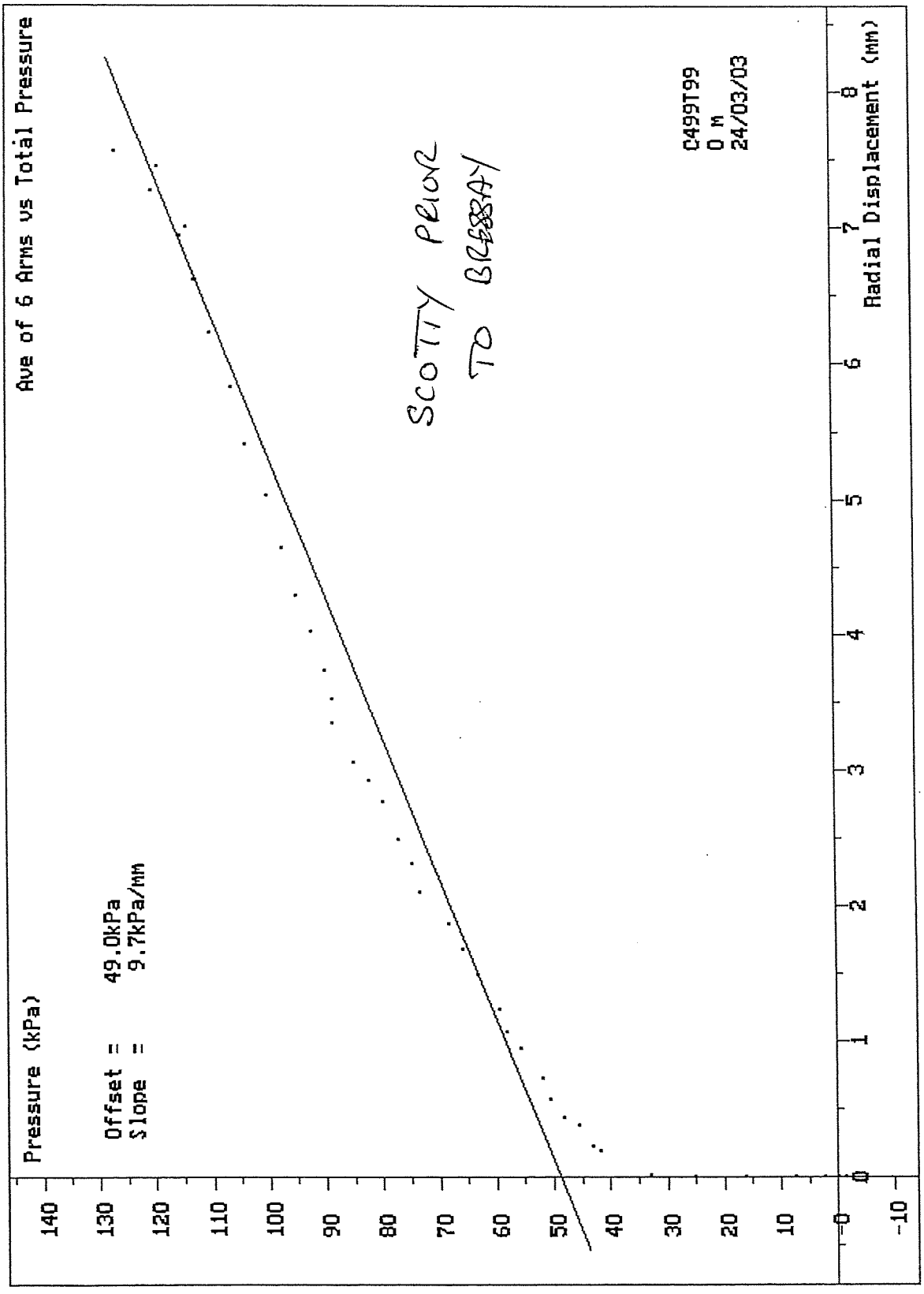

SCREEN DUMP Test: C499T99 Date: 24/03/03 Depth: 0.00m

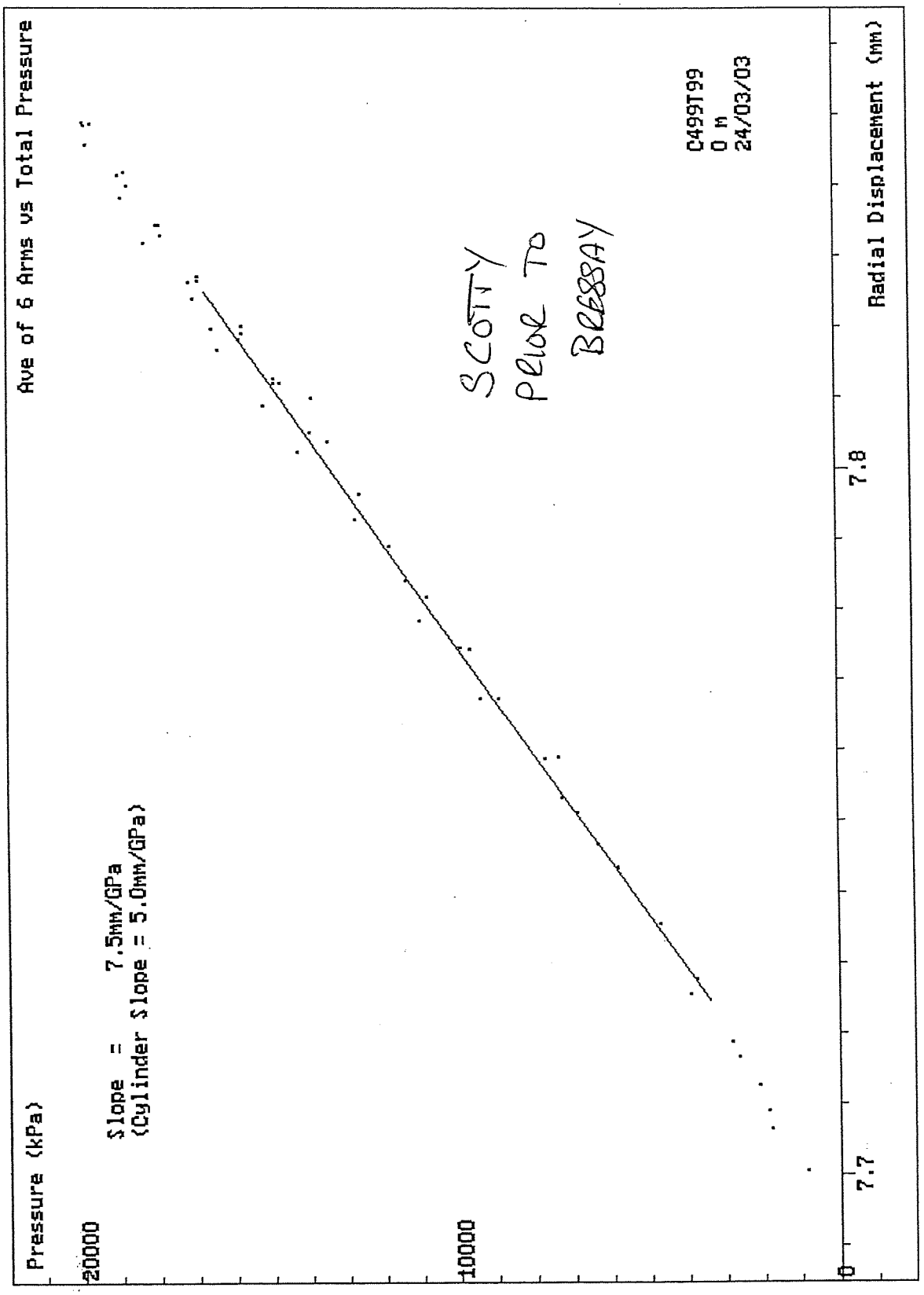

SCREEN DUMP Test: C499T99 Date: 24/03/03 Depth: 0.00m

APPENDIX C THE TEST PROCEDURE

1 Coring the Pocket

The HPD test is carried out in a 101mm pocket that has been formed by coring or more rarely by rock rollering. Coring is the conventional method because the recovered core can give some information about the pocket before the instrument is placed. Samples of the core are normally of sufficient quality to permit standard laboratory testing, which can then be compared with the pressuremeter results.

The pocket itself should be at least 2 metres long. This allows the user some choice about the exact point in the pocket in which to place the HPD. Note the following crucial measurements:

(a) From the foot of the instrument to the centre of the measuring section is 0.9 metres.
(b) The expanding part of the instrument is about 0.6 metres.
(c) The instrument is 2 metres long - if the BW extension rod is added to this then the effective length from the foot of the pressuremeter to the start of the rotary drill string is 3 metres. If the pocket is longer than 3 metres then the diameter of the drill rod used to place the pressuremeter must not exceed 75mm; this together with two thicknesses of hose, is the maximum that will fit into a 101mm pocket.

From these dimensions it is apparent that the instrument must be at least 1.3 metres into the pocket, and for safety we would suggest 1.5 metres into the pocket as a minimum. There is evidence that the very lowest part of the pocket should be avoided as this is often the area most spoiled by the coring, but as the test centre is some distance from the foot of the instrument this is not normally a problem.

Soft patches in the core suggest a point that ought to be in the test section. However soft patches at the ends of the expanding section may result in the membrane bursting before the pocket has been properly loaded.

Heavily fractured material around the test centre, although not likely to burst the membrane, will present problems of a different kind. The analyses that currently exist for the pressuremeter test assume that the material is intact - if this is not the case, then although the data may be good, deciding what they mean may prove complex.

It is a truism that the quality of the test is dependent on the quality of the initial coring. However many good tests have been made in pockets where no core at all was recovered. Standard coring practice is designed to preserve the core without regard for the borehole wall. This is the opposite of what the priorities need to be for the pressuremeter test.

Details about the core are noted on the Test Record Sheet as they can be useful in interpreting the test results.

2 Description of the Test

The test that the HPD makes is a loading test. Pressure is applied to the instrument and readings are taken of this pressure and the resulting displacements of the cavity. Plotting pressure against displacement gives a test curve with a characteristic 'S' shape made familiar by the Menard type pressuremeters (MPM) and for this reason the test tends to be carried out and analysed using techniques originally developed for the MPM.

The HPD makes two kinds of test:

A) The material yields well before the maximum pressure capability of the equipment is reached.
B) Tests where the maximum pressure capability of the HPD is the limiting factor.

All the tests on this contract were of type [A], but the movement after failure varied greatly; in some tests being very small. Only one test was limited by the maximum pressure capability of the system, but the material had started to fail.

3 Tests in material which can be failed - Type A

It is the loading curve of these tests that tend to take the 'S' shaped form. At the start of the test the membrane is lying on the body of the HPD. There are then several distinct parts to the test:

(1) Pressure is applied, the membrane lifts off the body of the HPD and expands out to touch the sides of the borehole. Hence there are large displacements for very little pressure.

(2) Further increments of pressure define the first curve of the 'S' shape; this curve is the instrument taking up the contour of the pocket and the cuttings left behind by the coring being squeezed out.

(3) Following this is a linear part of the loading curve. The pressure being applied is remoulding the material adjacent to the HPD that has been failed by the coring process, but is not yet sufficient to extend the zone of failure into fresh material. In this part of the test the pressure is increasing but is having little effect on the strain.

(4) Once the pressure is sufficient to extend the zone of failed material the upper curve of the 'S' starts to be defined, eventually reaching an almost linear condition once more where strain is increasing rapidly for very little increase in pressure.

(5) At this stage the cavity can be unloaded and the full unloading curve be drawn. The first part of this will be nearly linear, curving away as the pressure and hence the strain reduce to zero.

There are several ways of using the data contained in the pressure/strain curve but the most common is to use it to derive fundamental parameters about the strength of the material being tested. Therefore the precise manner in which the test is carried out should be chosen to make it easier to assess these parameters.

The slope of the initial linear part can give a value for the initial shear modulus G_i but because this part of the curve is sensitive to the disturbance produced by the coring the derived value is of little significance in itself.

FIGURE 1 Example of HPD test in a material showing large deformation

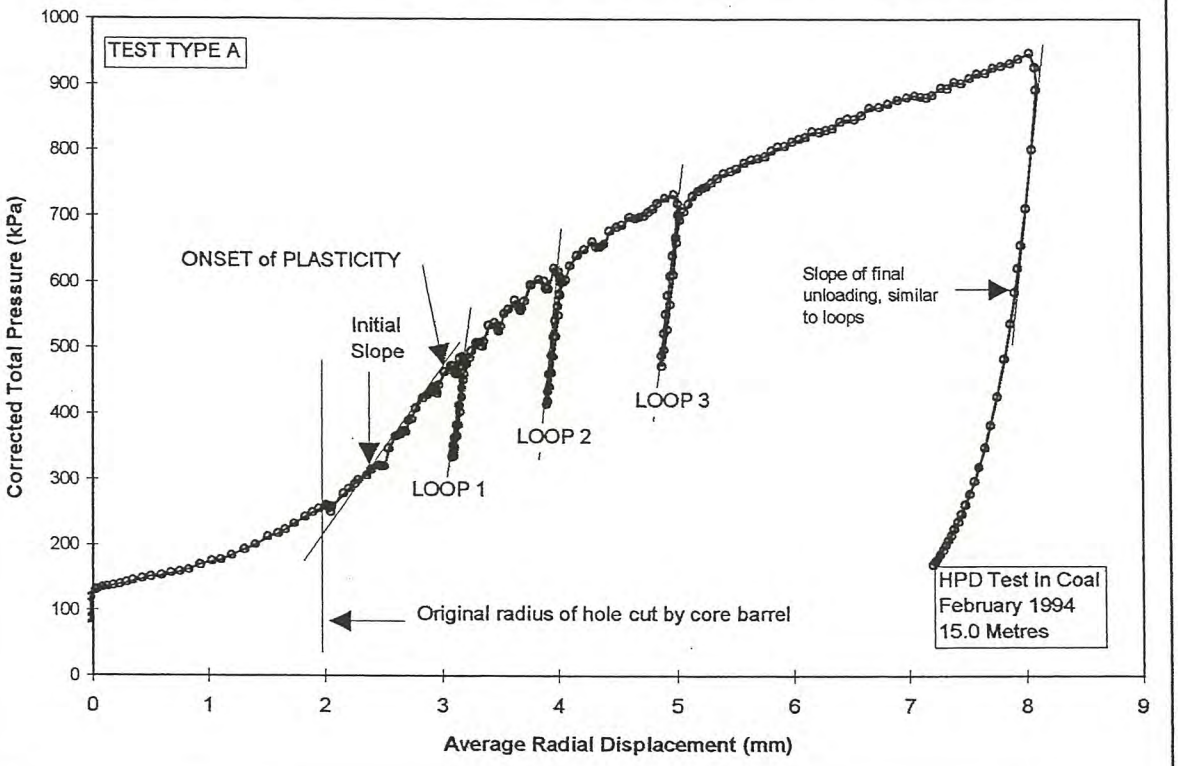

A better estimate of G can be made by taking unload/reload loops at intervals along the loading path. To do this a little of the pressure that has been applied is released and then reapplied in a controlled manner, taking readings of the changing strain. This produces a characteristic loop. The slope of the best fit straight line through the long axis of the loop can be used to derive G_r.

The value of G produced in this way is relatively insensitive to the initial drilling disturbance. The shear modulus is probably the single most useful parameter that the HPD test can produce, and it is used extensively in design calculations. Because of this significance it is usual to take at least two loops at suitable points on the test curve (even if the engineer supervising the test specifies only one). Suitable points would be on the linear part of the curve and as soon as there are indications of failure. Loops can also be taken on the unloading curve.

The ratio of G_i to G_r allows some assessment to be made about the extent of the disturbance created by the coring of the pocket.

Deductions about the undrained shear strength, Cu, are made from the part of the curve following yield until the end of loading.

Creep Readings:
From the linear part of the curve, can be deduced the insitu lateral stress, p_o. There are several methods. We use a modified version of the Marsland & Randolph argument (see references, Appendix F). Another aid to identifying the part of the curve where p_o may lie is to use creep strain, and this is frequently specified in contracts. To derive creep strain each pressure increment applied to the test cavity is held for a fixed period of time. The change of strain over

this time period is recorded. Plots of this creep strain can in certain circumstances allow an estimate to be made of p_o.

Current thinking is that for an 'A' type test creep readings should only be taken during the linear phase, where the lateral stress must lie. After this point, when the material is failing, holding the pressure for extended periods of time will allow any excess pore water pressure generated by the expansion to dissipate, seriously affecting the shear strength analysis which assumes that the expansion is undrained.

Creep readings serve no purpose during an unload/reload loop and there is no point in taking them when unloading the test cavity.

The time period we use in the absence of further instructions is 30 seconds, with an initial 10 or 20 seconds allowed for settling.

The exploration of creep effects is important for other reasons not directly related to the insitu lateral stress. Before taking a reload loop all residual creep in the material should be allowed to slow to an apparent stop, otherwise it is possible that the loop will be spoiled. As a guide the average loop will take three minutes - therefore the creep strain must be demonstrated to be insignificant over a similar time span.

4 Tests in material where all deformation is elastic - Type B Test:

Tests where the material does not fail before reaching the maximum pressure capability of the HPD need to be treated with great care. Such a test will have only the parts 1 - 3 of the 'S' shape curve described above. This means that for a large change in pressure there is little apparent strain. Any errors in the displacement sensing system will have important consequences for the results.

Frequently in material of this type the consulting engineer will only be looking for a value for modulus, because making assessments of p_o or c_u is dependent on the material at least starting to fail.

It is important therefore that there should be absolutely no possibility of creep in the material spoiling any unload/reload loop, and we would recommend holding the pressure for a significant length of time before taking a loop. Note also that the value of modulus is certain to be high, probably in excess of 1GPa. This indicates that the displacements seen during the loop will be very small, and therefore the pressure drop should be substantial to obtain the maximum possible definition of strain. This in turn implies that the ideal unload /reload loop be started from a point on the loading curve close to the maximum pressure limit.

In a 'Type B' test, if unusually large creep behaviour is seen at any point then we would advise exploring this creep behaviour by making pressure holds at increasing stress levels and for longer periods of time. Creep, if present, has important consequences for the final design.

FIGURE 2 Example of an HPD test where all rock response is elastic

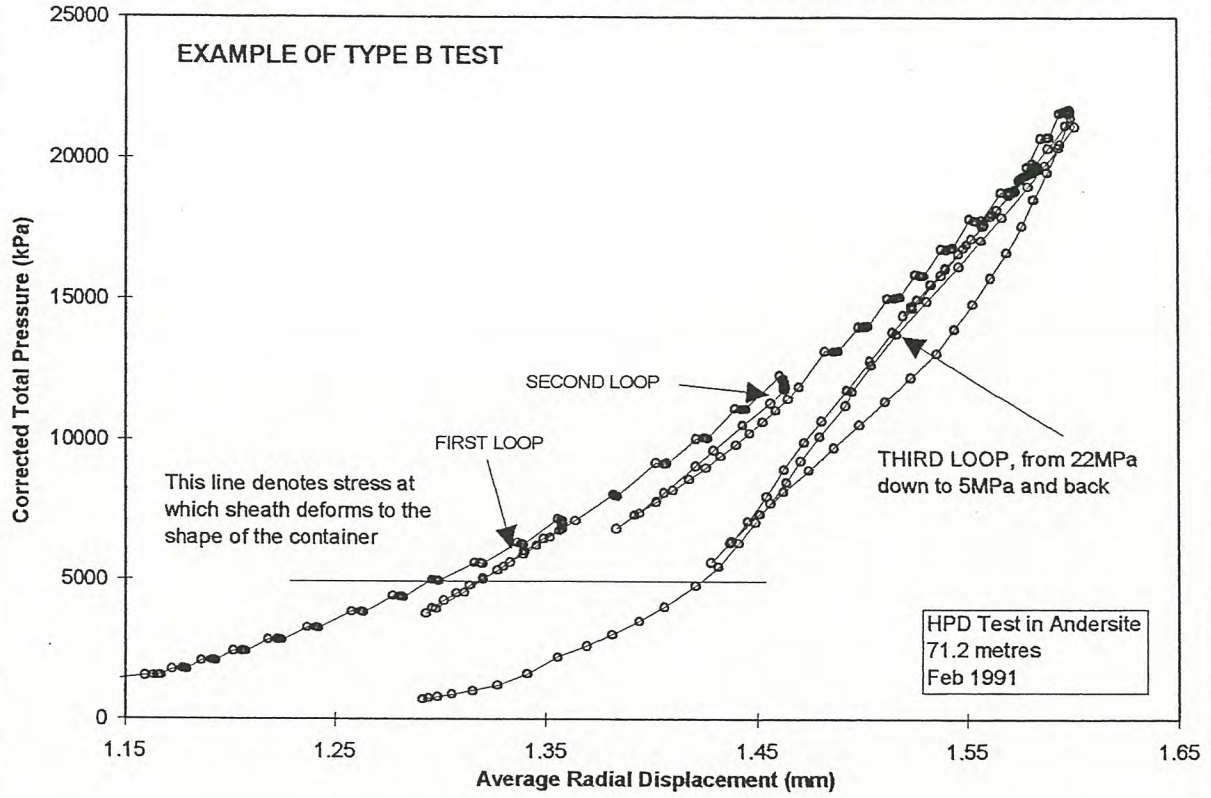

For type [B] tests it is necessary to recognise that the instrument itself is deforming under the influence of the large internal pressures. Removing this system error from the test data is not always straightforward and the engineer carrying out the test must ensure that sufficient information is available about the test and the characteristics of the instrument in order to facilitate the correction procedure.

Before the actual test is carried out there should be a corresponding calibration test in a special cylinder supplied with the HPD. This is always good practice but is especially important for a 'Type B' test.

Another technique that has proved rewarding is to make two loadings of the material. After reaching maximum pressure (20MPa) the cavity is unloaded to about 5MPa. It is then reloaded once more to maximum pressure before unloading to zero, taking unload/reload loops at appropriate stress levels.

A comparison of the two curves can be very revealing, particularly if there is uncertainty as to whether the material has begun to fail.

5 Concluding Remarks

This is a brief introduction only to the test; the intent is to ensure that the test is carried out in a manner that will recover the maximum amount of good quality data.

From remarks made above it is clear that we expect to gather more data than may have been specified.

It is difficult to separate a description of the test from a description of the analysis. An appreciation of what will be done with the data contributes significantly towards the success of the test.

APPENDIX D INTERPRETATION OF PRESSUREMETER TESTS

Deriving parameters from pre-bored pressuremeter tests in soil.

1. Introduction

There are two approaches to the interpretation of pressuremeter test data. The first, that developed by Menard, uses empirical correlations to allow measured co-ordinates of pressure and displacement to be inserted directly into design equations. This approach depends on a standardised test procedure and a large data bank of pressuremeter tests correlated with observations of the response of finished structures.

The second approach, which will be described briefly here and is the usual way of interpreting the pressuremeter test in the UK, relies on solving the boundary problem posed by the pressuremeter test.

The aim of the pressuremeter test is to expand a long cylindrical cavity within an undisturbed mass of soil. Fundamental strength properties of the material can be deduced from measurements made of cavity pressure and displacement.

In practice no instrument can be placed into the ground without affecting in some way the surrounding soil. In the case of a pre-bored pressuremeter test the disturbance is significant because the cavity wall is affected by the process of making the hole and is then completely unloaded prior to the placing of the instrument. The measured pressure/displacement curve does not represent the insitu response and must be redrawn to compensate for insertion disturbance prior to attempting to derive strength and stiffness parameters. The problem is two-fold:

- Expand the pressuremeter sufficiently far so that the effects of disturbance are erased by a new stress regime where the pressure applied by the instrument exceeds any previous stress experienced by the surrounding soil mass.
- Identify a point on the loading path that can be used as an origin for converting pressures and displacements to stresses and strains.

1.1 The pressuremeter test in soil - initially elastic response followed by failure in shear.

Consider that the soil is homogeneous, and shows elastic behaviour before failing in shear. The stress path followed by an element of soil adjacent to the cavity is given in figure 1.1 and the corresponding pressure /strain curve is shown alongside.

The radial stress, initially zero for a pressuremeter placed in a pre-bored hole, increases at the same rate as the circumferential stress decreases, regardless of whether the material is deforming under plane strain or plane stress conditions. The line 0 - 0 represents stress equality, so that in the ideal case considered here the point p_o is the insitu lateral stress.

Once the radial stress increases above the insitu stress then the shear stress in the soil at the cavity wall will increase. If the insitu lateral stress is low, then it is possible that the circumferential stress would go into tension. However in this example the insitu stress is high enough to ensure that the shear stress limit is reached before tensile stresses can be generated.

The pressure necessary to initiate shear failure is denoted p_f in figure 1.1. After this pressure the strain rate shows a substantial increase, and the form of this part of the pressure/strain curve

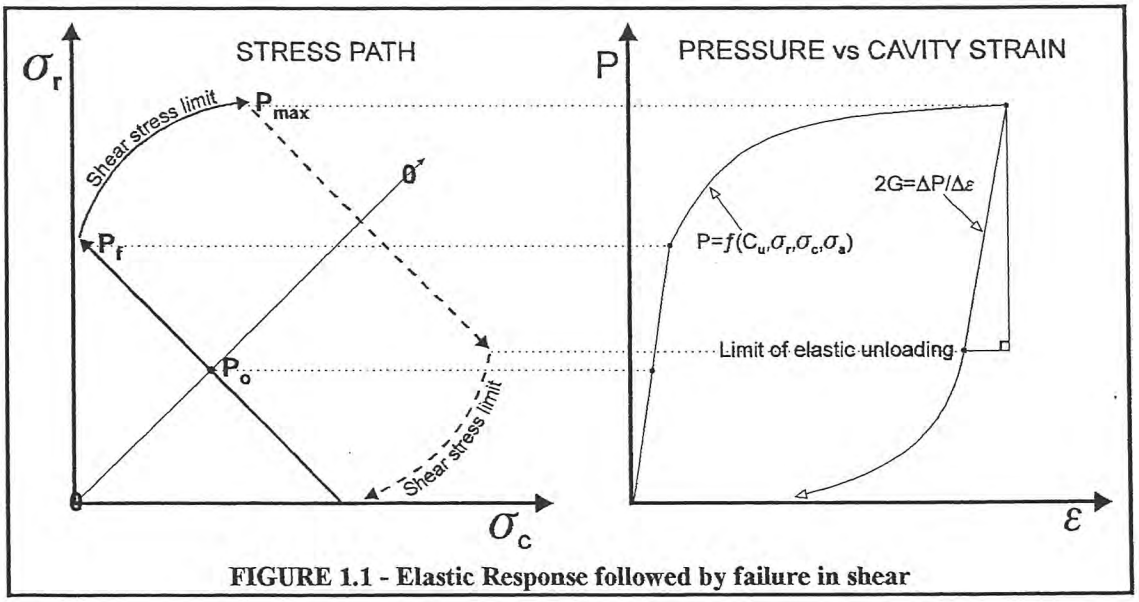

FIGURE 1.1 - Elastic Response followed by failure in shear

will be a function of the shear strength of the material. Radial stress and circumferential stress now increase together. If the shear stress limit is constant, and is not influenced by pressure, and if the material deforms at constant volume, then the failure shear strength can be determined by the analytical solution developed by Gibson & Anderson.

Before the shear stress limit is reached the pressuremeter response is elastic, both in loading and unloading. Were the installation to be perfect then the slope of the initial loading path would give the shear modulus of the material, using the classic procedure of Bishop, Hill & Mott. In practice, in a pre-bored test where significant unloading of the cavity wall has taken place prior to the pressuremeter being in position, the initial loading is *pseudo* elastic - it will under-estimate the true stiffness of the material. No such reservation applies to the initial unloading. In addition, small cycles of unloading and reloading taken after the shear stress limit is exceeded give plausible and repeatable estimates of the shear modulus (Hughes 1982).

As figure 1.1 implies, the complete unloading of the pressuremeter can also be analysed to give strength and stiffness parameters comparable with those obtained from the loading path.

1.2 Defining strain

For a pre-bored pressuremeter measuring the radius of the expanding cavity the conversion from displacement to strain is $[R-R_0]/R_0$, where R is the current radius of the cavity and R_0 is the original radius of the cavity *in the insitu state*. This is simple strain and when displacements are measured at the borehole wall is termed cavity strain, ε_c.

R_0 can be roughly approximated by the at rest radius of the instrument. Usually, in a pre-bored test, the initial part of the loading curve shows the instrument taking up the shape of the test cavity. The radius when this process is complete (indicated by a point of inflexion) is often taken to be R_0. In addition there are procedures for identifying when the applied pressure has reached the insitu lateral stress, and interpolating from this the corresponding radius which then becomes R_0.

Note that although the pressuremeter measures the radius of the cavity wall, ε_c is actually circumferential strain. It is usually expressed as a percentage.

Figure 1.2 shows how pressures and strains in the expanding borehole are defined.

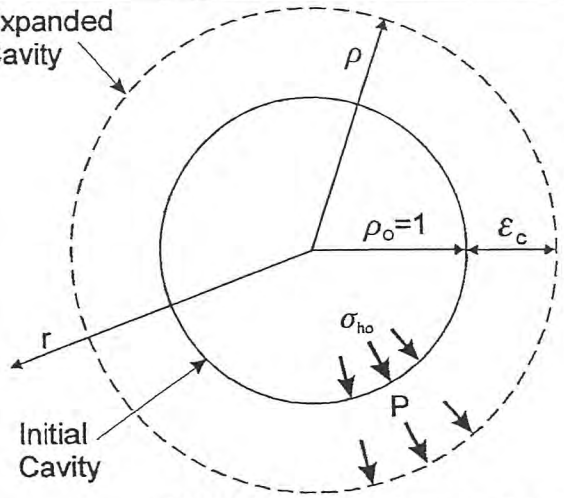

r = radius
ρ = radius of cavity
ρ_o = initial radius of cavity
P = pressure applied to cavity wall
σ_{ho} = insitu horizontal stress
ε_c = circumferential strain at cavity wall
= $[\rho-\rho_o]/\rho_o$

Constant area ratio $\Delta A/A$
= change of area/current area
= $[\pi(1+\varepsilon_c)^2 - \pi]/[\pi(1+\varepsilon_c)^2]$
= $1-1/(1+\varepsilon_c)^2$

FIGURE 1.2 Pressures and strains around the expanding cavity

The other strain commonly used is the constant area ratio, which is shear strain. As figure 1.2 indicates it can be expressed in terms of simple strain.

1.3 Average displacements versus the output of the separate axes

Although there are a number of displacement sensors in the probe recommended practice is to quote parameters from the average displacement curve. This is for two reasons:

1. The reference for the measured displacements is the body of the instrument itself - trying to separate the individual axes means assuming that the body of the instrument remains fixed at all times, which is not realistic.

2. All available analyses assume isotropic properties in the surrounding soil, and only the average pressure/strain curve represents this condition.

The High Pressure Dilatometer (HPD) has six equi-spaced arm followers in the same plane so that the effects of lateral translations of the instrument are cancelled by taking the average radius from a pair of opposing sensors. However because of the fairly poor fit to the borehole the probe moves in other directions than the horizontal plane and it is wise to use the average whenever possible to minimise these effects.

These remarks assume that the instrument is in full working order throughout the test - failure of a displacement follower means that alternative strategies must be adopted.

1.4 The analysis program

We use (and supply to others) software for analysing a pressuremeter test. The program is called **INSITU,** it has been in use for a number of years and is well proven.

To use the program the user must first read in a text file of test data in engineering units. The program needs to know the type of instrument being used, and the user may choose to enter additional background information about the test.

The next task is to identify for the program the nature of the individual data points. Broadly, speaking the options are these:

- a point can be part of the expansion curve
- or part of a reload loop

- or part of the contraction curve
- or part of a creep waiting period
- or none of the above. This might mean a 'rogue' data point, but it is more likely to be true of parts of the loading where the expansion was slowed prior to taking an unload/reload cycle. Data points recorded at this time are neither part of the expansion nor part of a cycle, and should be identified as such.

There is a quick on-screen routine for marking the points. Once marked, they appear in different colours and have different shapes (so that the distinction can be made clear on a black and white printout). Most of the analyses use a limited set of the available data - for example the Gibson & Anderson analysis for undrained shear strength uses only points on the expansion curve. The smoothest data are obtained when 'end creep' readings are plotted. These are the strains recorded at the end of a creep waiting period. Providing the creep interval is constant throughout the loading and providing there are sufficient steps of stress these are the ideal data to plot.

The program implements all the standard analyses mainly in a graphical form. As figure 1.1 implies, there are significant changes of gradient in the pressure/strain curve which denote critical soil parameters. The user of the program is provided with on-screen tools to mark these breakpoints or to obtain the slope of the loading curve. The tools can be visualised as rulers, and the chosen position of any ruler is stored by the program in the file of test data. The evidence for any derived parameter is a screen dump of the appropriate analysis showing the position of any rulers set by the user and quoting the parameter obtained.

Even when the user declines to make a choice it is good practice to provide the screen dump as evidence of why a choice is difficult.

The results for a test appear as a summary sheet of derived parameters followed by a number of plots showing the application of the various procedures.

Sometimes analyses are required which are not included in the INSITU program. In such instances commonly available spreadsheet software is used to implement the new analysis. Inevitably in such circumstances there is some risk of human error affecting the conversion of data in engineering units to the form required for analysis. INSITU has comprehensive export facilities and wherever possible is used as the data source for the spreadsheet.

2. ANALYSES FOR EXPANSION

2.1 Overview

The pressuremeter test is a sequence of measured co-ordinates of pressure and displacement of the cavity wall (once suitable corrections have been made to compensate for the response of the elastic membrane).

In order to solve the boundary problem, an origin for the expansion has to be determined. For insertion methods which imply stress *relief*, the origin is taken to be the point where insitu conditions are restored to the cavity. This means that an estimate of the insitu lateral stress has to be made, and the measured radius of the cavity at the point where the insitu lateral stress is restored is used to convert subsequent displacements to strain.

For a pre-bored pressuremeter test it is not normally possible to recognise the insitu lateral stress by inspection. However it is possible to recognise by inspection the shear stress limit (the point marked p_f in figure 1.1) as this is signified by the onset of a markedly non-linear response. An iterative procedure first suggested by Marsland & Randolph (1977) allows the insitu lateral stress to be inferred.

Once the origin is known, the expansion phase of the test can be used to determine the material shear strength. For an undrained expansion the classic procedure is that developed by Gibson & Anderson (1961) where the slope of the pressure /strain curve plotted on semi-log axes gives the shear strength directly and an estimate of the ultimate limit pressure. In most circumstances the assumption of failure at a constant shear strength is

reasonable, but the complete shear stress:shear strain response of a material deforming at constant volume can be described by applying the analysis due to Palmer (1972).

For materials where the expansion is drained, so that there are volumetric as well as shear strains to take into account, the analysis due to Hughes et al (1977) is used to derive the peak angle of internal friction and dilation. Manassero (1989) is a more complex analysis that offers a complete description of the shear strain versus volumetric strain response of a material deforming under drained conditions.

Estimates of shear modulus are obtained either from the slope of the pressure/strain curve at places where elastic response can be assumed, or (preferably) from the slope of the chord which bisects small rebound cycles. The values for shear modulus obtained in this second manner are repeatable and seem to be largely independent of any disturbance caused to the material by the placing of the pressuremeter. It is important, however, to correlate the measured stiffness with the strain range covered by the rebound cycle.

2.2 Marsland & Randolph (1977) Analysis

Marsland & Randolph analysis relies on being able to identify the onset of plastic behaviour, the yield stress p_f. The argument is as follows:

- that in the vicinity of the insitu lateral stress the soil behaves elastically and therefore the pressure/strain plot will be linear
- that this elastic behaviour will cease when the undrained shear strength of the soil is reached in the wall of the cavity, and hence the pressure /strain plot will begin to curve (see Figure 1.1).

This can be expressed as:

$$p_f = p_o + c_u \qquad \text{.....[2.1]}$$

From this it follows that p_o can be deduced by a process of iteration. Initially a guess is made of a value for p_o; using this guess to define a temporary strain origin a total pressure:log volumetric strain plot is then generated in order to derive a value for c_u. The sum of these two parameters is compared with the selected value of p_f. The choice of p_o is then suitably adjusted and the process repeated until a match is found. It is a straightforward matter to carry out this procedure on the computer.

The modified method in current use is a response to the difficulty that the Gibson & Anderson model is too simple for use in most materials and yield may occur at a shear stress that is different from the large strain shear strength. Hawkins et al (1990) suggested that the most appropriate choice was that value of shear stress pertaining at the apparent onset of plasticity, so that equation [2.1] above now becomes:

$$p_f = p_o + \tau_f \qquad \text{.....[2.2]}$$

τ_f can be obtained from a total pressure:log volumetric strain plot by selecting the slope at the pressure and strain corresponding to the choice of p_f (in practice, using the Palmer (1972) argument to identify the mobilised shear stress at failure).

The analysis is implemented graphically, using a number of rulers to identify significant points on the curve.

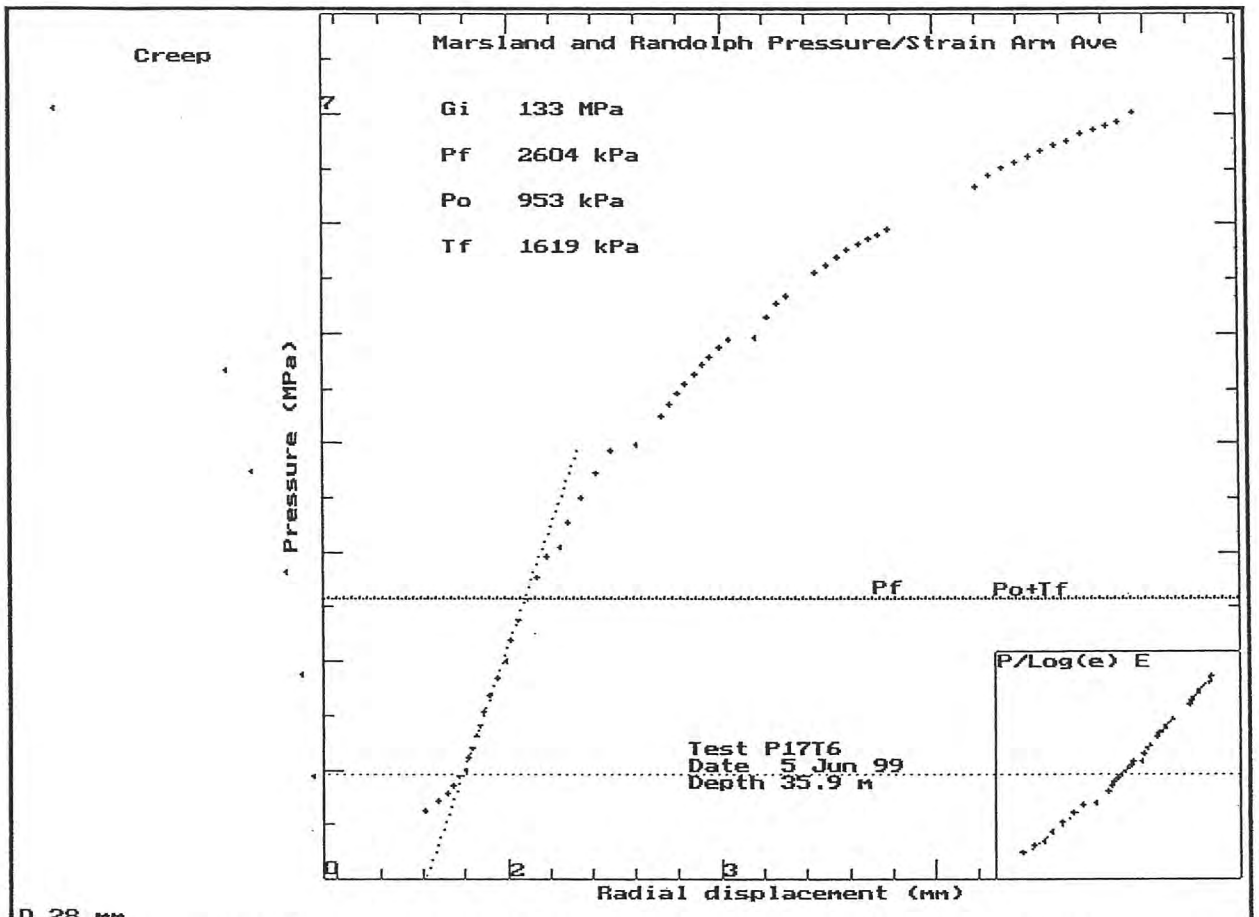

FIGURE 2.1. AN EXAMPLE OF THE MARSLAND & RANDOLPH ANALYSIS

The main problems associated with the analysis are these:

- The assumption of simple elastic response - in practice most soils exhibit marked non-linear elastic characteristics, so that the pressure at which the material appears to go fully plastic is more than one increment of shear stress above p_0.
- The assumption that the unloading of the cavity prior to the placing of the instrument is elastic and hence recoverable. It is obvious that in most tests this assumption is unjustified. This does not by itself affect the relationship between p_f and p_0 but it does mean that the associated yield strain (iterated from the two stresses) is too large, and hence the strain origin will be miscalculated.

2.3 Undrained shear strength (c_u)

There are two analyses for deriving estimates of undrained shear strength :

- **Gibson & Anderson (1961)**
- **Palmer (1972)**

Usually only parameters derived from the Gibson & Anderson analysis are quoted, although plots of the Palmer analysis are routinely supplied.

2.3.1 Gibson & Anderson (1961)

Prior to yield, the assumption of linear elastic behaviour means that pressures and shear strains measured at the borehole wall are related by

$$p_c - \sigma_{ho} = (\Delta\gamma)G \qquad \text{... [Equ. 2.3]}$$

where p_c is the total pressure applied to the cavity wall. For pressuremeters measuring changes in volume such as the Ménard probe for which the Gibson & Anderson solution was developed, shear strain γ is the change in volume divided by the *current* volume, usually expressed $\Delta V/V$. For pressuremeters measuring the radius of the cavity wall, γ is the change in area divided by the *current* area, $\Delta A/A$. Because plane strain expansion is assumed both expressions are identical.

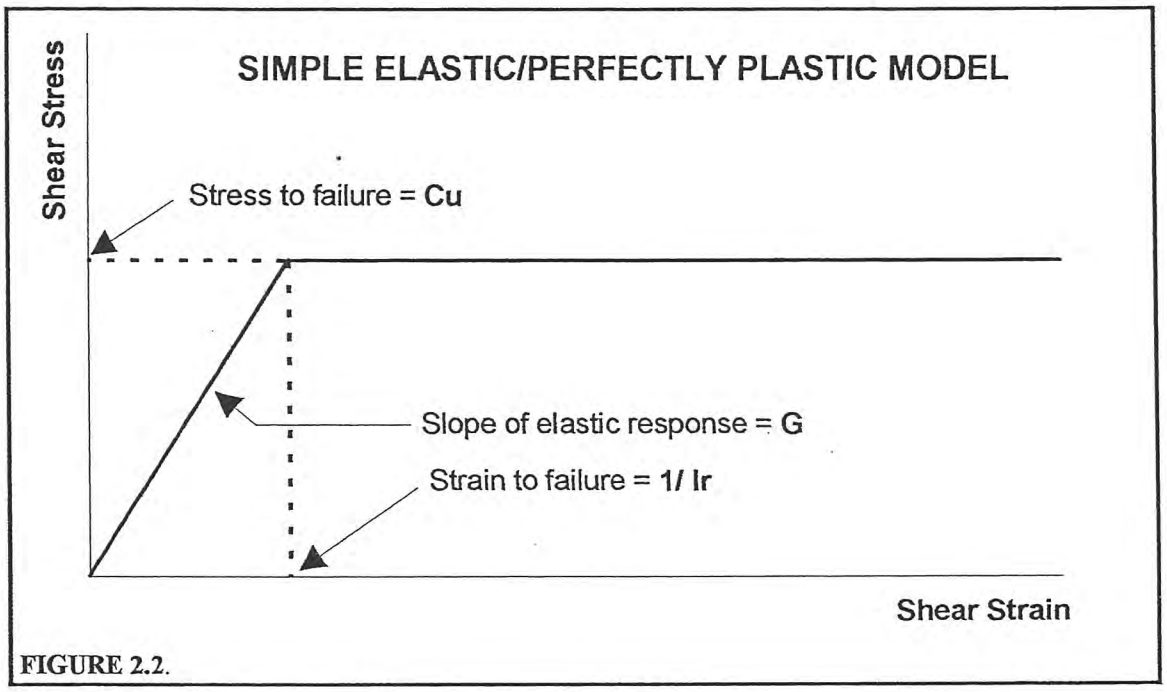

FIGURE 2.2.

For pressures exceeding the yield stress of the soil, the simple elastic/perfectly plastic solution is usually expressed in terms similar to the following:

$$p_c - \sigma_{ho} = c_u\{1+Ln[(G/c_u)(\Delta V/V)]\} \quad \text{... [Equ. 2.4]}$$

Strictly, equation 2.4 is a simplified version of the Gibson & Anderson solution developed by Windle & Wroth (1977).

Equation [2.4] can also be written:

$$p_c - \sigma_{ho} = c_u[1-Ln(c_u/G)+Ln(\Delta V/V)] \quad \text{... [Equ.2.5]}$$

From this it is clear that the change from simple elastic to perfectly plastic response occurs at a shear strain c_u /G at which point the log terms in equation [2.5] cancel and
$p_c - \sigma_{HO}$ equals the undrained shear strength c_u.

The limiting pressure p_{Limit} at which indefinite expansion of the borehole occurs is given by

$$p_{Limit} - \sigma_{ho} = c_u[1-Ln(c_u/G)] \quad \text{... [Equ. 2.6]}$$

Equations [2.4] and [2.6] can be combined to give the result

$$p_c = p_{Limit} + c_u\, Ln[\Delta V/V] \quad \text{... [Equ. 2.7]}$$

This is a particularly convenient form of the solution with the undrained shear strength and limit pressure being the gradient and intercept respectively of a plot of total pressure against the natural log of the shear strain at the cavity wall.

The analysis assumes constant shear strength, so the slope chosen should be that which best fits this assumption. There is no theoretical justification for selecting a slope at a specific strain and claiming this to be c_u. If the plot indicates that the gradient of the plastic phase is not more or less constant then the assumptions underpinning the analysis have been violated, and other strategies must be adopted.

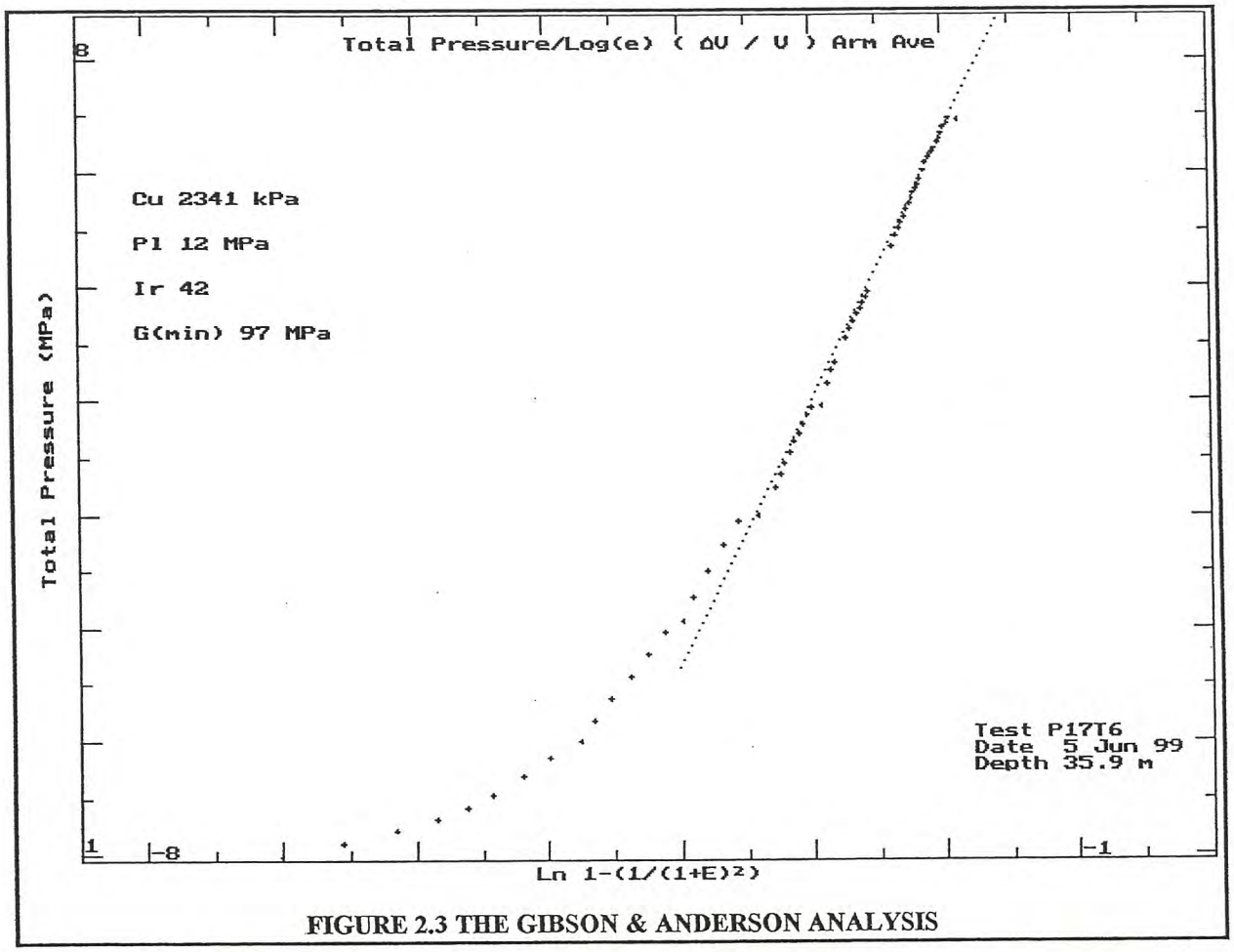

FIGURE 2.3 THE GIBSON & ANDERSON ANALYSIS

Equation [2.6] shows that if p_{Limit}, p_0, and c_u are known then the rigidity index I_r and the shear modulus at yield strain G_{min} can be determined without going outside the analysis for additional data. This has been done for the example plotted in Figure 2.3. In this example the rigidity index and the modulus value seem plausible, suggesting that the origin for strain is about right and that the material response is approximately linear elastic. The slope of the semi-log plot is relatively insensitive to the choice of the initial conditions so that the value for shear strength is better conditioned than that for all other parameters.

2.3.2 Palmer

The Palmer analysis (1972) shows that more information can be obtained from the pressuremeter test if fewer assumptions are made. The analysis shows that the pressure:strain graph is the integrated shear stress:shear strain curve. Taking the slope of the pressure:strain graph at any point gives the mobilised shear stress directly, and allows the complete shear stress:strain curve to be plotted. In terms of cavity strain the shear stress τ is:

$$\tau = \tfrac{1}{2}\varepsilon_c(1+\varepsilon_c)(2+\varepsilon_c)dP/d\varepsilon_c \qquad \text{.....[Equ. 2.8]}$$

More conveniently, perhaps, equation [2.8] can also be written in terms of shear strain as:

$$\tau = dP/d[\ln(\Delta V/V)] \qquad \text{.....[Equ. 2.9]}$$

This implies that the gradient at any strain of the semilog plot used for the Gibson & Anderson analysis gives the mobilised shear stress directly. The example below is the same test as Figure 2.3:

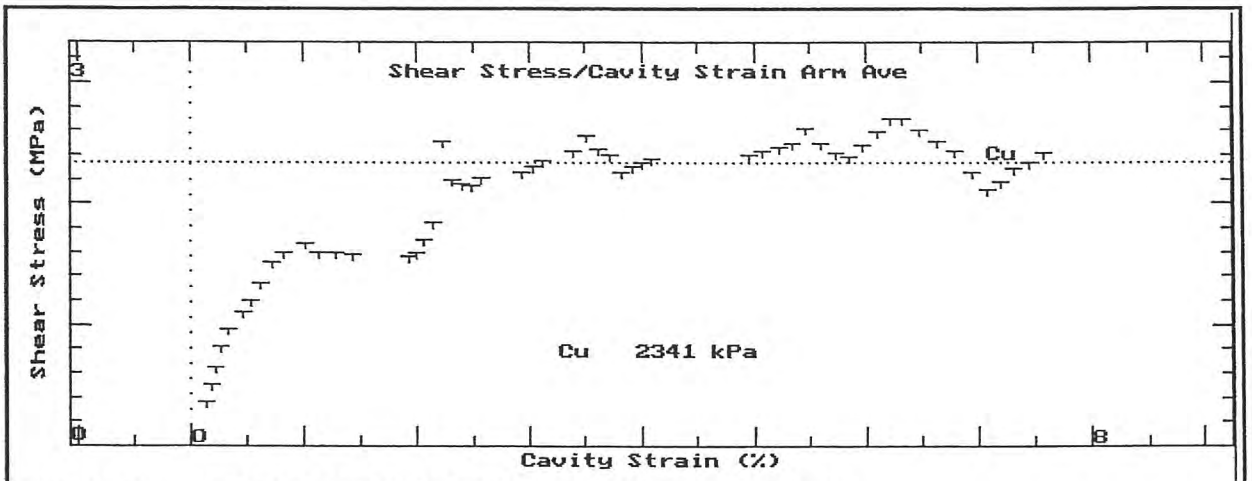

FIGURE 2.4 ` AN EXAMPLE OF THE PALMER (1972) ANALYSIS

The analysis is awkward to implement on the computer because the differentiation process highlights any irregularities in the data. This is especially irritating because the stress strain response must be a smooth curve. Possible strategies involve curve fitting the measured data prior to applying the solution, but this may be a mistake. Minor changes of gradient on the loading path are usually not random, but a response to some event such as the taking of an unload/reload cycle.

If the material does indeed deform in the manner required by Gibson & Anderson then the two analyses give identical answers. Included on the plot is a horizontal ruler marking the value of shear strength obtained from applying the previous Gibson & Anderson analysis. If there are clear indications of peak and residual shear strength then additional horizontal rulers are available to mark these values. However the true value of the plot is that it is a 'map' of the shear stress, and it is the form of the complete curve which is of interest.

The analysis is very sensitive to insertion disturbance - in particular insufficient allowance for stress relief will give an apparent peak in the stress/strain response. Figure 2.5 is an example.
A high peak followed by a fall to a much lower value may be real, but it may indicate the effects of disturbance. It is likely that the initial expansion is not occurring at constant volume, and as a consequence the analysis fails. The residual value of about 1900kPa may be a better choice, and there are indications here that if the expansion is taken far enough the effects of disturbance can be overcome. Note that it may take a substantial expansion for this to be achieved.

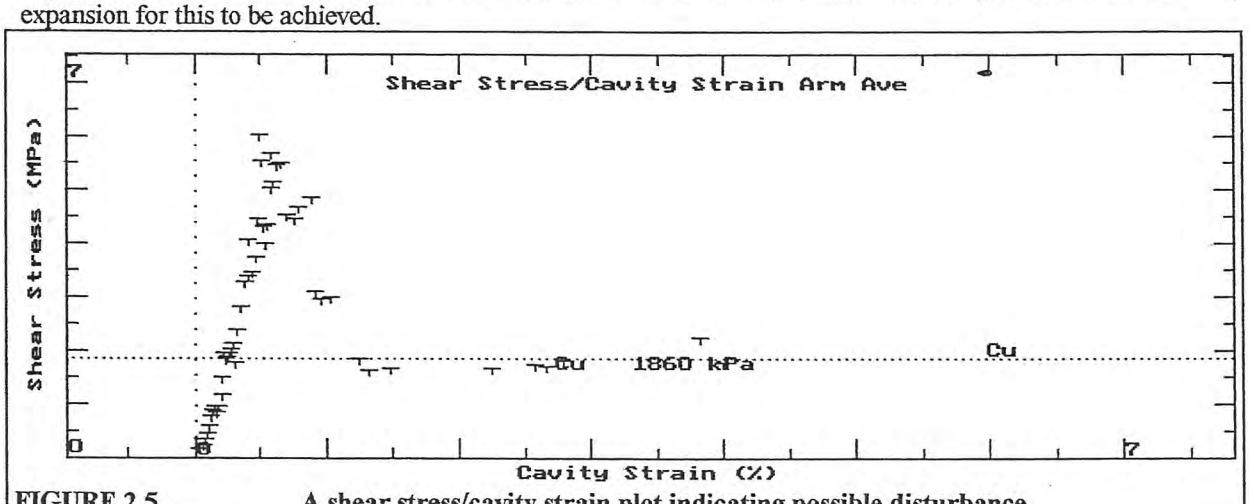

FIGURE 2.5 A shear stress/cavity strain plot indicating possible disturbance

2.4 Shear stress of sands

There are two significant analyses available for describing the shear stress/shear strain behaviour of sand:

- **Hughes et al (1977)**
- **Manassero (1989)**

2.4.1 Hughes et al (1977)

In addition to the usual conditions governing the expansion of a cylindrical cavity in plane strain this analysis assumes the following:

- A simple elastic/perfectly plastic model
- The expansion is fully drained, i.e. no pore water pressures are allowed to develop
- Following yield the sand deforms at a constant angle of internal friction
- Volumetric and shear strains are connected by Rowe's dilatancy law (1962)

Rowe's dilatancy law can be expressed as:

$$[1 + \sin \phi'/1 - \sin \phi'] = [1 + \sin \phi'_{cv}/1 - \sin \phi'_{cv}][\, 1 + \sin \Psi/1 - \sin \Psi] \quad .....[11]$$

where ϕ' is the peak angle of internal friction
ϕ'_{cv} is the critical state angle of friction
Ψ is the angle of dilation.

At failure the effective pressure p′ is :

$$p' = \sigma'_{ho}(1 + \sin \phi') \quad .....[12]$$

following failure:

$$\ln [p'] = S\ln[(\varepsilon_c/(1+\varepsilon_c) + c/2)] + A \quad .....[13]$$

where A is a constant
S is $[(1 + \sin \Psi) \sin \phi']/(1 + \sin \phi')$
c is a small elastic strain that has been shown (Hughes et al, appendix) to be negligible.

Equation [13] indicates that s is approximately the gradient of effective pressure plotted against cavity strain on log scales. Once obtained, both sin ϕ' and sin Ψ can be derived:

$$\sin \phi' = S/[1 + (S - 1) \sin \phi'_{cv}] \quad .....[14]$$

$$\sin \Psi = S + (S - 1) \sin \phi'_{cv} \quad .....[15]$$

The factor c/2 is usually ignored - it has been shown to introduce an error of about 0.03% in the strain scale for a typical dense sand, a negligible amount.

Withers et al (1989) shows that the same argument leads to a complete expression for the loading path, as follows:

$$p' = [2\sigma'_{ho}/(1+N)][(G/\sigma'_{ho})(1+n)[(1+N)/(1-N)]\, \varepsilon_c + (1-n)/2]^{[1-N/1+n]} \quad .....[16]$$

where n is $(1 - \sin \Psi)/(1 + \sin \Psi)$
N is $(1 - \sin \phi')/(1 + \sin \phi')$ and is the ratio of the minor to major principal effective stresses at failure.

Note that the power term [1-N]/[1+n] is the gradient of the log-log plot.

An example of the Hughes analysis is shown in figure 8. Note that both the ambient pore water pressure u_o and ϕ'_{cv} are required to implement the analysis. Because the expansion is drained the membrane normally collapses at the head of water pressure, and an estimate of u_o can often be made from this behaviour. ϕ'_{cv} must either be given or estimated.

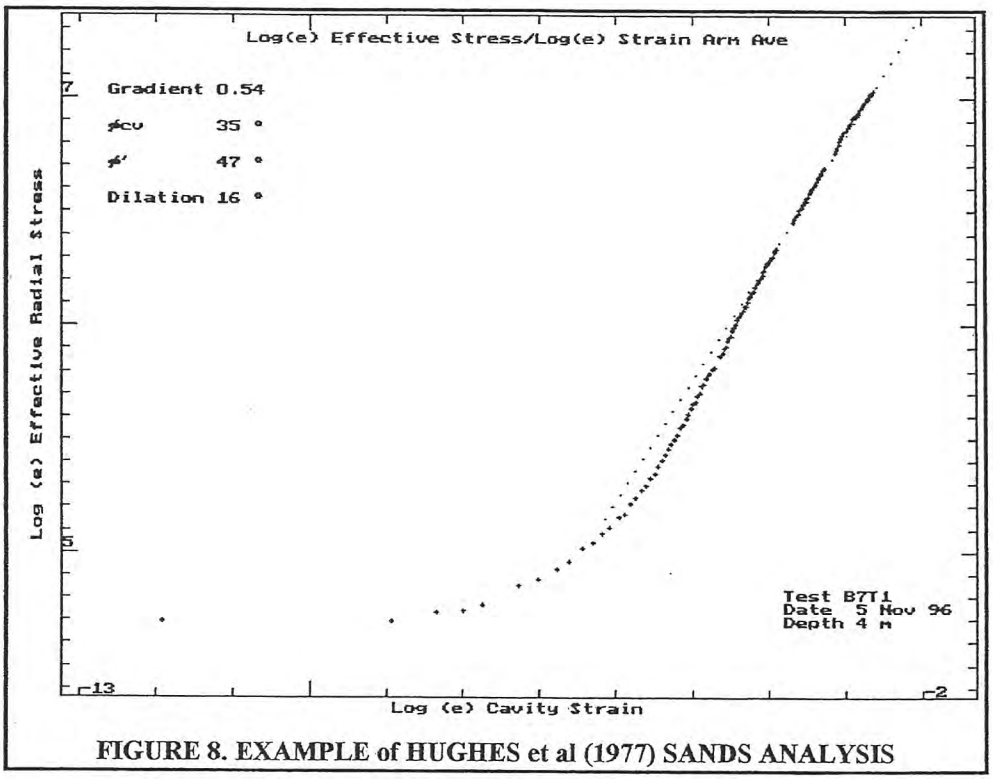

FIGURE 8. EXAMPLE of HUGHES et al (1977) SANDS ANALYSIS

Deciding on the strain origin for a test in sand is a problem. It is rarely the case that membrane lift-off gives a plausible value for σ_{ho} so a value has to be inferred. Despite the theoretical inappropriateness , the modified Marsland & Randolph method is often used to give an estimate. Because the material is only just plastic at the point where the failure shear stress is derived, the error is likely to be small.

Hughes et al assume a single value for the peak angle of internal friction throughout a typical SBP test, but this is often not the case. We have found that in dense sands the pressuremeter test often expands sufficiently to indicate a plateau in the shear stress, suggesting that the sand is approaching critical state.

2.4.2 Manassero (1989)

This analysis is a numerical procedure that essentially makes the same assumptions as that of Hughes et al (1977). The difference is that Rowe's dilatancy relationship is employed as a flow rule, so that the requirement for deformation at a single value of friction angle is not necessary.

The great advantage of this analysis is that it can produce a comprehensive stress/strain curve analogous to that of the Palmer (1972) analysis for an undrained expansion. The disadvantage is that the numerical method is very sensitive to minor fluctuations in the measured data. Manassero suggests that the measured data be fitted with a polynomial function prior to implementing the numerical calculations. However a polynomial curve is wrong in concept and better results can be obtained by employing a hyperbolic function.

The data here was much too noisy to attempt this method, with 'End of Creep' points too few and too widely spaced.

3 Shear Modulus

There are four parts of the pressuremeter curve capable of providing information concerning shear modulus:

- From the slope of the initial elastic loading phase
- From the slope of the chord bisecting small rebound cycles
- From the analysis for shear strength
- From the slope of the first part of the contraction curve

Whatever method is used to determine shear modulus, the value obtained is strain dependent.

3.1 The Initial Shear Modulus

Shear modulus derived from the slope of the initial part of the loading curve is quoted as part of the Marsland & Randolph analysis (see figure 2.1). In a pre-bored pressuremeter test, unless the probe is in good rock, this invariably underestimates the true elastic properties of the material because the initial part of the test is affected by the process of making a pocket.

As figure 1.1 shows, the calculation for shear modulus G is:

$$G = dP/2d\varepsilon_c \qquad .....[3.1]$$

Strictly, because the cavity strain ε_c is *simple* strain it is only the initial modulus for which this calculation is true. Once the expansion is underway modified calculations should be used that take account of the change in the reference condition.

3.2 Cycles of elastic unloading and reloading

Graphical plots of the reload loops are the preferred method of obtaining a value for shear modulus. The plots provided show the position of a cursor which has been placed by eye to bisect the loop. The slope of the cursor is the gradient of the reload loop and the program uses this slope to derive a value for shear modulus. This value is quoted in the top left hand corner of the plot together with an indication of the size of the loop expressed as the change of pressure and strain, and the co-ordinate of the centre of the loop. The equation used is:

$$G = [1+\varepsilon_c][dP/2d\varepsilon_c] \qquad .....[3.2]$$

In addition, the program carries out a regression analysis of the data points that are part of the reload loop. If the loop is good, that is symmetrical and without indications of scatter, then the two values of modulus obtained will be the same. However the regression analysis is sensitive to erroneous data points, which the visual technique can ignore. The value obtained by regression is quoted in the bottom right hand corner of the plot.

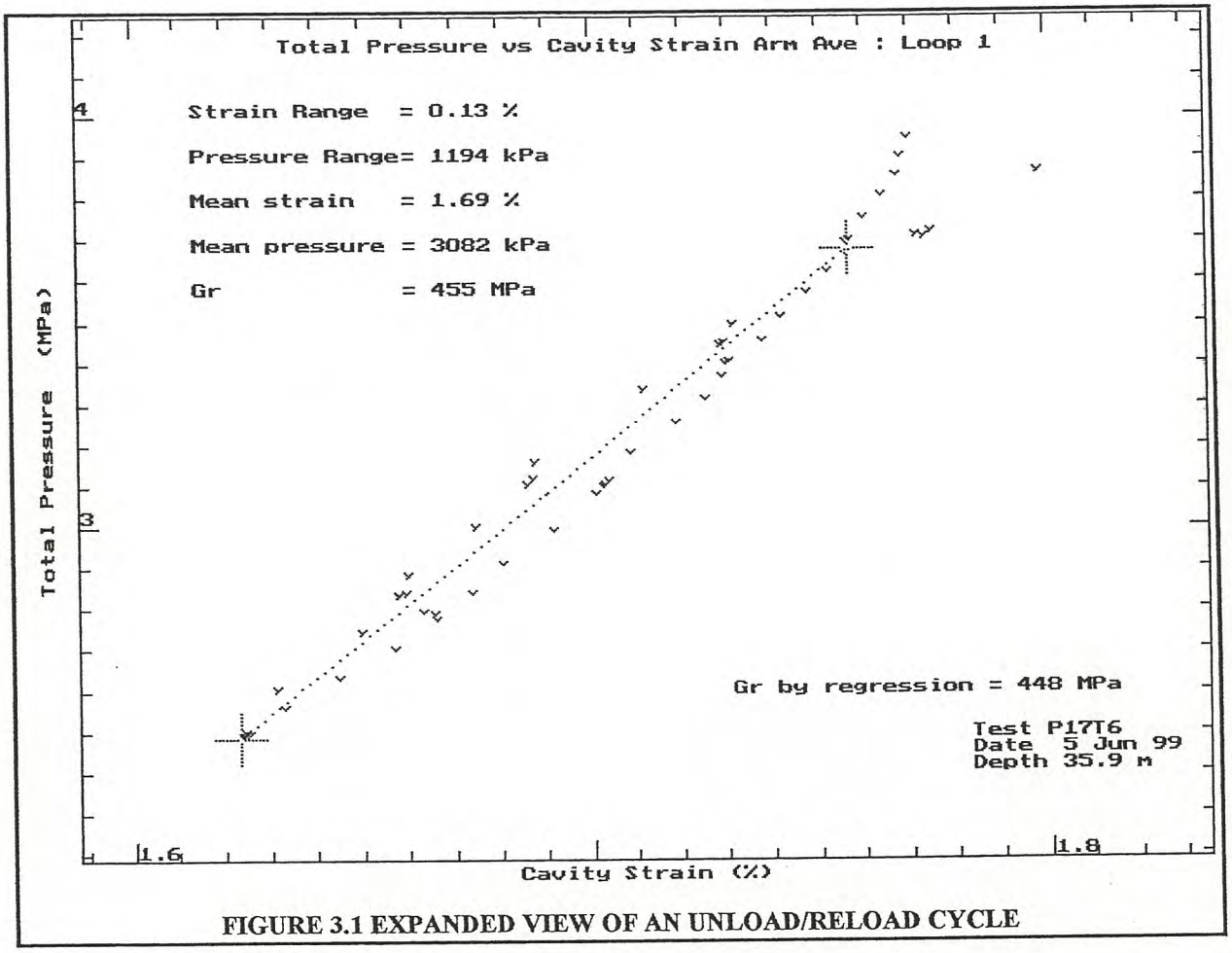

FIGURE 3.1 EXPANDED VIEW OF AN UNLOAD/RELOAD CYCLE

It is important that the effects of creep (for whatever cause) be minimised before starting the cycle, and in Figure 3.1 'deleted' points before the start of the unloading show where the pressure in the probe was held for a period of time.

3.3 Non-linear stiffness/strain response

In recent times it has become widely acknowledged that the stiffness/strain relationship is not linear. The unload/reload cycle can be made to give a comprehensive description of this non-linear relationship by looking at smaller steps of pressure/strain other than the points at the extreme ends of the cycle.

For reasons explained in Whittle et al (1992) it is preferable to examine one half of the rebound cycle only, that following the reversal of stress in a loop. The lowest recorded value of stress and strain then becomes the origin for subsequent data points until the original loading path is rejoined.

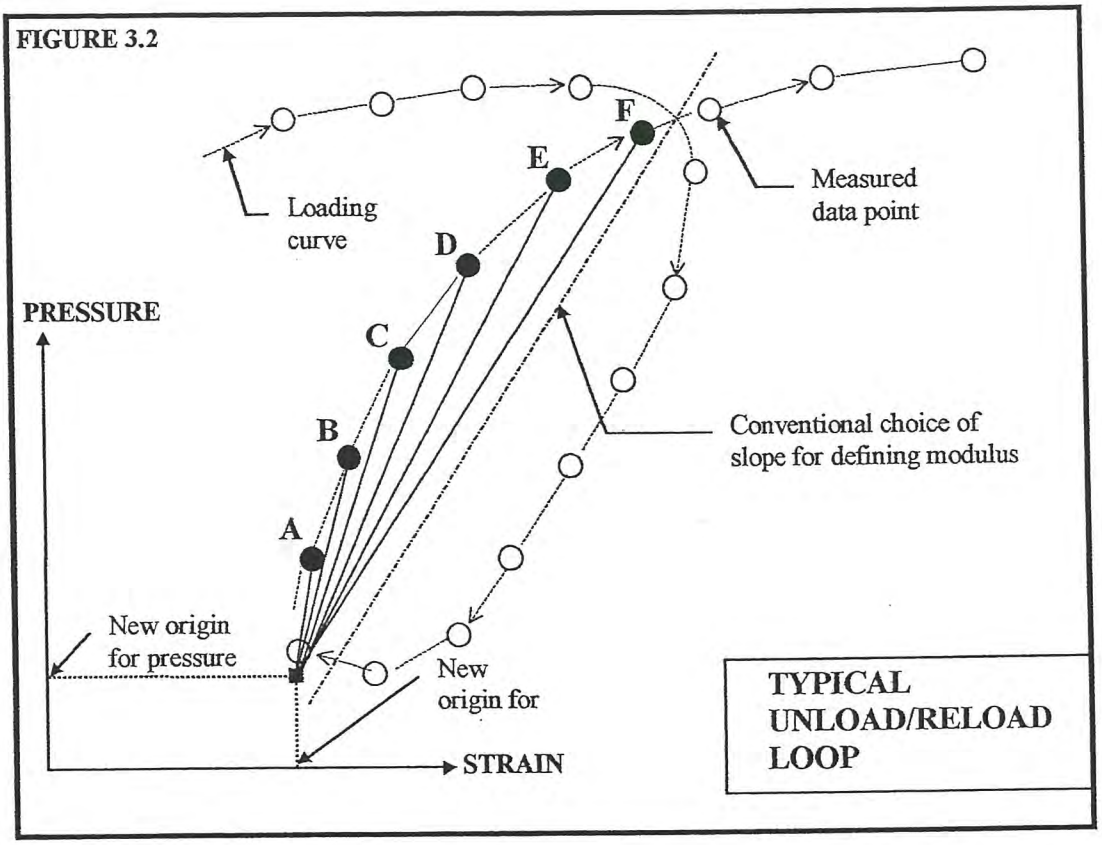

The reloading data can be plotted on axes of log Δp_c versus log $\Delta V/V$. Figure 3.3 is an example, using the same data as that in figure 3.2. The gradient of the best fit straight line to the data points gives the non-linear elastic exponent, where 1 is a linear elastic response.

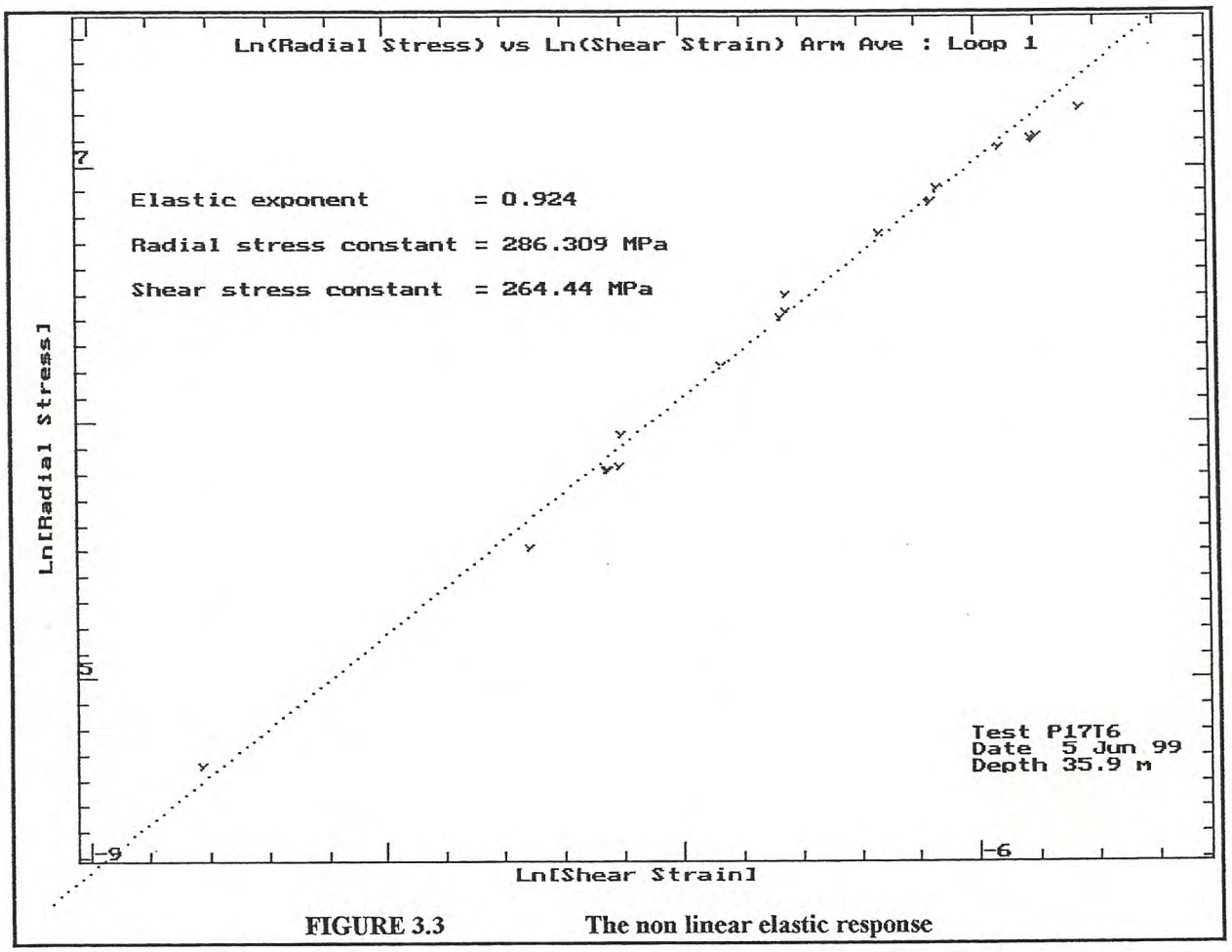

FIGURE 3.3 The non linear elastic response

The linear relationship between pressure and shear strain on log scales expands to a power law of the form

$$p_c = \eta\gamma^{\beta} \quad \text{... [3.3]}$$

where p_c is the change in radial stress at the cavity wall, γ is the corresponding shear strain and η and β are the intercept and gradient of the log log relationship.

Palmer (1972) shows for undrained plane strain loading the shear stress at any point on the pressure versus strain plot is given by

$$\tau = \gamma \frac{dP}{d\gamma} \quad \text{... [3.4]}$$

Substituting [3.3] into [3.4] gives

$$\tau = \gamma \frac{d(\eta\gamma^{\beta})}{d\gamma} \quad \text{... [3.5]}$$

The differential equation can now be solved

$$\tau = \gamma\left(\eta\beta\gamma^{\beta-1}\right) = \eta\beta\gamma^{\beta} \quad \text{... [3.6]}$$

Hence the shear stress is related to the radial stress measured at the cavity wall by

$$\tau = \beta p_c \quad \text{... [3.7]}$$

It is convenient at this point to replace the combined coefficient $\eta\beta$ in [3.6] with a single term α, where

$$\alpha = .\eta\beta \quad \text{... [3.8]}$$

Note that [3.8] can be turned into a general expression for secant shear modulus G_s by dividing both sides by the shear strain γ:

$$G_s = \eta\beta\gamma^{\beta-1} = \alpha\gamma^{\beta-1} \quad \text{... [3.9]}$$

and because the tangential modulus G_t is related to the secant modulus by the following relationship (Muir Wood 1990, Jardine 1992)

$$G_t = G_s + \gamma\left[\frac{dG_s}{d\gamma}\right] \quad \text{... [3.10]}$$

it follows from [3.9] that the solution to [3.10] is

$$G_t = \eta\beta^2\gamma^{\beta-1} = \alpha\beta\gamma^{\beta-1} \quad \text{... [3.11]}$$

Figure 3.3 shows an almost linear elastic response and for most tests in rock this is typical. Where the material is friable and behaves almost like a soil a more marked non-linear elastic response is apparent. Often loops carried out later in the loading when the applied stress is higher show the influence of grain crushing, revealed as a tendency for the exponent to become more non-linear. If the test is drained, meaning the mean effective stress increases throughout the loading, then successive loops will have a higher intercept.

Our practice is to give the exponent and intercept of the power law, and for comparative purposes to quote secant shear modulus parameters at three levels of plane shear strain, 10^{-2}, 10^{-3} and 10^{-4}. It is unwise to use the power law to predict modulus for strains smaller than 10^{-4}.

APPENDIX E SAMPLE CALCULATION OF A LINE OF DATA

What is described in some detail in this appendix is the steps necessary to convert the raw data output from the pressuremeter into engineering units.

In order to convert pressuremeter signals into calibrated data the following steps are taken:

A. The raw data is in units of volts, and needs to be corrected for zero offsets and scaled using the sensitivities quoted in the calibration data.

The calibrations for this particular test are presented as follows:-

INSTRUMENT CALIBRATIONS: P17T8 DEPTH: 43.90M DATE: 7 June 99

	ZERO		SLOPE	CORRECTION & COMPRESSION			
ARM 1	-2092.0mV	&	120.3 mV/mm	39.3kPa	&	12.1 kPa/mm	2.8 mm/GPa
ARM 2	-1992.5mV	&	120.0 mV/mm	39.3kPa	&	12.1 kPa/mm	2.8 mm/GPa
ARM 3	-1871.3mV	&	121.1 mV/mm	39.3kPa	&	12.1 kPa/mm	2.8 mm/GPa
ARM 4	-1808.8mV	&	120.5 mV/mm	39.3kPa	&	12.1 kPa/mm	2.8 mm/GPa
ARM 5	-1901.2mV	&	119.1 mV/mm	39.3kPa	&	12.1 kPa/mm	2.8 mm/GPa
ARM 6	-2058.9mV	&	120.2 mV/mm	39.3kPa	&	12.1 kPa/mm	2.8 mm/GPa
TPC A	-86.9mV	&	78.9 mV/MPa				
TPC B	-248.7mV	&	81.2 mV/MPa				

The line of raw data reads from left to right as follows. The units are volts:-

LINE	TPC A	ARM 1	ARM 2	ARM 3	ARM 4	ARM 5	ARM 6	TPC B	SIN	COS
357	0.6318	-0.9812	-1.0121	-1.4411	-1.3693	-1.4375	-1.4876	0.4929	-1.4189	1.8298

The first operation is to deduct the zero offsets. These are the figures found in the first column of the calibration information, but quoted here in volts. The columns for Sin and Cos disappear at this stage, as they are not transferred to the calibrated data file:

	TPC A	ARM 1	ARM 2	ARM 3	ARM 4	ARM 5	ARM 6	TPC B	
Output	0.6318	-0.9812	-1.0121	-1.4411	-1.3693	-1.4375	-1.4876	0.4929	
Zero	-0.0869	-2.0920	-1.9925	-1.8713	-1.8088	-1.9012	-2.0589	-0.2487	
Result	0.7187	1.1108	0.9804	0.4302	0.4395	0.4637	0.5713	0.7416	.....[1]

This result [1] can now be scaled. The information for this is found in the second column of calibration data, and is expressed as millivolts per millimetre to calculate displacement, and as millivolts per megaPascal to calculate pressure. As before, the results of the calculations are quoted in volts:

	TPC A	ARM 1	ARM 2	ARM 3	ARM 4	ARM 5	ARM 6	TPC B	
From [1]	0.7187	1.1108	0.9804	0.4302	0.4395	0.4637	0.5713	0.7416	
Slope	0.0789	0.1203	0.1200	0.1211	0.1205	0.1191	0.1202	0.0812	
Result	9.1090	9.2336	8.1700	3.5524	3.6473	3.8934	4.7529	9.1330	....[2]
	(MPa)	(mm)	(mm)	(mm)	(mm)	(mm)	(mm)	(MPa)	

At this point in the procedure, a choice has to be made about which total pressure cell or combination of cells to use in producing the calibrated data. The difference between the cells is because cell A is read at the beginning of a data scan and cell B at the end. The time taken to make the scan allows some pressure change to occur in the probe. In this example the average of cells A and B are used: (9.1090 + 9.133)/2 = 9.1210MPa.

B. The data is now in engineering units which reflect what is taking place inside the membrane. The remaining corrections are introduced to give a better representation of what is taking place at the point where the membrane bears on the borehole wall.

The displacement data is adjusted for the instrument displacements due to the pressure being applied to it. This is expressed as a linear movement in millimetres per GigaPascal of pressure being applied, and is found in the 5th column of the calibration details:

	ARM 1	ARM 2	ARM 3	ARM 4	ARM 5	ARM 6	
Correction Factor (mm/GPa)	2.8	2.8	2.8	2.8	2.8	2.8	column 5
Internal Pressure (MPa)	9.1210	9.1210	9.1210	9.1210	9.1210	9.1210	
Adjustment ((5)*[2])/1000	0.0255	0.0255	0.0255	0.0255	0.0255	0.0255	.....[3]
Internal Displacement (mm)	9.2336	8.1700	3.5524	3.6473	3.8934	4.7529	..... [2]
Corrected Displacement (mm)	9.2081	8.1445	3.5269	3.6218	3.8679	4.7274	.....[4]

C. The displacement data calculated so far is the movement measured by the arms to the inside of the membrane. The figures quoted in the calibrated data listings are the movement of the outside of the protective sheath. This is derived from the internal movement by assuming that the cross-section area of the membrane is a constant. A full explanation of this and the derivation of the equation used is discussed in the appendix on calibration technique.

The equation is $$E = \sqrt{[(R-t)^2 + D(2r+D)]} - (R-t)$$ ..... [a]

where
- E is the actual expansion of the pressuremeter
- 2R is the O.D of the pressuremeter at rest
- 2r is the I.D of the membrane at rest
- D is the movement measured by the strain arm
- t is the thickness of the Chinese lantern steel

For the pressuremeter used to produce this example:-

2R = 95.0 mm
2r = 82.0 mm
t = 0.53 mm

Because the membrane can be assumed to have the same thickness at all points on the cross-section the technique employed is to calculate a scale factor from the average displacement.

	ARM 1	ARM 2	ARM 3	ARM 4	ARM 5	ARM 6	
Corrected Displacements	9.2081	8.1445	3.5269	3.6218	3.8679	4.7274	...[4]
Average Displacement	5.5161	5.5161	5.5161	5.5161	5.5161	5.5161	.....[5]
Result of equation [a] using D = [5]	4.8849	4.8849	4.8849	4.8849	4.8849	4.8849	.....[6]
Scale Factor [6]/[5]	0.8856	0.8856	0.8856	0.8856	0.8856	0.8856	.....[7]
Apply [7] to [4]	8.1547	7.2128	3.1234	3.2075	3.4254	4.1866	.....[8]

D. The result, using displacements from [8] and the average total pressure quoted in kPa:

LINE	ARM 1	ARM 2	ARM 3	ARM 4	ARM 5	ARM 6	TPC	
357	8.1547	7.2128	3.1234	3.2075	3.4254	4.1866	9121.0	.....[9]

In practice the errors introduced by rounding-off calculations may result in small differences in the final figure. This is the line of data seen in the calibrated data file that is passed from the logging program to the analysis program.

E. However the conversion to data ready for analysis is not yet complete. The column for pressure is the pressure *inside* the membrane. What is required is the pressure on the *outside* of the membrane where it bears against the borehole wall. Before using the calibrated data file, therefore, the analysis program corrects the pressure data for the influence of the membrane, using the data in the calibrations for membrane correction. It is separately calculated for each arm position, although in practice an average correction value tends to be used. The correction figure is the sum of the zero figure (column 3 in the calibrations) plus the increased stiffness with strain (column 4):-

	ARM 1	ARM 2	ARM 3	ARM 4	ARM 5	ARM 6	
From Result [8]	8.1547	7.2128	3.1234	3.2075	3.4254	4.1866	
Average Displacement	4.8851	4.8851	4.8851	4.8851	4.8851	4.8851	..... [10]
kPa/mm (column 4)	12.1	12.1	12.1	12.1	12.1	12.1	..... [11]
Result [10]*[11] (kPa)	59.1	59.1	59.1	59.1	59.1	59.1	..... [12]
Correction zero (kPa)	39.3	39.3	39.3	39.3	39.3	39.3	(column 3)
Add zeroes to result [12]	98.4	98.4	98.4	98.4	98.4	98.4	..... [13]

This is the total membrane correction at each arm position and is now deducted from the total pressure cell readings. In this example because an average membrane correction has been used, the calculation is 9121.0kPa – 98.4kPa giving 9022.6kPa.

When the calibrated data is taken from the Analysis program the format differs from the PRN file produced by the logging program (see D, above). The analysis output gives the average radial displacement of opposing pairs of arms, together with a column of corrected pressure readings for each arm pair, and the uncorrected pressure:

LINE	Arms(1+4)/2	Arms (2+5)/2	Arms (3+6)/2	TPC 1	TPC 2	TPC 3	TPC
357	5.6811	5.3191	3.6550	9022.6	9022.6	9022.6	9121.0

APPENDIX F REFERENCES

ARNOLD, M. (1981)
An Empirical Evaluation of Pressuremeter Test Data, Civil Engineering Department, University of Adelaide, South Australia.

BAGUELIN, F., JEZEQUEL, J.F. and SHIELDS, D.H. (1978)
The Pressuremeter and Foundation Engineering, Transtech Publications, Clausthal, Germany ISBN O-87849-019-1

BELLOTTI, R., GHIONNA, V., JAMIOLKOWSKI, M., ROBERTSON, P. and PETERSON, R. (1989).
"Interpretation of moduli from self-boring pressuremeter tests in sand". *Géotechnique* Vol.XXXIX, no.2, pp.269-292.

BENOIT, J.(1983).
"Analysis of Self-Boring Pressuremeter Tests in Soft Clay", A dissertation submitted to the Department of Civil Engineering and the Committee on Graduate Studies of Stanford University in Partial Fulfilment of the Requirements of the Degree of Doctor of Philosophy.

BENOIT, J. and CLOUGH, G.W. (1985).
"Principal Stresses Derived from the Self-Boring Pressuremeter Tests in Soft Clays", The Pressuremeter and its Marine Applications, 2nd International Symposium.

BOLTON M.D. and WHITTLE R.W. (1999)
"A non-linear elastic/perfectly plastic analysis for plane strain undrained expansion tests." Géotechnique Vol. **49**, No.1, pp 133-141.

BRUZZI, D., GHIONNA, V., JAMIOLKOWSKI, M., LANCELLOTTA, R., & MANFREDINI G (1986).
"Self-Boring Pressuremeter in Po River Sand", 2nd International Symposium on The Pressuremeter and its Marine Applications.

CLARKE, B.G., CARTER, J.P. and WROTH, C.P. (1979).
"In Situ Determination of Consolidation Characteristics of Saturated Clays". Design Parameters in Geotechnical Engineering, VII ECSMFE, Brighton, Vol. 2, , pp 207- 211

CLARKE, B.G. (1981).
"In Situ Testing of Clay Using Cambridge Self-Boring Pressuremeter"
PhD Thesis, Cambridge University.

CLARKE, B.G and WROTH, C.P. (1984)
Analysis of Dunton Green retaining wall based on results of pressuremeter tests. *Géotechnique* **34**, No. 4, pp 549-561.

CLOUGH, G.W., and DENBY, G.M. (1980)
Self-boring Pressuremeter study of the San Francisco Bay Mud, J. Geotech Eng. Divn. ASCE V 106, No. GT1 pp 45-63

DALTON, J.C.P., HAWKINS, P.G.(1982)
Fields of Stress, some measurements of the in-situ stress in a meadow in the Cambridgeshire countryside. *Ground Engineering* Vol. 15, No. 4 pp 12 -23.

DENBY, G.M. and CLOUGH, G.W. (1980)
Self-boring Pressuremeter Tests in Clay. J. Geotech Eng. Divn. ASCE V 106 No. GT12 pp 1369-1387.

DENBY, G.M. (1978)
Self Boring Pressuremeter Study of the San Francisco Bay Mud. PhD Thesis, Department of Civil Engineering, Stanford University Technical Report, CE232

DENBY,G.M., COSTA,C.A., CLOUGH,G.W. and DAVIDSON,R.R. (1981)
"Laboratory and Pressuremeter Tests in Stiff Clay". Proceedings of the Tenth International Conference on Soil Mechanics and Foundation Engineering, Stockholm, Sweden.

DENBY, G.M. and HUGHES, J.M.O. (1982)
Horizontal stress interpretation of pressuremeter tests. Proc. ASCE Conf. on Updating Subsurface Sampling of Soils and Rocks and their In-Situ Testing, Santa Barbara, California.

ERVIN, M.C., BURMAN, B.C. and HUGHES, J.M.O.(1980).
The use of a high capacity pressuremeter for design of foundations in medium strength rock. International Conference on Structural Foundations on Rock, Sydney.

FAHEY, M. (1980)
A Study of the Pressuremeter Test in Dense Sand. PhD Thesis University of Cambridge.

FAHEY, M. and JEWELL, R.J. (1990)
Effect of Pressuremeter Compliance on Measurement of Shear Modulus. Paper submitted to The Third International Symposium on Pressuremeters, Oxford University 2 - 6 April 1990

FAHEY, M., and RANDOLPH, M.F. (1984)
Effect of disturbance on parameters derived from Self- boring Pressuremeter tests in sand. *Géotechnique* **34**, No. 1, pp 81-97

GHIONNA, V., JAMIOLKOWSKI, M., LACASSE, S., LADD, C.C., LANCELLOTTA, R. and LUNNE, T (1983).
Evaluation of Self-Boring Pressuremeter. Symposium International Vol. 2 Paris.

GHIONNA, V., JAMIOLKOWSKI, M., and LANCELLOTTA, R.(1982)
Characteristics of Saturated Clays as Obtained from SBP Tests. Proc. Int. Symp. Pressuremeter and its Marine Appls., Paris, pp 165-186.

GHIONNA, V., JAMIOLKOWSKI, M., LANCELLOTTA, R., TORDELLA, M.L. and LADD, C.C. (1981)
Performance of Self-Boring Pressuremeter tests in cohesive deposits. Dept of Civil Engineering, MIT, Report FHWA/RD- 81/173.

GHIONNA, V., JAMIOLKOWSKI, M., LANCELLOTTA, R. & MANASSERO, M (1989).
Limit Pressure of Pressuremeter Tests. Proc. of 12th ICSMFE, Rio De Janeiro.

GIBSON, R.E. and ANDERSON, W.F. (1961)
In situ measurement of soil properties with the pressuremeter, Civil Engineering and Public Works Review, Vol. 56, No. 658 May pp 615-618 .

HAWKINS, P.G., MAIR, R.J., MATHIESON, W.G. and MUIR WOOD, D. (1990)
Pressuremeter measurement of total horizontal stress in stiff clay, Proc. ISP.3 Oxford.

HOULSBY, G., CLARKE, B. and WROTH, C.P. (1986).
"Analysis of the unloading of a pressuremeter in sand". Proc. of the 2nd International Symposium on The Pressuremeter and its Marine Applications pp 245-262.

HUGHES, J.M.O. (1973).
An instrument for in situ measurement in soft clays, PhD Thesis, University of Cambridge

HUGHES,J.M.O., ERVIN, M.C. (1980)
Development of a High Pressure Pressuremeter for determining the engineering properties of soft to medium strength rocks.Proc. 3rd Aus.-NZ Conf. Geomechanics, Brisbane, pp.292-296.

HUGHES, J.M.O., WROTH, C.P. and PENDER, M.J. (1975).
A comparison of the results of special pressuremeter tests with conventional tests on a deposit of soft clay at Canvey Island, Internal Report No. CUED/C - SOILS TR 20, Cambridge University Engineering Department.

HUGHES, J.M.O., WROTH, C.P. and WINDLE, D. (1977)
Pressuremeter tests in sands, *Géotechnique* **4**, pp 455-477

JARDINE, R.J. (1991)
Discussing 'Strain-dependent moduli and pressuremeter tests' . *Géotechnique* **41**, No. 4., pp 621-624

JARDINE, R.J. (1992)
Nonlinear stiffness parameters from undrained pressuremeter tests. *Can. Geotech.* **29**, pp 436-447

JARDINE, R.J., POTTS, D.M., FOURIE, A.B. and BURLAND, J.B. (1986)
Studies of the influence of non-linear stress strain characteristics in soil structure interaction. *Géotechnique* **36**, No. 3, pp 377-396.

JEFFERIES, M.G. (1988)
Determination of horizontal geostatic stress in clay with self-bored pressuremeter. *Can. Geotech.* **25** (3), pp 559-573

JEWELL, R.J., FAHEY, M. and WROTH, C.P. (1980)
Laboratory Studies of the Pressuremeter Test in Sand. *Géotechnique* **30**, No. 4 pp 507-531

LACASSE, S. and LUNNE, T. (1982)
In Situ Horizontal Stress from Pressuremeter Tests". Proc. of the Symp. on the Pressuremeter and its Marine Applications, Paris.

LADANYI, B. (1973)
"Expansion of a Cavity in a Saturated Clay Medium". Journal of the Soil Mechanics and Foundation Engineering Division, ASCE, Vol. 89, No. SM4, Proc. Paper 3577, July 1973, pp 127-161.

MARSLAND, A. and RANDOLPH, M.F. (1977).
Comparison of the Results from Pressuremeter Tests and Large Insitu Plate Tests in London Clay. *Géotechnique* **27** No. 2 pp 217-243.

MAIR, R.J. and WOOD, D.M. (1987)
Pressuremeter Testing. Methods and Interpretation. Construction Industry Research and Information Association Project 335. Publ. Butterworths, London. ISBN 0-408-02434-8

MANASSERO, M. (1989)
Stress-Strain Relationships from Drained Self Boring Pressuremeter Tests in Sand. *Géotechnique* **39**, No.2.

MUIR WOOD, D. (1990)
Strain dependent soil moduli and pressuremeter tests. *Géotechnique*, **40**, pp 509-512.

NEWMAN, R.L., CHAPMAN, T.J.P. and SIMPSON, B. (1991)
"Evaluation of pile behaviour from pressuremeter tests". Proc. Xth European Conference on Soil Mechanics and Foundation Engineering, Florence, May 1991

PALMER, A.C. (1972)
Undrained plane-strain expansion of a cylindrical cavity in clay: a simple interpretation of the pressuremeter test, *Géotechnique* **22** No. 3 pp 451-457.

RANDOLPH, M.F. and WROTH, C.P. (1978)
An analytical solution for the consolidation around a driven pile. Int. J. Numer. Anal. Methods in Geomech.

ROBERTSON, P.K. and HUGHES, J.M.O. (1985)
"Determination of Properties of Sand from Self-Boring Pressuremeter Tests ". The Pressuremeter and Its Marine Applications, Second International Symposium.

ROWE, P.W. (1962)
"The Stress Dilatancy Relation for Static Equilibrium of an Assembly of Particles in Contact". Proceedings of the Royal Society. Vol. 269, Series A, pp 500-527.

WHITTLE, R.W. and DALTON, J.C.P. (1990)
Discussing 'Experience with the self boring rock pressuremeter'. *Ground Engineering*, Jan/Feb, pp 30-32.

WHITTLE R.W, DALTON J.C.P and HAWKINS P.G. (1992)
Shear Modulus and Strain Excursion in the Pressuremeter Test. Proc. Wroth Memorial Symposium, Oxford, July 1992.

WHITTLE R.W, HAWKINS P.G and DALTON J.C.P (1995)
The view from the other side - lift-off stress and the six arm self boring pressuremeter. The Pressuremeter and its New Avenues, Proc.4th International Symposium 17-19 May 1995.

WHITTLE R.W (1993)
Discussing 'The assessment of in situ stress and stiffness at seven overconsolidated clay and weak rock sites'. *Ground Engineering*, Sept 1993, pp 19-20.

WHITTLE R.W (1999)
Using non-linear elasticity to obtain the engineering properties of clay. Ground Engineering, May, vol. 32, no.5, pp 30-34.

WITHERS, N.J., HOWIE, J., HUGHES, J.M.O. and ROBERTSON, P.K. (1989)
Performance and Analysis of Cone Pressuremeter Tests in Sands, *Géotechnique* **39**, No. 3, pp 433-454.

WINDLE, D. (1976).
In situ testing of soils with a Self-boring Pressuremeter, PhD Thesis University of Cambridge

WINDLE, D. and WROTH, C.P.(1977)
The Use of a Self-boring Pressuremeter to determine the Undrained Properties of Clays. *Ground Engineering*, September.

WOOD, D.M. and WROTH, C.P. (1977)
Some laboratory experiments related to the results of pressuremeter tests. Internal Report No. CUED/C Soils TR 32, Cambridge University Engineering Department, also published in *Géotechnique* **27**, pp 181-201

WROTH, C.P.(1982)
British Experience with the Self Boring Pressuremeter in Proceedings of the Symposium on the Pressuremeter and its Marine Applications, Paris April 1982. Editions Techniq. 75737 Paris Cedex 15.

WROTH, C.P. (1984)
"The Interpretation of In Situ Soil Tests". Twenty Fourth Rankine Lecture, *Géotechnique* **34**, No. 4, pp 449-489